JÔNATAS PEDRO DA SILVA

SOIL ORGANIC MATTER FORMATION IN THE BYERS PENINSULA, MARITIME ANTARCTICA: ORIGIN AND BIOCHEMICAL COMPOSITION

VIÇOSA - MINAS GERAIS
2022

JÔNATAS PEDRO DA SILVA

SOIL ORGANIC MATTER FORMATION IN THE BYERS PENINSULA, MARITIME ANTARCTICA: ORIGIN AND BIOCHEMICAL COMPOSITION

Thesis submitted to the Soil and Plant Nutrition Graduate Program of the Universidade Federal de Viçosa in partial fulfillment of the requirements for the degree of *Doctor Scientiae*.

Adviser: Emanuelle Mercês Barros Soares

Co-advisers: Carlos Ernesto G. R. Schaefer
José João Lelis Leal de Souza

VIÇOSA - MINAS GERAIS
2022

Ficha catalográfica elaborada pela Biblioteca Central da Universidade Federal de Viçosa - Campus Viçosa

T
S586s
2022

Silva, Jônatas Pedro da, 1994-
Soil organic matter formation in the Byers Peninsula, maritme Antarctica: origin and biochemical composition / Jônatas Pedro da Silva. – Viçosa, MG, 2022.
1 tese eletrônica (181 f.): il. (algumas color.).

Texto em inglês.
Inclui apêndices.
Orientador: Emanuelle Mercês Barros Soares.
Tese (doutorado) - Universidade Federal de Viçosa, Departamento de Solos, 2022.
Inclui bibliografia.
DOI: https://doi.org/10.47328/ufvbbt.2022.801
Modo de acesso: World Wide Web.

1. Solos - Antártida. 2. Solos - Composição. 3. Solos - Teor de nitrogênio. 4. Solos - Teor de compostos orgânicos. 5. Mudanças climáticas. 6. Flora microbiana. I. Soares, Emanuelle Mercês, 1979-. II. Universidade Federal de Viçosa. Departamento de Solos. Programa de Pós-Graduação em Solos e Nutrição de Plantas. III. Título.

CDD 22. ed. 631.49989

JÔNATAS PEDRO DA SILVA

SOIL ORGANIC MATTER FORMATION IN THE BYERS PENINSULA, MARITIME ANTARCTICA: ORIGIN AND BIOCHEMICAL COMPOSITION

Thesis submitted to the Soil and Plant Nutrition Graduate Program of the Universidade Federal de Viçosa in partial fulfillment of the requirements for the degree of *Doctor Scientiae*.

APPROVED: December 16, 2022.

Assent:

Jônatas Pedro da Silva
(author)

Emanuelle Mercês Barros Soares
(Adviser)

“Os desafios são o que torna a vida interessante, e superá-los é o que dá sentido à vida.”

-Joshua J. Marine-

ACKNOWLEDGEMENTS

First of all, I thank God for giving me the gift of life!

To my mother Quitéria and my father Antônio for my existence, incentive to the studies and valuable advices that certainly contributed in my journey.

To my sisters (Késia, Cláudia, Claudeane and Claudete) and brothers (Josadaque and Jasiel) for their understanding, support, incentive and affection.

To the Department of Soils (DPS) of UFV for the opportunity given to me to do my PhD, as well as to CAPES/CNPq, PROANTAR and Permaclima for granting the scholarship.

To Professor Emanuelle Soares for his advice and trust.

To my co-advisors and friends Carlos Schaefer and J.J., for all the support, incentive, shared teachings and help that were primordial for the conclusion of this work. To Professor Carlos for the trust in sending me to Antarctica and providing me with one of the most incredible experiences of my life in that unique environment. To JJ for all the support, dedication, and patience, from the field collection to the elaboration of the articles and the acceptance hehehe.

To professor Teogenes Senna for the space given in his laboratory so that the analysis and processing of my material could be done.

To the other professors of the DPS/UFV for the knowledge acquired during the courses and conversations. To the DPS/UFV employees, specially Paloma Souza, technician of the Organic Matter and Residues Lab, who gave me technical support during the analyses in the lab.

To Dr. Tomás Veloso for all the support, support and knowledge shared.

I could not forget to thank my companion and friend Leonardo Barroso Vieira Silva for his advice, support, understanding, affection and motivation that he provided me until the end of this stage.

Last but not least, to all friends and colleagues who at some point contributed to this achievement, smiling and crying with me, especially Maria and Daniel, and my "gang" from LabMOR: Ferreira, Fernanda, Neilson, Naiara, Siro, Hugo, Paulo H., David, Victória, Heitor, Katherine. You have made our days lighter and more enjoyable.

Thank you so much!

“Não fiz o melhor, mas fiz de tudo para que o melhor fosse feito.
Não sou o que deveria, mas não sou o que eu era antes.”
-Martin Luther King-

ABSTRACT

SILVA, Jônatas Pedro da, D.Sc., Universidade Federal de Viçosa, December, 2022. **Soil organic matter formation in the Byers Peninsula, Maritime Antarctica: origin and biochemical composition**. Adviser: Emanuelle Mercês Barros Soares. Co-advisers: Carlos Ernesto Gonçalves Reynaud Schaefer and José João Lelis Leal de Souza.

The knowledge about the dynamics of soil organic matter (SOM) in Antarctica is fundamental to better understand the functioning of terrestrial ecosystems and to analyze the possible impacts of global climate change. Despite this, information on SOM in Maritime Antarctica is still incipient. Thus, we aimed to: i) analyze the elemental and biochemical constitution of the SOM; ii) calculate the soil C and N stocks; iii) perform the dating of the C present in the soils of the Byers Peninsula, Maritime Antarctica; iv) evaluate the soil microbial composition and activity, and; v) identify possible formation routes of the SOM present in the Antarctic biome. The Byers Peninsula with about 60 km^2 - is the largest ice-free area in Maritime Antarctica. It is designated a Specially Protected Antarctic Area (ASPA N° 126) due to its identification as a habitat of global importance, since it hosts breeding colonies of several birds and intense occupation of elephant seals. It is also considered the most important limnological site in the region and the most vulnerable to human interference. Thirteen soil profiles were opened and classified to represent vegetational, geological, geomorphological diversity and distance from the Rotche Dome glacier. The profiles were described and classified according to Soil Taxonomy and World Reference Base for Soil Resources (WRB). Samples were collected from all horizons for chemical and physical characterization. Vegetation material surrounding the profiles was also collected. The characterization of the SOM was done by physical fractionation, determining the POM and MAOM fractions. From these, the determination of the contents of C, N, C/N ratio and the isotopic signatures of $\delta^{13}C$ and $\delta^{15}N$ was made, as well as in the collected vegetal materials. In order to biochemically characterize the SOM present in these fractions and the vegetation, thermochemolysis analysis was performed with identification of the compounds by GC/MS to analyze whether there is a correlation between the composition of these vegetables and the biochemical composition of the SOM. Nuclear magnetic resonance spectroscopy (^{13}C NMR

CP/MAS) analysis was also performed in order to characterize the SOM at the molecular level and to identify the abundance of functional groups present in it. The C dating by the ^{14}C method was also performed to assess whether there is a correlation of this with glacier retreat. To understand the microbiological activity present in the Antarctic soils and its relationship with SOM and soil attributes, DNA was extracted from selected samples for identification of the organisms. The high diversity of biotic and abiotic factors acting in Maritime Antarctica directly affects the accumulation, transformation, and stabilization of SOM. Due to the greater presence of ecological niches, greater plant diversity with the presence of vascular plants, and the marked action of avifauna, these factors differentiate the processes involved in the redistribution of SOM between Maritime and Continental Antarctica, in addition to the humidity factor (in the form of net precipitation) being a key factor in the most active humification processes in the soils studied.

Keywords: Dynamics of soil organic matter. Elemental and biochemical composition. C and N stocks. Microbial composition. Formation routes of the SOM.

RESUMO

SILVA, Jônatas Pedro da, D.Sc., Universidade Federal de Viçosa, dezembro de 2022. **Formação da matéria orgânica do solo na Península Byers, Antártica Marítima: origem e composição bioquímica**. Orientador: Emanuelle Mercês Barros Soares. Co-orientadores: Carlos Ernesto Gonçalves Reynaud Schaefer e José João Lelis Leal de Souza.

O conhecimento sobre a dinâmica da matéria orgânica do solo (MOS) na Antártica é fundamental para melhor compreensão do funcionamento dos ecossistemas terrestres e análise dos possíveis impactos das mudanças climáticas globais. Apesar disso, as informações sobre a MOS na Antártica Marítima ainda são incipientes. Assim, objetivamos: i) analisar a constituição elementar e bioquímica da MOS; ii) calcular os estoques de C e N do solo; iii) realizar a datação do C presente nos solos da Península Byers, Antártica Marítima; iv) avaliar a composição e atividade microbiana do solo, e; v) identificar possíveis rotas de formação da MOS presente no bioma Antártico. A Península Byers com cerca de 60 km^2 – é a maior área livre de gelo da Antártica Marítima. Designada uma Área Antártica Especialmente Protegida (ASPA Nº. 126) devido a sua identificação como habitat de importância global, uma vez que abriga colônias de reprodução de diversas aves e de intensa ocupação de elefantes marinhos. É também considerado o mais importante sítio limnológico da região e o mais vulnerável à interferência humana. Treze perfis de solos foram abertos e classificados de forma a representar diversidade vegetacional, geológica, geomorfológica e distância da geleira Rotche Dome. Os perfis foram descritos e classificados conforme o Soil Taxonomy e World Reference Base for Soil Resources (WRB). Amostras foram coletadas em todos os horizontes para caracterização química e física. O material referente a vegetação circundante aos perfis também foi coletado. A caracterização da MOS foi realizada a partir do fracionamento físico, determinando as frações MOP e MAM. A partir dessas, foi feita a determinação dos teores de C, N, razão C/N e as assinaturas isotópicas de $\delta^{13}C$ e $\delta^{15}N$, assim como nos materiais vegetais coletados. Com o intuito de caracterizar bioquimicamente a MOS presente nessas frações e a vegetação, foi realizada a análise de termoquimólise com identificação dos compostos por GC/MS, para analisar se há correlação entre a composição desses vegetais e a composição bioquímica da MOS. Foi realizada

também a análise de espectroscopia de ressonância magnética nuclear (^{13}C RMN CP/MAS) com o objetivo de caracterizar a nível molecular a MOS e identificar a abundância de grupos funcionais presentes nesta. Foi realizada também a datação do C pelo método do ^{14}C, para avaliar se há correlação deste com o recuo da geleira. Para a compreensão da atividade microbiológica presente nos solos da Antártica Marítima e sua relação com a MOS e os atributos do solo, foi feita a extração de DNA de amostras selecionadas para identificação dos organismos. A elevada diversidade de fatores bióticos e abióticos que atuam na Antártida Marítima afeta diretamente a acumulação, transformação e estabilização da MOS. Devido à maior presença de nichos ecológicos, maior diversidade de plantas com a presença de plantas vasculares, e a marcada ação da avifauna, estes fatores diferenciam os processos envolvidos na redistribuição da MOS entre a Antártida Marítima e Continental, para além do fator humidade (sob a forma de precipitação líquida) ser um fator chave nos processos de humificação mais ativos nos solos estudados.

Palavras-chave: Dinâmica da matéria orgânica do solo. Composição elementar e bioquímica. Estoques de C e N. Composição microbiana. Rotas de formação da MOS.

SUMMARY

GENERAL INTRODUCTION

The melting process in the Antarctic Peninsula, encompassing its westernmost portion, called the South Shetlands Islands (Maritime Antarctica), began soon after the Last Glacial Maximum and continued throughout the Holocene (Ingólfsson et al., 2003, 1998; Oliva et al., 2016; Simms et al., 2011), and according to climate projections made by the IPCC (2014), will continue in the near future. This glacial retreat has resulted in the formation of large ice-free areas, among them the largest located on Livingston Island, in the Byers Peninsula, in the western portion of the island (Oliva et al., 2016). Existing records of early deglaciation in this area come from ^{14}C dating of basal Lake Limnopolar sediments, estimating an age of 8.3 cal. ky BP (calibrated thousands of years before present) (Toro et al., 2013), and from several minimum ages of other lake sediment records that ranged from 4 to 5 cal. ky BP (Björck et al., 1996).

In the latter half of the twentieth century, maritime Antarctica was considered to be the fastest warming region in the Southern Hemisphere, with average air temperature increases of 0.2-0.4 °C recorded every decade since the 1950's (Adams et al., 2009). This increase in surface air temperature in the soils of this region, intensified by the current global climate change scenario and increased greenhouse gas (GHG) emissions, will bring widespread effects under the Maritime Antarctic and its other polar ecosystems, as already reported in the literature through global climate change models (Turner et al., 2014), resulting in glacier recession (Cook et al., 2005), the disintegration of ice shelves and rising sea levels (Vaughan et al., 2003), as well as increased areas of exposed soils allowing colonization and expansion of plant (Amesbury et al., 2017; Charman et al., 2018) and microbial communities. This expansion tends to favor the mineralization of soil organic matter (SOM) and consequent release of GHG's such as C-CO_2 and N-N_2O, due to the increased activity of these organisms in the soil.

Consequently, increased air temperature resulting from global warming is expected to strongly affect vegetation expansion, biological activity, physical and chemical soil attributes, as well as SOM dynamics in periglacial environments, causing carbon (C) losses from these ecosystems (Schaefer et al., 2017; Thomazini et al., 2016). As these environments have low species diversity, low total biomass production, slow nutrient cycling rates, and simplified food chains with few trophic levels (Saba et al., 2014; Victoria et al., 2013), they become highly sensitive to disturbances or processes (such as, temperature and moisture changes, human activities, mass movements, etc.), consequently presenting a very slow recovery rate (Bockheim et al., 2013; Victoria et al., 2013; Zhu et al., 2014). Thus, understanding the dynamics of SOM in Antarctica is critical for better understanding the functioning of terrestrial ecosystems and analysis of possible impacts of global climate change (Beyer et al., 2004; Michel et al., 2006; Simas et al., 2006). Information about the nature and dynamics of SOM in Maritime

Antarctica is still incipient, making it necessary to know its elemental and biochemical constitution (C, N, P, S, lignin, tannins, polyphenols, lipids), possible sources of origin or formation routes, and composition of the physical fractions of SOM to better understand the mechanisms and processes of organic matter formation and protection in this environment. Through this understanding, it will be possible to make projections for future scenarios regarding C stocks in this environment, as well as how SOM dynamics may be affected.

In this context, we hypothesize that, (i) the SOM of Maritime Antarctica, specifically in the Byers Peninsula, may reveal a pre-glacial contribution due to the antiquity of the ice-free areas and the low contribution of vegetation in the present period; (ii) part of the organic C present in the soils of Maritime Antarctica are of complex, lacustrine and/or marine origin, besides terrestrial; (iii) part of the organic carbon present in these soils may come from microbial contributions, and, (iv) the current predominant vegetation in Maritime Antarctica, composed mainly of cryptogams (algae, mosses and lichens) and only two angiosperms (*Deschampsia antarctica* and *Colobanthus quitensis*), presents a variable contribution to the organic matter in these soils. Thus, the objectives of this work were: (i) to characterize the elemental, isotopic and biochemical composition of SOM fractions in Byers Peninsula soils and in plant materials, (ii) to determine the C and N contents and stocks in the different soil groupings (patterned soils located on high and low platforms, raised beach, and acid sulfate soil) as well as in the fractions of particulate (POM) and mineral-associated organic matter (MAOM) and in more abundant plant samples in the study area, iii) analyze the fungal and bacterial diversity present in Byers Peninsula soils and their interactions, and finally, iii) evaluate the differences in SOM composition as a function of soil age.

In paper 1 of this thesis, we present data on the ^{14}C dating of selected profiles to understand the thaw evolution and the eventual accumulation of C during the events since the last glacial maximum. The first paper was recently published in the journal *Geoderma*. In paper 2, we discuss the microbial diversity present in the soils of the Byers Peninsula, with the main focus on the bacterial and fungal communities. In paper 3, we discuss the elemental, biochemical and molecular composition of SOM in these soils, with the aim of understanding more about their dynamics in this environment, their fragility in the face of global climate change, and the possible sources of input and mechanisms behind the permanence of this SOM in the region.

Bibliographic references

Adams, B., Arthern, R., Atkinson, A., Barbante, C., Bargagli, R., Bergstrom, D., Bertler, N.A.N., Bindschadler, R., Bockheim, J., Boutron, C., Bromwich, D., Chown, S., Comiso, J., Convey, P., Cook, A., Prisco, G. Di, Fahrbach, E., Fastook, J., Forcada, J., Gili, J.-M., Gugliemin, M., Gutt, J., Hellmer, H., Hennion, F., Heywood, K.J., Hodgson, D., Holland, D., Hong, S., Huiskes, A., Isla, E., Jacobs, S., Jones, A., Lenton, A., Marshall, G., Mayewski, P., Meredith, M., Metzl, N., Monaghan, A., Garabato, A.C.N., Newsham, K., Orejas, C., Peck, L., Pörtner, H.-O., Rintoul, S., Robinson, S., Roscoe, H., Rossi, S., Scambos, T., Shanklin, J., Smetacek, V., Speer, K., Stevens, M., Summerhayes, C., Trathan, P., Turner, J., Veen, K. van Der, Vaughan, D., Verde, C., Webb, D., Wiencke, C., Dworth, P.W., Worby, T., Worland, R., Yamanouchi, T., 2009. The instrumental period. Antarct. Clim. Chang. Environ. 1–32.

Amesbury, M.J., Roland, T.P., Royles, J., Hodgson, D.A., Convey, P., Griffiths, H., Charman, D.J., 2017. Widespread Biological Response to Rapid Warming on the Antarctic Peninsula. Curr. Biol. 27, 1616-1622.e2. https://doi.org/10.1016/j.cub.2017.04.034

Beyer, L., White, D.M., Pingpank, K., Bölter, M., 2004. Composition and Transformation of Soil Organic Matter in Cryosols and Gelic Histosols in Coastal Eastern Antarctica (Casey Station, Wilkes Land). Cryosols 525–556. https://doi.org/10.1007/978-3-662-06429-0_26

Björck, S., Hjort, C., Ingólfsson, Ó., Zale, R., Ising, J., 1996. Holocene deglaciation chronology from lake sediments, in: Geomorphological Map of Byers Peninsula, Livingston Island. British Antarctic Survey Cambridge, pp. 49–51.

Bockheim, J., Vieira, G., Ramos, M., López-Martínez, J., Serrano, E., Guglielmin, M., Wilhelm, K., Nieuwendam, A., 2013. Climate warming and permafrost dynamics in the Antarctic Peninsula region. Glob. Planet. Change 100, 215–223. https://doi.org/10.1016/J.GLOPLACHA.2012.10.018

Charman, D.J., Amesbury, M.J., Roland, T.P., Royles, J., Hodgson, D.A., Convey, P., Griffiths, H., 2018. Spatially coherent late Holocene Antarctic Peninsula surface air temperature variability. Geology 46, 1071–1074. https://doi.org/10.1130/G45347.1

Cook, A.J., Fox, A.J., Vaughan, D.G., Ferrigno, J.G., 2005. Retreating glacier fronts on the Antarctic Peninsula over the past half-century. Science (80-.). 308, 541–544. https://doi.org/10.1126/SCIENCE.1104235/SUPPL_FILE/COOK.SOM.PDF

Ingólfsson, Ó., Hjort, C., Berkman, P.A., Björck, S., Colhoun, E., Goodwin, I.D., Hall, B., Hirakawa, K., Melles, M., Möller, P., Prentice, M.L., 1998. Antarctic glacial history since the Last Glacial Maximum: an overview of the record on land. Antarct. Sci. 10, 326–344.

https://doi.org/10.1017/S095410209800039X

Ingólfsson, Ó., Hjort, C., Humlum, O., 2003. Glacial and Climate History of the Antarctic Peninsula since the Last Glacial Maximum. Arctic, Antarct. Alp. Res. 35, 175–186. https://doi.org/10.1657/1523-0430(2003)035[0175:GACHOT]2.0.CO;2

IPCC, 2014. Climate Change 2013 - The Physical Science Basis. Cambridge University Press, Cambridge. https://doi.org/10.1017/CBO9781107415324

Michel, R.F.M., Schaefer, C.E.G.R., Dias, L.E., Simas, F.N.B., Benites, V. de M., Mendonça, E. de S., 2006. Ornithogenic Gelisols (Cryosols) from Maritime Antarctica. Soil Sci. Soc. Am. J. 70, 1370–1376. https://doi.org/10.2136/SSSAJ2005.0178

Oliva, M., Antoniades, D., Giralt, S., Granados, I., Pla-Rabes, S., Toro, M., Liu, E.J., Sanjurjo, J., Vieira, G., 2016. The Holocene deglaciation of the Byers Peninsula (Livingston Island, Antarctica) based on the dating of lake sedimentary records. Geomorphology 261, 89–102. https://doi.org/10.1016/J.GEOMORPH.2016.02.029

Saba, G.K., Fraser, W.R., Saba, V.S., Iannuzzi, R.A., Coleman, K.E., Doney, S.C., Ducklow, H.W., Martinson, D.G., Miles, T.N., Patterson-Fraser, D.L., Stammerjohn, S.E., Steinberg, D.K., Schofield, O.M., 2014. Winter and spring controls on the summer food web of the coastal West Antarctic Peninsula. Nat. Commun. 2014 51 5, 1–8. https://doi.org/10.1038/ncomms5318

Schaefer, C.E.G.R., Pereira, T.T.C., Almeida, I.C.C., Michel, R.F.M., Corrêa, G.R., Figueiredo, L.P.S., Ker, J.C., 2017. Penguin activity modify the thermal regime of active layer in Antarctica: A case study from Hope Bay. CATENA 149, 582–591. https://doi.org/10.1016/j.catena.2016.07.021

Simas, F.N.B., Schaefer, C.E.G.R., Melo, V.F., Guerra, M.B.B., Saunders, M., Gilkes, R.J., 2006. Clay-sized minerals in permafrost-affected soils (Cryosols) from King George Island, Antarctica. Clays Clay Miner. 54, 721–736. https://doi.org/10.1346/CCMN.2006.0540607

Simms, A.R., Milliken, K.T., Anderson, J.B., Wellner, J.S., 2011. The marine record of deglaciation of the South Shetland Islands, Antarctica since the Last Glacial Maximum. Quat. Sci. Rev. 30, 1583–1601. https://doi.org/10.1016/j.quascirev.2011.03.018

Thomazini, A., Francelino, M.R., Pereira, A.B., Schünemann, A.L., Mendonça, E.S., Almeida, P.H.A., Schaefer, C.E.G.R., 2016. Geospatial variability of soil CO2–C exchange in the main terrestrial ecosystems of Keller Peninsula, Maritime Antarctica. Sci. Total Environ. 562, 802–811. https://doi.org/10.1016/j.scitotenv.2016.04.043

Toro, M., Granados, I., Pla, S., Giralt, S., Antoniades, D., Galán, L., Cortizas, A.M., Lim, H.S., Appleby, P.G., 2013. Chronostratigraphy of the sedimentary record of Limnopolar Lake, Byers Peninsula, Livingston Island, Antarctica. Antarct. Sci. 25, 198–212. https://doi.org/10.1017/S0954102012000788

Turner, J., Barrand, N.E., Bracegirdle, T.J., Convey, P., Hodgson, D.A., Jarvis, M., Jenkins, A., Marshall, G., Meredith, M.P., Roscoe, H., Shanklin, J., French, J., Goosse, H., Guglielmin, M., Gutt, J., Jacobs, S., Kennicutt, M.C., Masson-Delmotte, V., Mayewski, P., Navarro, F., Robinson, S., Scambos, T., Sparrow, M., Summerhayes, C., Speer, K., Klepikov, A., 2014. Antarctic climate change and the environment: an update. Polar Rec. (Gr. Brit). 50, 237–259. https://doi.org/10.1017/S0032247413000296

Vaughan, D.G., Marshall, G.J., Connolley, W.M., Parkinson, C., Mulvaney, R., Hodgson, D.A., King, J.C., Pudsey, C.J., Turner, J., 2003. Recent Rapid Regional Climate Warming on the Antarctic Peninsula. Clim. Chang. 2003 603 60, 243–274. https://doi.org/10.1023/A:1026021217991

Victoria, F. de C., de Albuquerque, M.P., Pereira, A.B., Simas, F.N.B., Spielmann, A.A., Schaefer, C.E.G.R., 2013. Characterization and mapping of plant communities at Hennequin Point, King George Island, Antarctica. Polar Res. 32, 19261. https://doi.org/10.3402/polar.v32i0.19261

Zhu, R., Bao, T., Wang, Q., Xu, H., Liu, Y., 2014. Summertime CO2 fluxes and ecosystem respiration from marine animal colony tundra in maritime Antarctica. Atmos. Environ. 98, 190–201. https://doi.org/10.1016/J.ATMOSENV.2014.08.065

Paper 1

Paper published in the special issue "*Permafrost affected soils and climate change - from soil development to carbon storage and biological functioning*" by Georderma journal.

da Silva, J.P., Lelis Leal de Souza, J.J., Mercês Barros Soares, E., Schaefer, C.E.G.R., 2022. Soil organic matter accumulation before, during, and after the last glacial maximum in Byers Peninsula, Maritime Antarctica. Geoderma 116221. https://doi.org/10.1016/j.geoderma.2022.116221

PAPER 1: SOIL ORGANIC MATTER ACCUMULATION BEFORE, DURING, AND AFTER THE LAST GLACIAL MAXIMUM IN BYERS PENINSULA, MARITIME ANTARCTICA

Jônatas Pedro da Silva [a,b,*], José João Lelis Leal de Souza[b], Emanuelle Mercês Barros Soares [b], Carlos Ernesto G. R. Schaefer [b]

[a] Ph. D. student Program in Soils and Plant Nutrition, Department of Soils, Federal University of Viçosa - UFV, Viçosa - MG, Brazil

[b] Department of Soils, Federal University of Viçosa - UFV, Viçosa - MG, Brazil

[*] Corresponding author:

Telephone: +55 31 9 8357-2450

E-mail: jpedro.agronomo@gmail.com

Abstract

Organic matter is incorporated into soil by biological activity, and its preservation depends on composition and organic-mineral interactions. Frost activity, dry and cold climate, and glacial retreat-advance dynamics complexify soil organic matter storage in Antarctica. Byers Peninsula is the largest ice-free area in Antarctica and hosts a high diversity of vegetable and animal species. We hypothesize that (i) the SOM in the Byers Peninsula may reveal a distinct composition due to the antiquity of the ice-free areas not entirely obliterated by the advancing glaciers during the LGM; and (ii) the advancing ice caps at Byers allowed the accumulation of organic carbon at sheltered points of the Peninsula. Thus, the objectives of this work were: i) to characterize physically and chemically selected soils at Byers Peninsula, with emphasis on organic C and N stocks in different soil types, and ii) SOM dating of representative soil profiles. Thirteen soil profiles were dug, described, and classified. The plant species present at each site were identified. Chemical and physical attributes were determined. The C and N contents, $\delta^{13}C$ and $\delta^{15}N$ ratio isotopes were determined in the SOM physical size-fractionated particles. The C and N stocks were calculated for each SOM fraction. The deepest horizon of six soil profiles were dated by the ^{14}C method. Soils from Byers Peninsula showed a diverse and varied biochemical nature of SOM, resulting in varying content of C and N. The $\delta^{13}C$ weighted mean of the SOM reflects the dominant vegetation type present in each sampling location, except for pre-Holocene soils and soils influenced by ornithogenesis. The highest organic C and N pools were recorded at subsurface horizons and attributed to the organo-mineral association fraction in upper platforms. For all soil

groups, there was a significant overlap of $\delta^{13}C$ and enrichment of $\delta^{15}N$ in all fractions of SOM, requiring the combination of these two signatures to identify possible sources of contribution to SOM in this environment. The oldest soils, subjected to early-mid Holocene uplift, revealed an endolithic signature of pre-LGM age, the first recorded in Maritime Antarctica to this day. This first pre-LGM SOC record can indicate the initial modern colonization of Maritime Antarctica and suggests that ice caps advance during LGM was limited. Soils formed during and after the LGM in low platforms have a lacustrine signature indicating an influence of snowmelt, ice thawing, and permafrost degradation in selecting hygrophilous species. Soils formed in raised beaches have the lowest organic C and N stocks, and the isotopic composition of SOM indicates ancient ornithogenic influence.

Keywords: Radiocarbon dating, isotopic composition, C stock, N cycle, Endolithic-derived SOC, ice-free areas.

1. Introduction

The weather and climate of Antarctica limit its colonization by both microorganisms and vegetation. Less severe climate conditions (Boy et al., 2016) in the South Shetlands Islands (Maritime Antarctica - western portion of the Antarctic Peninsula) enabled old colonization of large ice-free areas by seabirds and mammals (Emslie et al., 2020; Liu et al., 2005), and incorporation of soil organic carbon (SOC) in Antarctic soils (Beyer, 2000; Beyer et al., 2000; Bockheim and Haus, 2014; Park et al., 2007). Consequently, the Antarctic Peninsula, encompassing all of Maritime Antarctica, represents the largest SOC stock in Antarctic soils, with estimated values on the order of 600 Mt from Antarctic Peninsula soils, out of a total C stock of 725 Mt estimated for all of Antarctica (Bockheim and Haus, 2014; Claridge et al., 2000).

The glacial retreat in the Antarctic Peninsula and South Shetlands Islands began shortly after the Last Glacial Maximum, it continued throughout the Holocene (Hodgson et al., 2014; Ingólfsson et al., 2003, 1998a; Oliva et al., 2016; Simms et al., 2011), and it will continue in the near future, according to climate projections (IPCC, 2014). The retraction of glaciers resulted in extensive ice-free areas, including the largest, located on the western sector of Livingston Island, in the Byers Peninsula (Oliva et al., 2016). Existing records of early deglaciation in this area come from ^{14}C dating of basal sediments from Lake Limnopolar, which reported an estimated age of 8.3 cal. ky BP (calibrated thousands of years before present) (Toro et al., 2013), and various minimum ages from other lake sediment records that ranged between 4 and 5 cal. ky BP (Björck et al., 1996a).

In the latter half of the 20th century, Maritime Antarctica was considered the fastest-warming region in the Southern Hemisphere, with average increases in air temperature of up to 0.4 °C being recorded every decade since the 1950s (Adams et al., 2009). The increase in air

temperature, intensified by the current scenario of global climate change (Turner et al., 2014a), will result in the recession of glaciers (Cook et al., 2005), the disintegration of ice shelves, and rise of sea levels (Vaughan et al., 2003), in addition to an increase in exposed soil areas allowing for colonization and expansion of plant communities (Amesbury et al., 2017; Charman et al., 2018).

The increase in air temperature and glacier retreat resulting from global warming are expected to affect vegetation expansion and biological activity due to their high sensitivity and rapid response to climate change (Cannone et al., 2012; Cary et al., 2010; Convey et al., 2011; Mendonça et al., 2011; Simas et al., 2008; Thomazini et al., 2014; Zhu et al., 2014a, 2014b); soil physical and chemical attributes through the exposure of new areas to physical, chemical and biological weathering, which results in soil deepening and restructuring, serving as a substrate for primary colonization by various opportunistic organisms (Kennedy, 1995), as well as soil organic matter (SOM) dynamics in periglacial environments causing losses of carbon (Balks et al., 2013; Cannone et al., 2006; Díaz-Puente et al., 2021; Michel et al., 2014; Navas et al., 2008a; Schaefer et al., 2017; Thomazini et al., 2016; Turner et al., 2014b). As a consequence of this warming, the melting of permafrost can stimulate root respiration, decomposition of organic carbon, and increase CO_2 emissions from soils (Carvalho et al., 2013; Mendonça et al., 2011; Thomazini et al., 2014).

However, the feedbacks related to organic carbon exchange are still uncertain, with positive feedbacks (caused by intensified SOC mineralization due to warming) or negative (resulting from excessive input of plant-derived carbon overcoming soil decomposition) depending on the intensity of climate change (Cannone et al., 2012). Although climate variables directly affect the C cycle through net primary production and decomposition, the SOC stock maintenance depends on physicochemical stabilization of C associated with clay fraction and geochemical soil properties (Doetterl et al., 2015a).

Compared to tropical and temperate regions, the periglacial environments propitiate shallower skeletal soils and lower net primary productivity (Doetterl et al., 2015a; Moura et al., 2012). Between soils on the same site there is a great variation in C and N stocks, varying according to soil class, vegetation cover and presence of animals (Pires et al., 2017). Birds and mammals increase up to more than tenfold SOC stocks in soils by nidification compared to the stocks in non-nesting areas (Beyer et al., 2004; Simas et al., 2007). The periglacial environments are susceptible to disturbances and show a prolonged recovery rate (Bockheim et al., 2013; Victoria et al., 2013; Zhu et al., 2014a) due to low species diversity, low total biomass production, slow nutrient cycling rates, and food chains with few trophic levels (Saba et al., 2014; Victoria et al., 2013).

Therefore, we hypothesize that (i) the SOM in parts of Maritime Antarctica, specifically in the Byers Peninsula, may reveal a distinct composition due to the antiquity of the ice-free areas not entirely obliterated by the advancing glaciers during the LGM; and (ii) the advancing ice caps at Byers allowed the accumulation of organic carbon at sheltered points of the Peninsula. Thus, the objectives of this work were: i) to characterize physically and chemically selected soils at Byers Peninsula, with emphasis on organic C and N stocks in different soil types (patterned-ground soils, high platforms, raised beaches, and acid-sulfated soils), and ii) SOM dating of representative soil profiles.

2. Material and Methods

2.1. Study area

With about 60 km^2, the Byers Peninsula is the most extensive ice-free area in Maritime Antarctica (Figure 1). The Peninsula is located at the western end of Livingston Island and between the Bransfield Strait and the Drake Passage (62° 34' – 62° 41'S and 60° 56' - 61° 12'W). Climatic data from 2002 to 2010 show an average annual temperature of -2.8°C at 70 m above sea level (m.a.s.l.), and precipitation ranging from 500 to 800 mm (Bañón et al., 2013). Runoff is restricted to the summer season and is mainly related to snowmelt and active layer thaw (Toro et al., 2013).

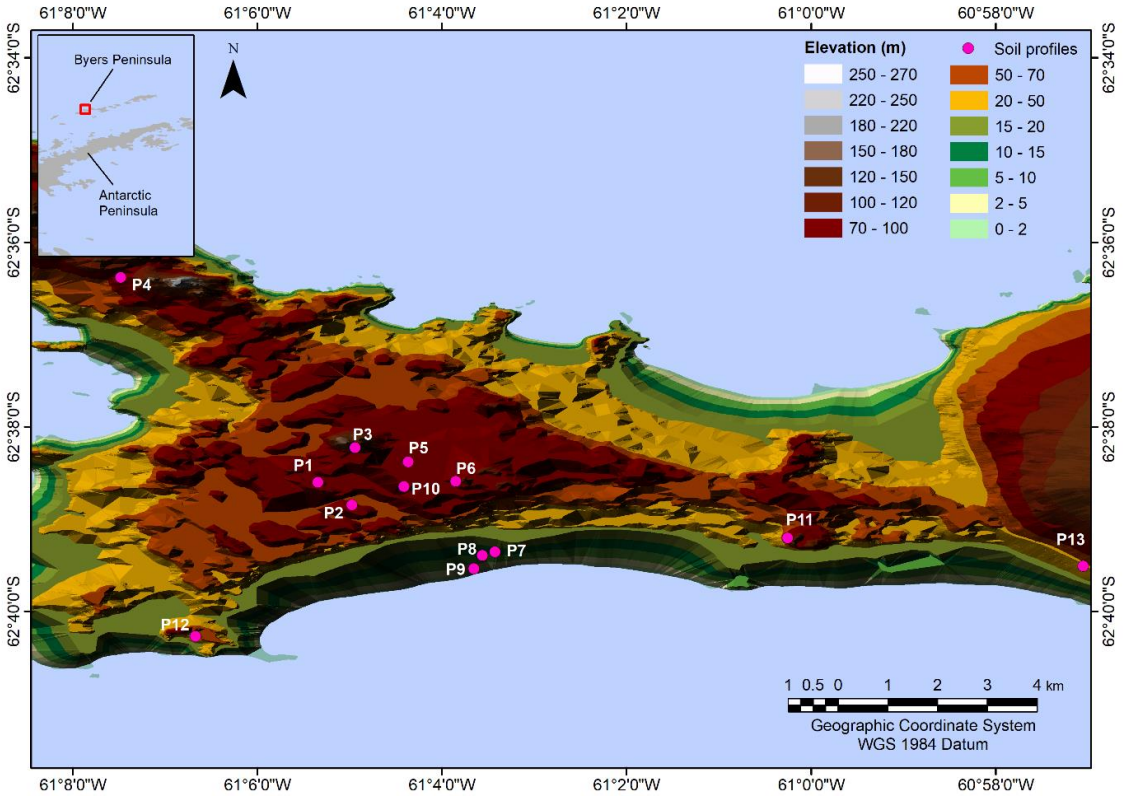

Figure 1. Location of Byers Peninsula in the South Shetlands and distribution of soil profiles collected in Byers Peninsula, Livingston Island, Antarctica Maritime.

The geology of Byers Peninsula is predominantly composed of Paleo-Mesozoic claystone, Juro-Cretaceous conglomerate, pyroclastic rocks interspersed with Cretaceous basalt, Paleogenous basaltic-andesitic intrusions, and Quaternary sedimentary rocks (Alfaro et al., 2010; Hobbs, 1968; Ruiz-Fernández and Oliva, 2016; Smellie et al., 1980). Ten levels of raised beaches, at elevations between 2 and 84 m.a.s.l., expose marine sedimentary materials. Low platforms between 50 and 70 m.a.s.l. occur on Cretaceous clastic sedimentary rocks. A cryoplanar surface, developed on volcanic tuffs, is the upper platform, above 70 m.a.s.l. Cliffs and isolated hills of Juro-Cretaceous volcanic and volcanoclastic rocks occur between 140 and 265 m.a.s.l. Shallow and loam Cryosols, Leptosols, and Regosols are the main soil groups in Byers Peninsula (Moura et al., 2012; Navas et al., 2008b, 2006).

Byers Peninsula has a diverse vegetation (Benayas et al., 2013). Fifty-six species of lichen and 42 species of mosses, of which 17 are endemic to the Byers Peninsula (Ochyra et al., 2008; Wirtz et al., 2003). The vegetation cover is more abundant in flat and high raised beaches, being mainly composed of several species of mosses, abundant in poorly drained environments (example, *Sanionia uncinata, Sanionia George-uncinata, Andreaea gainni, Polytrichum juniperinum, Hymenoloma grimmiaceum, Brachythecium austrosalebrosum, Warnstorfia*

sarmentosa, among other species), vascular plants, consisting of two flowering species, *Deschampsia antartica* and *Colobanthus quitensis* (Vera, 2011), and lichens distributed at higher places and abundantly on the rocks, with *Usnea auranteaco-ater* as the most abundant.

Peninsula Byers was selected as an Antarctic Specially Protected Area (ASPA N° 126) by the Protocol on Environmental Protection to the Antarctic Treaty (also known as the Madrid Protocol) in 1991. The Peninsula is home to breeding colonies of terns (*Sterna vittata*), seagulls (*Larus dominicanus*), penguins (*Pygoscelis antarctica* and *Pygoscelis papua*), petrels (*Oceanites oceanicus*, *Fregetta tropica*, *Daption capense,* and *Macronectes giganteus*), from cormorants (*Phalacrocorax atriceps*), skuas (*Stercorarius antarcticus*), Antarctic doves (*Chionis albus*), and intense occupation by sea elephants (*Mirounga leonina*). It is also considered the most important limnological site in the group of South Shetlands Islands and the most vulnerable to human interference (Oliva et al., 2016).

2.2. Selection, description, and classification of soil profiles and plant materials

Thirteen soil profiles were dug, described, and classified according to the Soil Taxonomy (ST) and the World Reference Base (WRB) (Tables S1 and S2). Although these systems are based on genetic principles, the approaches used emphasize the role of soil processes in soil taxonomic systems (Bockheim and Gennadiyev, 2000).

The plant species present in each site were identified and listed according to the specific literature for Antarctic vegetation, such as Ochyra (1998), Ochyra et al. (2008) and Putzke and Pereira (2001) for mosses and Olech (2004), Øvstedal and Smith (2001) and Redón (1985) for lichens (Table S1). The most abundant species (Table 1) from each site were also collected to analyze their elemental composition (C and N contents) and their isotopic signatures ($\delta^{13}C$ and $\delta^{15}N$).

Table 1. Identified and collected plant species on soils from the Byers Peninsula, Maritime Antarctic.

Soil profile	Coordinates	Dominant Species	Group	Identification
P2	62° 38’ 50.90” S 61° 04’ 58.54” W	*Hymenoloma grimmiaceum* (Müll. Hal.) Ochyra	Moss	HG
P3	62° 38’ 13.6” S 61° 04’ 56.3” W	*Usnea aurantiaco-atra* (Jacq.) Bory	Lichen	UA
P4	62° 38’ 22.9” S 61° 07’ 28.7” W	*Sanionia uncinata* (Hedw.) Loeske	Moss	SU
P6	62° 38’ 35.5” S	*Sanionia Geroge-uncinata*	Moss	SGU

P7	61° 03’ 51” W 62° 39’ 21.4” S 61° 03’ 25.4” W	*Brachythecium austrosalebrosum* (Müll. Hall.) Paris	Moss	BA
P7	62° 39’ 21.4” S 61° 03’ 25.4” W	*Warnstorfia sarmentosa* (Wahlenb.) Hedenäs	Moss	WS
P9	62° 39’ 32.4” S 61° 03’ 39.2” W	*Deschampsia antarctica* É. Desv.	Grassy	DA
P11	62° 39’ 12.4” S 61° 00’ 15.1” W	*Polytrichum juniperinum*	Moss	PJ
P12	62° 40’ 16.4” S 61° 06’ 40.1” W	*Andreaea gainii* Cardot	Moss	AG

2.3. Soil Attributes

Gravel content was determined in laboratory after sieving. The fine sand and coarse sand contents were determined by the sedimentation cylinder method. The silt and clay contents in the fine soil fraction were determined by the pipette method after being stirred for 16 h with 0.1 M NaOH. Once soils are gravelly and collecting undisturbed samples with the volumetric ring is virtually impossible, we measured total porosity in undisturbed samples collected to micromorphological descriptions. Representative samples of the surface horizons were taken to prepare the thin sections. For this purpose, field-oriented and preserved blocks collected in the field were oven dried at 40 °C for one week and vacuum impregnated (5 kPa) with polyester resin diluted in 30% (volume) styrene monomer. Thin sections were made following the method of Fitzpatrick (1984). Percentage area covered by pores in thin sections was measured using JMicroVision v.1.2.7. The soil density was calculated according to the formula: Soil density = (total porosity/ particle density) + 1. Particle density was determined after drying a quantity of soil to 105°C and then dividing the mass by the volume of the particles, excluding spaces among them (Teixeira et al., 2017).

The pH was determined in 1:2.5 soil: deionized water and 1 mol L^{-1} KCl solution. The potential acidity was extracted with 0.5 mol·L^{-1} $Ca(OAc)_2$ buffered at pH 7.0 and quantified by titration with 0.0606 mol·L^{-1} NaOH. Exchangeable Ca^{2+}, $Mg^{2+,}$ and Al^{3+} were extracted with KCl 1 mol·L^{-1} and determined by atomic absorption. Na^+, K^+, and P were extracted with Melich-1 (EMBRAPA, 2011). Exchangeable K^+ and Na^+ were determined by flame. Available phosphorus content was determined by photocolorimetry. The potential acidity (H + Al) was extracted by 1 mol L^{-1} ammonium acetate solution at pH 7. The cation exchange capacity was calculated as the sum of the cations. The P adsorption capacity of the soil was determined after stirring for 1 hour with 2.5 g of soil in 0.01 mol L^{-1} $CaCl_2$ containing 60 mg of P L^{-1}. The suspension was filtered, and the remaining P in solution was determined by photocolorimetry (P-rem).

2.4. Soil organic matter analysis

The SOM was physically size-fractionated as: a) particulate organic matter (POM), and; b) mineral-associated organic matter (MAOM) (Cambardella and Elliott, 1992). The C and N contents, $\delta^{13}C$ and $\delta^{15}N$ ratio isotopes were determined in these fractions in all soil horizons and the plant materials to assess their contribution to the organic C and N stocks in soils of Byers Peninsula and identify the link between the isotopic signatures of plant and soil SOM. All these determinations were made using an Isotope Ratio Mass Spectrometer (IRMS) Flash EA - Delta V in the *Centro de Isótopos Estáveis Prof. Dr. Carlos Ducatti* - UNESP. The weighted $\delta^{13}C$ and $\delta^{15}N$ mean of SOM was calculated for samples according to mass and signature of each physical fraction. The organic C and N contents were determined by a proportional mass sum of POM and MAOM fractions. The organic carbon to nitrogen ratio (C/N) was calculated based on the mass of the fractions.

Total C content was determined by a Perkin Elmer Series II 2400 CHN S/O Elemental Analyzer and a formula considering extracted C by the Walkley-Black method (Gatto et al., 2009). The inorganic C and N contents were determined by the difference between the total and the organic fraction content.Based on these data, it was possible to calculate the organic stock of C and N present in the soils using the following equation (Veldkamp, 1994):

$$S = ((C\ or\ N) * t * Ds)/10$$

Where *S* is the organic stock of C or N in Mg ha^{-1}; *C* and *N* is the content of these elements in the SOM fractions, in g kg^{-1}; *t* is the thickness of the soil layer, in cm, and *Ds* is the density of the soil in g cm^{-3}.

The organic stock of C and N in soil profiles were calculated as the sum of each layer. The values are expressed as Mg ha^{-1}.

2.5. Radiocarbon dating

The deepest horizon of six soil profiles were dated by the ^{14}C method. The soil profiles were selected to represent geomorphological, geological, and vegetable diversity, as well as different distances from the glacier. To measure the radiocarbon content in the samples, dating by Accelerator Mass Spectrometry (AMS) was performed by BETA ANALYTIC Laboratory. The analytical result ("BP" or "pMC") is obtained by measuring the $^{14}C/^{13}C$ sample in relation to the $^{14}C/^{13}C$ in oxalic acid II (NIST-4990C) in a particle accelerator using SNICS ion source. The result of the AMS analysis is corrected as a function of the total fractionation of the $\delta^{13}C$ of the graphite. The $\delta^{13}C$ of the sample is obtained by analyzing it in an isotope ratio mass spectrometer

(IRMS). The IRMS performs the separation and measurement of the CO_2 masses (44, 45, and 46), and the calculation of the $\delta^{13}C$ of the sample. Calibration of radiocarbon age expressed in years before the present (BP) was performed using the High Probability Density Band Method (HPD): SHCAL13 (Hogg et al., 2013; Ramsey, 2009).

2.6 Data Analysis

Statistical analyzes were performed using R geostatistical software (R Core Team, 2019). Principal Component Analysis (PCA) was done using the stats package. For Spearman's correlation, the corrplot package was applied, where probability values of 5% or less ($p \leq 0.05$) were considered statistically significant based on Student's "t" test. PCA's were carried out to explore general trends in soil attributes (chemical and physical parameters) and assess which main variables associated with MOS could be grouped or separated according to soil groups. Spearman's correlation analysis was used as a function of the variables studied in the PCA, as a complementary tool to elucidate these results. The low sample size disallows the execution of robust statistical procedures to ensure that the sample is considered representative of a population and that the statistical result can be generalized to a larger population. However, the number of samples is sufficient for determination of patterns. It is important to highlight that the reduced number of research samples is an inherent characteristic of Antarctic expeditions due to logistical difficulties and access limitations imposed on ASPA.

3. Results

Six Cryosols, three Gleysols, two Arenosols, one Cambisol, and one Leptosol were collected (Table S1). These profiles were developed at marine terraces, high and low platforms, between 15 and 140 m.a.s.l. The thickness of the soils varies between 10 and 205 cm (Table S2). Permafrost occurs discontinuously on platforms and top of ridges from 10 cm deep. Organic intrusions, wavy transition between horizons, and patterned ground evidence of cryoturbation in high and low platforms.

Soils are extremely acidic to moderately alkaline (Table S5). Except for the soil derived from pyritized andesite, all soils have base saturation above 50%, mostly hypereutrophic. The order of base dominance is $Ca^{2+}>Mg^{2+}>Na^{+}>K^{+}$. The values observed for Mehlich-1 extractable P ranged from 0.9 to 953.80 mg dm^{-3}. The P-rem contents ranged from 3.0 to 52.20 mg L^{-1}. The lowest levels of P and P-rem were found in the sulfated soil, while the highest content of P was found in the high platforms. Raised beaches presented the highest P-rem, suggesting a low affinity between clays, clay minerals, and SOM with P (Tonello et al., 2020). Low values of P-rem in the acid sulfate soil indicate high affinity between clay minerals and P, and high reactivity of this soil, demonstrating a very high capacity to adsorb P.

All soils are covered by vegetation, except for the soil profile derived from pyritized andesite and the soil on the highest raised beach. Thirteen two species were identified in soils collected from igneous ridges and talus, 28 species were identified on cryoplanar surfaces with patterned soils, 19 species in soils collected from raised beaches, and five species on cryoplanar surfaces without patterned soils. Most of the identified species were mosses, and the low platforms are the most diverse sites. Despite the high salinity registered, mainly in coastal soils, no halophyte species were identified in the study area.

The total C content varied between 0.06 and 1.57%; inorganic C contents represents in average 47.7% of total C. The total N content varied between 0.003 and 0.085%; inorganic N contents represents in average 36.7% of total N. The inorganic C and N stocks represented in average, respectively, 46.9.3 and 34.4% of the total stocks. As this study is focused on organic fractions, the inorganic fraction's data is presented and discussed in Supplementary Material.

3.1. Isotopic composition of SOM fractions and organic C and N levels

In general, the organic C and N contents in the MOAM and MOP fractions decreased with increasing depth. On the other hand, soil profiles in surface pattern ground (P2, P3, P5, and P10) tend to increase organic C and N contents in depth. The organic C content of the POM fraction varied between 0.13 and 6.62 mg g^{-1} of soil, or 0.03 and 0.91% of carbon (Table S3). The organic N content of the POM fraction varied between 0.05 and 1.01 mg g^{-1} of soil, or 0.01 and 0.14% (Table S3). The highest organic contents of C and N were observed in the high and low platforms, highlighting the P4 and P3 profiles (Figure 2). The raised beaches, in turn, stood out with the lowest organic C content associated with the POM fraction.

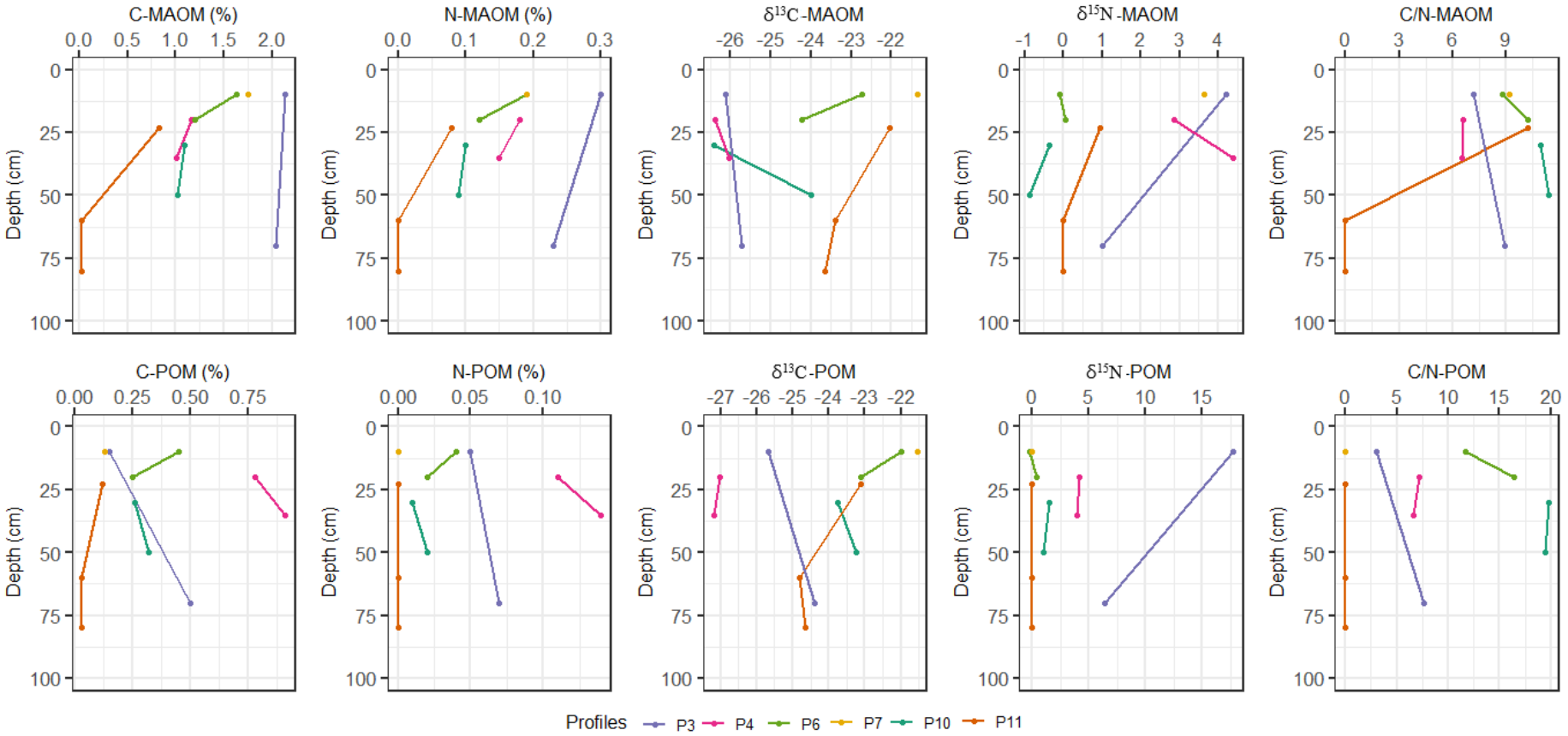

Figure 2. Soil C and N content, isotopic signature, and C/N ratio in the MAOM and POM fractions of the ^{14}C dated soil profiles collected in the Byers Peninsula.

The organic C content of the MAOM fraction varied between 0.12 and 8.10 mg g^{-1} of soil, or 0.03 and 2.14% of carbon (Table S3). The organic N content of the POM fraction varied between 0.01 and 0.79 mg g^{-1} of soil, or 0.01 and 0.30%. The soils of the high and low platforms, mainly those with patterned ground, have the highest organic C and N contents.

Soils with a high relative proportion of POM over MAOM are distinguished between: i) soils developed in raised beaches, with high $\delta^{13}C$, and; ii) sulfated soils and soils in non-patterned ground on cryoplanated surfaces, with low values of $\delta^{13}C$. These profiles have more than 50% of the organic C content associated with the POM fraction (Table S3). On the other hand, the profiles with MAOM over POM dominance are distinguished between: i) soils developed on patterned ground cryoplanated surfaces, with high values of $\delta^{13}C$; ii) soils developed in talus and cliffs, with low values of $\delta^{13}C$, and; iii) a flooded raised beach. The profiles developed on cryoplanated surfaces with patterned ground (P5, P6, and P12) have more than 80% of the organic C content associated with the MAOM. Profiles developed in talus (P2 and P3), cliffs (P10 and P11), and a flooded raised beach (P7) have more than 60% of the organic content of organic C associated with the mineral phase.

The P4 has the highest C and N contents associated with the POM fraction. This soil profile is on the upper plateau and derived from Paleozoic marine sedimentary rocks. The P6 has the highest C and N contents associated with the MAOM fraction. This soil is developed on the upper platform with patterned ground.

C/N ratio showed high variation between the profiles. Values ranged between 3.05 and 19.80 in the POM fraction and from 6.55 to 15.64 in the MAOM fraction. The highest C/N ratios in the POM fraction were observed in P10, P6, and P2 soils. All raised beaches (P7, P8, P9, and P13) and three patterned-ground soils (P5, P11, and P12) have the lowest C/N ratios or event did not allow to calculate the C/N ratio once their N contents were undetectable (minimum necessary for detection of N in the sample is 0.01%). The highest values of C/N associated with the MAOM fraction were registered in subsurface horizons of soils on the upper platform and raised beaches.

In general, the isotopic C ratio values associated with MAOM and POM are similar and varied below 3‰ with depth. The $\delta^{13}C$ values range from −27.73‰ to −17.44‰. Soils on the upper platforms registered the most depleted $\delta^{13}C$ values. Soil profiles in the lowest raised beaches (P8 and P9) registered enriched $\delta^{13}C$ values associated with the MAOM fraction compared to the POM fraction in subsurface horizons. The $\delta^{13}C$ in the soils showed a similar ^{13}C enrichment pattern with depth.

The $\delta^{15}N$ values varied between -0.23 to 18.43‰, and the MAOM fraction is generally depleted in comparison to the POM fraction. The acid sulfate soil (P1) and a soil in the upper

platform (P3) have the richest $\delta^{15}N$ values. These soil profiles registered a depletion of $\delta^{15}N$ with depth. The content of N isotopes associated with the POM fraction of P5, P8, P9, P12, and P13 was below the detection limit.

The isotopic signature of the SOM indicated similarity with marine organic materials for most of the soil profiles on low platforms and the acid sulfated soil profile (P1, P2, P5, and P12 – Table S3) (Burkins et al., 2000). The $\delta^{15}N$ values of the two well-drained soils on raised beaches (P8 and P9) indicated ornithogenic organic materials. On the other hand, $\delta^{13}C$ supported the ornithogenic signature in the upper levels of raised beaches (P7 and P13) (Burkins et al., 2000; Liu et al., 2006). The high platforms showed isotopic signatures oscillating between marine and lacustrine-derived organic matter, except for P4, where $\delta^{13}C$ showed a signature associated with endolithic-derived organic matter.

3.2. Isotopic composition of plants

Considering all samples together (moss, lichen, and grass), the total organic carbon (TOC) and total nitrogen (TN) contents had high values of coefficient of variation (above 20%). The TOC content ranged between 31.91 and 408.90 mg g^{-1} of dried biomass (Table 2). The TN varied from 17.24 to 1.67 mg g^{-1} of dry biomass. The C/N ratio of plant biomass varied between 55.37 to lichen and 15.41 to grass. The plant materials showed a high range of $\delta^{13}C$, from -27.91 to -21.42‰, and from -11.05 to 31.66 ‰ in terms of the isotopic signature of $\delta^{15}N$. The $\delta^{13}C$ weighted mean of the SOM reflects the dominant vegetation type present in each sampling location, except for P3, P4, P9, and P11.

Table 2. Isotopic composition of the vegetable samples and C and N levels

Plants Samples	Type of materials	Profiles	C (%)	$\delta^{13}C$ (‰)	TN (%)	$\delta^{15}N$ (‰)	C/N Ratio
HG	Moss	P2	3.19	-25.01	0.17	-0.49	18.76
UA	Lichen	P3	40.89	-21.49	0.74	-11.05	55.25
SU	Moss	P4	13.13	-25.12	0.60	-2.28	21.88
SGU	Moss	P6	23.81	-25.04	1.43	7.41	16.65
BA	Moss	P7	19.73	-21.42	0.79	-0.79	24.97
WS	Moss	P7	28.09	-23.80	1.22	0.40	23.02
DA	Grass	P9	26.57	-27.91	1.72	31.66	15.44
PJ	Moss	P11	7.15	-27.17	0.35	-2.52	20.42
AG	Moss	P12	20.02	-23.95	0.99	-2.59	20.22

3.3. Organic C and N stocks in soils

The organic C stock varied between 5.1 and 109.2 Mg ha^{-1}; the organic N stock varied between 0.2 and 12.5 Mg ha^{-1}. The organic C and N stocks increased with increase of altitude in Byers Peninsula (Figure 3). The high platforms registered up to 3.5 and 8.3 higher organic C and N stocks compared to raised beaches.

In general, the MAOM provides the greatest contribution to the organic C and N stocks, varying between 60.2 and 82.1%, respectively. The POM fraction contributed up to 39.7 and 17.9% to organic C and N stocks in the soil profiles. The soils developed in the high and low platforms contribute to more than 80% of the organic C and N stocks in Byers Peninsula. The lowest organic C stock was observed in the acid-sulfated soil, contributing only 6.5% of the total organic stock. As for the N stocks, the smallest were observed among the raised beaches. These soils represent only 6.5% of the organic N stock in the Byers Peninsula.

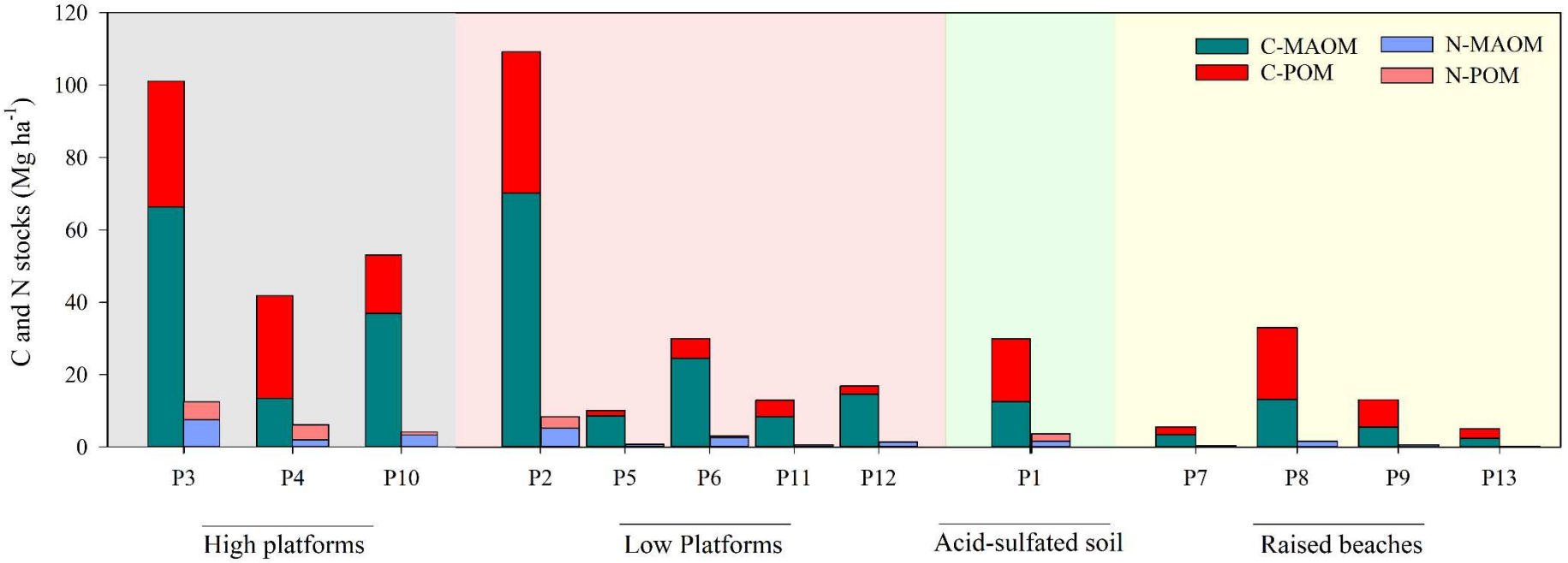

Figure 3. C and N stocks (Mg ha^{-1}) in the soil profiles studied. The full bar represents the total stock. The colors represent the C and N stocks in the fractions.

3.4. ^{14}C Age

All soil profiles are dated from Holocene (Table 3), except for a soil profile on the summit of a cliff on volcanic rock (P11) and another soil developed on platform on Cenozoic sedimentary rocks (P4). The oldest profile (P4) dates from before the Last Glacial Maximum, with 31,690 +/- 30 cal. yr BP, in a high platform developed on Cenozoic sedimentary rocks. The most recent ^{14}C soil corresponded to a pour-drainage soil on marine terrace level (P7), where this dates from 1,220 +/- 30 cal. yr BP.

Table 3. Age of dated horizons and additional information of soil profiles.

Profile	Profile feature	GPS Coordinates	Depth (cm)	Laboratory Number	$\delta^{13}C$ (‰)	Age ^{14}C (cal. yr BP)
P4	High platforms	62° 38' 22.9" S 61° 07' 28.7" W	20-35	Beta - 570240	-26.6	31,690 +/- 170
P11	High platforms/ Patterned-ground	62° 39' 12.4" S 61° 00' 15.1" W	60-80	Beta - 570244	-25.1	12,030 +/- 40
P3	High platforms/ Patterned-ground	62° 38' 13.6" S 61° 04' 56.3" W	10-70	Beta - 570239	-23.5	3,490 +/- 30
P6	High platforms	62° 38' 35.5" S 61° 03' 51" W	10-20	Beta - 570241	-22.0	3,290 +/- 30
P10	High platforms/ Patterned-ground	62° 38' 38.9" S 61° 04' 24.5" W	30-50	Beta - 570243	-23.6	2,350 +/- 30
P7	Raised beaches	62° 39' 21.4" S 61° 03' 25.4" W	0-10	Beta - 570242	-23.6	1,220 +/- 30

3.5. Statistical analysis

The first two principal components (PC) registered high eigenvalues (Figure 4a). The third PC and higher returned eigenvalues below 1.0 and hardly explain more variance than any of the original variables taken alone (1/31 = 3.22%), so they were excluded from further interpretation. The first component (PC1) explained 29.9% of the total variance and is mainly composed of original variables which express soil reactivity and isotopic fractionation of SOM, which are CEC, $\delta^{15}N$-POM, $\delta^{15}N$-MAOM, $\delta^{13}C$-POM, MAOM, clay, and sand contents (Figure 4b). The second component (PC2) explained 22.1% of the total variance of the data and is composed of original variables which express acidity and weathering, which are H+Al, pH, V,

and BS. The antagonism between δ^{15}N-MAOM and δ^{15}N-POM, clay, C, and N stocks expresses the difference between SOM-rich soils with marine-derived organic matter and poorly SOM soils with SOM derived from ornithic input. As the stocks in the POM and MAOM fractions, the organic C and N stocks showed a high affinity with the clay, silt, and P contents.

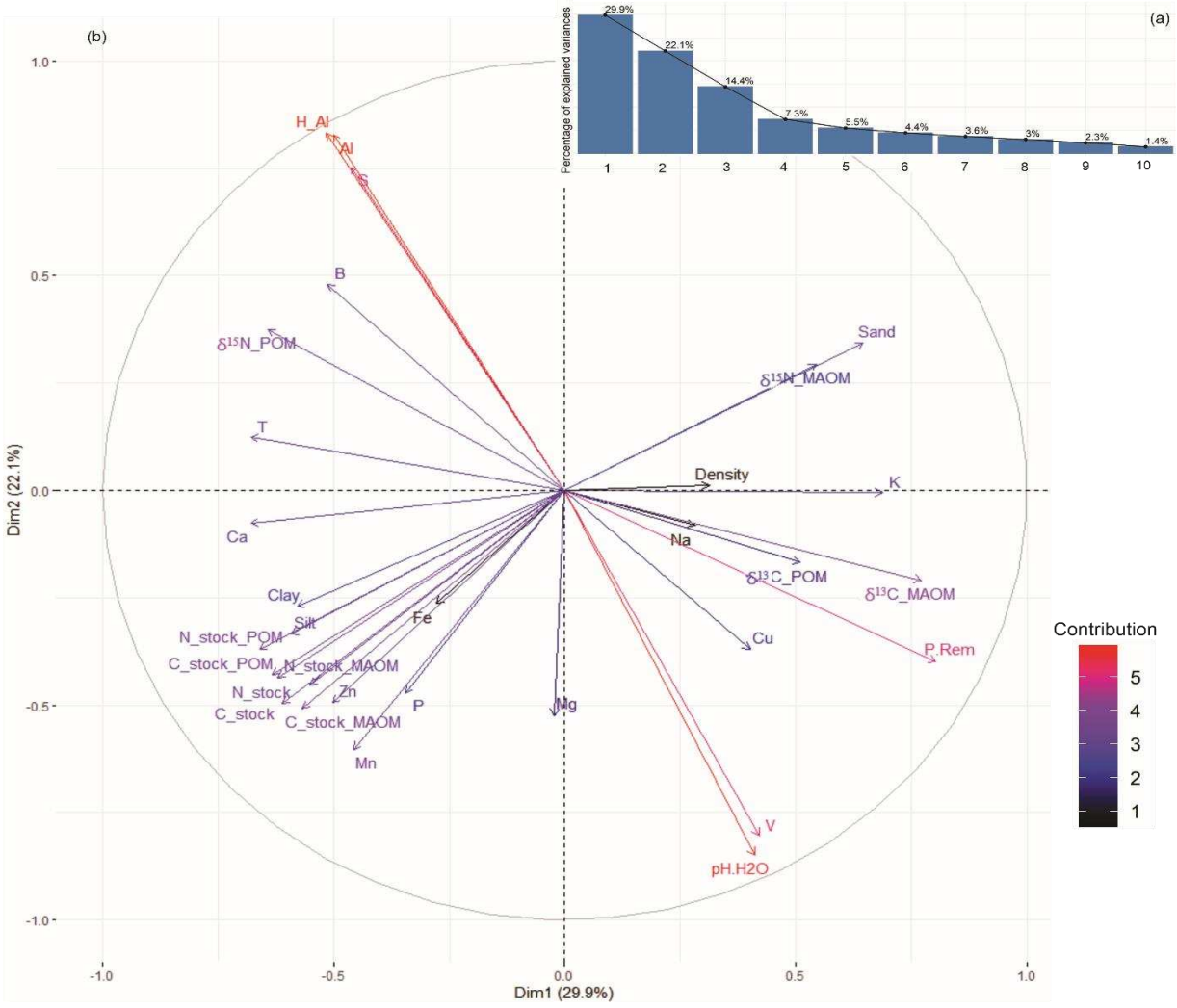

Figure 4. Eigenvalues of correlation matrix and explained variance per principal component (a). Soil properties distributed in PC1xPC2 plot (b).

4. Discussion

The low diversity of soil groups in Byers Peninsula reflects the dominance of periglacial processes (Ruiz-Fernández and Oliva, 2016). Discontinuous permafrost is registered in the first two meters in crioplanation surfaces and cliffs; Cryosol dominances in Byers Peninsula could be attributed to permafrost occurrence in the first 50 cm below the surface (Ferreira et al., 2017;

Hauck et al., 2007; Obu et al., 2020; Vieira et al., 2010). Gleysols, Leptosols, and Cambisols occupy degraded permafrost sites, once they also occur in high altitude. Arenosols occur in raised beaches uplifted by glacial retreat and glacioeustatic readjustment (Hall, 2010; Hall and Perry, 2004).

Low water availability and leaching induce limited weathering and pedogenesis. Consequently, the chemical and physical characteristics are determined mainly by parent material (Moura et al., 2012; Thomazini et al., 2020). In general, the soils in Byers Peninsula have a weak developed structure, lack B horizon and are shallow, skeletal, hypereutric and depleted in organic matter.

The similarity of organic C content among the Byers Peninsula and other sites in Maritime Antarctica (Carvalho et al., 2013; Francelino et al., 2011; Simas et al., 2008) indicates a climatic control of primary productivity. The intensification of glacial retreat, expansion of vegetation, and increased soil biological activity in ice-free areas increase C-CO_2 emissions (La Scala et al., 2010; Mendonça et al., 2011; Thomazini et al., 2020, 2016).

The increase in temperature in this polar environment contributes to greater mineralization of the organic compounds contributed to this system, including N mineralization, which favors an increase in the C/N ratio of the soil due to the scarcity of this element (Day et al., 2008).

For most of the horizons, the observed C/N ratio varied between 3.05 and 19.80, in both physical fractions of SOM, characterizing a high quality and high lability SOM. This range is recurrent in environments with bird and mammal contributions (Park and Day, 2007). The values observed in this study were low and with great oscillation between horizons of the same profile, even in areas where there was the presence of *Deschampsia antarctica*, where usually a range between 15 to 17 C/N ratio is reported because the deposition of *D. antarctica* or *Colobantus quitensis* residues (Day et al., 2008). Such characteristics reflect in the current C stocks in these soils. The weak structure and low clay content limit the efficiency of physicochemical processes of SOC stabilization. As net primary production is incipient in this environment and SOM is highly labile, they result in a disbalance between sequestration and emission of C (Doetterl et al., 2015b).

While the $\delta^{13}C$ values for most samples were similar, the $\delta^{15}N$ values allowed distinguishing soils with different SOM origins. The observed values of $\delta^{13}C$ show that the organic matter in the Byers Peninsula soils is mainly from Antarctic C_3 plants, deriving from lichens, lake algae, and mosses, with or without mixing of fresh Antarctic animal excrements (Liu et al., 2006). This result indicates a low contribution to the local SOM by the grass in Maritime

Antarctica, *Deschampsia antarctica*. However, it is challenging to use isolated $\delta^{13}C$ values for the identification of contributing sources of SOM in this environment due to the significant overlap of values found even in different materials, similar to observations made in a previous study when they tried to assess the influences of guano as an isolated source of contribution for SOM (Liu et al., 2006).

The use of $\delta^{15}N$ as a primary tracer for identifying organic matter sources is not commonly used, mainly due to the complexities of the N cycle. Several simultaneous abiotic and biotic processes influence N isotopic fractionation in most terrestrial ecosystems (Burkins et al., 2000). Consequently, the application of $\delta^{15}N$ as a primary tracer for determining soil organic origin is generally limited. However, previous studies registered a contrast $\delta^{15}N$ for high altitude soils, related to endolithic autotrophs, and lower altitudes, which signals indicated lacustrine organisms (Barrett et al., 2006; Burkins et al., 2000). In the present study, the signature pattern for Byers Peninsula was contrasting; while most soils on low platforms showed a signature of marine origin, the raised beaches showed isotopic signals suggesting ornithogenic organic matter, consistent with the colonization of penguins from these areas.

The high platform presented uncertain isotopic composition, with $\delta^{13}C$ and $\delta^{15}N$ values varying between the signature of organic material of lacustrine or marine origin. The marine origin is discarded once paleolimnological and geomorphological evidence in lakes indicate the timing of the onset of the deglaciation of the Byers Peninsula is 7.5 cal. kyr BP (Oliva et al., 2016). The enriched $\delta^{15}N$ is attributed to hygrophilous vegetation (França et al., 2015; Minick et al., 2019), covering soils saturated by water from snowmelt, active layer thaw during summer, and permafrost degradation (Carvalho et al., 2013; Hopkins et al., 2009).

The use of isolated isotopic signatures, such as $\delta^{13}C$ and $\delta^{15}N$, to identify SOM sources in Antarctic soils still needs further investigation to distinguish between the isotopic signatures of their different materials and sources of MOS in the Antarctic environment. However, using $\delta^{15}N$, $\delta^{13}C$, and bioelements can help envision changes in the composition and constitution of SOM over time (Liu et al., 2006).

4.1 Pre-LGM SOC

The P4 profile, developed in the high platform, is the oldest soil profile, with C dating from the pre-LGM period. This soil recorded a different $\delta^{13}C$ between SOM and vegetation cover. Although mosses cover soil, the endolithic signature of SOM indicates that this soil was formed through interactions between minerals, cryptogamic and microbial photoautotrophs and without higher plant organisms (vascular plants) for the production of SOM in this environment.

The previous oldest record of C dating in the Byers Peninsula, 8.3 cal. kyr BP (Toro et al., 2013), was surpassed by the value found in P4. Located on the Ray Promontory, on rocky crests at the western extremity of the Byers Peninsula, this profile was dated ~32 cal. kyr BP. The glacial retreat after 35 cal. kyr BP (Hillenbrand et al., 2010) exposed newly ice-free hard bottom areas available for colonization. Archaea, bacteria, and viruses can tolerate environmental extremes and colonize fresh rock in the first stage of soil formation (Mergelov et al., 2018). Freezing-thawing cycles, frost dehydration, and hydraulic pressure create frost-shattered rock fragments, which favored endolithic niche colonization in depth. Endolithic organisms accelerate weathering of primary minerals and incorporate organic carbon compounds, such as melanin, sporopollenin-like substances, aliphatic and aromatic OC, and various biopolymers (Mergelov et al., 2018; Saiz-Jimenez, 1995). These compounds are highly resistant to oxidation and persist over time in soil. This first pre-LGM SOC record can indicate the initial modern colonization of Maritime Antarctica and suggests that ice caps advance during LGM was limited (Simms et al., 2011).

The endolithic origin of SOM is described as limited to sites colonized by lichens and far from sources of liquid water or where lacustrine productivity is low (Faucher et al., 2017; Hopkins et al., 2009). In the present study, the profile has a water layer at depth, and mosses mainly cover the surface of the area. Thus, soils that present an endolithic isotopic signature associated with SOM may present subsurface water or even a high primary production, as long as they are polygenetic and the contribution time of the current vegetation is not sufficient to alter the older C and N isotopic signature.

4.2 Post-LGM SOC

Warm phases between 17-14 cal. kyr BP and 11-10 cal. kyr BP initiated deglaciation of some inner shelf areas and a few outer coastal lands (Simms et al., 2011). Lichen and moss colonized volcanic plugs exhumed by ice thinning and glacial retreat. The C and N stocks in the soils developed on plugs are limited by erosion. Lithic contact proximity to the surface and gravel content suggest frequent erosion favored by altitude and slope.

The highest C and N stocks in upper platforms suggest a climatic optimum between 4-3 cal. kyr BP (Ingólfsson et al., 1998b). These mild and humid conditions favor high primary activity and clay formation in Maritime Antarctica. Most of the C stored in these profiles is due to primary production by the local vegetation present in the area; the UA lichen, very abundant, has 40.89% of C, whereas AG and SU mosses account for 13.13 and 20.02% of C, respectively. The higher organic C stock in Late Holocene soils corroborates with the results of previous studies, who also observed higher contents of TOC and NT in areas with more significant

colonization by lichens and mosses (Cannone et al., 2008; Otero et al., 2013). Among the low platforms, P2 showed the highest organic C and N stocks. Most of the C stored in these profiles is associated with the mineral fraction of the soil, indicating its physical protection

During this warm phase, the weathering of mafic rocks formed clay soils, which physically protected soil organic matter against degradation. The organo-mineral association has received increasing attention for its persistence in terrestrial ecosystems (Almeida et al., 2018; Kleber et al., 2015), resulting in considerable C stocks in Antarctic soils. In the present study, organic C and N stocks were great, mainly in patterned ground soils, associated with higher altitudes in the landscape of the Byers Peninsula, with more than 80% of C associated with the MAOM fraction. This result is attributed to cryoturbation and slow upward/downward movements. Cryoturbation is a typical process in cryogenic soils of Maritime Antarctica (Michel et al., 2014; Ping et al., 2015), and it is primarily responsible for the distribution of SOM within soil (Tarnocai et al., 2009). It is the mixing of materials from different horizons and soil layers down to bedrock due to freezing and thawing. Cryoturbation commonly creates SOM-rich pockets into mineral horizons, including the top of permafrost. Gross C and N mineralization rates were substantially lower in these buried pockets due to low and, for most of the year, subzero soil temperatures and frequent waterlogging during the short unfrozen period (Kaiser et al., 2007; Schnecker et al., 2014). In addition, the turnover of C present in organo-mineral associations is much longer than that of C associated with POM, free or occluded OM, ranging from decades to millennia (Kleber et al., 2015), helping to explain the permanence of C in these soils, despite the low input at present. Cryoturbation process is more effective in medium texture soils than clay soils. As well in the studied sites, sandy and loam soils exhibit weak cohesion and a high propensity to mix soil horizons and SOC enrichment in deep horizons (Palmtag and Kuhry, 2018).

The second mechanism which influences SOM distribution and preservation is clay and clay minerals migration through soil due to the movement of solution in the pores to the freezing front. Fibrous or partially decomposed organic matter accumulation on top of the permafrost table is observed widely in soils with shallow permafrost under both tundra and forest vegetation (Bockheim and Tarnocai, 1998). The temperatures above the freezing water point during spring and summer favor organo-mineral compounds migration down the soil profile. The illuviation of these clay particle follows freezing gradient and accumulate above the permafrost table. On the other hand, the low air temperatures in the fall and winter seasons induce an ascending water migration which flows from permafrost to the dried seasonally freezing layer. Due to the seasonal thawing–freezing cycles and the drastic differences in the mechanical and thermophysical properties of its raw organic material and mineral soil, a complicated swirl (vortex) pattern of cryoturbation in the soil profile could be formed.

Desiccation crack networks and the lateral sliding of soil aggregates along melting ice lenses increase fine particles and TOC contents in-depth (Oliva and Ruiz-Fernández, 2015; Simas et al., 2008; Thomazini et al., 2020). Repetitive freeze-thaw cycles induce internal particle translocation and some plastic deformation of fine organic particles, which can adhere and accumulate to the face of aggregates (Van Vliet-Lanoë and Fox, 2018). This physicochemical process reduces the accessibility of microorganisms to SOM and reduces its decomposition (Diochon et al., 2013; Ping et al., 2015).

The third mechanism is descending migration of OM in the soil profiles. It is related to the cryogenic mass exchange and, particularly, to cryoturbation manifesting itself in the transport of organic matter in a dissolved state, and its precipitation and deposition above the permafrost table (Zubrzycki et al., 2014). Low mobile humus can accumulate in these conditions due to the very low temperatures and low decay rates (Lupachev et al., 2017; Mcguire et al., 2009). The migration in the fall and winter seasons mainly occurs in the opposite direction together with ascending water flows to the dried seasonally freezing layer.

After the climate optimum, a distinct climate cooling occurred with glacier advance and soil erosion (Björck et al., 1996b). A warmer phase at 1.5 cal. ky BP briefly interrupts the arid climate and promotes a new colonization phase (Björck et al., 1993) registered in the raised beaches. The raised beaches register the last warm phase due to the coarser sandy texture of these soils, reducing the organo-mineral interaction, resulting in SOM migration in-depth (Dieckow et al., 2009; Plante et al., 2006). Besides, the strong winds, high salinity of these soils, and trampling and crawling of animals in these areas difficult colonization of raised beaches (Vera, 2011). Consequently, the SOM is constantly eroded or degraded, and C and N stocks are still low.

The time of deglaciation and geomorphic implications resulting from this process are restricted to ice-free environments in Antarctica Maritima, of which Byers Peninsula is a notable example (Oliva et al., 2016). The data register advance and retreat of the local glaciers, indicating different episodes of C accumulation in soils. This information is relevant to understanding the landscape evolution better.

The Holocene paleoclimatic history of the South Shetland Islands is controversial and incomplete, and continued research is necessary. The first record of pre-LGM SOC in the Byers Peninsula adds an urgent need to improve the geochronology of this area and assist in interpreting the paleoenvironmental stages experienced, not only in Maritime Antarctica but also in the Peninsular Antarctica and the Weddell Sea sectors. Future studies with higher sample size should be executed to perform more robust statistical analysis. A higher number of samples in the same geomorphological and pedological contexts could clarify the SOC stock diversity into same soil group and identify a typical isotopic signal for each age group.

5. Conclusion

1. Mosses and lichens are the organisms that most contribute the C and N (primary source) to SOM on the Byers Peninsula. The high diversity of SOM contents reflects an occupation of these organisms driven by glacier retreat and permafrost degradation. The similar SOM content among Byers and sites where deglaciation is recent suggests a climatic control of organic C and N stocks in Antarctica.

2. Cryoturbation is an important mechanism for SOM stabilization by favoring organo-mineral interactions. The MAOM fraction in turbic soils increases up to four times the organic C and N stocks in subsurface horizons than in horizons of soils not undergoing cryoturbation. Among the profiles subjected to cryoturbation, the oldest (P11) has the lowest C-MAOM contents, this indicates that in the long term, this mechanism may undergo changes allowing degradation of this more stable SOM. Thus, future studies should explore the persistence of SOM preservation mechanisms by cryoturbation and their implications on long-term organic C and N stocks in this environment.

3. Isotopic C and N signatures identified three sources of SOM: i) a Pre-LGM endolithic-derived organic matter. It registers the initial colonization of the Maritime Antarctica in ancient deglaciation - the first recorded in Maritime Antarctica to this day; b) a Holocene marine/lacustrine-derived organic matter on low and high platforms. Chronology and topography of these areas suggest that the Holocene degradation of permafrost favors hydrophilic vegetation occupation, and; c) a limited ornithic contribution in sandy soils on raised beaches. The persistence of the ornithic signal in the highest raised beaches indicates the Byers Peninsula as one of the first bird-occupied areas in the Maritime Antarctica.

4. Pre-LGM soils formed on rocky crests are proxies of pre-Holocene environments. Subaerial endolithic SOM in upper platforms that we report in this study have a great potential to provide insights into early principles of organo-mineral interactions and soil production from hard rocks in Antarctica.

Acknowledgments

We thank the CNPq (Conselho Nacional de Desenvolvimento Científico e Tecnológico), CAPES (Coordenação de Aperfeiçoamento de Pessoal de Nível Superior) and FAPEMIG (Fundação de Amparo à Pesquisa do Estado de Minas Gerais) for financial support. We are grateful to INCT da Criosfera, TERRANTAR and MARINHA DO BRASIL (PROANTAR PROGRAM) for financial

support and field assistance. We thank the reviewers for their careful reading of the manuscript and their constructive remarks.

SUPPLEMENTARY DATA IN THE APENDIX A

Bibliographic references

Adams, B., Arthern, R., Atkinson, A., Barbante, C., Bargagli, R., Bergstrom, D., Bertler, N.A.N., Bindschadler, R., Bockheim, J., Boutron, C., Bromwich, D., Chown, S., Comiso, J., Convey, P., Cook, A., Prisco, G. Di, Fahrbach, E., Fastook, J., Forcada, J., Gili, J.-M., Gugliemin, M., Gutt, J., Hellmer, H., Hennion, F., Heywood, K.J., Hodgson, D., Holland, D., Hong, S., Huiskes, A., Isla, E., Jacobs, S., Jones, A., Lenton, A., Marshall, G., Mayewski, P., Meredith, M., Metzl, N., Monaghan, A., Garabato, A.C.N., Newsham, K., Orejas, C., Peck, L., Pörtner, H.-O., Rintoul, S., Robinson, S., Roscoe, H., Rossi, S., Scambos, T., Shanklin, J., Smetacek, V., Speer, K., Stevens, M., Summerhayes, C., Trathan, P., Turner, J., Veen, K. van Der, Vaughan, D., Verde, C., Webb, D., Wiencke, C., Dworth, P.W., Worby, T., Worland, R., Yamanouchi, T., 2009. The instrumental period. Antarct. Clim. Chang. Environ. 1–32.

Alfaro, P., López-Martínez, J., Maestro, A., Galindo-Zaldívar, J., Durán-Valsero, J.J., Cuchí, J.A., 2010. Recent tectonic and morphostructural evolution of Byers Peninsula (Antarctica): insight into the development of the South Shetland Islands and Bransfield Basin. J. Iber. Geol. 36, 21.

Almeida, L.F.J., Hurtarte, L.C.C., Souza, I.F., Soares, E.M.B., Vergütz, L., Silva, I.R., 2018. Soil organic matter formation as affected by eucalypt litter biochemistry — Evidence from an incubation study. Geoderma 312, 121–129. https://doi.org/10.1016/J.GEODERMA.2017.10.004

Amesbury, M.J., Roland, T.P., Royles, J., Hodgson, D.A., Convey, P., Griffiths, H., Charman, D.J., 2017. Widespread Biological Response to Rapid Warming on the Antarctic Peninsula. Curr. Biol. 27, 1616-1622.e2. https://doi.org/10.1016/J.CUB.2017.04.034

Balks, M.R., López-Martínez, J., Goryachkin, S. V., Mergelov, N.S., Schaefer, C.E.G.R., Simas, F.N.B., Almond, P.C., Claridge, G.G.C., Mcleod, M., Scarrow, J., 2013. Windows on Antarctic soil–landscape relationships: comparison across selected regions of Antarctica. Geol. Soc. London, Spec. Publ. 381, 397–410. https://doi.org/10.1144/SP381.9

Bañón, M., Justel, A., Velázquez, D., Quesada, A., 2013. Regional weather survey on Byers Peninsula, Livingston Island, South Shetland Islands, Antarctica. Antarct. Sci. 25, 146–156. https://doi.org/10.1017/S0954102012001046

Barrett, J.E., Virginia, R.A., Wall, D.H., Cary, S.C., Adams, B.J., Hacker, A.L., Aislabie, J.M., 2006. Co-variation in soil biodiversity and biogeochemistry in northern and southern Victoria Land,

Antarctica. Antarct. Sci. 18, 535–548. https://doi.org/10.1017/S0954102006000587

Benayas, J., Pertierra, L., Tejedo, P., Lara, F., Bermudez, O., Hughes, K.A., Quesada, A., 2013. A review of scientific research trends within ASPA No. 126 Byers Peninsula, South Shetland Islands, Antarctica. Antarct. Sci. 25, 128–145. https://doi.org/10.1017/S0954102012001058

Beyer, L., 2000. Properties, formation, and geo-ecological significance of organic soils in the coastal region of East Antarctica (Wilkes Land). CATENA 39, 79–93. https://doi.org/10.1016/S0341-8162(99)00090-9

Beyer, L., Pingpank, K., Wriedt, G., Bölter, M., 2000. Soil formation in coastal continental Antarctica (Wilkes Land). Geoderma 95, 283–304. https://doi.org/10.1016/S0016-7061(99)00095-6

Beyer, L., White, D.M., Pingpank, K., Bölter, M., 2004. Composition and Transformation of Soil Organic Matter in Cryosols and Gelic Histosols in Coastal Eastern Antarctica (Casey Station, Wilkes Land). Cryosols 525–556. https://doi.org/10.1007/978-3-662-06429-0_26

Björck, S., Håkansson, H., Olsson, S., Barnekow, L., Janssens, J., 1993. Palaeoclimatic studies in South Shetland Islands, Antarctica, based on numerous stratigraphic variables in lake sediments. J. Paleolimnol. 8, 233–272. https://doi.org/10.1007/BF00177858

Björck, S., Hjort, C., Ingólfsson, Ó., Zale, R., Ising, J., 1996a. Holocene deglaciation chronology from lake sediments, in: Geomorphological Map of Byers Peninsula, Livingston Island. British Antarctic Survey Cambridge, pp. 49–51.

Björck, S., Olsson, S., Ellis-Evans, C., Håkansson, H., Humlum, O., De Lirio, J.M., 1996b. Late holocene palaeoclimatic records from lake sediments on James Ross Island, Antarctica. Palaeogeogr. Palaeoclimatol. Palaeoecol. 121, 195–220. https://doi.org/10.1016/0031-0182(95)00086-0

Bockheim, J.., Tarnocai, C., 1998. Recognition of cryoturbation for classifying permafrost-affected soils. Geoderma 81, 281–293. https://doi.org/10.1016/S0016-7061(97)00115-8

Bockheim, J., Vieira, G., Ramos, M., López-Martínez, J., Serrano, E., Guglielmin, M., Wilhelm, K., Nieuwendam, A., 2013. Climate warming and permafrost dynamics in the Antarctic Peninsula region. Glob. Planet. Change 100, 215–223. https://doi.org/10.1016/J.GLOPLACHA.2012.10.018

Bockheim, J.G., Gennadiyev, A.N., 2000. The role of soil-forming processes in the definition of taxa in Soil Taxonomy and the World Soil Reference Base. Geoderma 95, 53–72. https://doi.org/10.1016/S0016-7061(99)00083-X

Bockheim, J.G., Haus, N.W., 2014. Distribution of Organic Carbon in the Soils of Antarctica, in: Soil Carbon. Springer International Publishing, Cham, pp. 373–380. https://doi.org/10.1007/978-3-319-04084-4_37

Boy, J., Godoy, R., Shibistova, O., Boy, D., McCulloch, R., De La Fuente, A.A., Morales, M.A., Mikutta, R., Guggenberger, G., 2016. Successional patterns along soil development gradients formed by

glacier retreat in the Maritime Antarctic, King George Island. Rev. Chil. Hist. Nat. 89, 1–17. https://doi.org/10.1186/S40693-016-0056-8/FIGURES/9

Burkins, M.B., Virginia, R.A., Page Chamberlain, C., Wall, D.H., 2000. ORIGIN AND DISTRIBUTION OF SOIL ORGANIC MATTER IN TAYLOR VALLEY, ANTARCTICA. Ecology 81, 2377–2391. https://doi.org/10.1890/0012-9658

Cambardella, C.A., Elliott, E.T., 1992. Particulate Soil Organic-Matter Changes across a Grassland Cultivation Sequence. Soil Sci. Soc. Am. J. 56, 777. https://doi.org/10.2136/sssaj1992.03615995005600030017x

Cannone, N., Binelli, G., Worland, M.R., Convey, P., Guglielmin, M., 2012. CO2 fluxes among different vegetation types during the growing season in Marguerite Bay (Antarctic Peninsula). Geoderma 189–190, 595–605. https://doi.org/10.1016/J.GEODERMA.2012.06.026

Cannone, N., Ellis Evans, J.C., Strachan, R., Guglielmin, M., 2006. Interactions between climate, vegetation and the active layer in soils at two Maritime Antarctic sites. Antarct. Sci. 18, 323–333. https://doi.org/10.1017/S095410200600037X

Cannone, N., Wagner, D., Hubberten, H.W., Guglielmin, M., 2008. Biotic and abiotic factors influencing soil properties across a latitudinal gradient in Victoria Land, Antarctica. Geoderma 144, 50–65. https://doi.org/10.1016/j.geoderma.2007.10.008

Carvalho, J.V.D.S., Mendonça, E.D.S., La Scala, N., Reis, C., Reis, E.L., Schaefer, C.E.G.R., 2013. CO 2 -C losses and carbon quality of selected Maritime Antarctic soils. Antarct. Sci. 25, 11–18. https://doi.org/10.1017/S0954102012000648

Cary, S.C., McDonald, I.R., Barrett, J.E., Cowan, D.A., 2010. On the rocks: the microbiology of Antarctic Dry Valley soils. Nat. Rev. Microbiol. 2010 82 8, 129–138. https://doi.org/10.1038/nrmicro2281

Charman, D.J., Amesbury, M.J., Roland, T.P., Royles, J., Hodgson, D.A., Convey, P., Griffiths, H., 2018. Spatially coherent late Holocene Antarctic Peninsula surface air temperature variability. Geology 46, 1071–1074. https://doi.org/10.1130/G45347.1

Claridge, G.G.C., Campbell, I.B., Sheppard, D.S., 2000. Carbon Pools in Antarctica and Their Significance for Global Climate Change, in: Global Climate Change and Cold Regions Ecosystems. CRC Press, pp. 71–90. https://doi.org/10.1201/9781482278637-12

Convey, P., Hopkins, D.W., Roberts, S.J., Tyler, A.N., 2011. Global southern limit of flowering plants and moss peat accumulation. Open Acad. 30. https://doi.org/10.3402/POLAR.V30I0.8929

Cook, A.J., Fox, A.J., Vaughan, D.G., Ferrigno, J.G., 2005. Retreating glacier fronts on the Antarctic Peninsula over the past half-century. Science (80-.). 308, 541–544. https://doi.org/10.1126/SCIENCE.1104235/SUPPL_FILE/COOK.SOM.PDF

Day, T.A., Ruhland, C.T., Xiong, F.S., 2008. Warming increases aboveground plant biomass and C stocks in vascular-plant-dominated Antarctic tundra. Glob. Chang. Biol. 14, 1827–1843. https://doi.org/10.1111/J.1365-2486.2008.01623.X

Díaz-Puente, F.J., Schmid, T., Pelayo, M., Rodríguez-Rastrero, M., Herraiz, M.J.S., O'Neill, T., López-Martínez, J., 2021. Abiotic factors influencing soil microbial activity in the northern Antarctic Peninsula region. Sci. Total Environ. 750, 141602. https://doi.org/10.1016/j.scitotenv.2020.141602

Dieckow, J., Bayer, C., Conceição, P.C., Zanatta, J.A., Martin-Neto, L., Milori, D.B.M., Salton, J.C., MacEdo, M.M., Mielniczuk, J., Hernani, L.C., 2009. Land use, tillage, texture and organic matter stock and composition in tropical and subtropical Brazilian soils. Eur. J. Soil Sci. 60, 240–249. https://doi.org/10.1111/J.1365-2389.2008.01101.X

Diochon, A., Gregorich, E.G., Tarnocai, C., 2013. Evaluating the quantity and biodegradability of soil organic matter in some Canadian Turbic Cryosols. Geoderma 202–203, 82–87. https://doi.org/10.1016/J.GEODERMA.2013.03.013

Doetterl, S., Stevens, A., Six, J., Merckx, R., Van Oost, K., Casanova Pinto, M., Casanova-Katny, A., Muñoz, C., Boudin, M., Zagal Venegas, E., Boeckx, P., 2015a. Soil carbon storage controlled by interactions between geochemistry and climate. Nat. Geosci. 2015 810 8, 780–783. https://doi.org/10.1038/ngeo2516

Doetterl, S., Stevens, A., Six, J., Merckx, R., Van Oost, K., Casanova Pinto, M., Casanova-Katny, A., Muñoz, C., Boudin, M., Zagal Venegas, E., Boeckx, P., 2015b. Soil carbon storage controlled by interactions between geochemistry and climate. Nat. Geosci. 8, 780–783. https://doi.org/10.1038/ngeo2516

Emslie, S.D., Romero, M., Juáres, M.A., Argota, M.R., 2020. Holocene occupation history of pygoscelid penguins at Stranger Point, King George (25 de Mayo) Island, northern Antarctic Peninsula. The Holocene 30, 190–196. https://doi.org/10.1177/0959683619875814

Faucher, B., Lacelle, D., Davila, A., Pollard, W., Fisher, D., McKay, C.P., 2017. Physicochemical and Biological Controls on Carbon and Nitrogen in Permafrost from an Ultraxerous Environment, McMurdo Dry Valleys of Antarctica. J. Geophys. Res. Biogeosciences 122, 2593–2604. https://doi.org/10.1002/2017JG004006

Ferreira, A., Vieira, G., Ramos, M., Nieuwendam, A., 2017. Ground temperature and permafrost distribution in Hurd Peninsula (Livingston Island, Maritime Antarctic): An assessment using freezing indexes and TTOP modelling. Catena 149, 560–571. https://doi.org/10.1016/J.CATENA.2016.08.027

Fitzpatrick, E.A., 1984. Micromorphology of Soils. Micromorphol. Soils. https://doi.org/10.1007/978-94-009-5544-8

França, M.C., Alves, I.C.C., Castro, D.F., Cohen, M.C.L., Rossetti, D.F., Pessenda, L.C.R., Lorente, F.L.,

Fontes, N.A., Junior, A.Á.B., Giannini, P.C.F., Francisquini, M.I., 2015. A multi-proxy evidence for the transition from estuarine mangroves to deltaic freshwater marshes, Southeastern Brazil, due to climatic and sea-level changes during the late Holocene. Catena 128, 155–166. https://doi.org/10.1016/j.catena.2015.02.005

Francelino, M.R., Schaefer, C.E.G.R., Simas, F.N.B., Filho, E.I.F., de Souza, J.J.L.L., da Costa, L.M., 2011. Geomorphology and soils distribution under paraglacial conditions in an ice-free area of Admiralty Bay, King George Island, Antarctica. CATENA 85, 194–204. https://doi.org/10.1016/J.CATENA.2010.12.007

Gatto, A., Barros, N.F. de, Novais, R.F., Silva, I.R., Mendonça, E. de S., Villani, E.M. de A., 2009. Comparaçao de métodos de determinação do carbono orgânico em solos cultivados com eucalipto. Rev. Bras. Ciência do Solo 33, 735–740. https://doi.org/10.1590/S0100-06832009000300026

Hall, B.L., 2010. Holocene relative sea-level changes and ice fluctuations in the South Shetland Islands. Glob. Planet. Change 74, 15–26. https://doi.org/10.1016/J.GLOPLACHA.2010.07.007

Hall, B.L., Perry, E.R., 2004. Variations in ice rafted detritus on beaches in the South Shetland Islands: a possible climate proxy. Antarct. Sci. 16, 339–344. https://doi.org/10.1017/S0954102004002147

Hauck, C., Vieira, G., Gruber, S., Blanco, J., Ramos, M., 2007. Geophysical identification of permafrost in Livingston Island, maritime Antarctica. J. Geophys. Res. Earth Surf. 112, 2–19. https://doi.org/10.1029/2006JF000544

Hillenbrand, C.-D., Larter, R.D., Dowdeswell, J.A., Ehrmann, W., Ó Cofaigh, C., Benetti, S., Graham, A.G.C., Grobe, H., 2010. The sedimentary legacy of a palaeo-ice stream on the shelf of the southern Bellingshausen Sea: Clues to West Antarctic glacial history during the Late Quaternary. Quat. Sci. Rev. 29, 2741–2763. https://doi.org/10.1016/j.quascirev.2010.06.028

Hobbs, G., 1968. The geology of the South Shetland Islands: IV. The geology of Livingston Island. Br. Antarct. Surv. Sci. Reports 47, 34.

Hodgson, D.A., Graham, A.G.C., Roberts, S.J., Bentley, M.J., Cofaigh, C.Ó., Verleyen, E., Vyverman, W., Jomelli, V., Favier, V., Brunstein, D., Verfaillie, D., Colhoun, E.A., Saunders, K.M., Selkirk, P.M., Mackintosh, A., Hedding, D.W., Nel, W., Hall, K., McGlone, M.S., Van der Putten, N., Dickens, W.A., Smith, J.A., 2014. Terrestrial and submarine evidence for the extent and timing of the Last Glacial Maximum and the onset of deglaciation on the maritime-Antarctic and sub-Antarctic islands. Quat. Sci. Rev. 100, 137–158. https://doi.org/10.1016/j.quascirev.2013.12.001

Hogg, A.G., Hua, Q., Blackwell, P.G., Niu, M., Buck, C.E., Guilderson, T.P., Heaton, T.J., Palmer, J.G., Reimer, P.J., Reimer, R.W., Turney, C.S.M., Zimmerman, S.R.H., 2013. SHCal13 Southern Hemisphere Calibration, 0–50,000 Years cal BP. Radiocarbon 55, 1889–1903. https://doi.org/10.2458/AZU_JS_RC.55.16783

Hopkins, D.W., Sparrow, A.D., Gregorich, E.G., Elberling, B., Novis, P., Fraser, F., Scrimgeour, C.,

Dennis, P.G., Meier-Augenstein, W., Greenfield, L.G., 2009. Isotopic evidence for the provenance and turnover of organic carbon by soil microorganisms in the Antarctic dry valleys. Environ. Microbiol. 11, 597–608. https://doi.org/10.1111/j.1462-2920.2008.01830.x

Ingólfsson, Ó., Hjort, C., Berkman, P.A., Björck, S., Colhoun, E., Goodwin, I.D., Hall, B., Hirakawa, K., Melles, M., Möller, P., Prentice, M.L., 1998a. Antarctic glacial history since the Last Glacial Maximum: an overview of the record on land. Antarct. Sci. 10, 326–344. https://doi.org/10.1017/S095410209800039X

Ingólfsson, Ó., Hjort, C., Berkman, P.A., Björck, S., Colhoun, E., Goodwin, I.D., Hall, B., Hirakawa, K., Melles, M., Möller, P., Prentice, M.L., 1998b. Antarctic glacial history since the Last Glacial Maximum: an overview of the record on land. Antarct. Sci. 10, 326–344. https://doi.org/10.1017/S095410209800039X

Ingólfsson, Ó., Hjort, C., Humlum, O., 2003. Glacial and Climate History of the Antarctic Peninsula since the Last Glacial Maximum. Arctic, Antarct. Alp. Res. 35, 175–186. https://doi.org/10.1657/1523-0430(2003)035[0175:GACHOT]2.0.CO;2

IPCC, 2014. Climate Change 2013 - The Physical Science Basis. Cambridge University Press, Cambridge. https://doi.org/10.1017/CBO9781107415324

Kaiser, C., Meyer, H., Biasi, C., Rusalimova, O., Barsukov, P., Richter, A., 2007. Conservation of soil organic matter through cryoturbation in arctic soils in Siberia. J. Geophys. Res. 112, G02017. https://doi.org/10.1029/2006JG000258

Kennedy, A.D., 1995. Antarctic terrestrial ecosystem response to global environmental change. Annu. Rev. Ecol. Syst. 26, 683–704. https://doi.org/10.1146/ANNUREV.ES.26.110195.003343

Kleber, M., Eusterhues, K., Keiluweit, M., Mikutta, C., Mikutta, R., Nico, P.S., 2015. Mineral–Organic Associations: Formation, Properties, and Relevance in Soil Environments, in: Advances in Agronomy. Elsevier Ltd, pp. 1–140. https://doi.org/10.1016/bs.agron.2014.10.005

La Scala, N., de Sá Mendonça, E., Vanir de Souza, J., Panosso, A.R., Simas, F.N.B., Schaefer, C.E.G.R., 2010. Spatial and temporal variability in soil CO2–C emissions and relation to soil temperature at King George Island, maritime Antarctica. Polar Sci. 4, 479–487. https://doi.org/10.1016/J.POLAR.2010.07.001

Liu, X.-D., Li, H.-C., Sun, L.-G., Yin, X.-B., Zhao, S.-P., Wang, Y.-H., 2006. δ13C and δ15N in the ornithogenic sediments from the Antarctic maritime as palaeoecological proxies during the past 2000 yr. Earth Planet. Sci. Lett. 243, 424–438. https://doi.org/10.1016/j.epsl.2006.01.018

Liu, X., Sun, L., Xie, Z., Yin, X., Wang, Y., 2005. A 1300-year record of penguin populations at Ardley Island in the Antarctic, as deduced from the geochemical data in the ornithogenic lake sediments. Arctic, Antarct. Alp. Res. 37, 490–498. https://doi.org/10.1657/1523-0430(2005)037[0490:AYROPP]2.0.CO;2

Lupachev, A., Abakumov, E., Gubin, S., 2017. The Influence of Cryogenic Mass Exchange on the Composition and Stabilization Rate of Soil Organic Matter in Cryosols of the Kolyma Lowland (North Yakutia, Russia). Geosci. 2017, Vol. 7, Page 24 7, 24. https://doi.org/10.3390/GEOSCIENCES7020024

Mcguire, A.D., Anderson, L.G., Christensen, T.R., Scott, D., Laodong, G., Hayes, D.J., Martin, H., Lorenson, T.D., Macdonald, R.W., Nigel, R., 2009. Sensitivity of the carbon cycle in the Arctic to climate change. Ecol. Monogr. 79, 523–555. https://doi.org/10.1890/08-2025.1

Mendonça, E. de S., La Scala, N., Panosso, A.R., Simas, F.N.B., Schaefer, C.E.G.R., 2011. Spatial variability models of CO 2 emissions from soils colonized by grass (Deschampsia antarctica) and moss (Sanionia uncinata) in Admiralty Bay, King George Island. Antarct. Sci. 23, 27–33. https://doi.org/10.1017/S0954102010000581

Mergelov, N., Mueller, C.W., Prater, I., Shorkunov, I., Dolgikh, A., Zazovskaya, E., Shishkov, V., Krupskaya, V., Abrosimov, K., Cherkinsky, A., Goryachkin, S., 2018. Alteration of rocks by endolithic organisms is one of the pathways for the beginning of soils on Earth. Sci. Rep. 8, 3367. https://doi.org/10.1038/s41598-018-21682-6

Michel, R.F.M., Schaefer, C.E.G.R., López-Martínez, J., Simas, F.N.B., Haus, N.W., Serrano, E., Bockheim, J.G., 2014. Soils and landforms from Fildes Peninsula and Ardley Island, Maritime Antarctica. Geomorphology 225, 76–86. https://doi.org/10.1016/j.geomorph.2014.03.041

Minick, K.J., Mitra, B., Li, X., Noormets, A., King, J.S., 2019. Water Table Drawdown Alters Soil and Microbial Carbon Pool Size and Isotope Composition in Coastal Freshwater Forested Wetlands. Front. For. Glob. Chang. 2, 7. https://doi.org/10.3389/ffgc.2019.00007

Moura, P.A., Francelino, M.R., Schaefer, C.E.G.R., Simas, F.N.B., de Mendonça, B.A.F., 2012. Distribution and characterization of soils and landform relationships in Byers Peninsula, Livingston Island, Maritime Antarctica. Geomorphology 155–156, 45–54. https://doi.org/10.1016/j.geomorph.2011.12.011

Navas, A., López-Martínez, J., Casas, J., Machín, J., Durán, J.J., Serrano, E., Cuchi, J.-A., 2006. Soil Characteristics along a Transect on Raised Marine Surfaces on Byers Peninsula, Livingston Island, South Shetland Islands. Antarctica 467–473. https://doi.org/10.1007/3-540-32934-X_60

Navas, A., López-Martínez, J., Casas, J., Machín, J., Durán, J.J., Serrano, E., Cuchi, J.-A., Mink, S., 2008a. Soil characteristics on varying lithological substrates in the South Shetland Islands, maritime Antarctica. Geoderma 144, 123–139. https://doi.org/10.1016/j.geoderma.2007.10.011

Navas, A., López-Martínez, J., Casas, J., Machín, J., Durán, J.J., Serrano, E., Cuchi, J.-A., Mink, S., 2008b. Soil characteristics on varying lithological substrates in the South Shetland Islands, maritime Antarctica. Geoderma 144, 123–139. https://doi.org/10.1016/j.geoderma.2007.10.011

Obu, J., Westermann, S., Vieira, G., Abramov, A., Ruby Balks, M., Bartsch, A., Hrbáček, F., Kääb, A.,

Ramos, M., 2020. Pan-Antarctic map of near-surface permafrost temperatures at 1 km2 scale. Cryosphere 14, 497–519. https://doi.org/10.5194/TC-14-497-2020

Ochyra, R., 1998. The moss flora of King George Island, Antarctica, Polish Academy of Sciences.

Ochyra, R., Smith, R.L., Bednarek-Ochyra, H., 2008. The illustrated moss flora of Antarctica. Cambridge University Press.

Olech, M., 2004. Lichens of King George Island, Antarctica. Institute of Botany of the Jagiellonian University, Kraków.

Oliva, M., Antoniades, D., Giralt, S., Granados, I., Pla-Rabes, S., Toro, M., Liu, E.J., Sanjurjo, J., Vieira, G., 2016. The Holocene deglaciation of the Byers Peninsula (Livingston Island, Antarctica) based on the dating of lake sedimentary records. Geomorphology 261, 89–102. https://doi.org/10.1016/J.GEOMORPH.2016.02.029

Oliva, M., Ruiz-Fernández, J., 2015. Coupling patterns between para-glacial and permafrost degradation responses in Antarctica. Earth Surf. Process. Landforms 40, 1227–1238. https://doi.org/10.1002/esp.3716

Otero, X., Fernández, S., de Pablo Hernandez, M.A., Nizoli, E.C., Quesada, A., 2013. Plant communities as a key factor in biogeochemical processes involving micronutrients (Fe, Mn, Co, and Cu) in Antarctic soils (Byers Peninsula, maritime Antarctica). Geoderma 195–196, 145–154. https://doi.org/10.1016/j.geoderma.2012.11.018

Øvstedal, D., Smith, R., 2001. Lichens of Antarctica and South Georgia: a guide to their identification and ecology, XII. ed. Cambridge University Press, Cambridge.

Palmtag, J., Kuhry, P., 2018. Grain size controls on cryoturbation and soil organic carbon density in permafrost-affected soils. Permafr. Periglac. Process. 29, 112–120. https://doi.org/10.1002/PPP.1975

Park, J.H., Day, T.A., 2007. Temperature response of CO2 exchange and dissolved organic carbon release in a maritime Antarctic tundra ecosystem. Polar Biol. 30, 1535–1544. https://doi.org/10.1007/S00300-007-0314-Y/TABLES/4

Park, J.H., Day, T.A., Strauss, S., Ruhland, C.T., 2007. Biogeochemical pools and fluxes of carbon and nitrogen in a maritime tundra near penguin colonies along the Antarctic Peninsula. Polar Biol. 30, 199–207. https://doi.org/10.1007/S00300-006-0173-Y/TABLES/2

Ping, C.L., Jastrow, J.D., Jorgenson, M.T., Michaelson, G.J., Shur, Y.L., 2015. Permafrost soils and carbon cycling. SOIL 1, 147–171. https://doi.org/10.5194/SOIL-1-147-2015

Pires, C.V., Schaefer, C.E.R.G., Hashigushi, A.K., Thomazini, A., Filho, E.I.F., Mendonça, E.S., 2017. Soil organic carbon and nitrogen pools drive soil C-CO2 emissions from selected soils in Maritime Antarctica. Sci. Total Environ. 596–597, 124–135. https://doi.org/10.1016/j.scitotenv.2017.03.144

Plante, A.F., Conant, R.T., Stewart, C.E., Paustian, K., Six, J., 2006. Impact of Soil Texture on the Distribution of Soil Organic Matter in Physical and Chemical Fractions. Soil Sci. Soc. Am. J. 70, 287–296. https://doi.org/10.2136/sssaj2004.0363

Putzke, J., Pereira, A., 2001. The Antarctic mosses: With special reference to the South Shetland Islands. Editora da ULBRA, Canoas.

R Core Team, 2019. R: A language and environment for statistical computing. https://doi.org/10.1016/j.dendro.2008.01.002

Ramsey, C.B., 2009. Bayesian Analysis of Radiocarbon Dates. Radiocarbon 51, 337–360. https://doi.org/10.1017/S0033822200033865

Redón, J., 1985. Líquenes antárticos. Instituto Antártico Chileno (INACH), Santiago de Chile.

Ruiz-Fernández, J., Oliva, M., 2016. Relative Paleoenvironmental Adjustments Following Deglaciation of the Byers Peninsula (Livingston Island, Antarctica). Arctic, Antarct. Alp. Res. 48, 345–359. https://doi.org/10.1657/AAAR0015-014

Saba, G.K., Fraser, W.R., Saba, V.S., Iannuzzi, R.A., Coleman, K.E., Doney, S.C., Ducklow, H.W., Martinson, D.G., Miles, T.N., Patterson-Fraser, D.L., Stammerjohn, S.E., Steinberg, D.K., Schofield, O.M., 2014. Winter and spring controls on the summer food web of the coastal West Antarctic Peninsula. Nat. Commun. 2014 51 5, 1–8. https://doi.org/10.1038/ncomms5318

Saiz-Jimenez, C., 1995. Microbial melanins in stone monuments. Sci. Total Environ. 167, 273–286. https://doi.org/10.1016/0048-9697(95)04588-R

Schaefer, C.E.G.R., Pereira, T.T.C., Almeida, I.C.C., Michel, R.F.M., Corrêa, G.R., Figueiredo, L.P.S., Ker, J.C., 2017. Penguin activity modify the thermal regime of active layer in Antarctica: A case study from Hope Bay. CATENA 149, 582–591. https://doi.org/10.1016/J.CATENA.2016.07.021

Schnecker, J., Wild, B., Hofhansl, F., Eloy Alves, R.J., Bárta, J., Čapek, P., Fuchslueger, L., Gentsch, N., Gittel, A., Guggenberger, G., Hofer, A., Kienzl, S., Knoltsch, A., Lashchinskiy, N., Mikutta, R., Šantrůčková, H., Shibistova, O., Takriti, M., Urich, T., Weltin, G., Richter, A., 2014. Effects of Soil Organic Matter Properties and Microbial Community Composition on Enzyme Activities in Cryoturbated Arctic Soils. PLoS One 9, e94076. https://doi.org/10.1371/journal.pone.0094076

Simas, F.N.B., Schaefer, C., Mendonça, E., Silva, I., Santana, R., Ribeiro, A., 2007. Organic carbon stocks in permafrost-affected soils from Admiralty Bay, Antarctica, in: Antarcica: A Keystone in a Changing World - Online Proceedigns of the 10th ISAES. p. 4. https://doi.org/10:3133/of2007-1047.srp076

Simas, F.N.B., Schaefer, C.E.G.R., Filho, M.R.A., Francelino, M.R., Filho, E.I.F., da Costa, L.M., 2008. Genesis, properties and classification of Cryosols from Admiralty Bay, maritime Antarctica. Geoderma 144, 116–122. https://doi.org/10.1016/J.GEODERMA.2007.10.019

Simms, A.R., Milliken, K.T., Anderson, J.B., Wellner, J.S., 2011. The marine record of deglaciation of the South Shetland Islands, Antarctica since the Last Glacial Maximum. Quat. Sci. Rev. 30, 1583–1601. https://doi.org/10.1016/j.quascirev.2011.03.018

Smellie, J.L., Davies, R.E.S., Thomson, M.R.A., 1980. Geology of a Mesozoic intra-arc sequence on Byers Peninsula, Livingston Island, South Shetland Islands. Britsh Antactic Surv. Bull. 50, 55–76.

Tarnocai, C., Canadell, J.G., Schuur, E.A.G., Kuhry, P., Mazhitova, G., Zimov, S., 2009. Soil organic carbon pools in the northern circumpolar permafrost region. Global Biogeochem. Cycles 23, n/a-n/a. https://doi.org/10.1029/2008GB003327

Teixeira, P., Donagemma, G., Teixeira, W., 2017. Manual de métodos de análise de solo. Embrapa, Brasília.

Thomazini, A., Francelino, M.R., Pereira, A.B., Schünemann, A.L., Mendonça, E. de S., Michel, R.F.M., Schaefer, C.E.G.R., 2020. The current response of soil thermal regime and carbon exchange of a paraglacial coastal land system in maritime Antarctica. L. Degrad. Dev. 31, 655–666. https://doi.org/10.1002/ldr.3479

Thomazini, A., Francelino, M.R., Pereira, A.B., Schünemann, A.L., Mendonça, E.S., Almeida, P.H.A., Schaefer, C.E.G.R., 2016. Geospatial variability of soil CO2–C exchange in the main terrestrial ecosystems of Keller Peninsula, Maritime Antarctica. Sci. Total Environ. 562, 802–811. https://doi.org/10.1016/J.SCITOTENV.2016.04.043

Thomazini, A., Teixeira, D.D.B., Turbay, C.V.G., La Scala, N., Schaefer, C.E.G.R., Mendonça, E.D.S., 2014. Spatial Variability of CO2 Emissions from Newly Exposed Paraglacial Soils at a Glacier Retreat Zone on King George Island, Maritime Antarctica. Permafr. Periglac. Process. 25, 233–242. https://doi.org/10.1002/PPP.1818

Tonello, M.S., Hebner, T.S., Sterner, R.W., Brovold, S., Tiecher, T., Bortoluzzi, E.C., Merten, G.H., 2020. Geochemistry and mineralogy of southwestern Lake Superior sediments with an emphasis on phosphorus lability. J. Soils Sediments 20, 1060–1073. https://doi.org/10.1007/S11368-019-02420-5/TABLES/6

Toro, M., Granados, I., Pla, S., Giralt, S., Antoniades, D., Galán, L., Cortizas, A.M., Lim, H.S., Appleby, P.G., 2013. Chronostratigraphy of the sedimentary record of Limnopolar Lake, Byers Peninsula, Livingston Island, Antarctica. Antarct. Sci. 25, 198–212. https://doi.org/10.1017/S0954102012000788

Turner, J., Barrand, N.E., Bracegirdle, T.J., Convey, P., Hodgson, D.A., Jarvis, M., Jenkins, A., Marshall, G., Meredith, M.P., Roscoe, H., Shanklin, J., French, J., Goosse, H., Guglielmin, M., Gutt, J., Jacobs, S., Kennicutt, M.C., Masson-Delmotte, V., Mayewski, P., Navarro, F., Robinson, S., Scambos, T., Sparrow, M., Summerhayes, C., Speer, K., Klepikov, A., 2014a. Antarctic climate change and the environment: an update. Polar Rec. (Gr. Brit). 50, 237–259.

https://doi.org/10.1017/S0032247413000296

Turner, J., Barrand, N.E., Bracegirdle, T.J., Convey, P., Hodgson, D.A., Jarvis, M., Jenkins, A., Marshall, G., Meredith, M.P., Roscoe, H., Shanklin, J., French, J., Goosse, H., Guglielmin, M., Gutt, J., Jacobs, S., Kennicutt, M.C., Masson-Delmotte, V., Mayewski, P., Navarro, F., Robinson, S., Scambos, T., Sparrow, M., Summerhayes, C., Speer, K., Klepikov, A., 2014b. Antarctic climate change and the environment: an update. Polar Rec. (Gr. Brit). 50, 237–259. https://doi.org/10.1017/S0032247413000296

Van Vliet-Lanoë, B., Fox, C.A., 2018. Frost Action. Interpret. Micromorphol. Featur. Soils Regoliths 575–603. https://doi.org/10.1016/B978-0-444-63522-8.00020-6

Vaughan, D.G., Marshall, G.J., Connolley, W.M., Parkinson, C., Mulvaney, R., Hodgson, D.A., King, J.C., Pudsey, C.J., Turner, J., 2003. Recent Rapid Regional Climate Warming on the Antarctic Peninsula. Clim. Chang. 2003 603 60, 243–274. https://doi.org/10.1023/A:1026021217991

Veldkamp, E., 1994. Organic Carbon Turnover in Three Tropical Soils under Pasture after Deforestation. Soil Sci. Soc. Am. J. 58, 175–180. https://doi.org/10.2136/sssaj1994.03615995005800010025x

Vera, M.L., 2011. Colonization and demographic structure of Deschampsia antarctica and Colobanthus quitensis along an altitudinal gradient on Livingston Island, South Shetland Islands, Antarctica. Polar Res. 30, 7146. https://doi.org/10.3402/polar.v30i0.7146

Victoria, F. de C., de Albuquerque, M.P., Pereira, A.B., Simas, F.N.B., Spielmann, A.A., Schaefer, C.E.G.R., 2013. Characterization and mapping of plant communities at Hennequin Point, King George Island, Antarctica. Polar Res. 32, 19261. https://doi.org/10.3402/polar.v32i0.19261

Vieira, G., Bockheim, J., Guglielmin, M., Balks, M., Abramov, A.A., Boelhouwers, J., Cannone, N., Ganzert, L., Gilichinsky, D.A., Goryachkin, S., López-Martínez, J., Meiklejohn, I., Raffi, R., Ramos, M., Schaefer, C., Serrano, E., Simas, F., Sletten, R., Wagner, D., 2010. Thermal state of permafrost and active-layer monitoring in the antarctic: Advances during the international polar year 2007–2009. Permafr. Periglac. Process. 21, 182–197. https://doi.org/10.1002/PPP.685

Wirtz, N., Lumbsch, H.T., Green, T.G.A., Türk, R., Pintado, A., Sancho, L., Schroeter, B., 2003. Lichen fungi have low cyanobiont selectivity in maritime Antarctica. New Phytol. 160, 177–183. https://doi.org/10.1046/J.1469-8137.2003.00859.X

Zhu, R., Bao, T., Wang, Q., Xu, H., Liu, Y., 2014a. Summertime CO2 fluxes and ecosystem respiration from marine animal colony tundra in maritime Antarctica. Atmos. Environ. 98, 190–201. https://doi.org/10.1016/J.ATMOSENV.2014.08.065

Zhu, R., Ma, D., Xu, H., 2014b. Summertime N2O, CH4 and CO2 exchanges from a tundra marsh and an upland tundra in maritime Antarctica. Atmos. Environ. 83, 269–281. https://doi.org/10.1016/j.atmosenv.2013.11.017

Zubrzycki, S., Kutzbach, L., Pfeiffer, E.-M., 2014. Permafrost-affected soils and their carbon pools with a focus on the Russian Arctic. Solid Earth 5, 595–609. https://doi.org/10.5194/se-5-595-2014

Paper 2

PAPER 2: ASSESSMENT OF MICROBIAL INDEXES OF BACTERIAL AND FUNGAL COMMUNITIES IN SELECTED SOILS ON THE BYERS PENINSULA, MARITIME ANTARCTICA

Jônatas Pedro da Silva [a, b], Tomás Gomes Reis Veloso [c], José João Lelis Leal de Souza [b], Emanuelle Mercês Barros Soares [b], Carlos Ernesto G. R. Schaefer [b]

[a] Ph. D. student Program in Soils and Plant Nutrition, Department of Soils, Federal University of Viçosa - UFV, Viçosa - MG, Brazil

[b] Department of Soils, Federal University of Viçosa - UFV, Viçosa - MG, Brazil

[c] Department of Microbiology, Federal University of Viçosa - UFV, Viçosa - MG, Brazil

[*] Corresponding author:

Telephone: +55 31 9 8357-2450

E-mail: jpedro.agronomo@gmail.com

Abstract

The life forms in the Antarctic biome have evolved influenced by extremely low temperatures, low availability of water, low C and N contents, freeze-thaw cycles, low radiation in winter, and high UV radiation in summer. Despite all the existing restricted conditions, recent studies using microbial DNA sequencing technologies have shown the magnitude of the microbial diversity in the Antarctic continent. The present study aimed to characterize and compare bacterial and fungal diversity using metabarcoding in surface and subsurface soil samples from characteristic and representative profiles of the Byers Peninsula, Maritime Antarctica. The intracellular DNA from living cells was used. The later steps of DNA extraction steps were performed using Nucleospin Soil® (Macherey-Nagel) according to the manufacturer's protocol. The bacterial and fungal communities were accessed by amplifying the sequences of the chromosomal coding for the bacterial V3-V4 region of 16S rRNA and fungal internal transcribed spacer 1 (ITS1). ^{14}C dating method was applied to the soil organic matter of six selected soil profiles. To assess the influence of abiotic factors that influence and control microbial community analyses of physical, chemical, and SOM-associated attributes of Byers Peninsula soils were carried out. The 14,048 bacterial ASVs were distributed in 11 phyla, 132 classes, 309 orders, 485 families, and 864 genera. Almost all samples presented 50% of their sequences assigned to Actinobacteriota and Proteobacteria phylas. Regarding the fungal community, the 1,619 ASVs were assigned to 7 phyla, 21 orders, 46 classes, 71 families, and 104 genera. Mortierellomycota, Ascomycota, and Basidiomycota are the main phyla found. Although we used the most updated database, up to 6% of the bacterial phyla and 40% of fungal phyla were not identified due to the limitation of microbial databases. Overall, the species diversity of bacteria was much higher than that of fungi in all the profiles evaluated. The Late Holocene soil profile, described in the youngest level of raised

beaches, hosts the highest bacterial and fungal diversity. The distance from the glacier seems less relevant to fungal and bacterial communities than the ^{14}C age of soil organic matter. In contrast to the distance from the glacier among the collection points, the moisture regime was a crucial factor in the behavior observed among the microbial indices analyzed. The fungal community composition is statistically correlated to nutrient availability, soil reactivity and soil organic matter composition. On the other hand, the bacteria community composition was not correlated with soil attributes. We observed a substantial bacterial and fungal diversity in the soils evaluated in this study. The fungal community depended more on the soil reservoir of nitrogen and carbon. The results found in our research can act as a base for future research to elucidate more the microbial role in these soils and the potential use of these microorganisms in biotechnological issues.

Keywords: Microbial indexes**,** microbial DNA sequencing technologies, metabarcoding, bacterial V3-V4 region, fungal internal transcribed spacer 1 (ITS1), soil features, soil surface horizons, ASPA N° 126

1. Introduction

The life forms in the Antarctic biome have evolved influenced by extreme low temperatures, low water available, low C and N contents, freeze-thaw cycles, low radiation in winter, and high UV radiation in summer [1]. Biota is restricted to small invertebrates, microorganisms, an abundant flora of mosses and lichens, and three flowering species: *Deschampsia antarctica* Desv. (Poaceae), *Colobanthus quitensis* (Kunth) Bartl (Caryophyllaceae), and *Poa annua* L. (Poaceae), accidentally introduced in the 1980s [2]. Despite all the existing restricted conditions, recent studies have shown the magnitude of the microbial diversity in the Antarctic continent [3,4].

The continent of Antarctica plays a fundamental role in the energy balance of the Earth, mainly related to atmospheric and climatic dynamics [5]. The ice-free areas represent less than 1% of the continent [6,7], and are considered oases in this cold desert, once they host a large part of the continent's biodiversity [8]. Maritime Antarctica is the hottest and wettest region in Antarctica. Liquid annual precipitation between 350 and 500 mm, average monthly temperatures > 0°C during the austral summer, and rarely < -12 °C in the winter [9], favor bird nidification, mammal occupation of the coast, and denser vegetation cover [10].

Maritime Antarctica has experienced intense climate change in recent decades [11], leading to changes in this environment, such as reduced glacier ice volume, glacial retreat, increased plant populations, and microbial activity [12]. Considered the westernmost portion of Peninsular Antarctica, this has less severe climatic conditions [13]. The deglaciation process in this region began at least 10 ky BP ago, at the beginning of the Holocene [14,15], enabling the appearance of large portions of ice-free areas and their colonization.

Among these areas, the Byers Peninsula stands out, where, besides being the largest ice-free area in Maritime Antarctica [16], it is considered to have the highest biodiversity in terms of flora and fauna [17].

Although most of the continent is dominated by ice-covered glaciers, there has been a significant retreat in the last decades due to climate change [18]. Global climate changes have influenced vegetation expansion, biological activity, and soil chemical and physical attributes in these periglacial landscapes [19,20]. Microbial diversity and functions in Maritime Antarctica soils are influenced and dictated by a wide range of abiotic factors (temperature, water availability, pH, C and N contents, nutrient balance, texture, among other physical and chemical soil attributes) [1,21], with temperature and moisture being considered the most critical variables [21,22]. These factors together influence the chemical composition of these environments and reflect on the availability of nutrients essential for the establishment and development of microbial communities [22].

The microbiota plays a crucial role in soil formation and biogeochemical cycles [6], contributing to the weathering of minerals in soils [23]. Bacterial and fungal species, considered the main biochemical engineers of soil, are responsible for organic matter decomposition and nutrient cycling, regulating 90% of energy flow, mainly through catabolic reactions leading to C decomposition, transformation and mineralization, and nutrient cycling [24]. They can also act as biological regulators and ecosystem engineers, physically altering soil and regulating resource availability for other species [25]. The interaction between biotic and abiotic processes remains one of the fundamental issues in research and the understanding of ecosystem dynamics and is strictly associated with the initial development of soils under adverse environmental conditions, such as in Antarctica [26]. Therefore, studies combining data on microbial communities and soil characteristics are essential to obtain a global view of its interactions.

We use molecular techniques to characterize the soil microbial diversity in the Byers Peninsula, Maritime Antarctica. Few studies have applied metabarcoding approaches to characterize fungal communities in this environment [27]. So, the present study aimed to characterize and compare bacterial and fungal diversity using metabarcoding in surface (nine profiles) and subsurface (three profiles) soil samples from characteristic and representative profiles (low and high platforms and raised beachs) of the Byers Peninsula, Maritime Antarctica. Using samples from different locations makes it possible to observe better the effects of abiotic variables that influence dynamics in this environment. Furthermore, to gain insight into the abiotic factors that influence and control community diversity, structure, and composition, microbial profiles have been associated with medium-term microenvironmental variables and soil chemical properties [21].

2. Material and Methods

2.1. Study site and soil sampling

The Byers Peninsula (BP), with about 60 km^2, is the most extensive ice-free area in Maritime Antarctica (Figure 1) - located at the western end of Livingston Island between the Bransfield Strait and the Drake Passage (between the respective latitudes and longitudes, 62° 34' – 62° 41' S and 60° 56' - 61° 12' W). It was designated an Antarctic Specially Protected Area (ASPA N° 126) due to its identification as a habitat of global importance since it is home to breeding colonies of terns (*Sterna vittata*), seagulls (*Larus dominicanus*), penguins (*Pygoscelis antarctica* and *Pygoscelis papua*), petrels (*Oceanites oceanicus*, *Fregetta tropica*, *Daption capense* and *Macronectes giganteus*), from cormorants (*Phalacrocorax atriceps*), skuas (*Stercorarius antarcticus*) and Antarctic doves (*Chionis albus*) and intense occupation by sea elephants (*Mirounga leonina*).

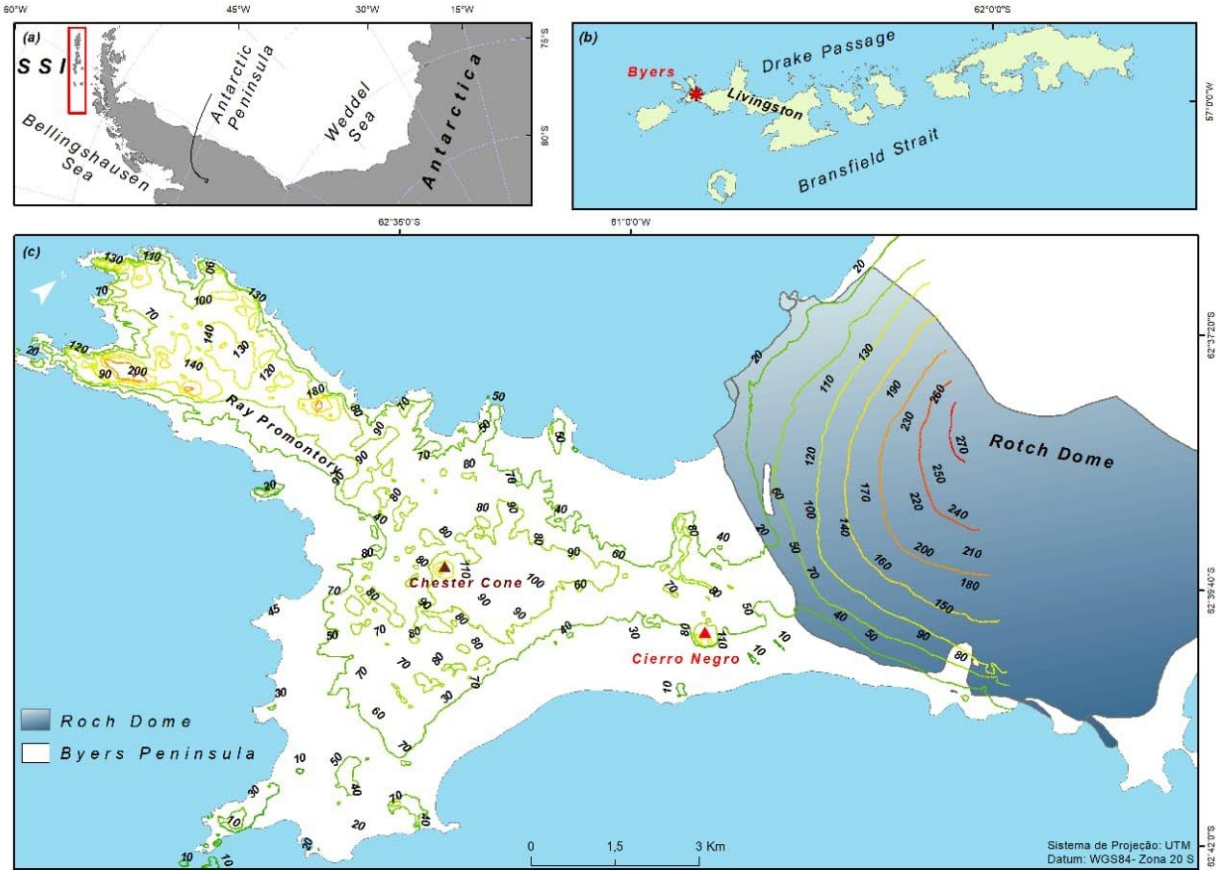

Figure 1. Location of the study area. a) South Shetlands Islands (SSI). b) Location of Livingston Island between the South Shetlands. c) Byers Peninsula and its main location points (Ray Promontory, Chester Cone, Cierro Negro, and Rotch Dome Glacier).

Thirteen soil profiles were sampled to represent the plant diversity, geomorphological, geological, and distance from water bodies and the glacier. The soil profiles (Figure 1) were described, collected, and classified according to the Soil Taxonomy (ST) and the World Reference Base (WRB) (Supplementary Material 1 and 2), classifying soils using diagnostic horizons, properties, and materials. Although these systems are based on genetic principles, the approaches used to emphasize the role of soil processes in soil taxonomic systems [28].

2.2. Soil physical, chemical, and SOM analysis

The samples were air dried and sieved through a 2 mm sieve before physic and chemical analyses [29]. Coarse and fine sand, silt, and clay were determined by the sieve-pipette method after dispersion with 0.1 M NaOH. Soil pH was measured with a glass electrode in a 1:2.5 suspension v/v soil and deionized water (H_2O pH). The potential acidity (H + Al) was extracted by 1 M ammonium acetate solution at pH 7. The contents of exchangeable Ca^{2+}, $Mg^{2+,}$ and Al^{3+} were determined in a 1 M KCl extract. Exchangeable K^+ and Na^+ were determined after Melhich-1 extraction. From these results, the sum of bases (SB), base saturation (V), aluminum saturation (m), equivalent cation exchange capacity (ECEC), and total cation exchange capacity (CEC) were calculated.

A Mehlich-1 extraction solution determined the available phosphorus content (P). The P adsorption capacity of the soil was determined after stirring for 1 hour with 2.5 g of soil in 0.01 M $CaCl_2$ containing 60 mg of P L^{-1}. The suspension was filtered, and the remaining P in solution (P_{REM}) was determined by photocolorimetry [30].

The C and N contents, $\delta^{13}C$ and $\delta^{15}N$ ratio isotopes were determined in the physical size-fractionated particles of soil organic matter (SOM): a) particulate organic matter (POM), and; b) mineral-associated organic matter (MAOM) [31]. Such determinations were performed on all soil horizons and plant materials. They were made using an isotope ratio mass spectrometer (IRMS) Flash EA - Delta V at the Center for Stable Isotopes Prof. Dr. Carlos Ducatti - UNESP. Based on these determinations and the determination of soil density, it was possible to calculate the stocks by fractions and total. The soil density was calculated according to the formula: Soil density = (total porosity/ particle density) + 1. Particle density was determined after drying a quantity of soil to 105°C and then dividing the mass by the volume of the particles, excluding spaces among them [29].

The biochemical composition of the SOM fractions (POM and MAOM), as well as the plant materials, was evaluated using an off-line TMAH -mediated thermochemolysis procedure as described in Chefetz et al. (2000) and Del Rio et al. (1998).

The deepest horizons of six soil profiles were dated by the ^{14}C method. The soil profiles were selected to represent geomorphological, geological, and vegetable diversity, as well different distances from

the glacier. The samples were physically pretreated to remove vegetal fragments. After that, non-hydrolysable carbon was isolated with two h treatments with HCl 1.0 mol L^{-1} at 90 °C until the supernatant was clear or up to 5 times. To measure the radiocarbon content in the samples, dating by Accelerator Mass Spectrometry (AMS) was performed by BETA ANALYTIC Laboratory. Calibration of radiocarbon age expressed in years before the present (BP) was performed using the High Probability Density Band Method (HPD): SHCAL13 [34,35].

2.3. DNA extraction, PCR, and sequencing

Eight grams of soil were used for DNA extraction. The intracellular DNA from living cells was separated from the extracellular DNA from dead cells to avoid overestimating diversity [36]. The cell lysis was performed in a Precellys 24 High-Powered Bead Mill Homogenizer (Bertin technologies) for 50 s at 4000 rpm. The later DNA extraction steps were performed using Nucleospin Soil® (Macherey-Nagel) according to the manufacturer's protocol. The quality of DNA extraction was evaluated by electrophoresis in 0.8 % agarose gel stained with Ethidium Bromide under UV light.

The bacterial and fungal communities were accessed by amplifying the sequences of the chromosomal sequence coding for the bacterial V3-V4 region of 16S rRNA and the fungal internal transcribed spacer 1 (ITS1). For that, the pair of primers 341F(5'-CCTAYGGGRBGCASCAG-3')/ 806R (5'-GGACTACNNGGGTATCTAAT-3') [37] and ITS1F(5'-CTTGGTCATTTAGAGGAAGTAA-3')/ITS2(5'-GCTGCGTTCTTCATCGATGC-3') were used. The PCR libraries were quantified and pooled according to ref Veloso et al. (2020). The sequencing of the 16S and ITS1 libraries was performed in separate runs using the NovaSeq 6000 platform.

2.4. Bioinformatic analyses of bacterial V3-V4 region and fungal ITS1 region

All raw reads were demultiplexed using qiime2 [39]. The denoising and removal of chimeras were performed using the plugin DADA2 [40], where all reads with two or more expected errors were removed. All high-quality ASVs of 16S and ITS markers were annotated using the SILVA 138 [41] and UNITE [42] databases. All downstream analyses were performed in the software R version 4.1.2 (2021-11-01) using the package phyloseq v. 1.36.0 [43] and 3.3.5.9000.

We built a Principal Coordinate Analysis (PcoA) to access the microbial beta-diversity based on Bray-Curtis dissimilarities between samples. The alpha indexes (Richness, evenness, dominance, and diversity) were calculated using the package *microbiome* available for R [44]. The Spearman's correlation index among these alpha indexes and soil features was calculated to evaluate the relations between these two compartments. Spearman's correlation, a non-parametric correlation measure, was used to evaluate monotonic reactions, whether linear or non-linear.

3. Results

3.1 Soil properties and classification

Samples from nine geographically distinct soil profiles were analyzed, having representatives from high (P3, P4, P10) and low platforms (P2, P5, P6, P11) and raised beaches (P7, P9). Among these profiles, three were classified as Cryosols (P2, P3, P10), three as Gleysols (P4, P5, P7), one as Leptosol (P6), one as Arenosol (P9), and one Cambisol (P11). Among the Cryosols, permafrost occurred on high and low platforms, with varying depths (60; 10 and 50 cm deep, respectively). The Gleysols presented poorly drained conditions, with a water layer visible from 10 cm depth in P7, 35 cm in P4, and 45 cm in P5. The Leptosol presented a well-drained condition despite the lithic contact at 20 cm depth. The Arenosol, described in the lowest marine terrace, showed intercalated depositions of clay and sand layers from 80 cm depth onwards, indicating different deposition phases.

The altitude range is 15 to 140 m.a.s.l., with the lowest altitude found on the marine terrace (P9) and the highest altitude on the high platform (P4). The surface horizon analyzed in these profiles also presented a variation in thickness ranging from 10 to 35 cm. The horizons and layers are dominantly yellow. The colors ranged from 5Y 6/4 to 10YR 3/2.

These surface horizons presented a weak to moderate subangular block structure for most samples, except in P6, which presented a moderate granular-type structure.

Sand and silt are the main particles. The sand content ranged from 20.3 to 97.9 %. Silt had contents ranging from 1.3 to 62.4 %. The clay content varies between 0.7 and 17.4 %.

The pH was moderately acidic to medium alkalinity (6.04 to 7.74), showing increased pH with increasing depth. The H^+ is the main source of acidity, and Al^{3+} is virtually absent, except in the surface horizon of a well-drained soil in raised beaches. The base saturation (V) of these soils characterized their eutrophication and demonstrated their incipient degree of weathering, with values ranging from 77.9 to 97.5%, represented mainly by the Ca^{2+} and Mg^{2+} contents.

As for the isotopic signatures of the SOM fractions analyzed in the studied samples, the $\delta^{13}C$ values in the POM fraction presented a variation of 5.64‰, with observed values ranging between -27.19 and -21.55‰. In the MAOM fraction, the variation was smaller, 5.19‰, with observed values between -26.55 and -21.36‰. As for the isotopic signature of $\delta^{15}N$, the variations in the fraction were higher, showing higher enrichment in ^{15}N of these samples. In the POM fraction, the $\delta^{15}N$ presented a variation of 17.94‰, with observed values ranging between -0.23 and 17.71‰. In the MAOM, the variation was slightly smaller, 16.67‰, with observed values ranging among the samples from -0.36 to 16.31‰. The samples examined were characterized by low TOC (0.3 to 9.9 g kg^{-1}) and low total nitrogen content (0 to 1.4 g kg^{-1}), which is quite common for Antarctic soils [45]. This high variation was reflected in the C/N ratio, which, even with

low values, varied between 4 and 15. The biochemical composition of the SOM in these samples was dominated almost exclusively by aliphatic compounds. Among these aliphatic compounds, the greatest dominant are lipid compounds of both plant and animal origin (cutin, suberin, microbial activity markers, bioactive and other lipids).

The dating performed on some of the soils studied, showed significant variation in ages between the ^{14}C dated (Figure S1). The profile with the oldest carbon is located on one of the highest platforms of the peninsula, P4, with contribution records from before the last glacial maximum (LGM), at 31,690 cal yr BP. One of the lower platforms (P11), showed C dated to the post-LGM period and the beginning of deglaciation of some areas, of 12,030 cal yr BP. The youngest profile was associated with the first raised beach level studied (P7), with only 1,220 cal yr BP. The other profiles (P3, P6, and P10) showed ages of 3,490, 3,290 and 2,350 cal yr BP, respectively, being placed in a context of climatic optimum for the Maritime Antarctic region, post-LGM and deglaciation of large tracts of land.

3.2 Microbial taxa

In total, 2,388,951 prokaryotic 16S rRNA reads (27,864 ASVs) and 586,478 fungal ITS region (1,619 ASVs) reads were obtained from 12 and 10 samples, respectively. After filtering, denoising, and removing the chimeric sequences, 1,554,745 16S and 559,393 ITS sequences were retained. The sampling effort was measured by the Zhang-Huang's estimator (Table S1), which showed that it was sufficient (above 0.99) to carry on the downstream analysis.

The 14,048 bacterial ASVs were distributed in 11 phyla, 132 classes, 309 orders, 485 families, and 864 genera. Almost all samples presented 50% of their sequences assigned to bacteria of phyla Actinobacteriota and Proteobacteria (Figure 2A), except for the sample collected in the surface horizon of soil profile on the highest altitude (P3H1), which presented Chloroflexi as the most abundant. Regarding the fungal community, the 1,619 ASVs were assigned to 7 phyla, 21 orders, 46 classes, 71 families, and 104 genera. The composition of fungal phyla varied more between the samples than the bacterial one (Figure 2B). The three main phyla found were Mortierellomycota, Ascomycota, and Basidiomycota. Many sequences could not be identified, ranging from 1.4 to 6.1% in the bacterial phylum, and from 1.3 to 39.6% in the fungal phylum (gray bars in Figure 2a and b, respectively), although we used the most recent database for fungi [46].

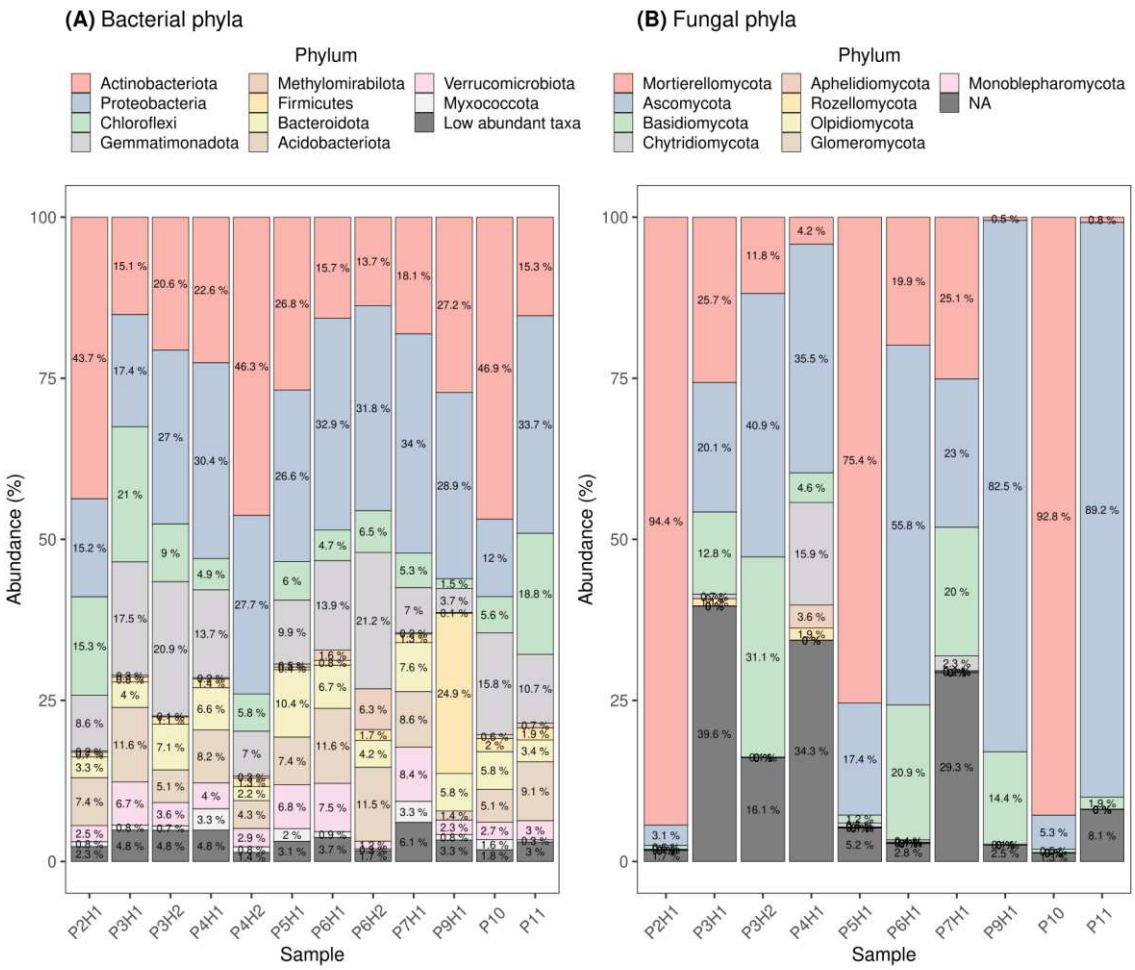

Figure 2. Relative abundance of taxonomic composition at the phylum level in nine soil profiles from Livingston Island. All fungal and the ten most abundant bacterial phyla are shown.

The ten most abundant organisms of the phylum bacteria were: Gemmatimonadaceae (2.16 to 17.33%); Micrococcaceae (0.18 to 32.30%); *Polaromonas* (0.057 to 18.56%); Gaiellales (0.67 to 5.73%); *Pseudomonas* (0.31 to 9.48%); *Ellin6067* (0.24 to 7.76%); P2-11E (0.64 to 8.90%); *Gaiella* (0.18 to 8.81%); *MB-A2-108* (0.22 to 6.96%) and *Pseudarthrobacter* (0.20 to 6.81%), and these were identified to the level of class (1), order (2), family (2), genus (6). For fungi, the most abundant were: *Mortierella antarctica* (0.35 to 91.82); *Aspergillus sydowii* (0.16 to 67.13%); *Verrucaria alpicola* (0.40 to 39.02%); *Mortierella* (0.50 to 38.56%); *Chaetomiaceae* (0.17 to 35.58%); *Mrakia frigida* (0.06 to 19.37%); *Acremonium biseptum* (0.05 to 28.12%); *Mortierella basiparvispora* (0.16 to 19.93%); *Phenoliferia psychrophila* (0.11 to 21.91%) and one fungus that could not be identified either at the phylum level (1.45 to 39.47%), and these were identified down to the genus (2) and species (7) level.

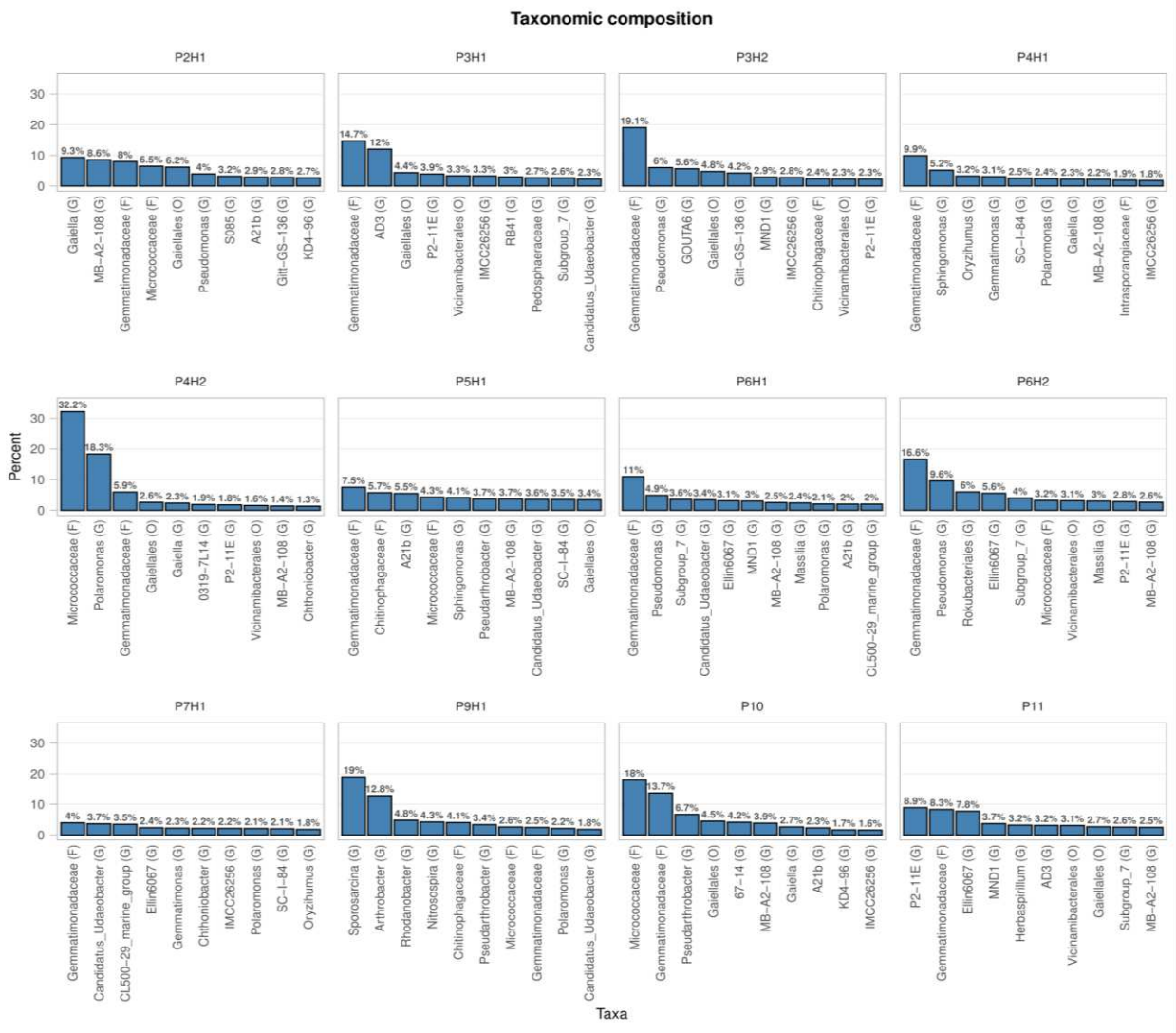

Figure 3. Ten most abundant genera per sample. When the identification of the genus (G) was not possible, the name of the family (F), Order (O), class (C), or phylum (P) was given instead.

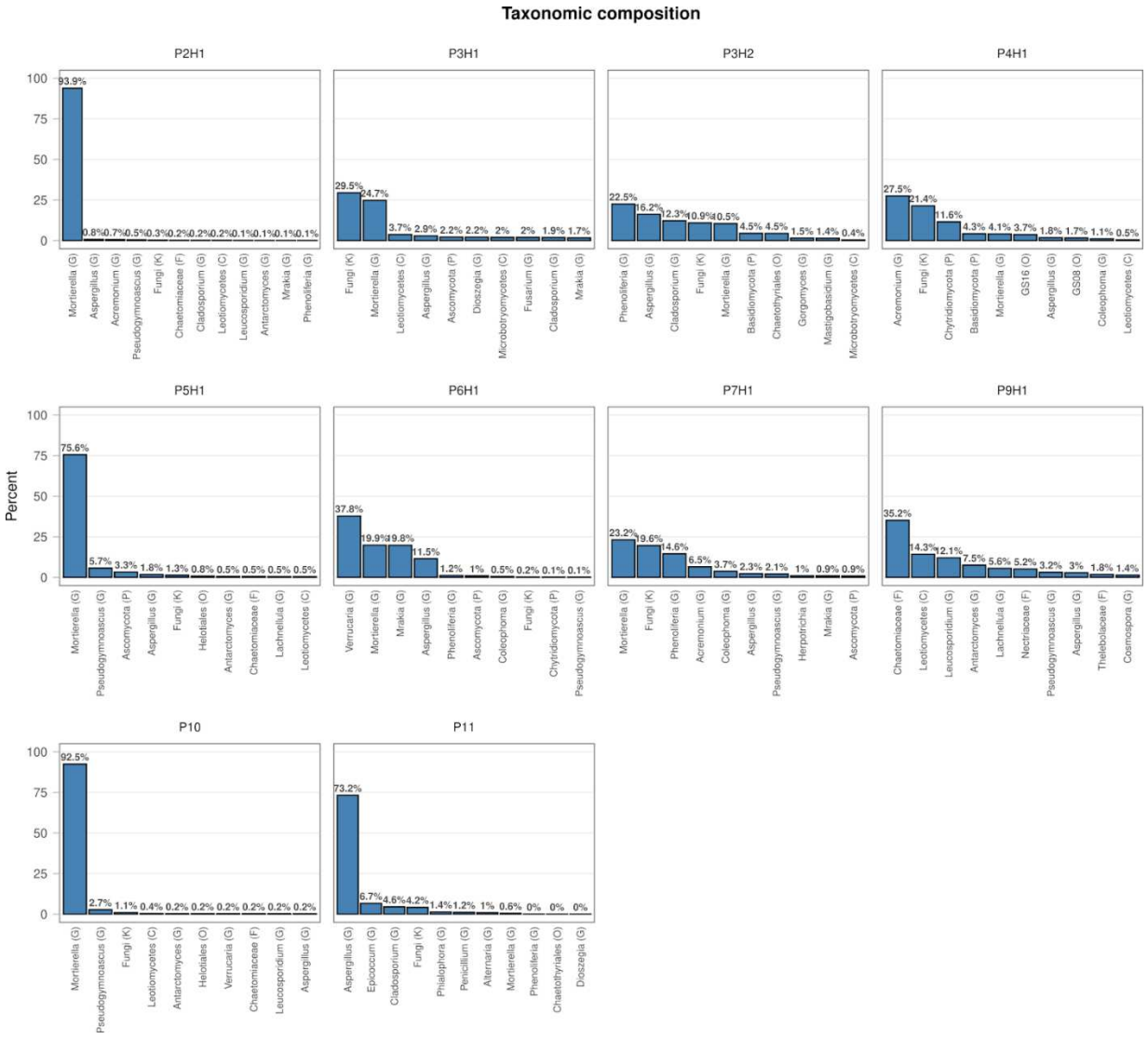

Figure 4. Ten most abundant fungal genera per sample. When the identification of the genus (G) was not possible, the name of the family (F), Order (O), class (C), or phylum (P) was given instead.

3.3 Microbial diversity

The Principal Coordinate Analyses (PcoA) indicated that each profile has a distinct microbial community. Most bacteria and fungi were found exclusively in one or two samples (Figure S2), i.e. most ASVs are not shared among many samples, showing that each soil has its typical microbial community.

The alpha diversity metric also varied among the samples (Figure 5C and 5D). Bacterial diversity among surface horizons ranged from 5.41 in the soil profile embedded in a high platform with lichen *Usnea auranteaco-atra* dominance (P10; 2,350 cal. yr BP) to 7.15 in the youngest soil (P7H1; 1220 cal. yr BP). The highest bacterial alpha diversity (7.15) was observed in the raised beach (P7), which also presented the

highest richness (3279) and evenness (0.88). On the other hand, the sample with the lowest richness index was P2H1, 1691. The youngest-dated soil (P7) showed the highest values for the bacterial alpha metric (Figure 5). The profiles with intermediate ages (2.3 to 12 cal ky BP; Figure S1) showed large oscillations between these values, not showing a pattern. The oldest profile (P4) showed values near and below the youngest profile. Among the subsurface samples analyzed, P3H2 showed the highest richness and diversity (1773 and 5.39, respectively), while P4H2 showed the lowest values for the same microbial indices (1441 and 4.1, respectively). Overall, the diversity of bacteria was much higher than that of fungi in all the profiles evaluated. Fungal diversity ranged from 0.61 on the surface of the most clayey profile (P2H1) to 3.9 on the surface of the youngest profile (P7H1).

The lowest fungal community richness was found on the surface horizon of the P11 profile, 79 (located near the glacier, 2.12 km). The profile with the highest fungal richness index (261) was the oldest (P4H1; 31,690 cal. yr BP), followed by the youngest profile (P7; 259). Interestingly, as observed for the bacterial community, the surface of the P7 profile showed high values for all alpha metric indexes (richness, evenness, and diversity; Figure 5). Despite showing lower richness than the P4 profile, the P7 profile showed higher diversity, since the diversity index takes into account the evenness and richness indices. Regarding the distance between the collected profiles and the glacier, no distribution pattern was observed between the alpha metric indices for the fungal and bacterial communities (Figure S1). As for the association between the ages of the dated profiles and the alpha metric indices, the oscillations of diversity and richness values were higher in the fungal community, but the pattern behavior was not so distinct from the bacterial community, differing more in terms of richness than diversity (Figure S1).

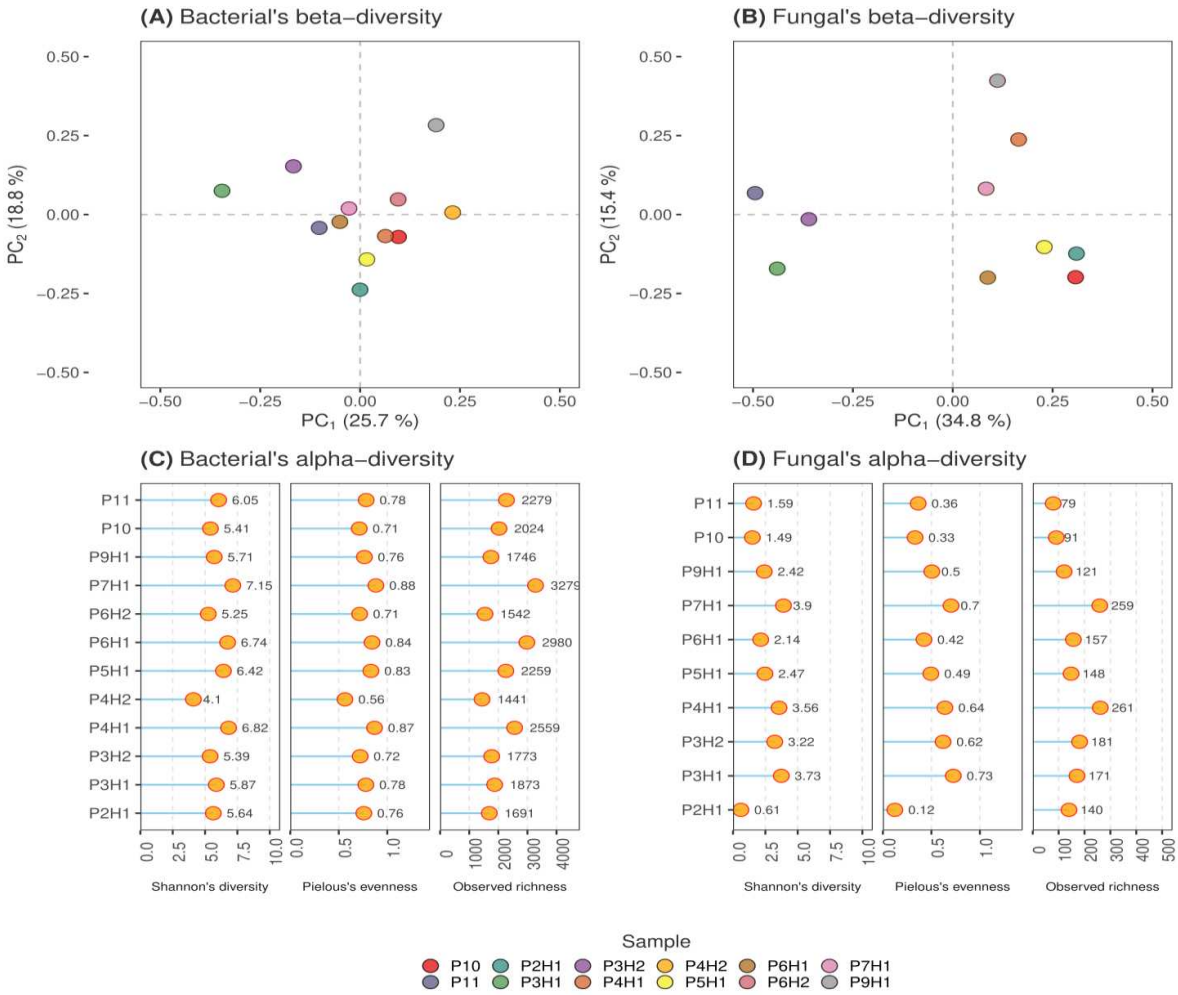

Figure 5. (A) Bacterial and (B) fungal beta-diversities in nine profiles sampled in the Byers Peninsula. The beta-diversity was accessed by building a principal component analysis (PcoA) based on Bray-Curtis distance of Hellinger transformed data. The percent of explanation for each axis is reported between parentheses. (C and D) Observed richness, Pielous' evenness, and diversity of Shannon for each profile/depth. The calculations for alpha-metrics used absolute counts of the rarefied abundance table.

Bacterial diversity and richness decrease with increasing depth. The lowest diversity and richness were observed in the subsurface horizon of the oldest profile (P4H2; 4.1 and 1441, respectively).

The linear distance between the sites and the modern glacier limit is not associated with the abundance and alpha diversity of microorganisms. Unlike the influence associated with the distance from the glacier among the collection points, the moisture regime was a crucial factor in the behavior observed among the microbial indices analyzed. Most of the profiles presented water in the subsurface, either in the form of W layer (water sheet) formed by snowmelt and/or degradation of permafrost, as P4, P5 and P7, or

the presence of permafrost itself, as P2, P3 and P10. It was noticeable that in the profiles with the presence of the water layer active the highest diversities of both bacteria and fungi occur (6.42 to 7.15 and 2.47 to 3.9, respectively), as well as the highest richnesses of these organisms (2,259 to 3,279 and 148 to 261, respectively). The profiles with permafrost or without the presence of water, showed close diversity and richness index values. The soils without the presence of water being higher for diversity of both organisms and for richness of bacteria.

3.4 Correlation analyses between physical-chemical and organic features of soil and microbial indexes

The fungal community is more correlated (23 significant correlations) with soil properties than the bacterial community (no significant correlation) (Figure 6). The fungal community composition is correlated to nutrient availability, soil reactivity and composition of soil organic matter. On the other hand, the bacteria community composition was not show to be correlated ($-0.5 > p < 0.5$) with any of the soil attributes.

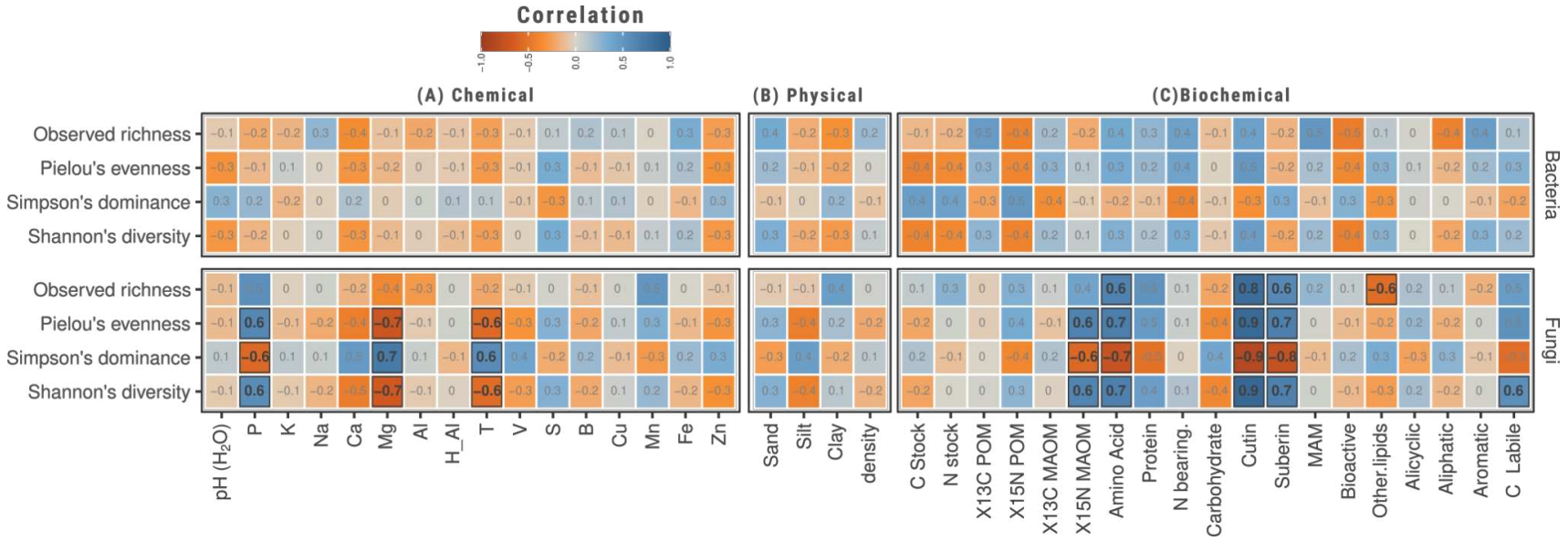

Figure 6. Correlation between soil features and microbial indexes. The value inside each tile represents the Spearman's correlation. All tiles with black outlines represent a significant correlation (p-value < 0.1)

The Redundancy Analysis (RDA, Figure 7) was done in order to verify which variables of the organic and physicochemical fractions most explain the variation in the bacterial and fungal communities. It is a canonical analysis where the dependent data matrix used contained the microbial sequence abundance data and the independent matrix contained the soil analysis data. For this, we used the first two axes (PC_1 and PC_2) due to them having the two largest gradients of microbial variation. The vectors of soil variables most parallel to each axis (PC_1 = X or PC_2 = Y) are the variables most correlated to microbial variation on each axis.

The Redundancy Analysis (RDA; figure 7) confirmed the results found in the correlation analysis among alpha metrics (richness, evenness, and diversity) and the soil factors. We found that while the bacterial beta-diversity is distributed more along the second component, the distribution of fungal beta-diversity occurs more along the first axis (PC_1), the axis that displays more variance in the beta-diversity, associated with the N isotopic fractionation and leaching.

Comparing graphs A and B (figure 7), we see that the arrows representing the variables associated with SOM are more parallel to Y (PC_2) in graph A (bacteria) and the X axis (PC_1) in graph B (fungi). Therefore, the larger gradient observed in fungi (the distribution of points on the PC_1 axis) correlates with the availability of these stocks of C, N, etc. This behavior makes sense since these organisms are all heterotrophic, and dependent on already pre-fixed carbon and nitrogen. On the other hand, these same variables are also related to the gradient of bacteria (Figure 7a), but on the second axis (PC_2), representing only the second largest variation in the bacterial community. Therefore, although they are important in the microbial community distribution, they are not related to the greatest variation gradient.

There is a clear distinction in PC_1 (Figure 7c) between bases and acids which occupy CEC. The base saturation decreases by leaching and/or by incorporation of SOM and deprotonated H^+ from organic clays; consequently, the content of acid in CEC increases. For the fungal community (Figure 7d), PC_1 showed a greater association with soil acidity and salinity.

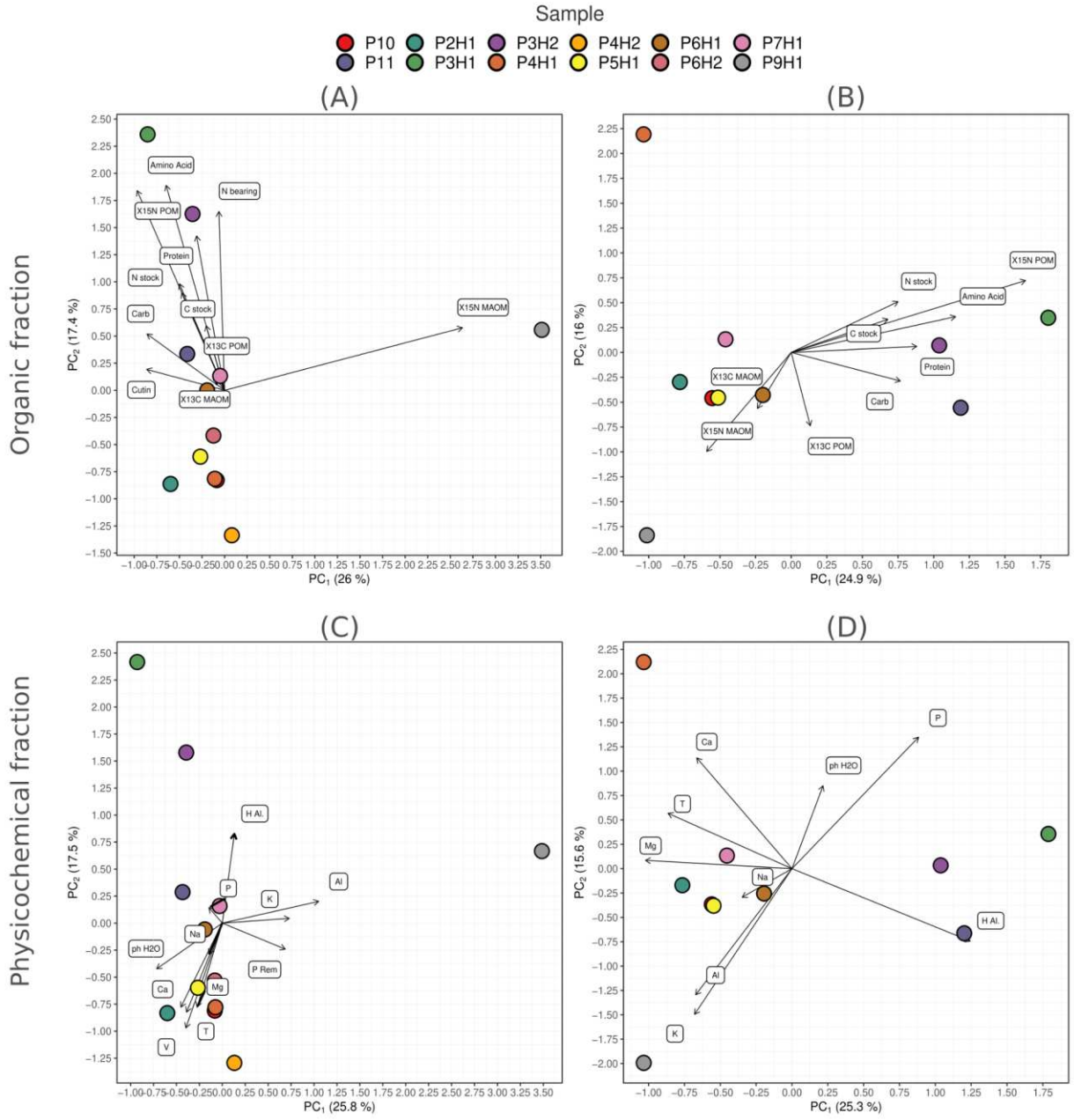

Figure 7: Redundancy Analysis (RDA) of bacterial (A, C) and fungal (B, D) communities and variables of the soil organic fraction (A, B) and physicochemical fraction (C, D). The numbers between parentheses display the percent of total variance explained by the axis.

4. Discussion

The Livingston Island provides an exceptional opportunity to understand better the interrelationships between biotic and abiotic factors acting on soil development and microbiological

properties in the absence of higher (vascular) plants. Although there are other studies about the bacterial [8] and fungal composition [47] present in soils of this island, to the best of our knowledge, this was only the second to study [48] at the same time both microbial communities. In view of the important role of the soil microbial community as the main actor in the biogeochemical cycling of these soils, in the present study provides information on the state of soil development and microbial community structure in the soils of the largest ice-free and most vegetation-covered area of maritime Antarctica, Byers Peninsula.

Previous studies indicated that the soil microbial community structure is influenced by local chemical and physical parameters, especially pH [49,50], grain size distribution, and soil moisture [51]. In Byers Peninsula, the Spearman's correlation showed a significant correlation of the microbial indexes with nutrient availability and composition of soil organic matter. In addition to correlation, redundancy analysis also showed that fungi depend more on soil organic composition than bacteria. Being basically heterotrophic organisms, these microorganisms cannot make their own food and require an external source to supply their nutritional needs [52,53]. In contrast, bacteria such as cyanobacteria can synthesize their food [53]. In addition, fungal biomass and activity are directly related to coarser soil fractions, unlike bacterial biomass and activity, which is more associated with finer fractions [54]. The texture of the studied soils was coarser, with abundant gravel in all profiles. Because of this, it is recognized that soil environmental factors change more rapidly in larger spaces than in smaller spaces, the greater association between the microbial indices associated with fungal communities and soil properties may be explainable.

Despite the importance attributed in several studies to pH as a critical factor for microbial communities and their growth [56–58], this predictor alone cannot play such an important role in shaping soil microbial diversity, with the ecological stability of the site playing a key role in the selection and maintenance of these communities [59]. The inexpressive correlation of pH with the microbial indices (diversity, evenness, richness) can be attributed to the fact that the pH values in the studied samples did not show significant variation, and the microbiological compositions are very varied between samples, resulting in the non-correlation between this attribute and the microbial indices[51]. The small variation in pH values may be attributed to the buffering of soil acidity by the high saturation by salts [60,61], since there is no presence of carbonates in the area and the base saturation ranged between 77.9 and 97.5%, reducing the relevance of this attribute in the correlation with microbial indices. Therefore, other physicochemical features of soil can be driving the microbial communities in these soils [62].

By evaluating the alpha-metrics, it was possible to observe the existing relationship between the microbial indices (diversity and richness of fungi and bacteria) and the dating done on the studied profiles. These data showed that the youngest dated profile (P7, 1,220 cal. yr BP) and the oldest (P4, 31,690 cal. yr BP) showed the highest values for the two microbial indices for both organisms. On the other hand, the profiles with intermediate ages (P10, 2,350; P6, 3,290; P3, 3,490 and P11, 12,030 cal. yr BP) showed greater

variability of these indices, without a pattern being seen as a function of age. This behavior can be explained through ecological niche theory [63,64]. Younger areas show many empty niches, which favor colonization by several organisms and result in a high diversity and richness. The intermediate areas between the dating have already undergone specific selections, culminating in specific niches due to resource competition, occurring in both selection and substitution of species, which results in high variability of diversity and richness indices, not allowing a standard behavior due to the instability of these environments. Finally, the older profile, having already gone through these selections, is possible in conditions of successional equilibrium close to a climax between organisms and specific niches selected and stable, thus allowing the observation of the high richness and diversity of fungi and bacteria.

In the present study, it was possible to observe a direct relationship between moisture regime in the studied profiles and microbial diversity and richness. The profiles with the presence of liquid water in the subsurface showed superior values compared to those with only the permafrost or those without water layer. Water is a limiting factor for microbial activity, where its absence or even soil rewetting processes affect the survival of certain microorganisms [65]. The absence of water is common in the soils of polar deserts [66]. Lack of water in soil can cause the death of many bacteria [67], although these organisms are more drought resistant than most fungi [68]. In wet permafrost-affected soils, on the other hand, rewetting of soil surface is common due to snowmelt and/or thawing of active layer in summer. High liquid available can provide favorable conditions for abrupt bacterial population growth compared to environments without the presence of water [69] This abrupt increase in soil rewetting conditions, a typical process that occurs in Maritime Antarctic soils, can cause variations among microbial diversity and richness indices, due to the reorganization of the microbiome as a function of resources such as moisture regime and nutrient availability. This can cause competition, alteration, and substitution in these communities, resulting in instability of this environment, which is reflected in the large variety of these indices among the bacterial and fungal communities in the soils of the Byers Peninsula, Maritime Antarctica.

4.1 Bacterial taxonomy and diversity

Although extreme climatic conditions on the Antarctic continent, studies focused on soil environments showed high bacterial diversity, with a high proportion of sequences that were only distinctly related to known sequences, indicating the existence of new species or genera [51,70–76]. In this study, we identified the dominant bacterial groups in a wide variety of soils on Livingston Island (Maritime Antarctica).

In the present study, the phyla Proteobacteria and Actinobacteriota were the most abundant. Among these, Actinobacteriota (13.63 to 47.1%), Proteobacteria (11.86 to 34%), Gemmatimonadata (3.68 to 20.51%), Chloroflexi (1.56 to 22.11%), Acidobacteriota (1.44 to 11.53%), and Bacteroidota (2.17 to

10.27%) are commonly found in temperate soils and are among the nine most abundant phylum described in soils [26,77,78], and also dominate microbial communities observed in Antarctic habitats [1,79–81]. The bacterial sequences detected in this study reveal a complex microbial community structure in different mineral soils under Antarctic Maritime climatic conditions [51]. Most of these bacterial sequences were detected with a high proportion of sequences that could not be affiliated with known genera identified in libraries. This is consistent with studies in other Antarctic soil environments [51,70–72,74].

The members of the phylum Proteobacteria constitute an average of 39% of soil bacterial communities, and its major members are classified into the classes Alphaproteobacteria, Betaproteobacteria, Gammaproteobacteria, and Deltaproteobacteria [77]. The class Gammaproteobacteria was the most abundant, with the genera *Polaromonas*, *Pseudomonas*, and *Ellin6067* as the main representatives.

The genus *Polaromonas* has been reported to have an interrelationship with microbial aging of Antarctic soils [26,82]. Its highest abundance was registered in the Pleistocene ^{14}C-dated horizon, the subsurface horizon of P4 associated with endolithic communities from the early colonization of these soils [83]. In addition to bacteria of the genus *Polaromas*, another genus associated with soil microbial weathering was the genus *Massilia* [84], which is in higher proportions in P6. Profile P6 had the highest organic C content, while profile P4 had the highest N content in its surface horizon, and these organisms may be associated with this C and N abundance. The second most representative bacterial genus was Pseudomonas. This genus has been described previously in exploratory work in Antarctica, where they have been associated with the degradation of polycyclic aromatic hydrocarbon and alkane compounds in soils [85,86]. The members of the genus *Ellin6067*, most abundant in profile P11 and P6, among the representatives of the class Gammaproteobacteria are functional microorganisms directly associated with the nitrogen cycle [87]. This clade associated with the genus *Nitrosospira* significantly contributes to ammonia-oxidizing bacteria, which can be found both in water and in epilithic biofilms [87,88]. In both profiles, the remarkable characteristic is the absence of permafrost and water layer, and this genus may be more associated with dry environments [89]. In addition, the highest diversity of mosses and lichens was observed and identified in these two profiles among the soils studied.

The phylum Actinobacteriota constitutes, on average, 13% of the soil bacterial communities [77]. In the analyzed samples, their abundance from 15.1 to 46.9%, mainly represented by the classes Actinobacteria (0.12% to 32.30%), Thermoleophilia (0.18% to 8.81%), and MB-A2-108 (0.13% to 7%). The predominance of this phylum is commonly reported in water [90] and soil [91,92] of Antarctica and was already reported as capable of surviving frozen for long periods (thousand to millions of years). The ubiquitous presence of these bacteria in the samples may be due to their high metabolic versatility, which allows them to be present in a wide range of very distinct soil types [93], contributing to carbon cycling and

performing an essential role in carbon cycling [94] and nitrogen fixation [95,96]. The species associated with the class Thermoleophilia are abundant and diverse, which play an essential role in geochemical cycling [97]. The main families found in this study were Solirubrobacteraceae, Gaiellaceae, and several uncultured taxa. The family Solirubrobacteraceae, which was most representative within the class Thermoleophilia, is distributed in six genera from six families, which were subsequently isolated from agricultural soils, activated sludge, and rhizospheric soil [98]. For these genera, identification at the species level was not possible to better visualize the genomic diversity of the Thermoleophilia class. However, representatives of these two cultured families may be able to fix CO_2 via the Calvin-Benson-Bassham (CBB) cycle and possess genes for *n*-alkane degradation, as main representatives *Gaiella occulta* and *Solirubrobacter soli* [98,99]. The taxa MB-A2-108, normally found associated with low soil organic carbon (SOC) environments [100,101], was present in all samples, where in general all showed low SOC contents.

4.2 Fungal taxonomy and diversity

Bacterial and fungal communities are key players in cycling the main elements of life: carbon, nitrogen, and phosphorus [96]. To date, about 1,000 fungal species have been described through macro- and/or micromorphology of colonies and fruiting bodies and DNA sequencing of mycelia of culturable fungi [102]. Our study used DNA sequencing with amplification of the ITS1 region to identify fungal representatives in Byers Peninsula soils. The wide variety of species recorded suggests that fungi make up the most diverse biota in Antarctic soils. The additional taxa identified through molecular research suggest an even greater diversity than estimated. However, fungi are commonly associated with higher organisms, and this diversity is still limited by the absence of large terrestrial animals and the limitation of higher plants, particularly those with woody components [102].

The fungal community was dominated by Mortierellomycota (0.63% to 94.38%), Ascomycota (3.17 % to 89.67%), Basidiomycota (0.48% to 31.29%), and Chytridiomycota (0.13% to 16.28%). The pattern of dominance observed in the fungal community structure of the Byers Peninsula soils indicates that a succession of species has already taken place. In environments newly colonized by fungi, the dominance of individuals of the genera Oomycota, Chytridiomycota, and Mucoromycota is usually observed, which in short precede saprophytic and pathogenic representatives, mainly from the phylum Ascomycota, and later colonization by the phylum Basidiomycota [103]. This dominance behavior was also observed in other studies conducted in Antarctica, both in soils [27] and lake sediments [104], both located in the Maritime Antarctic, thus indicating the dominance of these groups in the region's soils.

Mortierellomycota, had identification of 11 cultivated species (*Mortierella antarctica, M. basiparvispora, M. elongatula, M. alliacea, M. hyalina, M. polygonia, M. rishikesha, M. kuhlmanii, M. bainieri, M. alpina*) and three uncultured. The genus *Mortierella* has representative taxa that are commonly

found in Antarctica and abundant in associations with plants [105,106], lichens [107], and soil [108,109]. The species *M. antarctica* is considered endemic to the continent of Antarctica [109]. Species in the genus *Mortirrella* are characterized by producing bioactive fatty acids [109]. For example, *M. alpina* produces high levels of polyunsaturated fatty acids with antioxidant and antibacterial activities such as y-(gamma)linolenic acid and arachidonic acid [110], and *M. parvispora* produces arachidonic acid and di-homo-γ-linolenic acid [111].

The second most abundant phylum (Ascomycota) identified 68 cultivated and 67 uncultured species. The most representative genera were *Aspergillus* (0.22% to 73.98%), *Verrucaria* (0.16% to 39.85%), *Acremomium* (0.06% to 28.12%), *Cladosporium* (0.08% to 12%), *Pseudogymnoascus* (0.16% to 6.11%), *Epicoccum* (0.22% to 6.45%), and *Antarctomyces* (0.08% to 7.55%). While the *Verrucaria* genus comprises species that are usually found in the form of lichens, which are known as primary colonizers of soil in harsh conditions, the genus *Aspergillus* is comprised by well-known for their capacity to perform phosphate solubilization soils [112], enabling the use of this element for other organisms in soils where the scarcity of this nutrient occurs.

In the phylum Basidiomycota, 21 species were identified and 23 uncultured, among these, the most expressive genera in the samples were *Mrakia* (0.13% to 19.37%), *Phenoliferia* (0.05% to 22.12%), *Leucosporidium* (0.18% to 12.26%), *Mastigobasidium* (0.70% to 1.57%), and *Dioszegia* (0.06% to 1.99%). *Mrakia* and *Leucosporidium* are responsible for producing extracelular enzymes like pectinases that enable the organic matter decomposition [113,114]. Basidiomycetes are key players in producing cold-adapted enzymes for the organic matter decomposition, therefore their presence on this island enables the co-occurrence of other microorganisms. The phylum Basidiomycota is an essential decomposer fungi, where they strongly influence the rates and patterns of C release to the atmosphere, as well as the mineralization and immobilization of nutrients such as N and P in their biomass [115]. In the present study, the highest abundances of this phylum were associated with environments with higher C contents and higher plant density, dominated mainly by mosses and lichens (P3, P6, P7). Individuals belonging to this phylum can be isolated from soil, mosses, lichens, and even in the dung of penguins, petrels, and skuas [115].

Among the most abundant phyla, the Chytridiomycota was thelowest representativeness, where only one individual was identified to species level (*Paranamyces uniporus*) and five other species uncultured. As for the initial colonizers, especially representatives of the Chytridiomycota phylum, these were more abundant in profile P4, which presented pre-LGM ^{14}C dating data [83]. The ^{14}C dating, the isotopic signature reminiscent of trace contributions from endolithic communities [83], and the relative abundance of individuals of the phylum Chytridiomycota, considered one of the initial colonizers of environments, indicate that in this profile, the significant contribution of the fungal community to the microbial biomass. Furthermore, it was possible to observe that in the older profile, the abundance of fungi in succession to the initial colonizers was lower and there was a high abundance of taxa that were not amenable to identification

even with the use of current libraries. This may indicate that there is an even greater diversity of these organisms, which may be associated with early colonizers that have not yet been sequenced or new species of niche-specific fungi that have also not been identified.

Livingston Island is unique among the ecosystems of the South Shetland Islands. Although it has suffered from human interference associated with fishing and hunting, it has been little affected by tourism or research stations in recent decades. The retreat of the Rotch Dome glacier on the Byers Peninsula has provided a diverse and complex setting in terms of biogeochemical processes and agents (climate, fauna, flora, and microbiota) for the development of this environment. Thus, the Byers Peninsula is a highly suitable site for comparative studies with the rest of the Antarctic maritime region. It has a wide variety of freshwater bodies, which has made it a reference site for limnological studies, being considered the most important limnological site in the South Shetland Islands Archipelago (ISS) and the most vulnerable to human interference [16,17,116–119]. The Byers Peninsula is one of the most important areas from a geomorphological point of view [120]. Fluvial, periglacial, and cryogenic processes are dominant and decisive in soil formation in this environment, where Lithosols dominate, with widely distributed and discontinuous permafrost; Cryosols and Leptsols are also abundant [121]. The diverse vegetation dominated by lichens, mosses, and two species with flowers [122,123], and the favorable edaphoclimatic conditions for breeding and nesting of several mammals and birds, increase the importance of this environment considered a specially protected Antarctic area (ASPA No. 126) [16]. Given this, the microbial communities that act in this environment play a key role in maintaining ecosystem services, favoring the balance. Thus, more studies are still needed to better visualize the size of the microbial communities in Antarctic soils in general, given that these are more diverse than previously imagined, and this study further assisted in this visualization. However, the high abundance of taxa that have not been identified even with the help of the most up-to-date identification libraries needs to be further explored.

5. Conclusion

Despite the limitations in the databases, we observed a substantial diversity of bacteria and fungi in the soils evaluated in this study. These limitations found, reflect in the still underestimated microbial richness for the Antarctic environment.

The fungal community depend more on the soil reservoir of nitrogen and carbon, and some bacteria may act as key drivers for the input of carbon and nitrogen in these soils.

Permafrost represents a limitation for the microbial communities, directly affecting the diversity and richness of bacteria and fungi. In this regard, the conditions present in soils with permafrost limit the establishment of these communities more than the presence of water in liquid form (which by the results

exposed above allowed greater diversity and richness of bacteria and fungi) or the absence of water itself in the soil profile.

The behavior of the microbial communities, as a function of the ages observed for the soils studied, show a pattern of succession among these organisms from the colonization of more recent areas to the oldest areas that are already in a climax condition with their communities selected and well established.

Based on the large number of taxa that could not be identified, especially for fungi, it is of utmost importance further studies aimed at the replication of these organisms in laboratory conditions and their sequencing for better identification of these genera and species, which may be directly associated with the biogeochemical cycles that govern the various processes occurring in the soils of this environment.

Acknowledgments

We thank the CNPq (Conselho Nacional de Desenvolvimento Científico e Tecnológico), CAPES (Coordenação de Aperfeiçoamento de Pessoal de Nível Superior) and FAPEMIG (Fundação de Amparo à Pesquisa do Estado de Minas Gerais) for financial support. We are grateful to INCT da Criosfera, TERRANTAR and MARINHA DO BRASIL (PROANTAR PROGRAM) for financial support and field assistance. We thank the reviewers for their careful reading of the manuscript and their constructive remarks.

SUPPLEMENTARY DATA IN THE APENDIX B

Bibliographic references

1. Cary, S. C., McDonald, I. R., Barrett, J. E. & Cowan, D. A. On the rocks: the microbiology of Antarctic Dry Valley soils. *Nat. Rev. Microbiol. 2010 82* **8**, 129–138 (2010).
2. Olech, M. Human impact on terrestrial ecosystems in west Antarctica. in *Proceedings of the NIPR Symposium on Polar Biology* **9**, 299–306 (1996).
3. Czechowski, P., Clarke, L. J., Breen, J., Cooper, A. & Stevens, M. I. Antarctic eukaryotic soil diversity of the Prince Charles Mountains revealed by high-throughput sequencing. *Soil Biol. Biochem.* **95**, 112–121 (2016).
4. Lambrechts, S., Willems, A. & Tahon, G. Uncovering the Uncultivated Majority in Antarctic Soils: Toward a Synergistic Approach. *Front. Microbiol.* **10**, (2019).
5. Schellmann, K. & Kozel, S. A conquista da Antártica: signos e representações. *Rev. discente Expressões Geográficas* 15–26 (2005).
6. Cowan, D. A. *Antarctic Terrestrial Microbiology: Physical and Biological Properties of Antarctic Soils*. *Antarctic Terrestrial Microbiology: Physical and Biological Properties of Antarctic Soils* **9783642452**, (Springer Berlin Heidelberg, 2014).
7. Burton-Johnson, A., Black, M., Fretwell, P. T. & Kaluza-Gilbert, J. An automated methodology for differentiating rock from snow, clouds and sea in Antarctica from Landsat 8 imagery: a new rock outcrop map and area estimation for the entire Antarctic continent. *Cryosph.* **10**, 1665–1677 (2016).
8. Almela, P., Justel, A. & Quesada, A. Heterogeneity of Microbial Communities in Soils From the Antarctic Peninsula Region. *Front. Microbiol.* **12**, 280 (2021).
9. Singh, J., Singh, R. P. & Khare, R. Influence of climate change on Antarctic flora. *Polar Sci.* **18**, 94–101 (2018).
10. Abakumov, E. V. *et al.* Ornithogenic Factor of Soil Formation in Antarctica: A Review. *Eurasian Soil Sci.* **54**, 528–540 (2021).
11. Newsham, K. K. *et al.* Relationship between soil fungal diversity and temperature in the maritime Antarctic. *Nat. Clim. Chang.* **6**, 182–186 (2016).
12. Kim, D. *et al.* Passive warming effect on soil microbial community and humic substance degradation in maritime Antarctic region. *J. Basic Microbiol.* **58**, 513–522 (2018).
13. Boy, J. *et al.* Successional patterns along soil development gradients formed by glacier

retreat in the Maritime Antarctic, King George Island. *Rev. Chil. Hist. Nat.* **89**, 1–17 (2016).

14. Oliva, M. *et al.* The deglaciation of Barton Peninsula (King George Island, South Shetland Islands, Antarctica) based on geomorphological evidence and lacustrine records. *Polar Rec. (Gr. Brit).* **55**, 177–188 (2019).
15. Fernández-Fernández, J. M. *et al.* Ice thinning on nunataks during the glacial to interglacial transition in the Antarctic Peninsula region according to Cosmic-Ray Exposure dating: Evidence and uncertainties. *Quat. Sci. Rev.* **264**, 107029 (2021).
16. Oliva, M. *et al.* The Holocene deglaciation of the Byers Peninsula (Livingston Island, Antarctica) based on the dating of lake sedimentary records. *Geomorphology* **261**, 89–102 (2016).
17. Quesada, A., Camacho, A., Rochera, C. & Velázquez, D. Byers Peninsula: A reference site for coastal, terrestrial and limnetic ecosystem studies in maritime Antarctica. *Polar Sci.* **3**, 181–187 (2009).
18. Silva, A. B. *et al.* Spatial and temporal analysis of changes in the glaciers of the Antarctic Peninsula. *Glob. Planet. Change* **184**, 103079 (2020).
19. Schaefer, C. E. G. R. *et al.* Penguin activity modify the thermal regime of active layer in Antarctica: A case study from Hope Bay. *CATENA* **149**, 582–591 (2017).
20. Thomazini, A. *et al.* Geospatial variability of soil CO2–C exchange in the main terrestrial ecosystems of Keller Peninsula, Maritime Antarctica. *Sci. Total Environ.* **562**, 802–811 (2016).
21. Stomeo, F. *et al.* Abiotic factors influence microbial diversity in permanently cold soil horizons of a maritime-associated Antarctic Dry Valley. *FEMS Microbiol. Ecol.* **82**, 326–340 (2012).
22. Barrett, J. E. *et al.* Biogeochemical stoichiometry of Antarctic Dry Valley ecosystems. *J. Geophys. Res. Biogeosciences* **112**, 1010 (2007).
23. Uroz, S., Calvaruso, C., Turpault, M.-P. & Frey-Klett, P. Mineral weathering by bacteria: ecology, actors and mechanisms. *Trends Microbiol.* **17**, 378–387 (2009).
24. Spohn, M. Element cycling as driven by stoichiometric homeostasis of soil microorganisms. *Basic Appl. Ecol.* **17**, 471–478 (2016).
25. Saccá, M. L., Barra Caracciolo, A., Di Lenola, M. & Grenni, P. Ecosystem Services

Provided By Soil Microorganisms. in *Soil Biological Communities and Ecosystem Resilience* 9–24 (Springer International Publishing, 2017). doi:10.1007/978-3-319-63336-7_2

26. Meier, L. A. *et al.* Pedogenic and microbial interrelation in initial soils under semiarid climate on James Ross Island, Antarctic Peninsula region. *Biogeosciences* **16**, 2481–2499 (2019).
27. Rosa, L. H. *et al.* DNA metabarcoding uncovers fungal diversity in soils of protected and non-protected areas on Deception Island, Antarctica. *Sci. Rep.* **10**, 21986 (2020).
28. Bockheim, J. G. & Gennadiyev, A. N. The role of soil-forming processes in the definition of taxa in Soil Taxonomy and the World Soil Reference Base. *Geoderma* **95**, 53–72 (2000).
29. Teixeira, P., Donagemma, G. & Teixeira, W. *Manual de métodos de análise de solo*. (Embrapa, 2017).
30. Alvarez, V. H., Novais, R. F., Dias, L. E. & Oliveira, J. A. Determinação e uso do fósforo remanescente. *Bol. da Soc. Bras. Ciência do Solo* **25**, 27–32 (2000).
31. Cambardella, C. A. & Elliott, E. T. Particulate Soil Organic-Matter Changes across a Grassland Cultivation Sequence. *Soil Sci. Soc. Am. J.* **56**, 777–783 (1992).
32. Chefetz, B., Chen, Y., Clapp, C. E. & Hatcher, P. G. Characterization of Organic Matter in Soils by Thermochemolysis Using Tetramethylammonium Hydroxide (TMAH). *Soil Sci. Soc. Am. J.* **64**, 583–589 (2000).
33. Del Rio, J. C. *et al.* Structural characterization of bio- and geo-macromolecules by off-line thermochemolysis with tetramethylammonium hydroxide. *J. Chromatogr. A* **823**, 433–448 (1998).
34. Hogg, A. G. *et al.* SHCal13 Southern Hemisphere Calibration, 0–50,000 Years cal BP. *Radiocarbon* **55**, 1889–1903 (2013).
35. Ramsey, C. B. Bayesian Analysis of Radiocarbon Dates. *Radiocarbon* **51**, 337–360 (2009).
36. Högfors-Rönnholm, E., Christel, S., Engblom, S. & Dopson, M. Indirect DNA extraction method suitable for acidic soil with high clay content. *MethodsX* **5**, 136–140 (2018).
37. Yu, Y., Lee, C., Kim, J. & Hwang, S. Group-specific primer and probe sets to detect methanogenic communities using quantitative real-time polymerase chain reaction.

Biotechnol. Bioeng. **89**, 670–679 (2005).

38. Veloso, T. G. R. *et al.* Effects of environmental factors on microbiota of fruits and soil of Coffea arabica in Brazil. *Sci. Rep.* **10**, 14692 (2020).
39. Bolyen, E. *et al.* Reproducible, interactive, scalable and extensible microbiome data science using QIIME 2. *Nat. Biotechnol.* **37**, 852–857 (2019).
40. Callahan, B. J. *et al.* DADA2: High-resolution sample inference from Illumina amplicon data. *Nat. Methods* **13**, 581–583 (2016).
41. Quast, C. *et al.* The SILVA ribosomal RNA gene database project: improved data processing and web-based tools. *Nucleic Acids Res.* **41**, D590–D596 (2012).
42. Nilsson, R. H. *et al.* The UNITE database for molecular identification of fungi: handling dark taxa and parallel taxonomic classifications. *Nucleic Acids Res.* **47**, D259–D264 (2019).
43. McMurdie, P. J. & Holmes, S. phyloseq: An R Package for Reproducible Interactive Analysis and Graphics of Microbiome Census Data. *PLoS One* **8**, e61217 (2013).
44. Lahti, L., Shetty, S., Blake, T. & Salojarvi, J. Introduction to the microbiome R package. (2017). Available at: https://microbiome.github.io/tutorials/. (Accessed: 17th November 2022)
45. Cannone, N., Wagner, D., Hubberten, H. W. & Guglielmin, M. Biotic and abiotic factors influencing soil properties across a latitudinal gradient in Victoria Land, Antarctica. *Geoderma* **144**, 50–65 (2008).
46. Kõljalg, U. *et al.* The Taxon Hypothesis Paradigm—On the Unambiguous Detection and Communication of Taxa. *Microorganisms* **8**, 1910 (2020).
47. Newsham, K. K., Davey, M. L., Hopkins, D. W. & Dennis, P. G. Regional Diversity of Maritime Antarctic Soil Fungi and Predicted Responses of Guilds and Growth Forms to Climate Change. *Front. Microbiol.* **11**, 3575 (2021).
48. Guajardo-Leiva, S. *et al.* Source and acquisition of rhizosphere microbes in Antarctic vascular plants. *Front. Microbiol.* **13**, 3376 (2022).
49. Chong, C. W. *et al.* High levels of spatial heterogeneity in the biodiversity of soil prokaryotes on Signy Island, Antarctica. *Soil Biol. Biochem.* **42**, 601–610 (2010).
50. Siciliano, S. D. *et al.* Soil fertility is associated with fungal and bacterial richness, whereas pH is associated with community composition in polar soil microbial communities. *Soil*

Biol. Biochem. **78**, 10–20 (2014).

51. Ganzert, L., Lipski, A., Hubberten, H. W. & Wagner, D. The impact of different soil parameters on the community structure of dominant bacteria from nine different soils located on Livingston Island, South Shetland Archipelago, Antarctica. *FEMS Microbiol. Ecol.* **76**, 476–491 (2011).
52. Effmert, U., Kalderás, J., Warnke, R. & Piechulla, B. Volatile Mediated Interactions Between Bacteria and Fungi in the Soil. *J. Chem. Ecol. 2012 386* **38**, 665–703 (2012).
53. Gupta, A. *et al.* Microbes and Environment. *Princ. Appl. Environ. Biotechnol. a Sustain. Futur.* 43–84 (2017). doi:10.1007/978-981-10-1866-4_3
54. Chiu, C. Y., Chen, T. H., Imberger, K. & Tian, G. Particle size fractionation of fungal and bacterial biomass in subalpine grassland and forest soils. *Geoderma* **130**, 265–271 (2006).
55. Kandeler, E. *et al.* Structure and function of the soil microbial community in microhabitats of a heavy metal polluted soil. *Biol. Fertil. Soils 2000 325* **32**, 390–400 (2000).
56. Lauber, C. L., Hamady, M., Knight, R. & Fierer, N. Pyrosequencing-based assessment of soil pH as a predictor of soil bacterial community structure at the continental scale. *Appl. Environ. Microbiol.* **75**, 5111–5120 (2009).
57. Nacke, H. *et al.* Pyrosequencing-Based Assessment of Bacterial Community Structure Along Different Management Types in German Forest and Grassland Soils. *PLoS One* **6**, e17000 (2011).
58. Kaiser, K. *et al.* Driving forces of soil bacterial community structure, diversity, and function in temperate grasslands and forests. *Sci. Reports 2016 61* **6**, 1–12 (2016).
59. Cho, S. J., Kim, M. H. & Lee, Y. O. Effect of pH on soil bacterial diversity. *J. Ecol. Environ.* **40**, 1–9 (2016).
60. Souza, J. J. L. L. *et al.* Hydrogeochemistry of sulfate-affected landscapes in Keller Peninsula, Maritime Antarctica. *Geomorphology* **155**–**156**, 55–61 (2012).
61. Lopes, D. do V., Souza, J. J. L. L. de, Simas, F. N. B., Oliveira, F. S. de & Schaefer, C. E. G. R. Hydrogeochemistry and chemical weathering in a periglacial environment of Maritime Antarctica. *CATENA* **197**, 104959 (2021).
62. Dequiedt, S. *et al.* Biogeographical patterns of soil molecular microbial biomass as influenced by soil characteristics and management. *Glob. Ecol. Biogeogr.* **20**, 641–652 (2011).

63. Vandermeer, J. H. Niche theory. *Annu. Rev. Ecol. Syst.* 107–132 (1972).
64. Pocheville, A. The Ecological Niche: History and Recent Controversies. in *Handbook of Evolutionary Thinking in the Sciences* 547–586 (Springer Netherlands, 2015). doi:10.1007/978-94-017-9014-7_26
65. Meisner, A., Jacquiod, S., Snoek, B. L., Ten Hooven, F. C. & van der Putten, W. H. Drought legacy effects on the composition of soil fungal and prokaryote communities. *Front. Microbiol.* **9**, 294 (2018).
66. Van Horn, D. J. *et al.* Soil microbial responses to increased moisture and organic resources along a salinity gradient in a polar desert. *Appl. Environ. Microbiol.* **80**, 3034–3043 (2014).
67. Manzanera, M. Dealing with water stress and microbial preservation. *Environ. Microbiol.* **23**, 3351–3359 (2021).
68. Mekala, S. & Polepongu, S. Impact of climate change on soil microbial community. *Plant Biot. Interact. State Art* 31–41 (2019). doi:10.1007/978-3-030-26657-8_3/COVER
69. Denef, K. *et al.* Influence of dry–wet cycles on the interrelationship between aggregate, particulate organic matter, and microbial community dynamics. *Soil Biol. Biochem.* **33**, 1599–1611 (2001).
70. Shivaji, S., Reddy, G. S., Aduri, R. P., Kutty, R. & Ravenschlag, K. Bacterial diversity of a soil sample from Schirmacher Oasis, Antarctica. *Cell. Mol. Biol. (Noisy-le-grand).* **50**, 525–536 (2004).
71. Saul, D. J., Aislabie, J. M., Brown, C. E., Harris, L. & Foght, J. M. Hydrocarbon contamination changes the bacterial diversity of soil from around Scott Base, Antarctica. *FEMS Microbiol. Ecol.* **53**, 141–155 (2005).
72. Aislabie, J. M., Jordan, S. & Barker, G. M. Relation between soil classification and bacterial diversity in soils of the Ross Sea region, Antarctica. *Geoderma* **144**, 9–20 (2008).
73. Smith, J. J., Tow, L. A., Stafford, W., Cary, C. & Cowan, D. A. Bacterial Diversity in Three Different Antarctic Cold Desert Mineral Soils. *Microb. Ecol.* **51**, 413–421 (2006).
74. Shravage, B. V., Dayananda, K. M., Patole, M. S. & Shouche, Y. S. Molecular microbial diversity of a soil sample and detection of ammonia oxidizers from Cape Evans, Mcmurdo Dry Valley, Antarctica. *Microbiol. Res.* **162**, 15–25 (2007).

75. Yergeau, E., Newsham, K. K., Pearce, D. A. & Kowalchuk, G. A. Patterns of bacterial diversity across a range of Antarctic terrestrial habitats. *Environ. Microbiol.* **9**, 2670–2682 (2007).
76. Niederberger, T. D. *et al.* Microbial community composition in soils of Northern Victoria Land, Antarctica. *Environ. Microbiol.* **10**, 1713–1724 (2008).
77. Janssen, P. H. Identifying the dominant soil bacterial taxa in libraries of 16S rRNA and 16S rRNA genes. *Appl. Environ. Microbiol.* **72**, 1719–1728 (2006).
78. Chown, S. L. *et al.* The changing form of Antarctic biodiversity. *Nature* **522**, 431–438 (2015).
79. Bajerski, F. *et al.* Chryseobacterium frigidisoli sp. nov., a psychrotolerant species of the family Flavobacteriaceae isolated from sandy permafrost from a glacier forefield. *Int. J. Syst. Evol. Microbiol.* **63**, 2666–2671 (2013).
80. Chong, C. W., Pearce, D. A., Convey, P., Yew, W. C. & Tan, I. K. P. Patterns in the distribution of soil bacterial 16S rRNA gene sequences from different regions of Antarctica. *Geoderma* **181**–**182**, 45–55 (2012).
81. Pearce, D. A. *et al.* Metagenomic analysis of a southern maritime Antarctic soil. *Front. Microbiol.* **3**, 403 (2012).
82. Frey, B. *et al.* Weathering-Associated bacteria from the damma glacier forefield: Physiological capabilities and impact on granite dissolution. *Appl. Environ. Microbiol.* **76**, 4788–4796 (2010).
83. da Silva, J. P., Lelis Leal de Souza, J. J., Mercês Barros Soares, E. & Schaefer, C. E. G. R. Soil organic matter accumulation before, during, and after the last glacial maximum in Byers Peninsula, Maritime Antarctica. *Geoderma* 116221 (2022). doi:10.1016/j.geoderma.2022.116221
84. Qi-Wang, Ma, G. Y., He, L. Y. & Sheng, X. F. Characterization of bacterial community inhabiting the surfaces of weathered bricks of Nanjing Ming city walls. *Sci. Total Environ.* **409**, 756–762 (2011).
85. Aislabie, J., Foght, J. & Saul, D. Aromatic hydrocarbon-degrading bacteria from soil near Scott Base, Antarctica. *Polar Biol. 2000 233* **23**, 183–188 (2000).
86. Ma, H. *et al.* Pseudomonas, the dominant polycyclic aromatic hydrocarbon-degrading bacteria isolated from Antarctic soils and the role of large plasmids in horizontal gene

transfer. *Environ. Microbiol.* **8**, 455–465 (2006).

87. Gao, J. *et al.* The Tolerance of Anoxic-Oxic (A/O) Process for the Changing of Refractory Organics in Electroplating Wastewater: Performance, Optimization and Microbial Characteristics. *Process. 2021, Vol. 9, Page 962* **9**, 962 (2021).
88. Podlesnaya, G. V. *et al.* Diversity of nitrifying bacteria in microbial communities from water and epilithic biofilms of the Lake Baikal littoral zone. *Limnol. Freshw. Biol.* 1008–1010 (2020). doi:10.31951/2658-3518-2020-A-4-1008
89. Liu, H. *et al.* Insight into functional microorganisms in wet-dry conversion to alleviate the toxicity of chromium fractions in red soil. *Front. Microbiol.* **13**, 977171–977171 (2022).
90. Liu, K. *et al.* Bacterial community composition and diversity in Kalakuli, an alpine glacial-fed lake in Muztagh Ata of the westernmost Tibetan Plateau. *FEMS Microbiol. Ecol.* **93**, (2017).
91. Rego, A. *et al.* Actinobacteria and cyanobacteria diversity in terrestrial Antarctic microenvironments evaluated by culture-dependent and independent methods. *Front. Microbiol.* **10**, 1018 (2019).
92. Silva, L. J. *et al.* Actinobacteria from Antarctica as a source for anticancer discovery. *Sci. Reports 2020 101* **10**, 1–15 (2020).
93. van Bergeijk, D. A., Terlouw, B. R., Medema, M. H. & van Wezel, G. P. Ecology and genomics of Actinobacteria: new concepts for natural product discovery. *Nat. Rev. Microbiol. 2020 1810* **18**, 546–558 (2020).
94. Araujo, R. *et al.* Biogeography and emerging significance of Actinobacteria in Australia and Northern Antarctica soils. *Soil Biol. Biochem.* **146**, 107805 (2020).
95. Zhang, B. *et al.* Variation in Actinobacterial Community Composition and Potential Function in Different Soil Ecosystems Belonging to the Arid Heihe River Basin of Northwest China. *Front. Microbiol.* **10**, 2209 (2019).
96. Ortiz, M. *et al.* Microbial Nitrogen Cycling in Antarctic Soils. *Microorg. 2020, Vol. 8, Page 1442* **8**, 1442 (2020).
97. Hu, D., Zang, Y., Mao, Y. & Gao, B. Identification of molecular markers that are specific to the class thermoleophilia. *Front. Microbiol.* **10**, 1185 (2019).
98. Li, C. *et al.* Miltoncostaea marina gen. nov. sp. nov., and Miltoncostaea oceani sp. nov., a novel deep branching phylogenetic lineage within the class Thermoleophilia isolated from

marine environments, and proposal of Miltoncostaeaceae fam. nov. and Miltoncostaeales ord. nov. *Syst. Appl. Microbiol.* **44**, 126216 (2021).

99. Severino, R. *et al.* High-quality draft genome sequence of Gaiella occulta isolated from a 150 meter deep mineral water borehole and comparison with the genome sequences of other deep-branching lineages of the phylum Actinobacteria. *Microbiologyopen* **8**, e00840 (2019).
100. Goh, Y. K., Zoqratt, M. Z. H. M., Goh, Y. K., Ayub, Q. & Ting, A. S. Y. Discovering naturally-occurring microbiota in disease suppressive soil: Potential role of biological elements in suppressing Ganoderma boninense. *Biol. Control* **165**, 104787 (2022).
101. Fu, X., Wang, J., Xie, M., Zhao, F. & Doughty, R. Increasing temperature can modify the effect of straw mulching on soil C fractions, soil respiration, and microbial community composition. *PLoS One* **15**, e0237245 (2020).
102. Bridge, P. D. & Spooner, B. M. Non-lichenized Antarctic fungi: transient visitors or members of a cryptic ecosystem? *Fungal Ecol.* **5**, 381–394 (2012).
103. *Principles and Applications of Soil Microbiology*. (Elsevier, 2021). doi:10.1016/C2018-0-05260-3
104. Ogaki, M. B. *et al.* Diversity of fungal DNA in lake sediments on Vega Island, north-east Antarctic Peninsula assessed using DNA metabarcoding. *Extremophiles* **25**, 257–265 (2021).
105. Carvalho, C. R. *et al.* Cultivable fungi associated with bryosphere of bipolar mosses Polytrichastrum alpinum and Polytrichum juniperinum in King George Island, South Shetland Islands, Maritime Antarctica. *Polar Biol.* **43**, 545–553 (2020).
106. Rosa, L. H. *et al.* Opportunistic fungi found in fairy rings are present on different moss species in the Antarctic Peninsula. *Polar Biol.* **43**, 587–596 (2020).
107. Santiago, I. F., Soares, M. A., Rosa, C. A. & Rosa, L. H. Lichensphere: a protected natural microhabitat of the non-lichenised fungal communities living in extreme environments of Antarctica. *Extremophiles* **19**, 1087–1097 (2015).
108. Bridge, P. D. & Newsham, K. K. Soil fungal community composition at Mars Oasis, a southern maritime Antarctic site, assessed by PCR amplification and cloning. *Fungal Ecol.* **2**, 66–74 (2009).
109. Gomes, E. C. Q. *et al.* Cultivable fungi present in Antarctic soils: taxonomy, phylogeny,

diversity, and bioprospecting of antiparasitic and herbicidal metabolites. *Extremophiles* **22**, 381–393 (2018).

110. Melo, I. S. *et al.* Isolation and biological activities of an endophytic Mortierella alpina strain from the Antarctic moss Schistidium antarctici. *Extremophiles* **18**, 15–23 (2014).
111. Hou, C. New bioactive fatty acids. *Asia Pacific J. Clin.* **17**, 192–195 (2008).
112. Singh, S. M. *et al.* Phosphate solubilizing ability of two Arctic Aspergillus niger strains. *Polar Res.* **30**, (2011).
113. DA SILVA, M. K. *et al.* Extracellular hydrolytic enzymes produced by yeasts from Antarctic lichens. *An. Acad. Bras. Cienc.* **94**, 20210540 (2022).
114. Troncoso, E. *et al.* Identification and characterization of yeasts isolated from the South Shetland Islands and the Antarctic Peninsula. *Polar Biol.* **40**, 649–658 (2017).
115. Ludley, K. E. & Robinson, C. H. 'Decomposer' Basidiomycota in Arctic and Antarctic ecosystems. *Soil Biol. Biochem.* **40**, 11–29 (2008).
116. Convey, P., Greenslade, P., Richard, K. J. & Block, W. The terrestrial arthropod fauna of the Byers Peninsula, Livingston Island, South Shetland Islands - Collembola. *Polar Biol.* **16**, 257–259 (1996).
117. Rodriguez, P. & Rico, E. A new freshwater oligochaete species (Clitellata: Enchytraeidae) from Livingston Island, Antarctica. *Polar Biol.* **31**, 1267–1279 (2008).
118. Toro, M. *et al.* Limnological characteristics of the freshwater ecosystems of Byers Peninsula, Livingston Island, in maritime Antarctica. *Polar Biol.* **30**, 635–649 (2007).
119. Van de Vijver, B., Agius, J. T., Gibson, J. A. E. & Quesada, A. AN UNUSUAL SPINE-BEARING PINNULARIA SPECIES FROM THE ANTARCTIC LIVINGSTON ISLAND (SOUTH SHETLAND ISLANDS). *Diatom Res.* **24**, 431–441 (2009).
120. Benayas, J. *et al.* A review of scientific research trends within ASPA No. 126 Byers Peninsula, South Shetland Islands, Antarctica. *Antarct. Sci.* **25**, 128–145 (2013).
121. Moura, P. A., Francelino, M. R., Schaefer, C. E. G. R., Simas, F. N. B. & de Mendonça, B. A. F. Distribution and characterization of soils and landform relationships in Byers Peninsula, Livingston Island, Maritime Antarctica. *Geomorphology* **155**–**156**, 45–54 (2012).
122. Ochyra, R., Smith, R. L. & Bednarek-Ochyra, H. *The illustrated moss flora of Antarctica.* (Cambridge University Press, 2008).

123. Vera, M. L. Colonization and demographic structure of Deschampsia antarctica and Colobanthus quitensis along an altitudinal gradient on Livingston Island, South Shetland Islands, Antarctica. *Polar Res.* **30**, 7146 (2011).

Paper 3

PAPER 3: Biochemical, elemental and molecular composition of soil organic matter: a case study in soils of the Byers Peninsula, Maritime Antarctica

Jônatas Pedro da Silva [a, b]*, José João Lelis Leal de Souza [b], Deborah Pinheiro Dick [c, d], Rafael da Silva Teixeira [b], Emanuelle Mercês Barros Soares [b], Carlos Ernesto G. R. Schaefer [b]

[a] Ph. D. student Program in Soils and Plant Nutrition, Department of Soils, Federal University of Viçosa - UFV, Viçosa - MG, Brazil

[b] Department of Soils, Federal University of Viçosa - UFV, Viçosa - MG, Brazil

[c] Soil Science Department, Federal University of Rio Grande do Sul, UFRGS, Av. Bento Goncalves, 7712 Porto Alegre, 91540-000, Brazil

[d] Institute of Chemistry, UFRGS, Av. Bento Goncalves, 9500 Porto Alegre, 91501-970, Brazil

* Corresponding author:

Telephone: +55 31 9 8357-2450

E-mail: jpedro.agronomo@gmail.com

Abstract

The current knowledge state about the quality and SOM stocks in the polar regions still presents poorly constrained estimates. Understanding the SOM dynamics in Antarctica is fundamental for a better understanding of the functioning of terrestrial ecosystems and analysis of the possible impacts of global climate change. Our objective was to investigate the molecular organization of SOM, from several selected soils of the Byers Peninsula, Maritime Antarctica; to assess the potential vulnerability of soil organic matter to possible mineralization processes and to estimate the C and N stocks in these soils and their possible sources of input into this system. Thirteen soil profiles were dug, described and classified. Soil chemical and physical attributes were determined. The C and N contents and stocks, $\delta^{13}C$ and $\delta^{15}N$ ratio isotopes were determined in the SOM physical size-fractionated particles. The plant species present in each site was identified and listed according to the specific literature for Antarctic vegetation. The most abundant species from each site were also collected to analyze their elemental composition and their isotopic signatures. The biochemical composition of the SOM fractions (POM and MAOM) as well as the plant materials was evaluated using an off-line TMAH -mediated thermochemolysis procedure. Investigation by ^{13}C NMR CP/MAS was performed on global samples. In general, C and N stocks decreased with increasing soil depth for most of the profiles studied. The exception to this behavior was observed in profiles P1, P2, P3, P5 and P8. The profiles that presented the greatest C and N stocks were those associated with low and high platforms, with emphasis on soils with more pronounced evidence of cryoturbation. For all samples analyzed, the isotopic signatures of both $\delta^{13}C$ and $\delta^{15}N$ showed overlaps for both fractions of the MOS as well as in the plant materials. The isotopic signatures analyzed in the MAOM fraction, identified the contribution of marine organic materials (P1, P2, P5 and P12), ornithogenic organic materials (P7, P8, P9 and P13), and a signature

associated with endolithic organic matter in P4, the profile with the oldest record ever dated to Maritime Antarctica. The dominance of the compounds identified in the plant materials was lipid compounds, similar to the pattern observed for the SOM fractions. The presence of lignin-derived compounds was observed only in the *Deschampsia antarctica* grass with a relative abundance of 6.5%. Evaluating the structure of the carbon chains of the compounds identified in the SOM fractions, in general, there is a predominance in all profiles of aliphatic compounds (60% to 95% of relative abundance in MAOM fraction and 51% to 96% in the POM fraction). The predominance in all profiles is of compounds of lipid origin in both fractions (POM - 39.02 to 91.07% and MAOM - 40.39 to 96%). All analyzed samples by ^{13}C NMR-CP/MAS showed what the most abundant groups were alkyl C and aryl C groups, whose proportions ranged from 27 to 46%, and 32 to 46% respectively. The O-alkyl C and carbonyl C groups contributed in smaller proportions to the SOM_{HF} composition, between 13 and 35% and 6 and 22%, respectively. Byers Peninsula soils showed a diverse and varied biochemical nature of SOM, resulting in varying levels of C and N as well as their constituents, showing a large contribution of lipid compounds derived from both plant and animal sources, these being dominated by long chain hydrocarbons reflecting the hydrophobicity of this organic matter. Differences of SOM content indicate that deglaciation has led to the loss of a large portion of the labile organic matter and suggest that the residual organic matter acts to stabilize hydrolytic enzyme activities. The stabilizing action implies a saving in enzyme synthesis and to a certain extent should mitigate the biochemical degradation associated with the loss of soil organic matter. The largest C and N pools were recorded on the high and low platforms and in the organo-mineral association fraction, where not all Cryosols followed a pattern of increase in depth. The isotopic signatures found in the SOM fractions of the Byers Peninsula soils revealed a wide variation of potential C sources in these soils, these being reflective of the colonization of these areas and landscape development/transformation, indicating different geological stages of SOM accumulation in this area.

Keywords: off-line TMAH -mediated thermochemolysis, ^{13}C NMR CP/MAS, SOM fractions, C and N stocks, $\delta^{13}C$ and $\delta^{15}N$ isotopic signatures.

1. Introduction

The accelerated warming observed in the last 50 years for the Maritime Antarctica region will have widespread effects on this region and its other polar ecosystems (Turner et al., 2014). Consequently, it is expected that the increase in air temperature resulting from global warming will strongly affect the expansion of vegetation and the colonization of ice-free areas, biological activity, the physical and chemical attributes of the soil, as well as the dynamics of soil organic matter (SOM) in these periglacial environments (Amesbury et al., 2017; Charman et al., 2018; Schaefer et al., 2017; Thomazini et al., 2016). This expansion tends to favor SOM mineralization and consequent carbon (C) losses from these ecosystems, where the SOM composition is less resistant to microbial degradation

when compared to SOM from other global regions (Carvalho et al., 2013). Due to this possible degradation of SOM, polar SOM represents a vulnerable reservoir of organic carbon, susceptible to being remobilized under increasing temperatures (Abakumov, 2017).

Understanding the SOM dynamics in Antarctica is fundamental for a better understanding of the functioning of terrestrial ecosystems and analysis of the possible impacts of global climate change (Beyer et al., 2004; Michel et al., 2006; Simas et al., 2006). Accurate knowledge of their spatial distribution is needed, both in terms of quantity and quality (i.e. biodegradability capacity, biochemical and molecular composition, and degree of humification) (Abakumov, 2017; Fritz et al., 2015). Information on the nature and SOM dynamics in Maritime Antarctica is still incipient, making it necessary to know its elemental and biochemical constitution (C, N, P, S, lignin, tannins, polyphenols, lipids), its origin, and composition of physical fractions of SOM, for a better understanding of the mechanisms and processes of formation and estabilization of organic matter in this environment. Through this understanding, it will be possible to prospect for future scenarios regarding C stocks in this environment, as well as C emissions into the atmosphere.

The current knowledge state about the quality and SOM stocks in the polar regions still presents poorly constrained estimates (Hugelius et al., 2014). In specific for Antarctica this is due to the high content of the coarse soil fractions and the high variability of carbon content in the fine soil (Abakumov, 2017). Such uncertainties for SOM storage in polar environments become even more important for SOM quality (Abakumov and Mukhametova, 2014; Mishra et al., 2013). In previous investigations of the structure and molecular composition of organic matter in soils from East Antarctic by ^{13}C-NMR methods, it was shown that in the most common organomineral soils aliphatic carbon prevails over aromatic, due to the nature of the non-ligniferous material as precursor (Calace et al., 1995). Later it was shown that this feature is typical for many soils from different Antarctic soils (Abakumov, 2010) and even soils, formed on penguin rocks shows the same trends of prevalence of aliphatic compounds from aromatic ones (Abakumov and Fattakhova, 2015).

Our objective was to investigate the molecular organization of SOM, from several selected soils from the Byers Peninsula (Livingston Island - Maritime Antarctica); to assess the potential vulnerability of soil organic matter to possible mineralization processes and to estimate the C and N stocks in these soils and their possible sources of input into this system. This was addressed through a) the quantification of SOM, and b) the characterization of SOM quality through elemental analysis, isotope ratio mass spectrometry, solid-state ^{13}C-NMR spectroscopy, and gas chromatography coupled to mass spectrometry.

2. Material and Methods

2.1. Study area

Detailed information on the description and characterization of the study area (location, climatic condition, geomorphological characterization) can be found elsewhere (da Silva et al., 2022). Briefly, the study area is considered one of the largest ice-free areas in Maritime Antarctica. It is located in one of Antarctica's Specially Protected Areas (ASPA No. 126) (Oliva et al., 2016). The Byers Peninsula is subject to a polar oceanic climate regime (Barsch et al., 1985; Lopez-Martinez et al., 1996), and has a mutually varied and diverse vegetation and flora in terms of numbers of species already described (Benayas et al., 2013). In addition, it presents a diverse geology formed basically by pyritized andesite (Juro-Cretaceous), Pre-Holocene marine sediments, basalt, andesite, and volcanic (igneous) rocks (Juro-Cretaceous).

2.2. Selection, description and classification of soil profiles and plant materials

Aiming for greater geoenvironmental representativeness (altitude, presence of patterned soils, presence and absence of vegetation), thirteen soil profiles (Fig. 1) were dug, described and classified according to Soil Taxonomy (ST) and World Reference Base (WRB). At the study and comparison level, these profiles were grouped into: acid sulfated soil (P1), high platforms (P3, P4, P10), low platforms (P2, P5, P6, P11, P12), and high beaches (P7, P8, P9, P13). Detailed information about the profiles (general description of pedons; chemical, morphological and physical properties of soils) can be found elsewhere (da Silva et al., 2022).

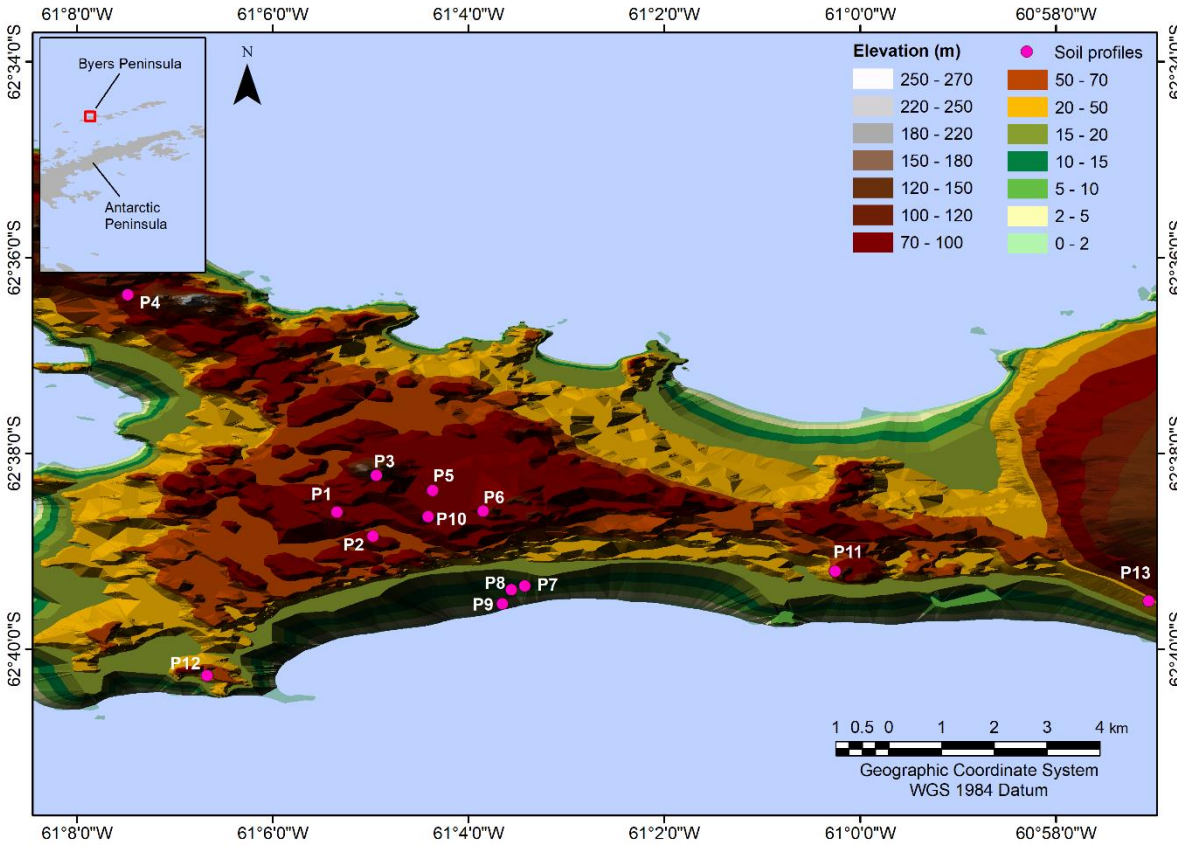

Figure 1. Location of Byers Peninsula in the South Shetlands and distribution of soil profiles collected in Byers Peninsula, Livingston Island, Maritime Antarctica (da Silva et al., 2022).

The plant species present in each site was identified and listed according to the specific literature for Antarctic vegetation, such as Ochyra (1998), Ochyra et al. (2008) and Putzke and Pereira (2001) for mosses and Olech (2004), Øvstedal and Smith (2001) and Redón (1985) for lichens (Table S1). The most abundant species from each site were also collected to analyze their elemental composition and their isotopic signatures (Table 1).

Table 1. Plant species identified and collected on soils from the Byers Peninsula, Antarctic Maritime

Soil profile	Coordinates	Dominant Species	Group	Identification	C (%)	$\delta^{13}C$ (‰)	N (%)	$\delta^{15}N$ (‰)	C/N Ratio
P2	62° 38’ 50.90” S 61° 04’ 58.54” W	*Hymenoloma grimmiaceum* (Müll. Hal.) Ochyra	Moss	HG	3.19	-25.01	0.17	-0.49	19.14
P3	62° 38’ 13.6” S 61° 04’ 56.3” W	*Usnea aurantiaco-atra* (Jacq.) Bory	Lichen	UA	40.89	-21.49	0.74	-11.05	55.37
P4	62° 38’ 22.9” S 61° 07’ 28.7” W	*Sanionia uncinata* (Hedw.) Loeske	Moss	SU	13.13	-25.12	0.60	-2.28	21.79
P6	62° 38’ 35.5” S 61° 03’ 51” W	*Sanionia Geroge-uncinata*	Moss	SGU	23.81	-25.04	1.43	7.41	16.69
P7	62° 39’ 21.4” S 61° 03’ 25.4” W	*Brachythecium austrosalebrosum* (Müll. Hall.) Paris	Moss	BA	19.73	-21.42	0.79	-0.79	25.12
P7	62° 39’ 21.4” S 61° 03’ 25.4” W	*Warnstorfia sarmentosa* (Wahlenb.) Hedenäs	Moss	WS	28.09	-23.80	1.22	0.40	23.05
P9	62° 39’ 32.4” S 61° 03’ 39.2” W	*Deschampsia antarctica* É. Desv.	Grassy	DA	26.57	-27.91	1.72	31.66	15.41
P11	62° 39’ 12.4” S 61° 00’ 15.1” W	*Polytrichum juniperinum*	Moss	PJ	7.15	-27.17	0.35	-2.52	20.67
P12	62° 40’ 16.4” S 61° 06’ 40.1” W	*Andreaea gainii* Cardot	Moss	AG	20.02	-23.95	0.99	-2.59	20.14

2.3. Soil organic matter analysis

Contents and stocks of C and N, $\delta^{13}C$ and $\delta^{15}N$ in the SOM fractions

The C and N contents, $\delta^{13}C$ and $\delta^{15}N$ ratio isotopes were determined in the SOM physical size-fractionated particles: a) particulate organic matter (POM), and; b) mineral-associated organic matter (MAOM) (Cambardella and Elliott, 1992). The fractions were separated and quantified after dispersion for 16 h in sodium hexametaphosphate solution (5 g L^{-1}) and sieving on 50 µm mesh. Such determinations were procedure in all soil horizons and the plant materials to assess their contribution to the C and N stocks in soils of Byers Peninsula and identify the link between the isotopic signatures of plant and soil SOM. All these determinations were made using an Isotope Ratio Mass Spectrometer (IRMS) Flash EA - Delta V in the *Centro de Isótopos Estáveis Prof. Dr. Carlos Ducatti* - UNESP. The weighted $\delta^{13}C$ and $\delta^{15}N$ mean of SOM was calculated for samples according to mass and signature of each physical fraction.

Once carbonates are absent in Byers Peninsula, total organic C (TOC) and total N (TN) were determined from the sum of the values present in the physical fractions in each horizon. Based on these data, it was possible to calculate the average stock of C and N present in the soils (in the horizons and profile by summing all horzons), using the following equation:

$$S = (C\ or\ N) * t * Ds$$

Where *S* is the stock of C or N in Mg ha^{-1}; *C* and *N* is the content of these elements in the SOM fractions, in g kg^{-1}; *t* is the thickness of the soil layer, in cm, and *Ds* is the density of the soil in g cm^{-3}. Once soils are gravelly and collecting undisturbed samples with the volumetric ring is virtually impossible, we measured total porosity in undisturbed samples collected by micromorphological analysis (Fitzpatrick, 1984). Particle density was determined after drying a quantity of soil to 105 °C and then dividing the mass by the volume of the particles, excluding spaces among them (Teixeira et al., 2017). The soil density was calculated according to the formula: Soil density = (total porosity/particle density) + 1.

Biochemical composition of MOS fractions and plant materials

The biochemical composition of the SOM fractions (POM and MAOM) as well as the plant materials was evaluated using an off-line TMAH -mediated thermochemolysis procedure as described in Chefetz et al. (2000) and Del Rio et al. (1998).

The samples were weighed (2 mg, 100 mg and 200 mg for the vegetable residues, MAOM and POM fractions respectively) and placed in tubes (snap glass vials), to which 200 µL of tetramethylammonium hydroxide - TMAH (25% in methanol - m/v) was added. The TMAH was evaporated under continuous nitrogen flow for 30 min at a temperature of 38 ºC, after complete evaporation the vials were sealed. The sealed vials were then placed in a muffle furnace at 300 °C for

30 min. After cooling to room temperature, the tubes were opened and all internal surfaces washed with dichloromethane - DCM (3 x 1 mL). The extracts were combined and to these were added 50 µl of internal standard (methyl nonadecanoate -19:0), then dried again under a stream of nitrogen. The samples were then diluted with a known volume of DCM (100 µL).

Subsequently, the TMAH thermochemolysis products were analyzed by gas chromatography-mass spectrometry on a Shimadzu QP 2010-SE GC-MS equipped with a Rtx-5MS column (30 m length; 0.25 mm inner diameter (ID); 0.25 µm film thickness). He Ultrapure was the carrier gas used at a flow rate of 3 mL min^{-1}, the ion source temperature was set to 200 °C, the interface temperature to 290 °C, and the oven temperature was increased from 60 °C to 300 °C at a rate of 15 °C min^{-1} up to 150 °C and then at a rate of 4 °C min^{-1} up to 300 °C, with initial analysis time at 3.50 min and final time at 48.5 min. The pyrolytic compounds were identified by their mass spectra and relative retention times. Most peaks were identified by comparison with the NIST library and some were confirmed by comparison with authentic standards.

The origin of the compounds was classified and categorized as compounds derived from carbohydrates, nitrogenous compounds (proteins, amino acids, and N-bearing), lipids (cutin, suberin, bioactive, microbial activity markers - MAM, and other lipids), lignin derivatives, and others. In addition to this characterization, the compounds were categorized as to the structure of their carbon chains, classifying them as alicyclic (aliphatic compounds that present rings, saturated or unsaturated, without the presence of benzene rings), the other aliphatic (compounds that present open carbonic chain, containing or not unsaturation), aromatics (compounds that present at least one benzene ring in their structure, as well as those also classified as heterocyclic or mononuclear aromatics, which are cyclic compounds containing, in the ring, one or more atoms other than carbon; in the present study, these were identified mainly in the nitrogen compounds). The ratio of aliphatic to aromatic chain compounds (Al/Ar) was determined by the ratio of the relative abundance of these compounds.

Evaluation of the molecular structure of SOM by ^{13}C NMR CP/MAS

The evaluation of the SOM molecular structure in Byers Peninsula soils was performed in 13 samples from 8 representative profiles (P2, P3, P4, P6, P7, P10, P11 and P12). These samples were selected based on their highest C-MOAM content and on their different pedogenic environments. Prior to the analyses of solid-state ^{13}C nuclear magnetic resonance spectroscopy (*^{13}C NMR CP/MAS)* the soil samples were treated with 10% (w/w) hydrofluoric acid (HF) solution to concentrate C and remove paramagnetic matter (Gonçalves et al., 2003).

Three 10 g subsamples of each selected soil horizon were treated with 30 ml of 10% (w/w) HF solution under mechanical shaken for 2 h. The suspension was centrifuged (10 min at 3000 rpm at 15 °C) and the supernatant was removed and discarded. This procedure was repeated five times. The material remaining in the tube (SOM_{HF}) was washed with 40 mL of deionized water three times to

remove residual HF and then freeze-dried. After drying, the samples were macerated in agate mortar. Mass recovery of samples after pre-treatment with HF 10% ranged from 4.5 to 13.31%.

The C and N contents were determined in the samples after treatment with 10% HF solution (SOM_{HF}) in an elemental analyzer (Perkin Elmer 2400). The C/N_{HF} ratio (w/w) and the R-factor (CN_{HF}/ C/N_{soil}) were calculated. The C enrichment after HF treatment (C_E) was calculated by the ratio C_{HF}/C_{soil}, where C content of the bulk soil samples was estimated from the sum between the contents of the SOM fractions, taking into account their masses and proportions.

Investigation by ^{13}C NMR CP/MAS was performed on global samples of P2H2, P2H3, P4H1 and P4H2. NMR analysis of other representative samples from the studied area will still be carried out.

The ^{13}C NMR analyses were performed in an Agilent spectrometer (Agilent Technologies, model DD2) operating at a resonance frequency of 125.7 MHz. The CPMAS (Cross Polarization magic angle spinning) procedure was used with a rotational speed of 10 kHz and a contact time for cross polarization of 1 ms. On average, 50,000 scans were accumulated and a line magnification between 250 and 400 Hz was applied. Chemical shifts were reported with respect to tetramethylsilane (0 ppm), which was adjusted with glycine (carboxyl C = 176.08 ppm). Chemical shifts of the ^{13}C NMR spectra were performed according to Knicker (2011), as follows: 0 - 45 ppm, alkyl C; 45 - 60 ppm, N/O-alkyl C; 60 - 110 ppm, O-alkyl C; 110 - 160 ppm, aryl C; and 160 - 220 ppm, carboxyl/carbonyl C. The contributions of the various C groups to the total C were calculated using MestreNova 8.1 by integrating the respective area and relating it to the total area of the spectrum. From these data, the following ratios were calculated: alkyl C/O-alkyl C (0-45 ppm/45-110 ppm) (Baldock et al., 1997); and alkyl C/aryl C (0-110 ppm/110-160 ppm).

2.4 Data Analysis

Statistical analyses were performed using the geostatistical software R (R Core Team, 2019). Principal Component Analysis (PCA) was performed using the stats package. For Spearman's correlation applied the corrplot package, where statistically significant from Student's t-test were considered probability values of 5% or less ($p \leq 0.05$). PCA's were performed to explore general trends in soil attributes (chemical and physical parameters) and to assess which major variables associated with SOM could be grouped according to soil groups.

3. Results

3.1 C and N stocks in the soil profiles

In general, C and N stocks decreased with increasing soil depth for most of the profiles studied. The exception to this behavior was observed in profiles P1, P2, P3, P5 and P8. P1, despite the high acidity, provided C and N accumulation at soil depth. P2, P3 and P5, both cryoturbated soils and with high C and N stocks, showed this tendency to increase in soil depth. P8, despite being a marine terrace

with intermediate formation time in the sequence of the studied profiles, drew attention to its stocks due to the abrupt increase of almost 10 times between the superficial horizon and the deepest one.

The global C and N stocks in soil profile showed great variation as a function of profile positioning in the landscape, ranging from 5.08 (from 0 to 50 cm depth) to 109.21 Mg ha^{-1} (from 0 to 105 cm depth) and from 0.21 (from 0 to 50 cm depth) to 12.52 Mg ha^{-1} (from 0 to 70 cm depth), respectively (Table S1). The profiles that presented the greatest C and N stocks were those associated with low (P2 – Fig. 2) and high platforms (P3, P4, P10 – Fig. 3), with emphasis on soils with more pronounced evidence of cryoturbation (patterned ground), respectively 109.21; 101.10; 41.85 and 53.04 Mg ha^{-1} of C and 8.31; 12.52; 6.16 and 4.15 Mg ha^{-1} of N.

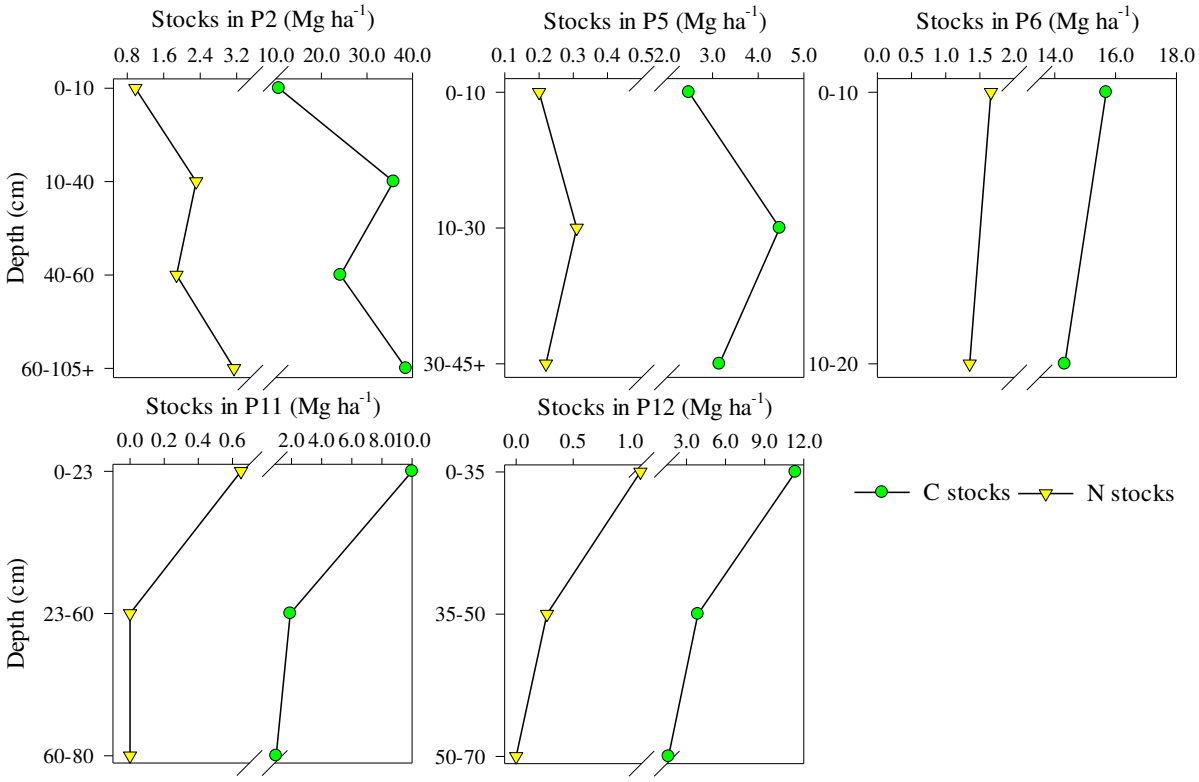

Figure 2. C and N stock (Mg ha^{-1}) in the different soil depth to the low platforms (P2, P5, P6, P11, P12).

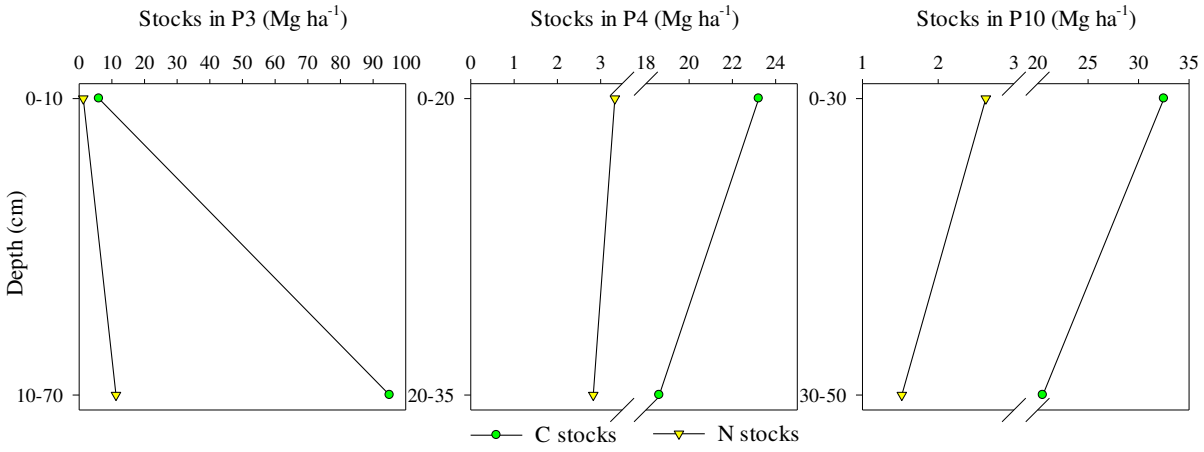

Figure 3. C and N stock (Mg ha^{-1}) in the different soil depth to the high platforms (P3, P4, P10).

The profiles corresponding to the marine terraces (P7, P8, P9 and P13 – Fig. 4) presented in general the lowest C and N stocks. P1 (Fig. 5), even though it is inserted in a desert sidewalk under an acid-sulfate soil patch, still showed considerable C and N stock values, higher than those observed for the marine terraces.

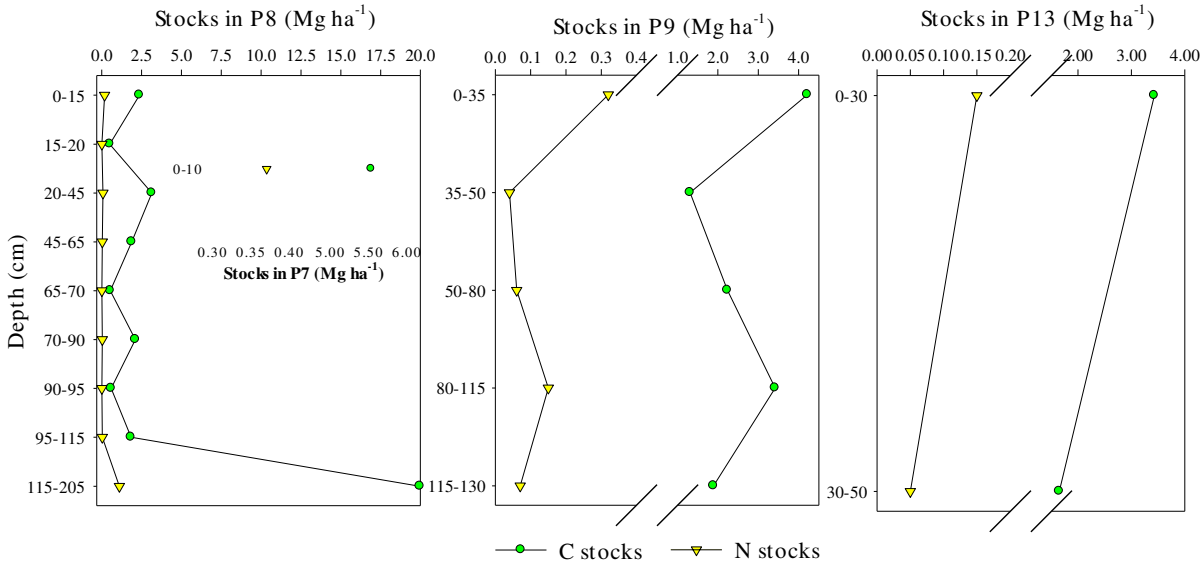

Figure 4. C and N stock (Mg ha^{-1}) in the different soil depth to the raised beaches (P7, P8, P9, P13).

Assessing the stocks at the SOM fraction level (Table S1), the MAOM showed the highest contribution to total stocks by profile, contributing on average 60.25% of the total C stock and 82.09% of the N stock, with C stocks ranging from 2.43 to 70.15 Mg ha^{-1}, and N stocks from 0.21 to 7.53 Mg ha^{-1}. The POM fraction showed an average contribution of 39.75% and 17.91% to C and N stocks, respectively, with C stocks ranging from 1.44 to 39.06 Mg ha^{-1}, and from 0 to 4.99 Mg ha^{-1} of N.

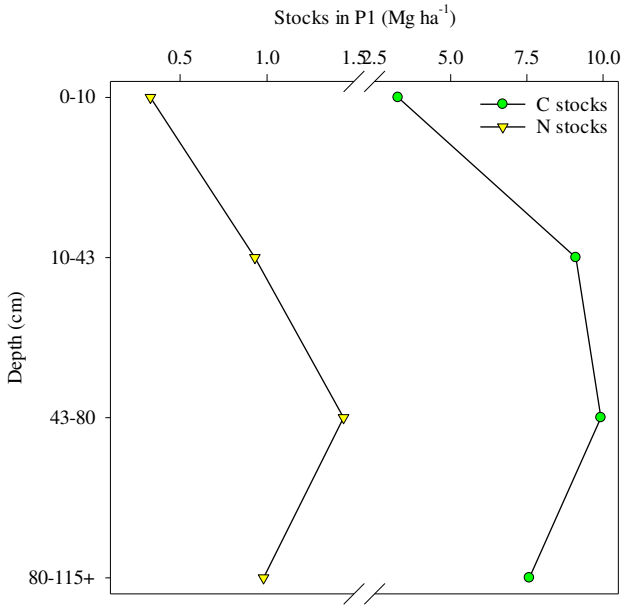

Figure 5. C and N stock (Mg ha^{-1}) in the acid-sulfated soil (P1).

3.2 Characterization of plant materials regarding their isotopic signature and their C and N contents

The analyzed plant materials (mosses, lichen and grasses) presented C contents ranging from 31.9 to 408.9 g kg^{-1} and N from 1.67 to 17.2 g kg^{-1} (Table 1). The highest TOC content observed was associated with the lichen *Usnea aurantiaco-atra* (UA) and the highest TN content was associated with the grass present on the Peninsula, *Deschampsia antarctica* (DA). The C/N ratio of these plant organisms showed great amplitude due to the high variation in C and N contents, where the lichen UA showed the highest C/N ratio 55.37 and the grass the lowest ratio of 15.41 (Table 1). Among the lichen and mosses these values were highly variable due to large fluctuations in N content.

The $\delta^{13}C$ isotopic signature of these materials showed an oscillation of up to 6.5‰ among these materials, with $\delta^{13}C$ values ranging from -27.9 to -21.4‰, characterizing this isotopic signature similar to that of plant materials with a C_3 photosynthetic pathway (Table 1). Except for *Brachytecium austrosalebrosum* (BA), the other mosses and the grass showed slightly more negative $\delta^{13}C$ than the lichen.

Compared to the relatively narrow range for the observations made of $\delta^{13}C$ values, the $\delta^{15}N$ isotopic composition of the Byers Peninsula plant organisms ranged more widely between -11 to 31.7‰, showing a range of up to 42.7‰ indicating a greater enrichment of this compartment. Mosses, due to the larger number of organisms examined, showed a range between -2.59 and 7.41‰. The lichen (UA) showed the most depleted in ^{15}N (-11.1‰), while the grass (DA) was the most enriched (31.7‰).

3.3 Isotopic composition of SOM fractions

The isotopic composition of organic matter from Byers Peninsula soils was analyzed and contrasted with patterns observed for local vegetation (Table 2) to identify primary sources of C and N input to the soil. In general, the $\delta^{13}C$ and $\delta^{15}N$ signatures in the POM and MAOM fractions showed overlap with those observed in the analyzed plant materials, where mainly the $\delta^{13}C$ signals also characterized the signature of materials with C_3 photosynthetic cycle, indicating possible trace contributions of these materials as primary sources of C and N in this environment. Only the topmost P13 sample skewed this pattern somewhat, with $\delta^{13}C$ values below -20‰ somewhat resembling the contribution of C_4 photosynthetic cycle material.

In the POM fraction, the $\delta^{13}C$ isotopic signatures ranged from -27.36 to -17.44‰, with a variation of up to 6.19‰ in P13, this being observed with increasing soil depth. The POM fraction of P2 and P4 profile were more depleted in ^{13}C with the most negative $\delta^{13}C$ values, -27,36 e -27.19‰ respectively, also presenting two of the highest POM C stocks of the analyzed soils (Table S1). On the other hand, the most ^{13}C-enriched profile was P13 with $\delta^{13}C$ of -17.44‰ (mean profile -20.53‰ ± 3.09). The $\delta^{15}N$ signatures were less expressive in the POM fraction, where due to the low N contents in this fraction for most of the profiles (raised beaches (P7, P8, P9, P13) and three low platforms (P5, P11, P12) with N contents below detectable - <0.001%), it made it impossible to identify the signature of most of the soil samples studied. However, the values obtained in the samples of this fraction ranged from -0.23 to 18.43‰ at POM. The P1 profile presented the greatest variation with increasing soil depth, where the values decreased up to 11.64‰; in this same profile, the largest $\delta^{15}N$ signature (18.43‰) was observed, this being observed at surface. The most depleted profile in ^{15}N was P6 (-0.23‰).

The MAOM fraction, presented isotopic signal of $\delta^{13}C$ ranging from -27.73 to -19.98‰, with variation within the profiles much lower than that observed in the POM (3.55‰) which was observed in the P2 profile. MAOM was also more distinct from POM in terms of the pattern of ^{13}C depletion with increasing depth. The profile with the most depleted ^{13}C signature was P1. The most enriched profile, as in the POM fraction, was P13. The $\delta^{15}N$ signatures showed a smaller oscillation than in the POM fraction, with values ranging from -0.87‰ in the most ^{15}N-impoverished profile (P10) to 16.31‰ in the most enriched profile (P9). In profiles P2, P4, P8, P9, P11 and P12 it was also observed that there was an enrichment of ^{13}C from the POM fraction to the MAOM, with $\delta^{13}C$ values becoming less negative.

Table 2. Isotopic composition of SOM fractions and C and N levels

Sample	Horizon thickness (cm)	C %	$\delta^{13}C$ (‰)	C (mg g soil^{-1})	N %	$\delta^{15}N$ (‰)	N (mg g soil^{-1})	C/N Ratio	C %	$\delta^{13}C$ (‰)	C (mg g soil^{-1})	N %	$\delta^{15}N$ (‰)	N (mg g soil^{-1})	C/N Ratio
	Particulate organic matter (POM)								Mineral-Associated Organic Matter (MAOM)						
P1H1	0-10	0.17	-26.25	1.33	0.02	18.43	0.12	11.28	0.29	-27.73	0.68	0.04	3.89	0.08	8.05
P1H2	10-43	0.17	-26.54	1.05	0.01	8.98	0.09	12.15	0.17	-27.29	0.65	0.02	5.95	0.09	7.52
P1H3	43-80	0.09	-26.60	0.52	0.01	6.79	0.08	6.28	0.18	-26.96	0.79	0.02	5.24	0.11	7.39
P1H4	80-115	0.12	-26.88	0.99	0.02	7.95	0.13	7.58	0.22	-27.11	0.34	0.03	3.91	0.04	8.14
P2H1	0-10	0.48	-26.27	3.18	0.04	3.84	0.27	11.67	0.86	-23.02	2.88	0.08	1.93	0.28	10.12
P2H2	10-40	0.59	-26.36	1.76	0.04	5.57	0.12	15.07	0.70	-25.31	4.91	0.04	4.87	0.31	15.64
P2H3	40-60	0.45	-26.39	1.91	0.03	4.67	0.14	13.54	0.87	-23.36	4.94	0.07	3.59	0.39	12.60
P2H4	60-105	0.58	-27.36	2.16	0.05	4.89	0.18	11.72	0.42	-26.57	2.66	0.03	5.26	0.21	12.80
P3H1	0-10	0.15	-25.68	1.32	0.05	17.71	0.43	3.05	2.14	-26.12	2.45	0.30	4.19	0.34	7.15
P3H2	10-70	0.50	-24.39	3.40	0.07	6.44	0.45	7.60	2.04	-25.70	6.50	0.23	1.00	0.73	8.94
P4H1	0-20	0.78	-27.03	5.76	0.11	4.18	0.80	7.21	1.17	-26.38	3.02	0.18	2.85	0.46	6.57
P4H2	20-35	0.91	-27.19	6.62	0.14	3.98	1.01	6.58	1.01	-26.04	2.77	0.15	4.38	0.42	6.55
P5H1	0-10	0.04	-25.77	0.19	0.00	0.00	0.00	0.00	0.27	-26.55	1.49	0.02	2.04	0.14	10.74
P5H2	10-30	0.04	-25.84	0.23	0.00	0.00	0.00	0.00	0.26	-26.23	1.27	0.02	1.91	0.10	12.25
P5H3	30-45	0.05	-25.70	0.21	0.00	0.00	0.00	0.00	0.20	-26.62	1.18	0.02	2.80	0.10	12.19
P6H1	0-10	0.45	-21.99	2.58	0.04	-0.23	0.22	11.69	1.63	-22.72	6.99	0.19	-0.08	0.79	8.80
P6H2	10-20	0.25	-23.11	0.81	0.02	0.41	0.05	16.45	1.20	-24.22	8.10	0.12	0.05	0.79	10.22
P7H1	0-10	0.13	-21.55	1.17	0.00	0.00	0.00	0.00	1.75	-21.36	1.88	0.19	3.64	0.21	9.15
P8H1	0-15	0.04	-24.32	0.41	0.00	0.00	0.00	0.00	0.75	-24.26	0.45	0.11	13.84	0.06	7.08

P8H2	15-20	0.04	-24.08	0.37	0.00	0.00	0.00	0.00	0.41	-22.96	0.17	0.05	12.97	0.02	8.83
P8H3	20-45	0.05	-24.24	0.51	0.00	0.00	0.00	0.00	0.42	-20.81	0.18	0.04	11.17	0.02	9.53
P8H4	45-65	0.04	-24.54	0.39	0.00	0.00	0.00	0.00	0.35	-22.06	0.12	0.03	11.36	0.01	11.11
P8H5	65-70	0.05	-24.30	0.43	0.00	0.00	0.00	0.00	0.30	-21.84	0.16	0.03	11.37	0.01	12.06
P8H6	70-90	0.05	-24.28	0.45	0.00	0.00	0.00	0.00	0.30	-21.47	0.13	0.03	11.87	0.01	11.62
P8H7	90-95	0.05	-24.58	0.49	0.00	0.00	0.00	0.00	0.28	-21.98	0.17	0.02	12.29	0.01	13.37
P8H8	95-115	0.04	-24.59	0.38	0.00	0.00	0.00	0.00	0.27	-21.20	0.12	0.02	13.13	0.01	11.50
P8H9	115-205	0.07	-23.19	0.66	0.00	0.00	0.00	0.00	0.96	-20.73	0.57	0.12	11.10	0.07	8.34
P9H1	0-35	0.04	-25.31	0.41	0.00	0.00	0.00	0.00	1.06	-24.73	0.37	0.17	16.31	0.06	6.25
P9H2	35-50	0.04	-27.20	0.42	0.00	0.00	0.00	0.00	0.40	-22.23	0.15	0.04	11.43	0.02	9.21
P9H3	50-80	0.03	-24.94	0.31	0.00	0.00	0.00	0.00	0.19	-23.21	0.17	0.01	10.64	0.01	12.77
P9H4	80-115	0.04	-24.85	0.34	0.00	0.00	0.00	0.00	0.54	-23.12	0.29	0.05	6.90	0.03	10.17
P9H5	115-130	0.05	-24.57	0.46	0.00	0.00	0.00	0.00	0.52	-23.76	0.35	0.05	6.89	0.03	11.04
P10H1	0-30	0.26	-23.75	1.53	0.01	1.53	0.08	19.80	1.09	-26.41	4.48	0.10	-0.36	0.41	10.94
P10H2	30-50	0.32	-23.25	2.11	0.02	0.98	0.11	19.42	1.02	-23.98	3.42	0.09	-0.87	0.30	11.38
P11H1	0-23	0.12	-23.12	0.91	0.00	0.00	0.00	0.00	0.83	-22.05	1.82	0.08	0.94	0.18	10.21
P11H2	23-60	0.03	-24.81	0.14	0.00	0.00	0.00	0.00	0.03	-23.39	0.19	0.00	0.00	0.00	0.00
P11H3	60-80	0.03	-24.66	0.14	0.00	0.00	0.00	0.00	0.03	-23.66	0.17	0.00	0.00	0.00	0.00
P12H1	0-35	0.05	-24.44	0.26	0.00	0.00	0.00	0.00	0.49	-23.48	2.12	0.05	3.76	0.23	9.26
P12H2	35-50	0.09	-23.95	0.38	0.00	0.00	0.00	0.00	0.28	-23.01	1.59	0.02	4.78	0.14	11.49
P12H3	50-70	0.06	-25.32	0.13	0.00	0.00	0.00	0.00	0.06	-23.89	0.48	0.00	0.00	0.00	0.00
P13H1	0-30	0.03	-17.44	0.27	0.00	0.00	0.00	0.00	0.17	-19.98	0.28	0.01	5.95	0.02	11.74
P13H2	30-50	0.03	-23.62	0.24	0.00	0.00	0.00	0.00	0.18	-20.28	0.16	0.01	4.53	0.01	12.18

For all samples analyzed, the isotopic signatures of both $\delta^{13}C$ and $\delta^{15}N$ showed overlaps for both fractions of the MOS as well as in the plant materials. However, the $\delta^{15}N$ values were broader, indicating a higher enrichment of ^{15}N. In addition to the large oscillation in the signatures between the fractions, they showed a very diverse pattern in depth in the profiles. In view of this, the weighted average of the $\delta^{13}C$ and $\delta^{15}N$ signatures in the MAOM fraction (most stable fraction) was applied to the signature of the surface horizons for the identification of the main sources of this SOM. The isotopic signatures analyzed in the MAOM fraction, as described in da Silva et al. (2022) identified the contribution of marine organic materials (P1, P2, P5 and P12), ornithogenic organic materials (P7, P8, P9 and P13), and a signature associated with endolithic organic matter in P4, the profile with the oldest record ever dated to Maritime Antarctica.

3.4 Biochemical composition of plant materials and SOM fractions as determined by Thermochemolysis TMAH off-line

The evaluation of the biochemical composition of SOM fractions and plant materials by off-line thermochemolysis allowed the identification of 231 compounds (Table S2): 2 lignin-derived compounds (p-hydroxyphenyl - P17&P18 and Guiacyl - G17&G18 structure), 7 amino acids, 2 proteins, 20 other nitrogen compounds, 7 carbohydrates, 9 cutin, 2 suberin, 4 MAM's, 54 bioactive compounds, 30 other lipid compounds, and 94 other compounds that did not fit the previous classifications.

The plant materials studied presented a diversity of origin of the compounds (Figure 6a), similar to what was observed in the SOM fractions. The dominance of the compounds identified in the plant materials was also lipid compounds (bioactive, cutin, suberin and other lipids), similar to the behavior observed for the SOM fractions. The presence of lignin-derived compounds was observed only in the *Deschampsia antarctica* (DA) grass with a relative abundance of 6.5%. Amino acids were more abundant in some mosses, especially in *Sanionia George-uncinata* (SGU) with 7%, and in DA with 3.1%. N-bearing compounds were more abundant in the mosses *Polytrichum juniperinum* (PJ) with 11.9%. Carbohydrates were less abundant only when compared to lipid compounds, being more abundant in the grass DA with 51% and in the lichen *Usnea auranteaco-ater* (UA) with 22.8%. Among the lipid compounds, suberin was the least abundant, being identified only in the grass DA, with 3.8% relative abundance. Cutin was most abundant in the mosses with *Andreaea gainii* (AG) and *Hymenoloma grimmiaceum* (HG) standing out, with 24.5 and 20.5%, respectively. Bioactive compounds were generally abundant in almost all materials analyzed, with the lowest abundance observed for DA, possibly associated with secondary metabolites of these plant organisms.

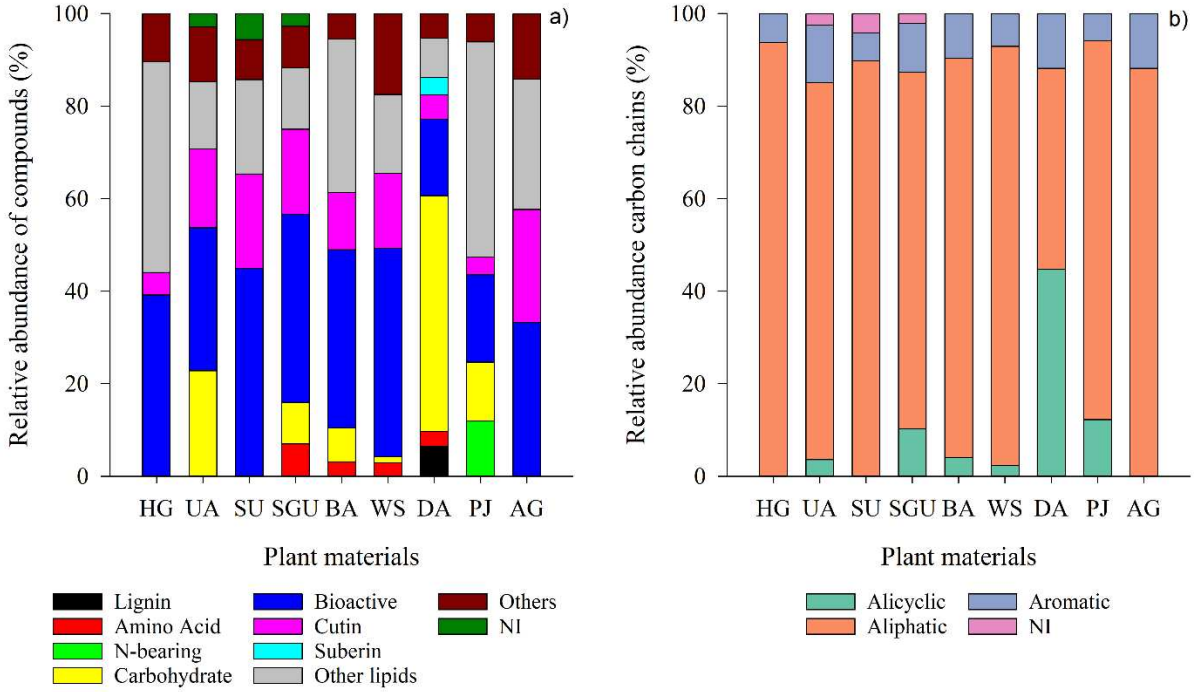

Figure 6 Relative abundance of the origin of the compounds (%) present in the plant material (a), and relative abundance carbon chains (%) of compounds (b)

As for the distribution of carbon chains in the plant organisms, the aliphatic chains were also more abundant as observed in the fractions with relative abundance ranging from 77.12 to 93.8% in the mosses, the lichen with 81.5%, and the grass with only 43.5%. The grass showed a high abundance of allicyclic chains (44.7%). Among the mosses, this type of structure was quite variable, not establishing a pattern for this type of chain. As for the aromatic chain compounds, despite the low representation, they presented a relative abundance ranging from 5.8 to 12.4%. The highest abundance of aromatic compounds was observed in the lichen, in sequence similar content was observed in the grass (DA) and in the AG moss, with 11.8%.

Evaluating the structure of the carbon chains of the compounds identified in the SOM fractions, in general, there is a predominance in all profiles of aliphatic compounds (60% to 95% of relative abundance in MAOM fraction and 51% to 96% in the POM fraction). In the MAOM fraction, the aliphatic compounds presented an increase of the relative abundance with the depth of the soils, whereas for the POM fraction a predominance of behavior was not observed with the increase of the depth. As for the aromaticity of the carbonic chains of the identified compounds in MAOM, in general, there was a tendency to decrease with the increase of the soil depth, in POM the behavior was contrary. The compounds with alicyclic chains were more restricted and less abundant when compared to the aliphatic and aromatic ones, however, in the profiles that these were present, their abundance was more notable at the surface.

The POM fraction showed less variation of origin/derivation of compounds, where, besides lipids (cutin, suberin, MAM, bioactive and other lipids) presented traces of contribution of compounds derived from carbohydrates. The MAOM fraction, showed greater diversity of origin of compounds, with emphasis on the presence of nitrogen compounds (0.45 to 32.43%) and lignin derivatives (P17&P18 - 0.83 to 1.41%) which were identified only in this fraction. This lignin fragment characterizes a lignin of the non-woody type.

The predominance in all profiles is of compounds of lipid origin in both fractions (POM - 39.02 to 91.07% and MAOM - 40.39 to 96%). Among the lipid compounds, bioactive and MAM were the most representative in both fractions of the studied profiles. The range of bioactive compounds identified was associated with hydrocarbons, which generally present antimicrobial activity or derivatives of secondary metabolites whether of animal or plant origin. As for the MAMs, they were concentrated in two main markers among the fatty acids, *palmitic acid* (C16 - represented in our results by *n-hexadecanoic acid*) and *stearic acid* (C18 - represented by *octadecanoic acid*) and their derivatives (*Hexadecanoic acid, ethyl ester* - palmitic acid methyl ester; and *Methyl stearate* - methylated stearic acid) which are used as proxies for microbial activity (Tadini et al., 2022).

The high platforms and low platforms with the presence of patterned soils showed higher diversity of compounds in the MAOM fraction when compared to the raised beaches and the acidic sulfate soil (Figure 7c and 8c). Among these profiles, P3, especially in depth, was the most diverse in terms of biochemical composition in the MAOM fraction. This profile is located in an area of occurrence of the lichen UA and the mosses *Sanionia uncinata* (SU) and *Andreaea gainii* (AG) possessing a tundra physiognomy (see Supplementary Material 1 in da Silva et al. (2022)). The P4 profile stood out in terms of its abundance of bioactive compounds, especially in the MAOM fraction on the surface, at 59%. P10, in turn, was the profile that presented the highest diversity of nitrogen compounds in subsurface (N-bearing = 32.43 %), being this profile inserted in a lichen (UA) and moss (BA) dominance area. The P5 profile, in the MAOM fraction of the studied profiles, was the only one that presented traces of lignin-derived compounds, and this was identified only in the subsurface. The POM fraction of these soils showed low diversity of compounds (Figure 7a and 8a), derived almost majorly from total lipids, with an emphasis on MAM's and bioactive compounds.

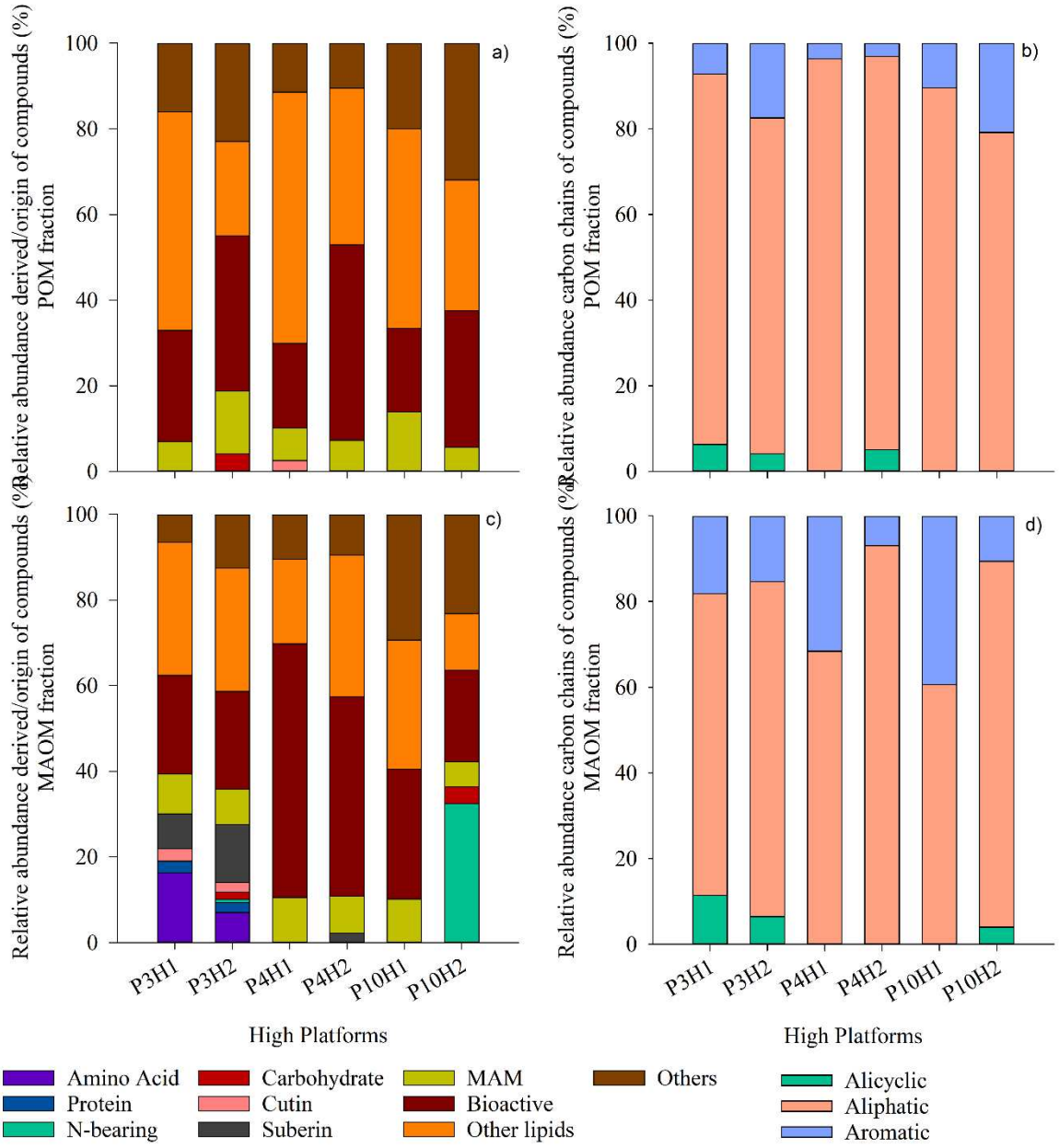

Figure 7. Relative abundance of the origin of the compounds (%) present in the POM (a) and MAOM (c) fractions; and relative abundance carbon chains of the compounds (%) in the POM (b) and MAOM (d) fractions of the high platforms

The carbon chains of the compounds identified in both fractions in the high platforms showed a high degree of aliphaticity and low aromaticity (Figure 7b and d), but the proportion of aromatic compounds from the high platforms in the MAOM fraction was the highest among all soil groups studied, especially the superficial horizons of profiles P4 and P10 with 31.64 and 39.41% of aromatic composition, indicating a more resistant and more stable SOM in the higher points of the Peninsula. In the MAOM the aliphatic/aromatic (Al/Ar) ratio was 3.7 and in the POM 8.3, with more than 75% of

the MOS constitution in these profiles aliphatic. In the lower platforms the degree of aliphaticity and aromaticity showed a similar pattern to the upper platforms (Figure 8b and d), but the Al/Ar ratio was inverse between the fractions, where in the MAOM it was 7.9 and in the POM 4.2. As for the compounds with alicyclic chains they were more abundant in the MAOM fraction in both high and low platforms.

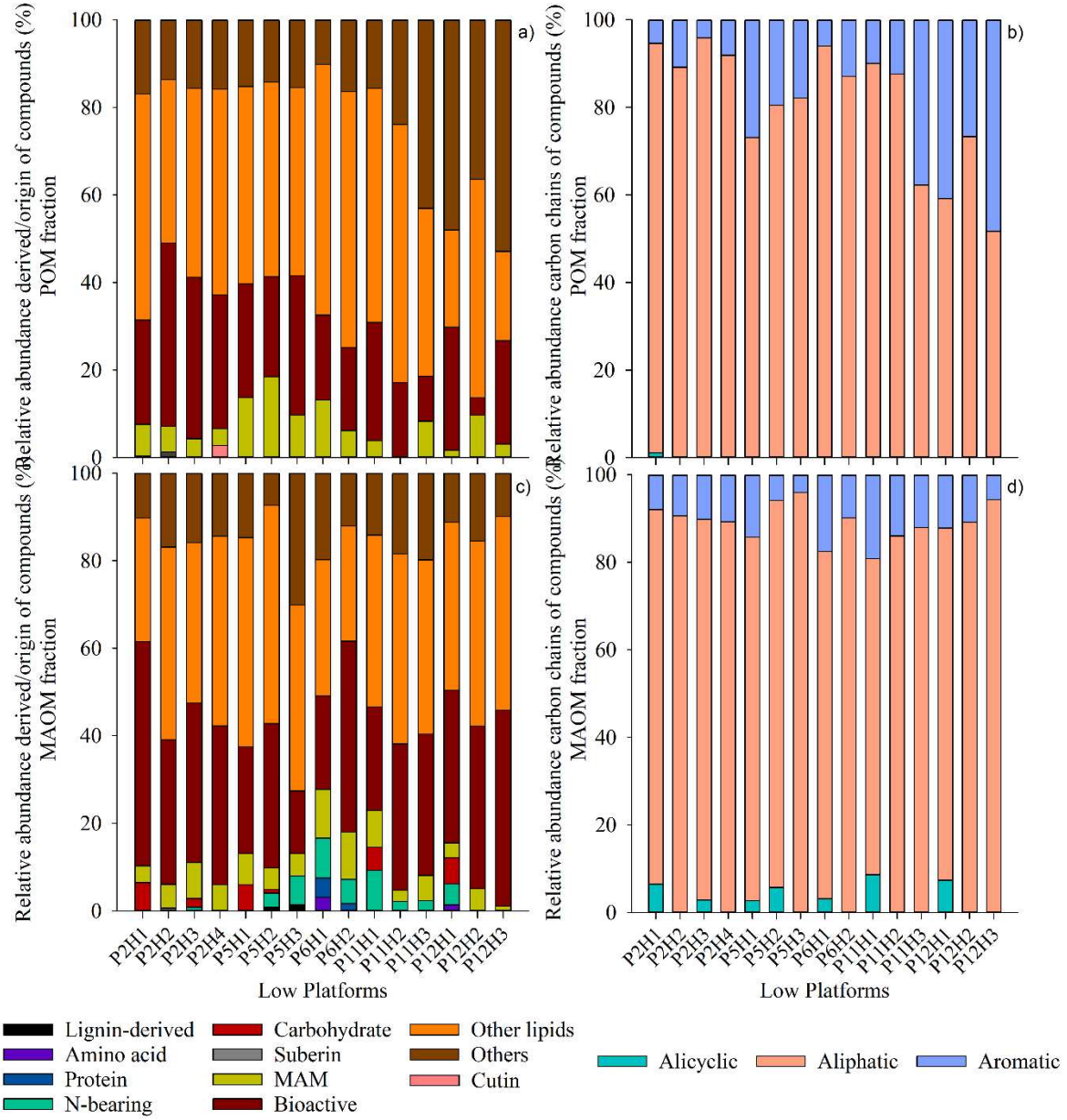

Figure 8. Relative abundance of the origin of the compounds (%) present in the POM (a) and MAOM (c) fractions; and relative abundance carbon chains (%) of the POM (b) and MAOM (d) fractions of the low platforms

In the raised beaches, the diversity of origin of the compounds was higher in MAOM than in POM, with emphasis on the abundance of nitrogen compounds present only in the samples of the MAOM fraction of these profiles (Figure 9c). In the MOP fraction, in addition to the absence of nitrogen, lignin-derived and carbohydrate-derived compounds, the lipid proportion was absent of cutin- and suberin-derived compounds, being dominated only by other lipid compounds possibly of animal origin, MAM's and bioactives (Figure 9a). In the raised beaches the abundance of the carbon chains (Figure 9b and d) showed a very similar behavior to the lower platforms, where in this group of soils, the aliphatic chain compounds were more abundant in the MAOM with an average of 88.82%, and in the POM presented the highest average for the aromatic compounds with an average abundance of 20.64%. The Al/Ar ratio in MAOM was 8.2 and in POM 3.8.

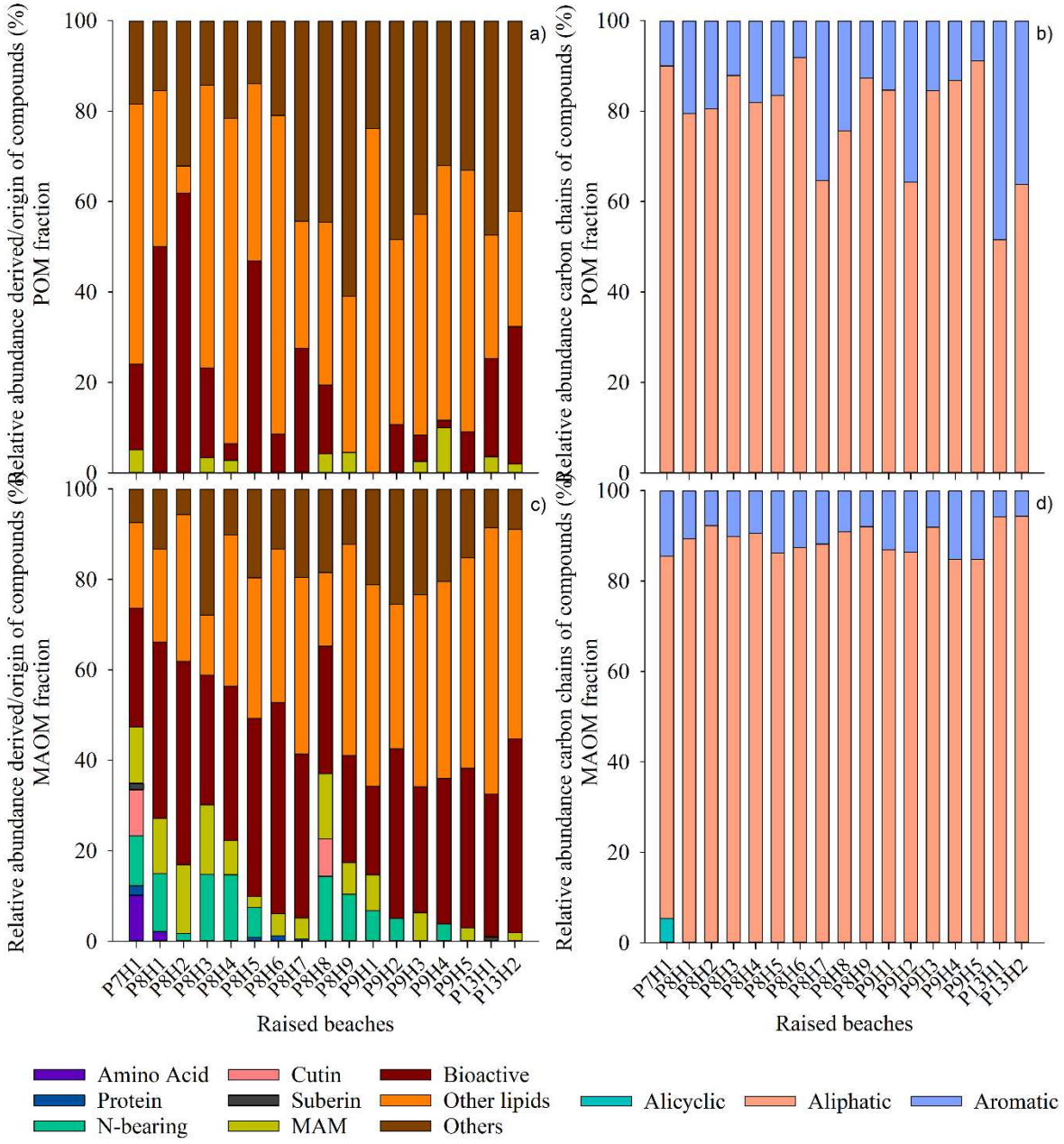

Figure 9. Relative abundance of the origin of the compounds (%) present in the POM (a) and MAOM (c) fractions; and relative abundance carbon chains (%) of the POM (b) and MAOM (d) fractions of the raised beaches

The sulfate acid soil profile (Figure 10) presented the biochemically poorest SOM, especially when compared to the MAOM fraction of the other soil groups described above. The MAOM fraction (Figure 10c), presented only MAM's compounds with an increasing increase in subsurface (from 0 to 17%), being that in the superficial horizon it was not detected the presence of these compounds in this fraction, bioactive compounds were more abundant along the profile and other lipids, being also observed traces of compounds derived from carbohydrates in the most subsurface soil layer. In the POM (Figure 10a), the diversity of compounds was similar, but in smaller proportions and without the presence of carbohydrates. The aromaticity of the compounds in the POM fraction of P1 (Figure 10b) was the lowest observed, with a mean value for the profile of 8.86%. Aliphatic compounds were represented by more than 90% of the compounds identified in the fraction, resulting in an Al/Ar ratio of 10.3. In the MAOM fraction this ratio was only 6.2.

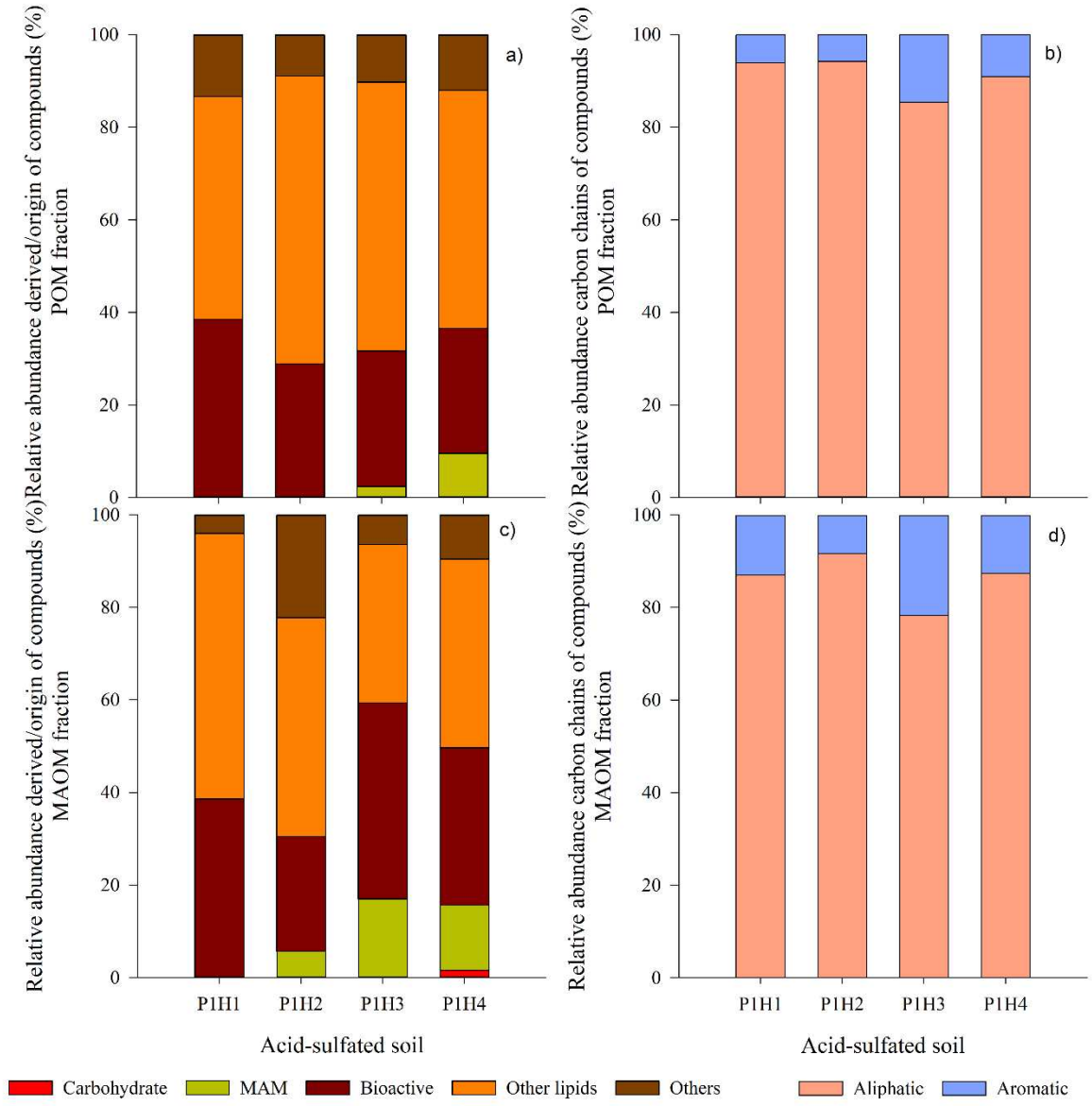

Figure 10. Relative abundance of the origin of the compounds (%) present in the POM (a) and MAOM (c) fractions; and relative abundance carbon chains (%) of the POM (b) and MAOM (d) fractions of the sulfated soil

3.5 Elemental composition after 10% HF solution pretreatment

After concentration of SOM by HF solution, the C and N contents ranged from 7.7 to 18.3% and 0.56 to 1.5%, respectively (Table 3). These results represent a significant increase of up to 27.3 and 34.6-fold for C and N, respectively, over the initial contents in the soil samples. The increase in C and N contents results from the dissolution and removal of the mineral fraction by the HF solution. The C/N ratio after HF either decreased (P2H2) or increased in comparison to the C/N of the bulk sample (Table 3), showing that enrichment in C and in N was not uniform among the analyzed samples. The R-factor of samples P2H3, P4H1 and P4H2 was greater than 1, indicating a preferential loss of N-bearing

compounds during HF treatment, whereas R-factor of 0.8 in P2H2 indicates a preferential loss of C-rich compounds.

Table 3. C and N contents, C/N ratio (w/w), R-factor and C_E (%) of the samples concentrated with 10% HF solution.

Samples	C_{HF} (%)	N_{HF} (%)	C/N_{HF}	R-factor	C_E (%)
P2H2	18,3	1,49	12,3	0.8	27.31
P2H3	12,11	0,73	16,6	1.3	17.81
P4H1	7,69	0,61	12,6	1.9	8.74
P4H2	10,08	0,56	18,0	2.7	10.72

3.6 Molecular composition investigated by ^{13}C NMR CP/MAS spectroscopy

Information about SOM molecular structure was provided by ^{13}C NMR spectra from two profiles of the Peninsula, P2 being representative of the low platforms and P4 representative of the high platforms (Figure 12a, b).

All analyzed samples showed the same ^{13}C NMR-CP/MAS spectra pattern (Figure 12) where the most abundant groups were alkyl C (0-45 ppm) and aryl C (110-160 ppm) groups (Table 4), whose proportions ranged from 27 to 46%, and 32 to 46% respectively. The O-alkyl C and carbonyl C groups contributed in smaller proportions to the SOM_{HF} composition, between 13 and 35% and 6 and 22%, respectively. A low proportion of O-alkyl groups was expected as shown by the thermochemolysis results (Figures 7a and c; Figures and 8a and c). However, the comparatively high proportion of aryl C and, consequently lower proportion of alkyl C obtained from the ^{13}C NMR spectra, disagrees with the data from Figures 7b, 7d, 8b and 8d.

Table 4. Distribution and proportion of main functional groups determined by ^{13}C NMR-CP/MAS and ratios Alkyl/Aryl (Al/Ar) and Alkyl/O-Alkyl (A/O-A) of the 10% HF-treated samples

Functional groups	Alkyl	O-alkyl	Aryl	Carbonyl/carboxyl		
Chemical shift range (ppm)	0-45	45-110	110-160	160-220		
Samples	----------%----------				Al/Ar	A/O-A
P2H2	46,1	13,8	35,9	22,1	1.7	3,3
P2H3	27,0	35,6	32,9	6,7	1.9	0,7
P4H1	33,3	22,0	39,0	8,0	1.4	1,5
P4H2	28,7	17,8	46,0	12,6	1.0	1,6

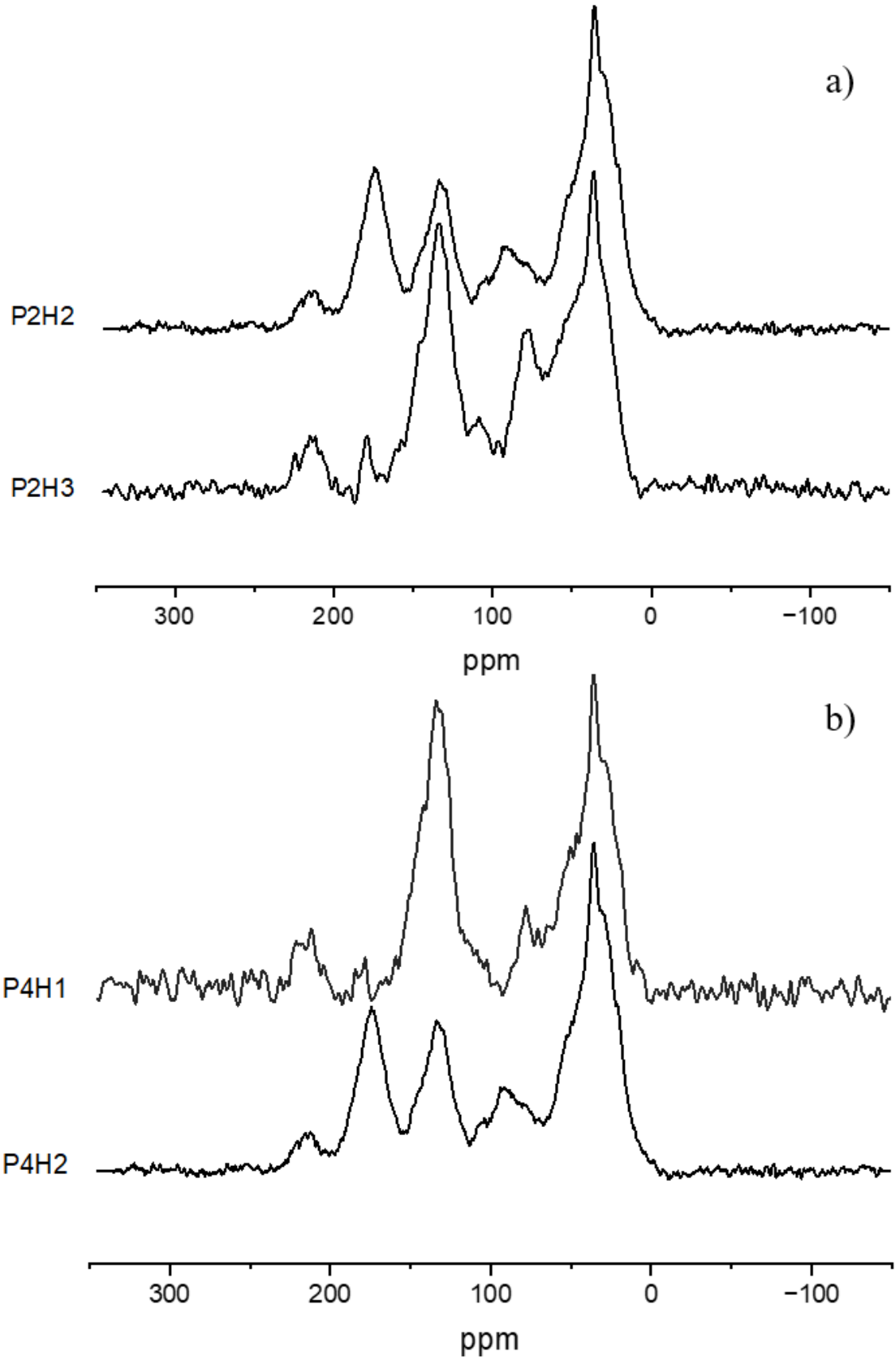

Figure 12. ^{13}C NMR CP/MAS spectra of the SOM samples from profiles P2 (a) and P4 (b), treated with 10% HF solution.

The pattern of variation of functional groups differed between the two profiles, with the exception of alkyl C groups, whose proportion decreased with depth in both sites (Figure 12, table 3). Sample P2H2 (Figure 12) was dominated by alkyl C groups (0-45 ppm), indicating the abundance of lipids in the sample. Some signals (45-110 ppm) can be attributed to cellulose since cellulose may be present in these soils associated with the cell wall of fungi, as the plant diversity is restricted to only the grass *Deschampsia antarctica* and *Colobanthus quitensis* in maritime Antarctica. The immediately underlying horizon (P2H3) showed a smaller proportion of alkyl C and a greater proportion of O-alkyl C. In low platform soils the subsuperficial horizons are more prone to microbial activity than in the surface resulting in a SOM richer in microbial-derived structures (e.g. carbohydrates) in detriment of alkyl C.

The spectra of the P4 profile (Figure 12b) were also dominated by both hydrophobic groups (alkyl C and Aryl-C). However, in P the decrease in the alkyl C proportion was accompanied by a decrease in O-alkyl C and an increase in C aryl and C carbonyl. The greater proportion of O-alkyls (carbohydrates/cellulose) and lower aryl C in the most superficial horizon (P4H1) indicates the higher lability of the SOM of this horizon and lower humification when compared to the SOM of the subsurface horizon (P4H2).

The aromatic signal band (160-110 ppm) in both soils does not resemble lignin due to the absence of the methoxyl group at 55ppm. This distinct pattern between the two soils was also confirmed by the alkyl C / aryl C ratio that showed a pattern of increase in P2 and decrease in P4 with depth. The alkyl C/O-alkyl C ratio also varied significantly among the samples examined, suggesting that the humification processes in the low platform soils (P2) and high platform soils (P4) are distinct from one another. In the low platform (P2), the index was much higher in P2H2 than in the subsequent horizon, reflecting greater progress in decomposition and humification in this horizon. On the high platform (P4), the behavior was the opposite, with a higher index in the subsurface, despite the small difference between the indices of the two horizons studied.

3.7 Principal Component and Correlation Analysis

Due to the great divergence in terms of contribution of the variables studied, three principal component analyses (PCAs) were performed to analyze the behavior of the variables related to the physical and chemical attributes of the soils (Figure 13), the biochemical composition of the SOM (Figure 14) and as to the stocks of C and N and the isotopic signatures of the samples studied as a function of the SOM fractions (Figure 15). For both PCAs the first two principal components (PC) were used which recorded the highest eigenvalues. The other PCs returned eigenvalues below 1.0 and hardly explained more variance than any of the original variables considered alone, so they were excluded from further interpretation.

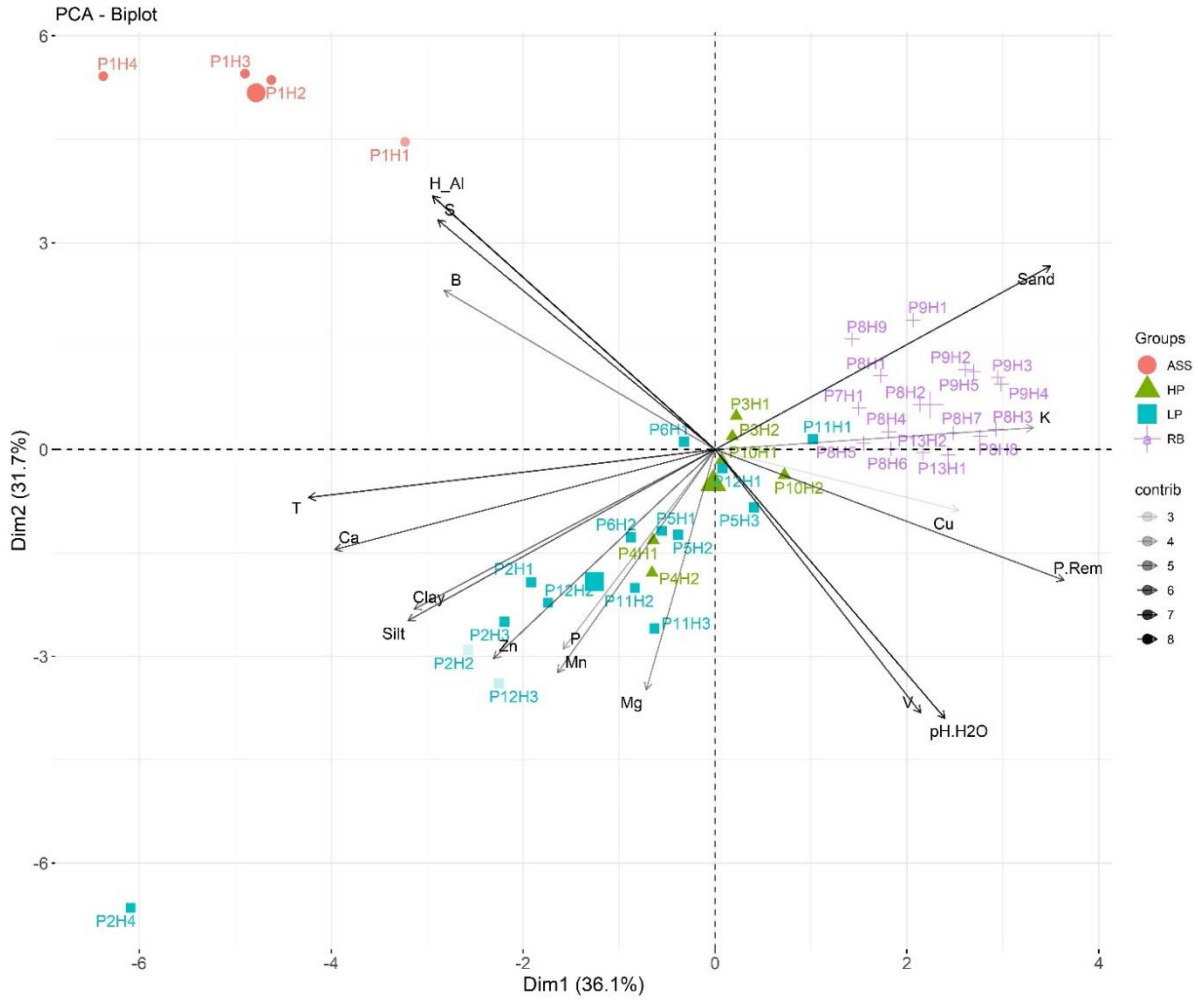

Figure 13. Principal component analysis - PCA with the separation of soil groups according to their chemical and physical soil attributes. Dim1 and Dim2: dimension axis.

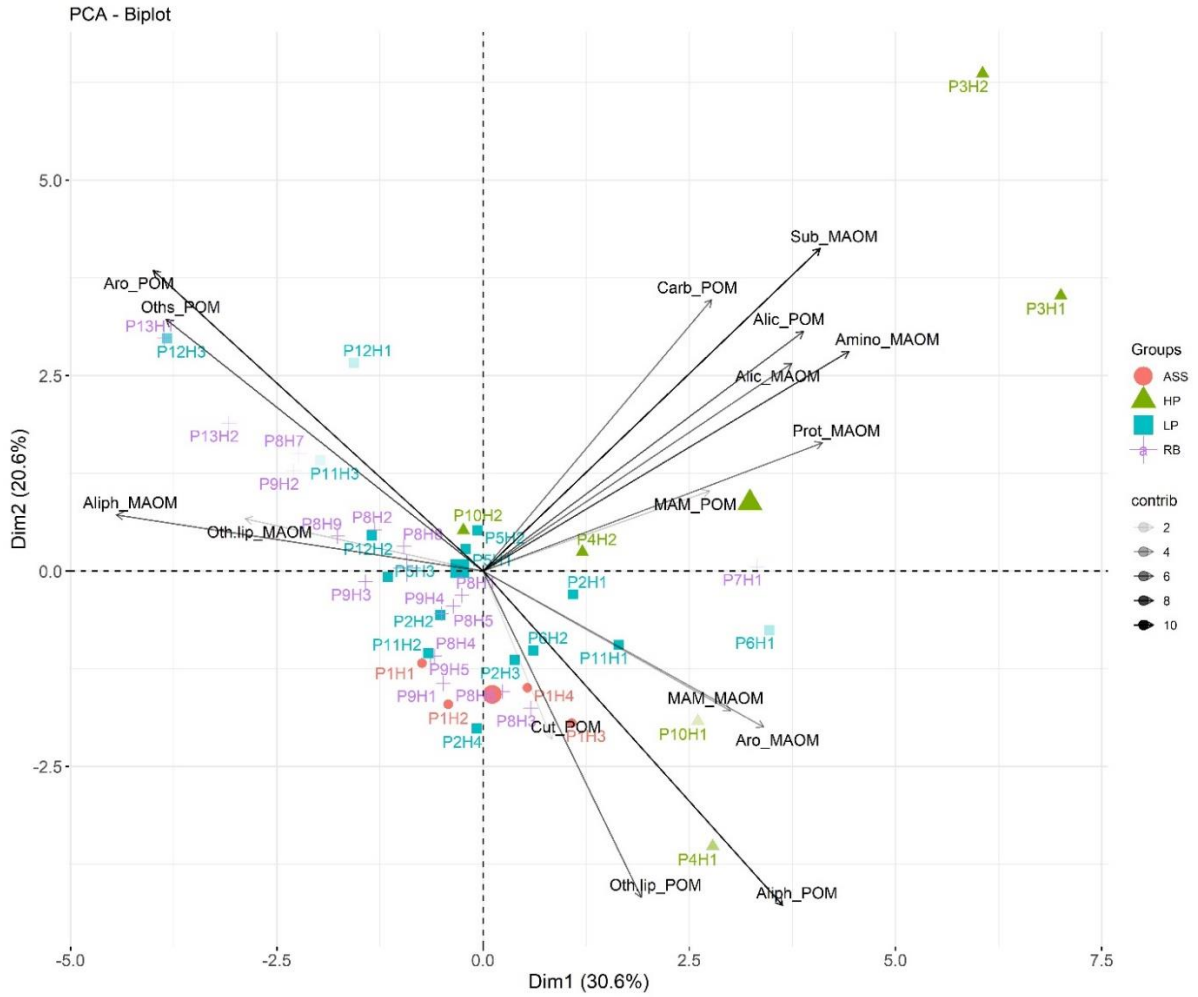

Figure 14. Principal component analysis - PCA indicating the separation of soil groups according to the biochemical composition of soil organic matter (origin/derivation of compounds and types of carbon chains of the compounds). Dim1 and Dim2: dimension axis.

In the first PCA (Figure 13) the eigenvalues above 1 of dimensions 1 and 2 together explained 67.8% of the variance. The remaining dimensions had eigenvalues below 1 and were excluded from the subsequent analysis. In the second PCA (Figure 14) the eigenvalues of dimensions 1 and 2 together explained 51.2% of the variance. In the third PCA (Figure 15) the eigenvalues of the first two dimensions explained 79.3% of the variance. Spearman's correlation analysis (Figure S1, S2a and b) was used in function of the variables studied in the PCA's, as a complementary tool to elucidate the results present in them. Both PCA's allowed for a grouping of characteristic variables for the groups of soils studied.

As for the physical and chemical attributes (Figure 13), the differentiation between soil groups and their association with specific attributes was more noticeable. The sulfate profile, P1, located in the desert floor, showed association mainly between the variables associated with the potential acidity of the soil (H+Al) and with the S and B, presenting a positive correlation between them. The high and low platforms showed a more comprehensive association of attributes, where the silt and clay fractions were

positively correlated, the cation exchange capacity was strongly influenced by the high Ca content, resulting in a positive correlation between these, and the P content in these profiles correlated positively with the Ca, Mn, and Zn content. As for the terraces, the variables associated with this environment were very specific and of great relevance for the characterization of this environment, these being the K content and high percentage of sand, a characteristic feature of marine terraces.

Regarding the biochemical composition of the SOM, analyzing the behavior of the aliphatic chain compounds among the soil groups showed that the more coastal profiles, represented by the raised beaches (P8, P9 and P13) and two low platforms (P11 and P12) presented the MAOM fraction more aliphatic and rich in oxygenated aliphatic compounds, which reflects the susceptibility of this SOM. In addition, these profiles stood out for the higher contribution of aromatic compounds in the POM fraction. On the other hand, the highest aliphatic contributions in the POM fraction and aromatic contributions in the MAOM fraction were associated with two high platforms (P4 and P10) and the acid sulfate soil profile (P1). The P3 profile showed great differentiation from the others and almost all of the contribution of alicyclic, nitrogenous, and carbohydrate compounds.

The total C and N stocks, as well as the stocks in the POM and MAOM fractions, showed a greater association with the profiles of the high and low platforms (Figure 15). The correlation between the total C and N stocks and between the C and N stocks in the fractions was greater than 50% for all (Figure S2b), showing the high correlation between C and N in the studied samples. In the MAOM fraction, the C and N stocks showed relatively higher values than in the POM fraction, in terms of contribution to the total stocks, thus the stocks in the MAOM fraction showed a high positive correlation with the total stocks of C and N. The $\delta^{13}C$ showed a high association with one of the raised beaches (P13), because this profile was observed the greatest variation (‰) of $\delta^{13}C$ in the POM fraction, as well as the highest values of $\delta^{13}C$ in both fractions (-17.44 ‰ in POM and -19.98 ‰ in MAOM), fully distinguishing between the isotopic signature of this profile with the others. In the MAOM fraction, $\delta^{15}N$ showed a greater association with raised beaches, due to the higher values observed in this group of soils, showing greater enrichment than in the other areas. The $\delta^{15}N$ in the POM fraction was more associated with the acid-sulfated soil profile (P1) and the highest platform (P3), where the highest values of $\delta^{15}N$ signature were observed.

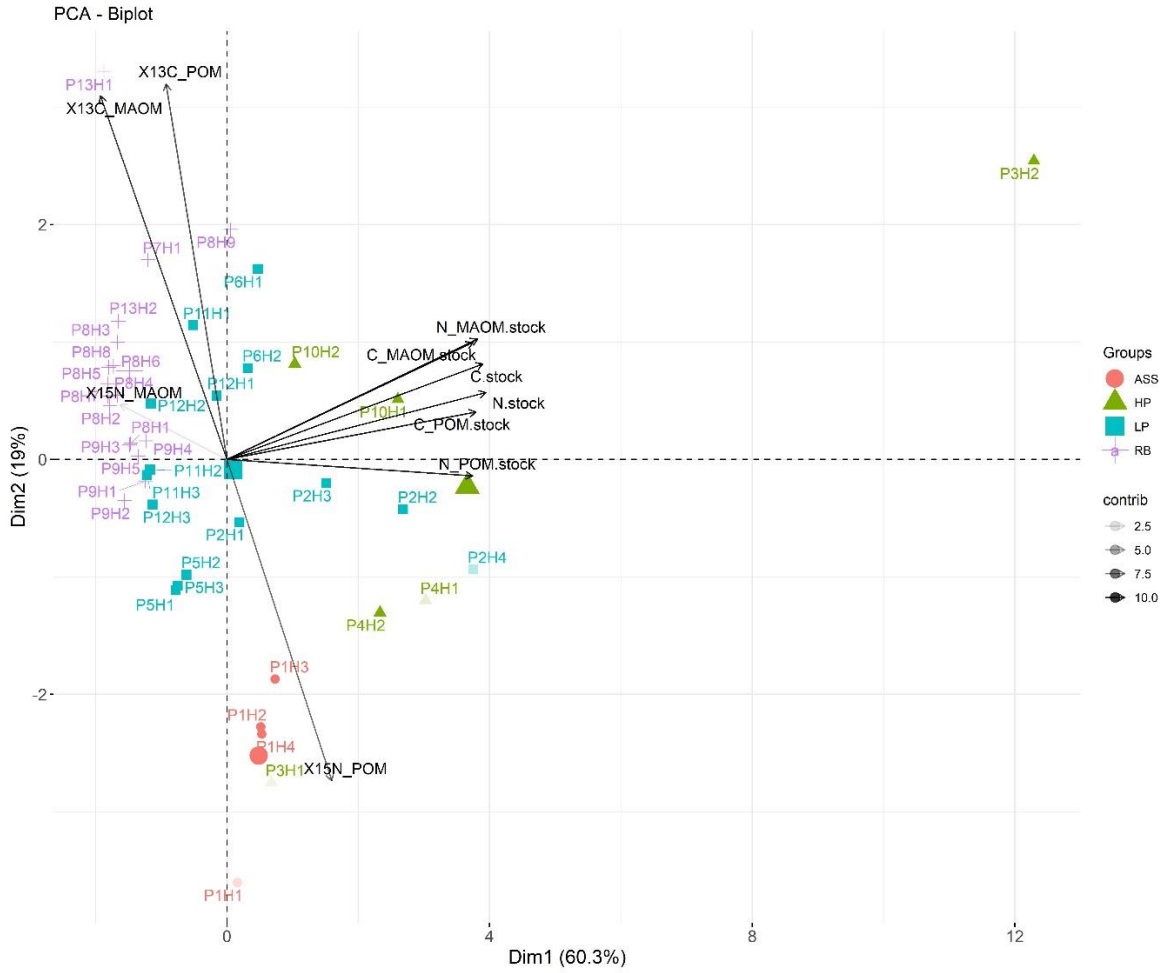

Figure 15. Principal component analysis - PCA indicating the separation of soil groups according to the C and N stocks and isotopic signatures of the studied samples as a function of SOM fractions (stock of C and N, $\delta^{13}C$ and $\delta\ ^{15}N$ of POM and MAOM fractions). Dim1 e Dim2: axis of dimensions.

4. Discussion

4.1 C and N in the soil profiles

The South Shetlands Islands and the Antarctic Peninsula have the highest stock of soil organic carbon (SOC) in the entire Antarctic continent, with estimated C stock of 600 Mt (Bockheim et al., 2013; Bockheim and Haus, 2014; Claridge et al., 2000) possibly due less severe climate conditions. This enabled an old colonization of large ice-free areas by seabirds and mammals (Emslie et al., 2020; Liu et al., 2005), and incorporation of organic C in Antarctic soils (Beyer, 2000; Beyer et al., 2000; Bockheim and Haus, 2014; Park et al., 2007). In the present study, there was a large variation in C and N stocks as a function of the positioning of the profiles in the landscape, this being a typical pattern for soils from polar environments (Lupachev et al., 2017; Zubrzycki et al., 2014).

More than 80% of the C and N stocks were associated with the most stable SOM fraction (MAOM). High stocks in the MAOM fraction were most significant in patterned ground soils associated with higher altitudes on the Peninsula. The higher preservation of these stocks in patterned soil

environments may be associated with cryoturbation. A process typical of cryogenic soils that allows more contact between fine solid-mineral soil particles with organic material, cryoturbed soils favor more stability of SOM and increased stocks at depth (Oliva and Ruiz-Fernández, 2015; Simas et al., 2008; Thomazini et al., 2020). This process implies reduced access by microorganisms to SOM, reducing the decomposition rate and increasing SOM stabilization in periglacial environments (Diochon et al., 2013; Ping et al., 2015).

Among the Cryosols, three profiles followed the pattern proposed in the literature of showing increased C and N stocks at depth (P1, P2 and P3). The other three Cryosols did not show this pattern (P10, P12 and P13), indicating that more factors besides cryoturbation may influence the stocks at depth in polar environments. The P1 profile, representative of acidic sulfate soils, has as a striking characteristic the high acidity and low N content, which makes it less favorable to microbial activity (Pires et al., 2017; Thomazini et al., 2015) resulting the accumulation of C and N at depth and the preservation of these stocks. The P2 profile, low platform developed on convex slope in a field of soils with a striated pattern formed through the periglacial solifluction process, can favor besides the formation of deeper soils, the increase of C stocks at depth, this being dependent on the vegetation at the surface (Fröjd et al., 2022). Moreover, this profile presented the highest clay content among the soils studied, which favors greater interaction between the organic fraction of the soil with the mineral fraction, enabling greater stability of the SOM through the organo-mineral association. P3, representative of the high platforms, among the Cryosols that showed increased C and N stocks at depth was the shallowest soil, possessing great abundance of vegetation on the surface, significant clay content and permafrost activity from 10 cm depth, this set of factors being favorable to the accumulation and increments of SOM at soil depth.

Organo-mineral association has received increasing attention for its the persistence in terrestrial ecosystems (Almeida et al., 2018; Kleber et al., 2015), resulting in considerable C stocks in Antarctic soils. In addition, the turnover of C present in organo-mineral associations is much longer than that of C associated with POM, free or occluded OM, ranging from decades to millennia (Kleber et al., 2015), helping to explain the permanence of C in these soils, despite the low input at the present time.

In addition to the physical protection provided to the SOM by the mineral fraction through the cryoturbation process, most of the C and N stocks in the soils of the Maritime Antarctic result from a primary production by fauna, microorganisms, algae and mainly by the abundant plant organisms in this environment. Among the plant organisms, lichens and mosses stand out for their high abundance in this environment, characterizing tundra-like environments. The lichen studied, UA, presents in its composition 40.9% of C, while the most abundant mosses in C content, AG and SU, presented 13.1 and 20.0% of C respectively. The high platforms that presented the greatest stocks of C and N are associated with this vegetation, corroborating previous studies, which also observed higher TOC and NT contents in areas colonized by lichens and mosses (Cannone et al., 2008; Otero et al., 2013).

The raised beaches had the lowest total stocks, possibly due to the coarser sandy texture of these soils, reducing the organo-mineral interaction, resulting in SOM migration in depth, since increases in clay in soil can result in reduced soil C loss, favoring an increase in the C stock (Dieckow et al., 2009; Plante et al., 2006). Other possible factors that explain the low C and N stock in the raised beaches may be associated with the difficulty of establishing plant species, due to the high salinity of these soils, and associated with this, the trampling and crawling of animals in these areas which are of larger agglomerations. Despite the lower C and N stocks, the POM fraction stood out over the MAOM in the raised beaches and acid-sulfated soils.

Following a pattern of low values observed for C/N ratios in Antarctic soils (Day et al., 2008), the C/N ratio of the SOM fractions in the studied profiles (Table S3, da Silva et al., 2022) was slightly low. This indicates that the SOM of these soils is more or less transformed compared to hystic materials of Cryosols embedded in areas dominated by mosses and plant litter (Lupachev et al., 2017). The highest C/N ratios were associated with the POM fraction, with values closer to the plant organisms studied, reflecting the primary contribution of the existing vegetation in these areas to the SOM.

4.2 Isotopic composition of the source materials and SOM fractions

Based on the observed $\delta^{13}C$ values of the mosses, lichen and grasses studied, the Byers Peninsula is dominated by organisms with a typical signature of terrestrial plants using the C_3 photosynthetic pathway, similar to observations made previously (Galimov, 2000; Hopkins et al., 2009; Lee et al., 2009; Park et al., 2007) with values ranging from -27.9 to -21.4‰. Most species of mosses and lichens have C/N ratios greater than 33 and grasses typically have a C/N ratio greater than 15, fitting these into the characteristic terrestrial vegetation classification (Lee et al., 2009). However, in the present study, the lichen *Usnea auranteaco-atra* showed a C/N ratio greater than 55 showing more depleted in ^{15}N, the grass *Deschampsia antarctica* showed more depleted in ^{13}C with a C/N ratio of 15, and the mosses showed the most diverse pattern from that portrayed in the literature, ranging from 16.7 to 25.1. The most striking feature in the distribution of $\delta^{13}C$ values is the specificity among species. Each taxonomic group has different values and within the group itself there are also distinct values, demonstrating the control of each species over the isotopic signature of $\delta^{13}C$, and this specificity may also be influenced by the different water utilization efficiency in the polar environment (Galimov, 2000; Lee et al., 2009).

The $\delta^{15}N$ values showed a wide variation among the organisms studied ($\Delta\delta^{15}N > 42‰$), and this can be attributed to the influence of nitrogen uptake derived from animals (Lee et al., 2009), precipitation, soil (Ellis et al., 2004), windborne particles (Bokhorst et al., 2007), or even through parasitic associations among organisms, such as the case of lichens that develop on mosses (Gaßmann and Ott, 2000). Most of the $\delta^{15}N$ values of the studied materials are shown to be strongly depleted in ^{15}N, which may reflect the assimilation of depleted ^{15}N sources, such as soil nitrate that can be easily depleted in the soils of several Antarctic regions (Michalski et al., 2005; Savarino et al., 2007).

The observed $\delta^{13}C$ values in the Byers Peninsula SOM fractions were very similar to those observed in the analyzed plant organisms, showing that the SOM of these soils has main derivation from Antarctic C_3 plants. This derivation is mainly associated with lichens, mosses, and algae, and may or may not have the contribution of fresh Antarctic animal droppings (Liu et al., 2006). In general, profiles P1 and P4 were the most depleted in ^{13}C in both fractions, indicating a contribution from an impoverished source, associating with endolithic communities or impoverished mosses (Burkins et al., 2000; Hopkins et al., 2009). In the case of profile P4, this endolitic contribution was also confirmed by the antiquity of the C dated in this soil (da Silva et al., 2022), with pre-LGM record, indicating the beginning of colonization of these areas. The relative increase in the observed values of $\delta^{13}C$ from the POM to the MAOM fraction in most of the studied profiles (P2, P4, P8, P9, P11 and P12), brings great indication of microbial contribution, where the enrichment of ^{13}C occurs due to microbial discrimination during decomposition/humification of SOM (Acton et al., 2013; Gautam et al., 2017; Sarangi et al., 2021).

Due to the significant overlap of $\delta^{13}C$ values even among distinct SOM sources, it becomes challenging to use isolated $\delta^{13}C$ values for the identification of possible contributing sources for SOM in this environment (Liu et al., 2006). Given this, for the identification of possible contributing sources for SOM fractions in Byers Peninsula soils, the isotopic signature of $\delta^{15}N$ was used as a complementary tool. Although the use of $\delta^{15}N$ is not common for identifying SOM sources (Burkins et al., 2000), previous studies have observed marked contrasts in $\delta^{15}N$ values, with soils from high altitudes possessing signatures associated with endolithic autotrophs, and low altitudes indicating signs of lacustrine/marine organisms (Barrett et al., 2006; Burkins et al., 2000). However, our data were contrasting to this observed pattern. Most of the soils embedded in the lower platforms showed a signature similar to that of organic matter of marine origin. The raised beaches showed a signature indicating ornithogenic contribution, consisting of colonization of these areas by penguins among other birds. Despite the uncertain isotopic composition in the raised platforms, oscillating between organic matter of lacustrine or marine origin, paleolimnological and geomorphological evidence rules out the possibility of marine contribution since the melting of most areas of the Byers Peninsula occurred at approximately 7.5 cal. kyr BP (Oliva et al., 2016).

4.3 Quality of SOM and plant materials

The quality of SOM is assigned based on its biochemical composition and the mineralization rate of its constituents. High quality SOM is characterized by a high mineralization rate, low amounts of recalcitrant compounds such as lignin and phenols, low C/N ratio and a high concentration of more labile compounds of microbial origin such as lipids, pepitides, carbohydrates and sugars in general, leading to a faster and more efficient accumulation of MAOM. Low-quality SOM, on the other hand, has a lower mineralization rate, due to the presence of larger amounts of aromatic compounds, and high C/N ratios, which will directly influence the slow decomposition rate of these organic materials

(Córdova et al., 2018; Cotrufo et al., 2013). SOM in Antarctic soils is generally of high quality, exhibiting intermediate to low C/N ratio values (Beyer et al., 2000; Carvalho et al., 2013) and low proportions of aromatic chains.

In the present study, the C/N ratio values in both fractions of the SOM, presented oscillations of the values in depth along the profiles. Considering that all samples are submitted to the same climatic condition and with poor vegetation cover (basically dominated by *Deschampsia antarctica* Desv., mosses and lichens), the differences found in the C/N ratios within the same profile and comparatively among them, can be attributed to the different soil moisture conditions (Carvalho et al., 2013). High C/N ratio is usually related to low decomposition of the SOM (Carvalho et al., 2013; Silva and Mendonça, 2007). In the studied samples the highest C/N ratio of 19 was observed in the POM fraction, whereas in the MAOM the values were not greater than 15. The values observed for the SOM fractions denote higher lability, and easy degradability by soil microorganisms, thus reflecting in the susceptibility of the C reservoirs in the marine Antarctic soils to mineralization and higher C-CO_2 emissions to the atmosphere. Thus, the quality of mainly the POM, can be used in several studies as proxies of resistance to degradation, and its correlation with the production and emission of C-CO_2, since this fraction is directly associated and closer to the materials that compose it.

Based on thermochemolysis, the SOM of the studied soils is dominated by aliphatic fragments. The biochemical composition revealed by thermochemolysis analysis showed between 60 and 95% abundance of aliphatic compounds in the fractions and on NMR between 46.5 and 62.6% in the samples analyzed. Similar previous observations have been made elsewhere on Livingston Island in the evaluation of humic acids with aliphatic fragments ranging between 65 and 69%, this predominance being caused by low lignin contents (Abakumov et al., 2022). This dominance can be associated with the abundance of mosses and lichens in this environment, where these organisms lead to the formation of aliphatic structural fragments.

As a highlight among the aliphatic chains observed in this study is the abundance of Alkyl C, both in the biochemical composition of the fractions and expressed in the NMR results. These long-chain hydrocarbons without the presence of oxygen in their structure are derived from plant biopolymers, such as cutin and wax, and microbial metabolites, and their hydrophobicity is directly related to the formation of more stable SOM (Savarese et al., 2021; Zhang et al., 2019). Thus, it is believed that the preservation of alkyl compounds in soil, may lead to the accumulation of SOM, based on a C sequestration mechanism in the progressively larger hydrophobic domains of SOM (Jandl et al., 2012; Piccolo et al., 2018; Spaccini et al., 2002). Given the above, it can be inferred as a possible hypothesis for the accumulation and maintenance of SOM in the soils of Byers Peninsula the abundant presence of these compounds (alkyl C), since in addition to the aromaticity present in both fractions of SOM, the contribution of alkyl C compounds was significantly higher than that of more labile compounds such as carbohydrates and nitrogen compounds.

The alkyl C/O-alkyl C ratio was used because it provides a better understanding of the extent of the decomposition process, a purpose for which this index was proposed (Baldock et al., 1997), and has since been used successfully in both temperate and tropical soils (Dick et al., 2005; Gonçalves et al., 2003; Höfle et al., 2013). However, the studied soils differ greatly in pedogenetic conditions, vegetation (table 1) and microbial diversity (Silva et al *in plero*) from the mentioned environments; thus, the use of this ratio for the same purpose should be taken with extreme caution.

The low proportion of O-Alkyl C compounds in the samples analyzed by NMR and the low proportion of oxygen-containing compounds identified by thermochemolysis, demonstrates the low oxidation state of the SOM in these soils, this being possibly caused by the humification processes of this SOM. As the predominance in these areas is of lower plant organisms, the precursors of humification of this SOM are formed from the dominant organisms, mosses and lichens; which have almost no aromatic structures, consisting basically of carbohydrates and proteins (Abakumov et al., 2022). This explains the presence of carbohydrates and amino acids/proteins in almost all the studied profiles, being due to the contribution of these organisms indicating their primary contribution to the biochemical composition of the SOM.

D. antarctica stands out among the contributions of carbohydrates to the SOM in the Byers Peninsula soils. *D. antarctica* has more than 49% of carbohydrates, but in the soils where it is present, there is no contribution to the SOM fractions. This demonstrates the low contribution of this vegetation to the local SOM. Concomitantly to what has been described, studies have shown that greenhouse gas emissions in areas where *D. antarctica* occurs are in order of magnitude of 514% higher in these maritime areas (La Scala et al., 2010). This can be explained by the biochemical composition of this plant, which helps to understand the low contribution of *D. antarctica* to SOM and the high CO_2 fluxes in the areas where they are located, due to the high percentage of carbohydrates present in its composition, where these compounds have short persistence in the soil due to its rapid mineralization by microorganisms (Otto and Simpson, 2006). On the other hand, this information reinforces the direct contribution of mosses and lichens with carbohydrates to the SOM fractions. In addition, plant-derived carbohydrates can be synthesized by microorganisms into new carbohydrates of microbial origin (Lowe, 1978), indicating that this contribution can be associated with the vegetation present in the area and also with microbial synthesis.

Referring to the higher proportion of aryl C than alkyl C in the NMR spectra diverging from the data obtained by thermochemolysis, two possible facts may account for the conflicting results obtained from the two analytical techniques, which might be contributing simultaneously to the results. Firstly, the TMAH-thermochemolise may have not attacked all the aromatic compounds, especially if there are polymerized structures, leading to an underestimation of their abundance (Higuchi, 2004; Khatami et al., 2019; Waggoner et al., 2015). Secondly, the loss of SOM during HF treatment (already mentioned by the discussion of the C/N ratio), occurred mainly with hydrophilic structures adsorbed on the MOAM (Chabbi et al., 2009; Rumpel et al., 2006), leading to a relative enrichment of aromatic

structures. In spite of these possible process, the ^{13}C NMR data reflects the composition of at least a considerable part of the SOM and are, therefore, reliable.

The vegetation of the studied area is almost exclusively non-ligniferous and such an expressive occurrence of aromatics groups in the composition of SOM from Antarctic soils was, initially, not expected. A possible source for the aryl groups in the SOM of P2 and P4 is the aerial transport of black-carbon-like material from forest fires in South America as proved by (Antony et al., 2014) while studying the molecular composition of dissolved organic matter (DOM) in East Antarctica. The authors were able to connect the presence of aromatic terrestrial material (tannin and lignin) and condensed aromatics in DOM to the air mass transport from Southern America over to their studied area transects.

Nevertheless, an *in situ* synthesis of aryl structures should also be considered. The formation of aromatic structures in DOM from East Antarctica was accomplished by photo-biochemical processes evidencing the interaction between light and microbes in the humification of Antarctic SOM (Antony et al., 2018). Accordingly, the photochemical-mediated processes dominate during Antarctic summer, which last on average 3 months (Bañón et al., 2013), whereas during winter microbial processes govern the DOM formation. Humification process with the formation of aromatic compounds in Antarctic SOM has been also verified (Abakumov and Alekseev, 2018; Beyer et al., 1995).

On the surface soils of the Byers Peninsula, as well as the Maritime Antarctic in general, it is notable the presence of plant communities whether isolated or associated (Pereira and Putzke, 2013), colonizing the most diverse environments in this ecosystem, being their distribution influenced by microclimatic conditions, position in the landscape, soil moisture, soil chemical characteristics and surface types (Francelino et al., 2011; Thomazini et al., 2016; Victoria et al., 2013). Thus, these factors in addition to influencing the establishment of these plant communities, associated with microbial activity in these soils, develop an important role in the dynamics of decomposition of plant residues and their contribution to the SOM in this environment. In turn, the contribution of these plant materials to the SOM, is directly associated with its composition/quality.

The biochemical characterization of the most abundant plant materials on the surface of the soils studied showed that the predominant composition of most of them (mosses and lichens), is associated with lipid and carbohydrate compounds. These compounds present in their composition O-alkyl chains, which indicates greater lability and easy access to decomposer microorganisms, especially in the early stages of decomposition, being accessed by these microorganisms in sequence the Alkyl C fraction (Bonanomi et al., 2013; Otto and Simpson, 2006; Zhang et al., 2013). In view of the above, it can be inferred that the contribution of these plant organisms to the SOM in Antarctic soils may be low due to the lability of their constituents, but due to the low microbial activity and the climatic conditions that dominate this environment, they favor relative accumulation and contribution to SOM stocks.

Besides the extreme climatic conditions in the Antarctic environment, another factor to which attention should be paid regarding the accumulation/degradation of SOM in this environment is the microbial activity in the soil, which is strongly influenced by microclimatic conditions, such as soil

temperature variation and water regime, which directly affect primary production and C uptake (Thomazini et al., 2016). Even with increasing temperatures and consequent glacier retreat and exposure of soils to plant and microbial colonization, microbial activity in this environment is still limited mainly due to climatic conditions. Analyzing the relative abundance of MAM's, the low expressivity and presence of these organisms in the soils of BP was remarkable. Given the presence of these markers in the samples studied, the distribution pattern indicates an activity, even if low, in the subsurface, contradictory to the pattern normally observed in soils of tropical and temperate regions, where in these environments the highest activity reported is associated with the surface of the soils (Stone et al., 2014).

Due to the absence of higher plants the precursors of SOM humification on the Byers Peninsula is directly associated with mosses and lichens, these organisms being poor in aromatic structures and lignin, the latter being the main precursor compound of humification from higher plants (Karmanov et al., 2015; Semenov et al., 2009). Despite the low proportion of aromatic fragments (5.8 to 12.5% - Figure 11b) and absence of lignin-derived compounds, mosses and lichens may contain up to 10% tannins and flavanoids in their biochemical composition, thus contributing to the aromaticity of the SOM (Abakumov et al., 2022) of the studied profiles. Other studies have already arrived at higher values of these compounds in the biochemical composition of mosses and lichens, the former being low in lignin containing up to 20% tannins and flavonoids, and lichens contain up to 2% tannins and flavonoids and up to 10% lignin (Orlov, 1990). In the present study, no lignin fragments were observed in the mosses or lichens analyzed.

The only plant organism that presented fragments derived from lignin in its composition was the grass D. antarctica, however, even the areas where this vegetation is dominant, it was not observed participation of these aromatic fragments in the SOM fractions of these soils. Only profile P5 presented fragments derived from lignin (P17&P18), and this contribution possibly came from the unidentified crustose lichen that was on the surface of this profile, colonizing the rocky fragments.

The high diversity of biotic and abiotic factors acting in maritime Antarctica directly affects the accumulation, transformation, and stabilization of SOM. Due to the greater presence of ecological niches, greater plant diversity with the presence of vascular plants, and the marked action of avifauna, these factors differentiate the processes involved in the redistribution of SOM between Maritime and Continental Antarctica, in addition to the humidity factor (in the form of net precipitation) being a key factor in the most active humification processes in the soils studied (Abakumov et al., 2022).

5. Conclusion

Byers Peninsula soils showed a diverse and varied biochemical nature of SOM, resulting in varying levels of C and N as well as their constituents, showing a large contribution of lipid compounds derived from both plant and animal sources, these being dominated by long chain hydrocarbons reflecting the hydrophobicity of this organic matter.

Differences of SOM content indicate that deglaciation has led to the loss of a large portion of the labile organic matter and suggest that the residual organic matter acts to stabilize hydrolytic enzyme activities. The stabilizing action implies a saving in enzyme synthesis and to a certain extent should mitigate the biochemical degradation associated with the loss of soil organic matter.

The largest C and N pools were recorded on the high and low platforms and in the organo-mineral association fraction, where not all Cryosols followed a pattern of increase in depth. The isotopic signatures found in the SOM fractions of the Byers Peninsula soils revealed a wide variation of potential C sources in these soils, these being reflective of the colonization of these areas and landscape development/transformation, indicating different geological stages of SOM accumulation in this area.

Acknowledgments

We thank the CNPq (Conselho Nacional de Desenvolvimento Científico e Tecnológico), CAPES (Coordenação de Aperfeiçoamento de Pessoal de Nível Superior) and FAPEMIG (Fundação de Amparo à Pesquisa do Estado de Minas Gerais) for financial support. We are grateful to INCT da Criosfera, TERRANTAR and MARINHA DO BRASIL (PROANTAR PROGRAM) for financial support and field assistance. We thank the reviewers for their careful reading of the manuscript and their constructive remarks.

SUPPLEMENTARY DATA IN THE APENDIX C

Bibliographic references

Abakumov, E., 2017. Characterisation of humic acids, isolated from selected sub-antarctic soils by 13C-NMR spectroscopy. Czech Polar Reports 7, 1–10. https://doi.org/10.5817/CPR2017-1-1

Abakumov, E., Alekseev, I., 2018. Stability of soil organic matter in Cryosols of the maritime Antarctic: Insights from 13C NMR and electron spin resonance spectroscopy. Solid Earth 9, 1329–1339. https://doi.org/10.5194/SE-9-1329-2018

Abakumov, E., Mukhametova, N., 2014. Microbial biomass and basal respiration of selected Sub-Antarctic and Antarctic soils in the areas of some Russian polar stations. Solid Earth 5, 705–712. https://doi.org/10.5194/SE-5-705-2014

Abakumov, E., Yaneva, R., Polyakov, V., Zhiyanski, M., 2022. Characterization of Humic Acids Isolated from Selected Soils of Livingston Island by CP/MAS 13C NMR and ESR Spectroscopy. Appl. Environ. Soil Sci. 2022. https://doi.org/10.1155/2022/7540077

Abakumov, E. V., 2010. The sources and composition of humus in some soils of West Antarctica. Eurasian Soil Sci. 43, 499–508. https://doi.org/10.1134/S1064229310050030

Abakumov, E. V, Fattakhova, Y.M., 2015. Structural composition of humic acids of ornitogenic soils on the data of 13-C NMR resonance [WWW Document]. Russ. Ornitol. URL https://scholar.google.com.br/scholar?hl=pt-BR&as_sdt=0%2C5&q=Structural++composition++of++humic++acids++of+ornitogenic+soils+on+the+data+of+13C-NMR+resonance&btnG= (accessed 4.13.22).

Acton, P., Fox, J., Campbell, E., Rowe, H., Wilkinson, M., 2013. Carbon isotopes for estimating soil decomposition and physical mixing in well-drained forest soils. J. Geophys. Res. Biogeosciences 118, 1532–1545. https://doi.org/10.1002/2013JG002400

Almeida, L.F.J., Hurtarte, L.C.C., Souza, I.F., Soares, E.M.B., Vergütz, L., Silva, I.R., 2018. Soil organic matter formation as affected by eucalypt litter biochemistry — Evidence from an incubation study. Geoderma 312, 121–129. https://doi.org/10.1016/J.GEODERMA.2017.10.004

Amesbury, M.J., Roland, T.P., Royles, J., Hodgson, D.A., Convey, P., Griffiths, H., Charman, D.J., 2017. Widespread Biological Response to Rapid Warming on the Antarctic Peninsula. Curr. Biol. 27, 1616-1622.e2. https://doi.org/10.1016/J.CUB.2017.04.034

Antony, R., Grannas, A.M., Willoughby, A.S., Sleighter, R.L., Thamban, M., Hatcher, P.G., 2014. Origin and Sources of Dissolved Organic Matter in Snow on the East Antarctic Ice Sheet. Environ. Sci. Technol. 48, 6151–6159. https://doi.org/10.1021/es405246a

Antony, R., Willoughby, A.S., Grannas, A.M., Catanzano, V., Sleighter, R.L., Thamban, M., Hatcher, P.G., 2018. Photo-biochemical transformation of dissolved organic matter on the surface of the coastal East Antarctic ice sheet. Biogeochemistry 141, 229–247. https://doi.org/10.1007/s10533-018-0516-0

Baldock, J.A., Oades, J.M., Nelson, P.N., Skene, T.M., Golchin, A., Clarke, P., 1997. Assessing the extent of decomposition of natural organic materials using solid-state 13C NMR spectroscopy. Soil Res. 35, 1061. https://doi.org/10.1071/S97004

Bañón, M., Justel, A., Velázquez, D., Quesada, A., 2013. Regional weather survey on Byers Peninsula, Livingston Island, South Shetland Islands, Antarctica. Antarct. Sci. 25, 146–156. https://doi.org/10.1017/S0954102012001046

Barrett, J.E., Virginia, R.A., Wall, D.H., Cary, S.C., Adams, B.J., Hacker, A.L., Aislabie, J.M., 2006. Co-variation in soil biodiversity and biogeochemistry in northern and southern Victoria Land, Antarctica. Antarct. Sci. 18, 535–548. https://doi.org/10.1017/S0954102006000587

Barsch, D., Blümel, W., Flügel, W., Mausbacher, R., Stäblein, G., Zick, W., 1985. Untersuchungen zum Periglazial auf der König-Georg-lns Südshetlandinseln/Antarktik. Reports Polar Res. 24.

Benayas, J., Pertierra, L., Tejedo, P., Lara, F., Bermudez, O., Hughes, K.A., Quesada, A., 2013. A review of scientific research trends within ASPA No. 126 Byers Peninsula, South Shetland Islands, Antarctica. Antarct. Sci. 25, 128–145. https://doi.org/10.1017/S0954102012001058

Beyer, B.L., Vogt, B., Erlenkeuser, H., 1995. Soil Organic Matter Composition and Transformation in a Swamp Soil from Algae of Coastal Continental Antarctica. Soil Biol. Biochem. 27, 1279–1288.

Beyer, L., 2000. Properties, formation, and geo-ecological significance of organic soils in the coastal region of East Antarctica (Wilkes Land). CATENA 39, 79–93. https://doi.org/10.1016/S0341-8162(99)00090-9

Beyer, L., Pingpank, K., Wriedt, G., Bölter, M., 2000. Soil formation in coastal continental Antarctica (Wilkes Land). Geoderma 95, 283–304. https://doi.org/10.1016/S0016-7061(99)00095-6

Beyer, L., White, D.M., Pingpank, K., Bölter, M., 2004. Composition and Transformation of Soil Organic Matter in Cryosols and Gelic Histosols in Coastal Eastern Antarctica (Casey Station, Wilkes Land). Cryosols 525–556. https://doi.org/10.1007/978-3-662-06429-0_26

Bockheim, J., Vieira, G., Ramos, M., López-Martínez, J., Serrano, E., Guglielmin, M., Wilhelm, K., Nieuwendam, A., 2013. Climate warming and permafrost dynamics in the Antarctic Peninsula region. Glob. Planet. Change 100, 215–223. https://doi.org/10.1016/J.GLOPLACHA.2012.10.018

Bockheim, J.G., Haus, N.W., 2014. Distribution of Organic Carbon in the Soils of Antarctica, in: Soil Carbon. Springer International Publishing, Cham, pp. 373–380. https://doi.org/10.1007/978-3-319-04084-4_37

Bokhorst, S., Huiskes, A., Convey, P., Aerts, R., 2007. External nutrient inputs into terrestrial

ecosystems of the Falkland Islands and the Maritime Antarctic region. Polar Biol. 30, 1315–1321. https://doi.org/10.1007/S00300-007-0292-0/FIGURES/3

Bonanomi, G., Incerti, G., Giannino, F., Mingo, A., Lanzotti, V., Mazzoleni, S., 2013. Litter quality assessed by solid state 13C NMR spectroscopy predicts decay rate better than C/N and Lignin/N ratios. Soil Biol. Biochem. 56, 40–48. https://doi.org/10.1016/j.soilbio.2012.03.003

Burkins, M.B., Virginia, R.A., Page Chamberlain, C., Wall, D.H., 2000. ORIGIN AND DISTRIBUTION OF SOIL ORGANIC MATTER IN TAYLOR VALLEY, ANTARCTICA. Ecology 81, 2377–2391. https://doi.org/10.1890/0012-9658

Calace, N., Campanella, L., Paolis, F. De, Petronio, B.M., 1995. Characterization of Humic Acids Isolated from Antarctic Soils. Int. J. Environ. Anal. Chem. 60, 71–78. https://doi.org/10.1080/03067319508027229

Cambardella, C.A., Elliott, E.T., 1992. Particulate Soil Organic-Matter Changes across a Grassland Cultivation Sequence. Soil Sci. Soc. Am. J. 56, 777. https://doi.org/10.2136/sssaj1992.03615995005600030017x

Cannone, N., Wagner, D., Hubberten, H.W., Guglielmin, M., 2008. Biotic and abiotic factors influencing soil properties across a latitudinal gradient in Victoria Land, Antarctica. Geoderma 144, 50–65. https://doi.org/10.1016/j.geoderma.2007.10.008

Carvalho, J.V.D.S., Mendonça, E.D.S., La Scala, N., Reis, C., Reis, E.L., Schaefer, C.E.G.R., 2013. CO 2 -C losses and carbon quality of selected Maritime Antarctic soils. Antarct. Sci. 25, 11–18. https://doi.org/10.1017/S0954102012000648

Chabbi, A., Kögel-Knabner, I., Rumpel, C., 2009. Stabilised carbon in subsoil horizons is located in spatially distinct parts of the soil profile. Soil Biol. Biochem. 41, 256–261. https://doi.org/10.1016/J.SOILBIO.2008.10.033

Charman, D.J., Amesbury, M.J., Roland, T.P., Royles, J., Hodgson, D.A., Convey, P., Griffiths, H., 2018. Spatially coherent late Holocene Antarctic Peninsula surface air temperature variability. Geology 46, 1071–1074. https://doi.org/10.1130/G45347.1

Chefetz, B., Chen, Y., Clapp, C.E., Hatcher, P.G., 2000. Characterization of Organic Matter in Soils by Thermochemolysis Using Tetramethylammonium Hydroxide (TMAH). Soil Sci. Soc. Am. J. 64, 583–589. https://doi.org/10.2136/sssaj2000.642583x

Claridge, G.G.C., Campbell, I.B., Sheppard, D.S., 2000. Carbon Pools in Antarctica and Their Significance for Global Climate Change, in: Global Climate Change and Cold Regions Ecosystems. CRC Press, pp. 71–90. https://doi.org/10.1201/9781482278637-12

Córdova, S.C., Olk, D.C., Dietzel, R.N., Mueller, K.E., Archontouilis, S. V., Castellano, M.J., 2018. Plant litter quality affects the accumulation rate, composition, and stability of mineral-associated soil organic matter. Soil Biol. Biochem. 125, 115–124. https://doi.org/10.1016/j.soilbio.2018.07.010

Cotrufo, M.F., Wallenstein, M.D., Boot, C.M., Denef, K., Paul, E., 2013. The Microbial Efficiency-Matrix Stabilization (MEMS) framework integrates plant litter decomposition with soil organic matter stabilization: do labile plant inputs form stable soil organic matter? Glob. Chang. Biol. 19, 988–995. https://doi.org/10.1111/gcb.12113

da Silva, J.P., Lelis Leal de Souza, J.J., Mercês Barros Soares, E., Schaefer, C.E.G.R., 2022. Soil organic matter accumulation before, during, and after the last glacial maximum in Byers Peninsula, Maritime Antarctica. Geoderma 116221. https://doi.org/10.1016/j.geoderma.2022.116221

Day, T.A., Ruhland, C.T., Xiong, F.S., 2008. Warming increases aboveground plant biomass and C stocks in vascular-plant-dominated Antarctic tundra. Glob. Chang. Biol. 14, 1827–1843. https://doi.org/10.1111/J.1365-2486.2008.01623.X

Del Rio, J.C., McKinney, D.E., Knicker, H., Nanny, M.A., Minard, R.D., Hatcher, P.G., 1998. Structural characterization of bio- and geo-macromolecules by off-line thermochemolysis with tetramethylammonium hydroxide. J. Chromatogr. A 823, 433–448. https://doi.org/10.1016/S0021-9673(98)00268-4

Dick, D.P., Nunes Gonçalves, C., Dalmolin, R.S.D., Knicker, H., Klamt, E., Kögel-Knabner, I., Simões, M.L., Martin-Neto, L., 2005. Characteristics of soil organic matter of different Brazilian Ferralsols under native vegetation as a function of soil depth. Geoderma 124, 319–333. https://doi.org/10.1016/J.GEODERMA.2004.05.008

Dieckow, J., Bayer, C., Conceição, P.C., Zanatta, J.A., Martin-Neto, L., Milori, D.B.M., Salton, J.C., MacEdo, M.M., Mielniczuk, J., Hernani, L.C., 2009. Land use, tillage, texture and organic matter stock and composition in tropical and subtropical Brazilian soils. Eur. J. Soil Sci. 60, 240–249. https://doi.org/10.1111/J.1365-2389.2008.01101.X

Diochon, A., Gregorich, E.G., Tarnocai, C., 2013. Evaluating the quantity and biodegradability of soil organic matter in some Canadian Turbic Cryosols. Geoderma 202–203, 82–87. https://doi.org/10.1016/J.GEODERMA.2013.03.013

Ellis, C.J., Crittenden, P.D., Scrimgeour, C.M., 2004. Soil as a potential source of nitrogen for mat-forming lichens. Can. J. Bot. 82, 145–149. https://doi.org/10.1139/b03-144

Emslie, S.D., Romero, M., Juáres, M.A., Argota, M.R., 2020. Holocene occupation history of pygoscelid penguins at Stranger Point, King George (25 de Mayo) Island, northern Antarctic Peninsula. The Holocene 30, 190–196. https://doi.org/10.1177/0959683619875814

Fitzpatrick, E.A., 1984. Micromorphology of Soils. Micromorphol. Soils. https://doi.org/10.1007/978-94-009-5544-8

Francelino, M.R., Schaefer, C.E.G.R., Simas, F.N.B., Filho, E.I.F., de Souza, J.J.L.L., da Costa, L.M., 2011. Geomorphology and soils distribution under paraglacial conditions in an ice-free area of Admiralty Bay, King George Island, Antarctica. CATENA 85, 194–204.

https://doi.org/10.1016/J.CATENA.2010.12.007

Fritz, M., Deshpande, B.N., Bouchard, F., Högström, E., Malenfant-Lepage, J., Morgenstern, A., Nieuwendam, A., Oliva, M., Paquette, M., Rudy, A.C.A., Siewert, M.B., Sjöberg, Y., Weege, S., 2015. Brief Communication: Future avenues for permafrost science from the perspective of early career researchers. Cryosphere 9, 1715–1720. https://doi.org/10.5194/TC-9-1715-2015

Fröjd, C., Trombotto Liaudat, D., Scheer, C., Pecker Marcosig, I., Kuhry, P., 2022. Soil organic carbon stocks in mountain periglacial areas of northern Patagonia (Argentina). Arctic, Antarct. Alp. Res. 54, 176–199. https://doi.org/10.1080/15230430.2022.2062102

Galimov, E.M., 2000. Carbon isotope composition of Antarctic plants. Geochim. Cosmochim. Acta 64, 1737–1739. https://doi.org/10.1016/S0016-7037(99)00328-2

Gaßmann, A., Ott, S., 2000. Growth Strategy and the Gradual Symbiotic Interactions of the Lichen Ochrolechia frigida. Plant Biol. 2, 368–378. https://doi.org/10.1055/s-2000-3711

Gautam, M.K., Lee, K.S., Song, B.Y., Bong, Y.S., 2017. Site related δ13C of vegetation and soil organic carbon in a cool temperate region. Plant Soil 418, 293–306. https://doi.org/10.1007/S11104-017-3284-Z/TABLES/5

Gonçalves, C.N., Dalmolin, R.S.D., Dick, D.P., Knicker, H., Klamt, E., Kögel-Knabner, I., 2003. The effect of 10% HF treatment on the resolution of CPMAS 13C NMR spectra and on the quality of organic matter in Ferralsols. Geoderma 116, 373–392. https://doi.org/10.1016/S0016-7061(03)00119-8

Higuchi, T., 2004. Microbial degradation of lignin: Role of lignin peroxidase, manganese peroxidase, and laccase. Proc. Japan Acad. Ser. B 80, 204–214. https://doi.org/10.2183/PJAB.80.204

Höfle, S., Rethemeyer, J., Mueller, C.W., John, S., 2013. Organic matter composition and stabilization in a polygonal tundra soil of the Lena Delta. Biogeosciences 10, 3145–3158. https://doi.org/10.5194/BG-10-3145-2013

Hopkins, D.W., Sparrow, A.D., Gregorich, E.G., Elberling, B., Novis, P., Fraser, F., Scrimgeour, C., Dennis, P.G., Meier-Augenstein, W., Greenfield, L.G., 2009. Isotopic evidence for the provenance and turnover of organic carbon by soil microorganisms in the Antarctic dry valleys. Environ. Microbiol. 11, 597–608. https://doi.org/10.1111/j.1462-2920.2008.01830.x

Hugelius, G., Strauss, J., Zubrzycki, S., Harden, J.W., Schuur, E.A.G., Ping, C.L., Schirrmeister, L., Grosse, G., Michaelson, G.J., Koven, C.D., O'Donnell, J.A., Elberling, B., Mishra, U., Camill, P., Yu, Z., Palmtag, J., Kuhry, P., 2014. Estimated stocks of circumpolar permafrost carbon with quantified uncertainty ranges and identified data gaps. Biogeosciences 11, 6573–6593. https://doi.org/10.5194/BG-11-6573-2014

Jandl, G., Baum, C., Blumschein, A., Leinweber, P., 2012. The impact of short rotation coppice

on the concentrations of aliphatic soil lipids. Plant Soil 350, 163–177. https://doi.org/10.1007/S11104-011-0892-X/TABLES/4

Karmanov, A.P., Kocheva, L.S., Karmanova, Y.A., 2015. INVESTIGATION OF LIGNIN FROM MOSS POLYTRICHUM COMMUNE. Chemistry plant raw Mater. 109.

Khatami, S., Deng, Y., Tien, M., Hatcher, P.G., 2019. Formation of water-soluble organic matter through fungal degradation of lignin. Org. Geochem. 135, 64–70. https://doi.org/10.1016/j.orggeochem.2019.06.004

Kleber, M., Eusterhues, K., Keiluweit, M., Mikutta, C., Mikutta, R., Nico, P.S., 2015. Mineral–Organic Associations: Formation, Properties, and Relevance in Soil Environments, in: Advances in Agronomy. Elsevier Ltd, pp. 1–140. https://doi.org/10.1016/bs.agron.2014.10.005

Knicker, H., 2011. Solid state CPMAS 13C and 15N NMR spectroscopy in organic geochemistry and how spin dynamics can either aggravate or improve spectra interpretation. Org. Geochem. 42, 867–890. https://doi.org/10.1016/j.orggeochem.2011.06.019

La Scala, N., de Sá Mendonça, E., Vanir de Souza, J., Panosso, A.R., Simas, F.N.B., Schaefer, C.E.G.R., 2010. Spatial and temporal variability in soil CO2–C emissions and relation to soil temperature at King George Island, maritime Antarctica. Polar Sci. 4, 479–487. https://doi.org/10.1016/J.POLAR.2010.07.001

Lee, Y. Il, Lim, H.S., Yoon, H. Il, 2009. Carbon and nitrogen isotope composition of vegetation on King George Island, maritime Antarctic. Polar Biol. 32, 1607–1615. https://doi.org/10.1007/S00300-009-0659-5/FIGURES/6

Liu, X.-D., Li, H.-C., Sun, L.-G., Yin, X.-B., Zhao, S.-P., Wang, Y.-H., 2006. δ13C and δ15N in the ornithogenic sediments from the Antarctic maritime as palaeoecological proxies during the past 2000 yr. Earth Planet. Sci. Lett. 243, 424–438. https://doi.org/10.1016/j.epsl.2006.01.018

Liu, X., Sun, L., Xie, Z., Yin, X., Wang, Y., 2005. A 1300-year record of penguin populations at Ardley Island in the Antarctic, as deduced from the geochemical data in the ornithogenic lake sediments. Arctic, Antarct. Alp. Res. 37, 490–498. https://doi.org/10.1657/1523-0430(2005)037[0490:AYROPP]2.0.CO;2

Lopez-Martinez, J., Thomson, M., Arche, A., Bjorck, S., 1996. geomorphological map of Byers peninsula, livingston island. BAS Geomap Ser. Cambridge, Br. Antarct. Surv.

Lowe, L.E., 1978. Chapter 2 Carbohydrates in Soil. Dev. Soil Sci. 8, 65–93. https://doi.org/10.1016/S0166-2481(08)70017-5

Lupachev, A., Abakumov, E., Gubin, S., 2017. The Influence of Cryogenic Mass Exchange on the Composition and Stabilization Rate of Soil Organic Matter in Cryosols of the Kolyma Lowland (North Yakutia, Russia). Geosci. 2017, Vol. 7, Page 24 7, 24.

https://doi.org/10.3390/GEOSCIENCES7020024

Michalski, G., Bockheim, J.G., Kendall, C., Thiemens, M., 2005. Isotopic composition of Antarctic Dry Valley nitrate: Implications for NOy sources and cycling in Antarctica. Geophys. Res. Lett. 32, 1–4. https://doi.org/10.1029/2004GL022121

Michel, R.F.M., Schaefer, C.E.G.R., Dias, L.E., Simas, F.N.B., Benites, V. de M., Mendonça, E. de S., 2006. Ornithogenic Gelisols (Cryosols) from Maritime Antarctica. Soil Sci. Soc. Am. J. 70, 1370–1376. https://doi.org/10.2136/SSSAJ2005.0178

Mishra, U., Jastrow, J.D., Matamala, R., Hugelius, G., Koven, C.D., Harden, J.W., Ping, C.L., Michaelson, G.J., Fan, Z., Miller, R.M., McGuire, A.D., Tarnocai, C., Kuhry, P., Riley, W.J., Schaefer, K., Schuur, E.A.G., Jorgenson, M.T., Hinzman, L.D., 2013. Empirical estimates to reduce modeling uncertainties of soil organic carbon in permafrost regions: a review of recent progress and remaining challenges. Environ. Res. Lett. 8, 035020. https://doi.org/10.1088/1748-9326/8/3/035020

Ochyra, R., 1998. The moss flora of King George Island, Antarctica, Polish Academy of Sciences.

Ochyra, R., Smith, R.L., Bednarek-Ochyra, H., 2008. The illustrated moss flora of Antarctica. Cambridge University Press.

Olech, M., 2004. Lichens of King George Island, Antarctica. Institute of Botany of the Jagiellonian University, Kraków.

Oliva, M., Antoniades, D., Giralt, S., Granados, I., Pla-Rabes, S., Toro, M., Liu, E.J., Sanjurjo, J., Vieira, G., 2016. The Holocene deglaciation of the Byers Peninsula (Livingston Island, Antarctica) based on the dating of lake sedimentary records. Geomorphology 261, 89–102. https://doi.org/10.1016/J.GEOMORPH.2016.02.029

Oliva, M., Ruiz-Fernández, J., 2015. Coupling patterns between para-glacial and permafrost degradation responses in Antarctica. Earth Surf. Process. Landforms 40, 1227–1238. https://doi.org/10.1002/esp.3716

Orlov, D.S., 1990. Soil humic Acids and General Theory Humification. Moscov state University, Moscow.

Otero, X., Fernández, S., de Pablo Hernandez, M.A., Nizoli, E.C., Quesada, A., 2013. Plant communities as a key factor in biogeochemical processes involving micronutrients (Fe, Mn, Co, and Cu) in Antarctic soils (Byers Peninsula, maritime Antarctica). Geoderma 195–196, 145–154. https://doi.org/10.1016/j.geoderma.2012.11.018

Otto, A., Simpson, M.J., 2006. Evaluation of CuO oxidation parameters for determining the source and stage of lignin degradation in soil. Biogeochemistry 80, 121–142. https://doi.org/10.1007/s10533-006-9014-x

Øvstedal, D., Smith, R., 2001. Lichens of Antarctica and South Georgia: a guide to their identification and ecology, XII. ed. Cambridge University Press, Cambridge.

Park, J.H., Day, T.A., Strauss, S., Ruhland, C.T., 2007. Biogeochemical pools and fluxes of carbon and nitrogen in a maritime tundra near penguin colonies along the Antarctic Peninsula. Polar Biol. 30, 199–207. https://doi.org/10.1007/S00300-006-0173-Y/TABLES/2

Pereira, A.B., Putzke, J., 2013. The Brazilian research contribution to knowledge of the plant communities from Antarctic ice free areas. An. Acad. Bras. Cienc. 85, 923–935. https://doi.org/10.1590/S0001-37652013000300008

Piccolo, A., Spaccini, R., Drosos, M., Vinci, G., Cozzolino, V., 2018. The Molecular Composition of Humus Carbon: Recalcitrance and Reactivity in Soils, in: The Future of Soil Carbon. Elsevier, pp. 87–124. https://doi.org/10.1016/B978-0-12-811687-6.00004-3

Ping, C.L., Jastrow, J.D., Jorgenson, M.T., Michaelson, G.J., Shur, Y.L., 2015. Permafrost soils and carbon cycling. SOIL 1, 147–171. https://doi.org/10.5194/SOIL-1-147-2015

Pires, C.V., Schaefer, C.E.R.G., Hashigushi, A.K., Thomazini, A., Filho, E.I.F., Mendonça, E.S., 2017. Soil organic carbon and nitrogen pools drive soil C-CO2 emissions from selected soils in Maritime Antarctica. Sci. Total Environ. 596–597, 124–135. https://doi.org/10.1016/j.scitotenv.2017.03.144

Plante, A.F., Conant, R.T., Stewart, C.E., Paustian, K., Six, J., 2006. Impact of Soil Texture on the Distribution of Soil Organic Matter in Physical and Chemical Fractions. Soil Sci. Soc. Am. J. 70, 287–296. https://doi.org/10.2136/sssaj2004.0363

Putzke, J., Pereira, A., 2001. The Antarctic mosses: With special reference to the South Shetland Islands. Editora da ULBRA, Canoas.

R Core Team, 2019. R: A language and environment for statistical computing. https://doi.org/10.1016/j.dendro.2008.01.002

Redón, J., 1985. Líquenes antárticos. Instituto Antártico Chileno (INACH), Santiago de Chile.

Rumpel, C., Rabia, N., Derenne, S., Quenea, K., Eusterhues, K., Kögel-Knabner, I., Mariotti, A., 2006. Alteration of soil organic matter following treatment with hydrofluoric acid (HF). Org. Geochem. 37, 1437–1451. https://doi.org/10.1016/J.ORGGEOCHEM.2006.07.001

Sarangi, V., Agrawal, S., Sanyal, P., 2021. The disparity in the abundance of C4 plants estimated using the carbon isotopic composition of paleosol components. Palaeogeogr. Palaeoclimatol. Palaeoecol. 561, 110068. https://doi.org/10.1016/J.PALAEO.2020.110068

Savarese, C., Drosos, M., Spaccini, R., Cozzolino, V., Piccolo, A., 2021. Molecular characterization of soil organic matter and its extractable humic fraction from long-term field experiments under different cropping systems. Geoderma 383, 114700. https://doi.org/10.1016/j.geoderma.2020.114700

Savarino, J., Kaiser, J., Morin, S., Sigman, D.M., Thiemens, M.H., 2007. Nitrogen and oxygen isotopic constraints on the origin of atmospheric nitrate in coastal Antarctica. Atmos.

Chem. Phys. 7, 1925–1945. https://doi.org/10.5194/ACP-7-1925-2007

Schaefer, C.E.G.R., Pereira, T.T.C., Almeida, I.C.C., Michel, R.F.M., Corrêa, G.R., Figueiredo, L.P.S., Ker, J.C., 2017. Penguin activity modify the thermal regime of active layer in Antarctica: A case study from Hope Bay. CATENA 149, 582–591. https://doi.org/10.1016/j.catena.2016.07.021

Semenov, V.M., Ivannikova, L.A., Tulina, A.S., 2009. Stabilization of organic matter in the soil. Agrokhimiya 77–96.

Silva, I.R., Mendonça, E.S., 2007. Matétia orgânica do solo, in: NOVAIS, R.F., ALVAREZ, V., BARROS, N.F., FONTES, R.L.F., CANTARUTTI, R.B., NEVES, J.C.L. (Eds.), Fertilidade Do Solo. Revista Brasileira de Ciência do Solo, Viçosa, p. 275.

Simas, F.N.B., Schaefer, C.E.G.R., Filho, M.R.A., Francelino, M.R., Filho, E.I.F., da Costa, L.M., 2008. Genesis, properties and classification of Cryosols from Admiralty Bay, maritime Antarctica. Geoderma 144, 116–122. https://doi.org/10.1016/J.GEODERMA.2007.10.019

Simas, F.N.B., Schaefer, C.E.G.R., Melo, V.F., Guerra, M.B.B., Saunders, M., Gilkes, R.J., 2006. Clay-sized minerals in permafrost-affected soils (Cryosols) from King George Island, Antarctica. Clays Clay Miner. 54, 721–736. https://doi.org/10.1346/CCMN.2006.0540607

Spaccini, R., Piccolo, A., Conte, P., Haberhauer, G., Gerzabek, M.H., 2002. Increased soil organic carbon sequestration through hydrophobic protection by humic substances. Soil Biol. Biochem. 34, 1839–1851. https://doi.org/10.1016/S0038-0717(02)00197-9

Tadini, A.M., Goranov, A.I., Martin-Neto, L., Bernardi, A.C.C., Oliveira, P.P.A., Pezzopane, J.R.M., Hatcher, P.G., 2022. Structural characterization using 2D NMR spectroscopy and TMAH-GC × GC-MS: Application to humic acids from soils of an integrated agricultural system and an Atlantic native forest. Sci. Total Environ. 815, 152605. https://doi.org/10.1016/J.SCITOTENV.2021.152605

Teixeira, P., Donagemma, G., … A.F.-B., 2017, U., 2017. Manual de métodos de análise de solo, Embrapa.

Thomazini, A., Francelino, M.R., Pereira, A.B., Schünemann, A.L., Mendonça, E. de S., Michel, R.F.M., Schaefer, C.E.G.R., 2020. The current response of soil thermal regime and carbon exchange of a paraglacial coastal land system in maritime Antarctica. L. Degrad. Dev. 31, 655–666. https://doi.org/10.1002/ldr.3479

Thomazini, A., Francelino, M.R., Pereira, A.B., Schünemann, A.L., Mendonça, E.S., Almeida, P.H.A., Schaefer, C.E.G.R., 2016. Geospatial variability of soil CO2–C exchange in the main terrestrial ecosystems of Keller Peninsula, Maritime Antarctica. Sci. Total Environ. 562, 802–811. https://doi.org/10.1016/J.SCITOTENV.2016.04.043

Thomazini, A., Mendonça, E.S., Teixeira, D.B., Almeida, I.C.C., La Scala, N., Canellas, L.P.,

Spokas, K.A., Milori, D.M.B.P., Turbay, C.V.G., Fernandes, R.B.A., Schaefer, C.E.G.R., 2015. CO2 and N2O emissions in a soil chronosequence at a glacier retreat zone in Maritime Antarctica. Sci. Total Environ. 521–522, 336–345. https://doi.org/10.1016/J.SCITOTENV.2015.03.110

Turner, J., Barrand, N.E., Bracegirdle, T.J., Convey, P., Hodgson, D.A., Jarvis, M., Jenkins, A., Marshall, G., Meredith, M.P., Roscoe, H., Shanklin, J., French, J., Goosse, H., Guglielmin, M., Gutt, J., Jacobs, S., Kennicutt, M.C., Masson-Delmotte, V., Mayewski, P., Navarro, F., Robinson, S., Scambos, T., Sparrow, M., Summerhayes, C., Speer, K., Klepikov, A., 2014. Antarctic climate change and the environment: an update. Polar Rec. (Gr. Brit). 50, 237–259. https://doi.org/10.1017/S0032247413000296

Victoria, F. de C., de Albuquerque, M.P., Pereira, A.B., Simas, F.N.B., Spielmann, A.A., Schaefer, C.E.G.R., 2013. Characterization and mapping of plant communities at Hennequin Point, King George Island, Antarctica. Polar Res. 32, 19261. https://doi.org/10.3402/polar.v32i0.19261

Waggoner, D.C., Chen, H., Willoughby, A.S., Hatcher, P.G., 2015. Formation of black carbon-like and alicyclic aliphatic compounds by hydroxyl radical initiated degradation of lignin. Org. Geochem. 82, 69–76. https://doi.org/10.1016/J.ORGGEOCHEM.2015.02.007

Zhang, J., Chi, F., Wei, D., Zhou, B., Cai, S., Li, Y., Kuang, E., Sun, L., Li, L.-J., 2019. Impacts of Long-term Fertilization on the Molecular Structure of Humic Acid and Organic Carbon Content in Soil Aggregates in Black Soil. Sci. Rep. 9, 11908. https://doi.org/10.1038/s41598-019-48406-8

Zhang, M., Schaefer, D.A., Chan, O.C., Zou, X., 2013. Decomposition differences of labile carbon from litter to soil in a tropical rain forest and rubber plantation of Xishuangbanna, southwest China. Eur. J. Soil Biol. 55, 55–61. https://doi.org/10.1016/j.ejsobi.2012.12.003

Zubrzycki, S., Kutzbach, L., Pfeiffer, E.-M., 2014. Permafrost-affected soils and their carbon pools with a focus on the Russian Arctic. Solid Earth 5, 595–609. https://doi.org/10.5194/se-5-595-2014

FINAL CONSIDERATIONS

The Holocene paleoclimatic history of the South Shetland Islands is controversial and incomplete, and continued research is necessary. The first record of pre-LGM SOC in the Byers Peninsula adds an urgent need to improve the geochronology of this area and assist in interpreting the paleoenvironmental stages experienced, not only in Maritime Antarctica but also in the Peninsular Antarctica and the Weddell Sea sectors. Future studies with higher sample size should be executed to perform more robust statistical analysis. A higher number of samples in the same geomorphological and pedological contexts could clarify the SOC stock diversity into same soil group and identify a typical isotopic signal for each age group.

Livingston Island is unique among the ecosystems of the South Shetland Islands. Although it has suffered from human interference associated with fishing and hunting, in recent decades, it has been little affected by tourism or research stations. The retreat of the Rotch Dome glacier on the Byers Peninsula has provided a diverse and complex setting in terms of biogeochemical processes and agents (climate, fauna, flora, and microbiota) for the development of this environment. Thus, the Byers Peninsula is a highly suitable site for comparative studies with the rest of the Antarctic maritime region. Given this, the microbial communities that act in this environment play a key role in maintaining ecosystem services, favoring the balance. Thus, more studies are still needed to better visualize the size of the microbial communities in Antarctic soils in general, given that these are more diverse than previously imagined, and this study further assisted in this visualization. However, the high abundance of taxa that have not been identified even with the help of the most up-to-date identification libraries needs to be further explored.

The high diversity of biotic and abiotic factors acting in maritime Antarctica directly affects the accumulation, transformation, and stabilization of SOM. Due to the greater presence of ecological niches, greater plant diversity with the presence of vascular plants, and the marked action of avifauna, these factors differentiate the processes involved in the redistribution of SOM between Maritime and Continental Antarctica, in addition to the humidity factor (in the form of net precipitation) being a key factor in the most active humification processes in the soils studied (Abakumov et al., 2022).

APPENDIX A. SUPPLEMENTARY DATA (PAPER 1)

Table S1. General description of pedons

Pedon	Soil Classification ST/WRB	Coordinates[1]	Altitude (m.a.s.l.)	General description
1	"Sulfuric" Typic Haploturbels/ Cambic Turbic Cryosol (Pantoorthodistric, Loamic, Ochric, Pantosulfidic, Epiyermic)	62° 38' 36.10" S 61° 05' 20.50" W	71	Soil developed on a convex slope in a field of *mudboils*. Soil derived from Juro-Cretaceous pyritized andesite. Desert gravel pavement with a rust varnish on the surface. Well-drained soil. No plant cover. Periglacial landscape in undulating relief. Presence of a sulfated horizon throughout the profile and *permafrost* from 60 cm in depth.
2	Aquic Haploturbels/ Cambic Endoreductaquic Turbic Cryosol (Geoabruptic, Pantohypereutric, Clayic, Ochric, Clayinovic, Endorapitic)	62° 38' 50.90" S 61° 04' 58.54" W	71	Soil developed on convex slope in a field of soils with a striated pattern. Soil derived from pre-Holocene marine sedimentary rock and colluvium, with a parental material discontinuity at 105 cm. Periglacial landscape in undulating relief. Well-drained soil. Predominant vegetation cover by *Sanionia uncinata*, *Leptogium puberulum*, *Hymenoloma grimmiaceum,* and tundra phytophysiognomy. *Permafrost* from 60 cm deep.
3	"Leptic" Skeleptic Typic Haploturbels/ Hyperskeletic Leptic Turbic Cryosol (Hypereutric, Clayic, Ochric)	62° 38' 13.6" S 61° 04' 56.3" W	140	Soil developed on middle third of concave/convex slope in field of polygonal soils. Soil derived from Juro-Cretaceous basalt. Periglacial landscape in undulating relief. Well-drained soil. Predominant vegetation cover on coarse gravel attached to the edges of the polygons. Occurrence of *Usnea aurantiacoater*, *Sanionia*

				uncinata, *Andreaea gainii,* and tundra phytophysiognomy. *Permafrost* from 10 cm deep.
4	Typic Endoaquents/ Pantohypereutric Reductigleyic Endoreductic Gleysol (Endoclayic, Ochric, Skeletic)	62° 38’ 22.9” S 61° 07’ 28.7” W	106	Soil developed on the upper plateau. Soil derived from sedimentary rock of pre-Holocene marine origin. Periglacial landscape in flat to gently undulating relief. Poorly drained soil with water depth from 35 cm in depth. Periglacial landscape in undulating to heavily undulating relief. Occurrence of *Sanonia uncinata*, *Leptogium puberulum*, *Lecida seatrapha, Bractecium austrosalebrosum,* and *Hennediela heinni*.
5	Typic Cryaquents/ Orthodystric EndoReductic Gleysol (Loamic, Ochric, Skeletic, Turbic)	62° 38’ 22.9” S 61° 04’ 21.8 W	114	Soil developed on interior of a rectilinear plateau in a field of polygonal soils. Soil derived from Juro-Cretaceous andesite. Periglacial landscape in smooth wavy to wavy relief. Poorly drained soil, with water depth from 45 cm. Predominant vegetation cover on coarse gravel attached to the edges of the polygons. Occurrence of *Leptogium puberulum*, and unidentified lichen crustosus.
6	Lythic Cryorthents/ Oligoeutric Cambic Umbric Leptosol (Clayic, Humic, Skeletic, Epiturbic)	62° 38’ 35.5” S 61° 03’ 51” W	120	Soil developed on straight top of a slope and wavy to heavily undulating regional relief. Soil derived from Juro-Cretaceous basalt. Periglacial landscape in flat to gently undulating relief. Well-drained soil, with lytic contact from 20 cm deep. Occurrence of *Usnea auranteacoater, Sanionia george-uncinata, Andreae gainni, Himontornia lugubris, Ocholecria frigida, Ocholecria antarctica, Andreae depressinervis, Microglaena antarctica, Placopsis contortuplicata, Cephaloziela varians, Lecida siatrapha, Hennediela heinni, Xanthoria candelaria, Prasiola*

				crispa, Verrucaria racoviqzae, Coloplaca athalina, Bartramia platens, and *Cistocolio niger*.
7	Typic Cryaquents/ Pantohyperdystric Fluvic Someriumbric Subaquatic Gleysol (Pantoarenic, Humic, Limnic, Pantonechic)	62° 39’ 21.4” S 61° 03’ 25.4” W	51	Soil developed on coastal shore at the highest raised beaches level. Soil derived from pre-Holocene marine sediment. Periglacial landscape in flat to gently undulating relief. Poorly drained soil. Occurrence of *Sanionia uncinata*, *Bartramia platens*, *Bryn pseudotrichetum*, *Wanstorfia sarmentosa*, *Leptogium puberulum*, *Deschampsia antarctica*, *Hennediela heinni, Bractecium austrosalebrosum,* and *cistocoleo niger*.
8	Typic Cryopsamments/ Pantohyperdystric Protic Akrofluvic Arenosol (Ochric, Pantonechic, Endoraptic)	62° 39’ 23.7” S 61° 03’ 33.6” W	22	Soil developed on coastal coast at the intermediate level of raised beaches. Soil derived from pre-Holocene marine sediment. Periglacial landscape in flat to gently undulating relief. Well-drained soil. Occurrence of *Sanionia uncinata*, *Bartramia platens*, *Bryn pseudotrichetum*, *Wanstorfia sarmentosa*, *Leptogium puberulum*, *Deschampsia antarctica*, *Hennediela heinni, Bractecium austrosalebrosum,* and *cistocoleo niger*.
9	Typic Cryopsamments/ Pantoorthodystric Protic Akrofluvic Arenosol (Ochric, Pantonechic, Raptic)	62° 39’ 32.4” S 61° 03’ 39.2” W	15	Soil developed on coastal coast at the lowest level of raised beaches. Soil derived from pre-Holocene marine sediment. Periglacial landscape in flat to gently undulating relief. Lines of rounded quartz pebbles at 35 and 50 cm depth. Clay and sandy sheets interspersed from 80 cm in depth. Well-drained soil. Occurrence of *Deschampsia antarctica*.

10	Glacic Haploturbels/ Cambic Epiturbic Amphiglacic Cryosol (Pantohypereutric, Clayic, Humic)	62° 38’ 38.9” S 61° 04’ 24.5” W	132	Soil developed on convex hill top in a field of polygonal soils. Soil derived from Juro-Cretaceous igneous rock. Periglacial landscape in flat to gently undulating relief. Poorly drained soil. *Permafrost* from 50 cm deep. Predominant vegetation cover on coarse gravel attached to the edges of the polygons. Occurrence of *Usnea aurantiacoater* and *Bractecium austrosalebrosum*.
11	Humic Eutrocryepts/ Pantohypereutric Endoleptic Cambisol (Clayic, Humic, Epiturbic)	62° 39’ 12.4” S 61° 00’ 15.1” W	123	Soil developed on a cliff in a field of polygonal soils. Soil derived from Juro-Cretaceous basalt. Periglacial landscape in undulating to heavily undulating relief. Fragmentary lytic contact from 80 cm depth. Predominant vegetation cover on coarse gravel attached to the edges of the polygons. Occurrence of *Deschampsia antarctica*, *Sanionia uncinata*, *Syntrichia filaris*, *Leptogium puberulum*, *Politrichium alpino*, *Hennediela heinni*, *Bracterium austrosalebrosum*, *Sanionia george-uncinata*, *Cistocolio niger* and *Psoroma hypnorum.*
12	Typic Haploturbels/ Pantocambic Endoleptic Turbic Cryosol (Pantohypereutric, Clayic, Humic, Skeletic)	62° 40’ 16.4” S 61° 06’ 40.1” W	82	Soil developed on a rectilinear plateau in a field of polygonal soils. Soil derived from Juro-Cretaceous igneous rocks. Periglacial landscape in flat to gently undulating relief. Permafrost from 70 cm and fragmentary lithic contact. Soil with clay plume migrating from the subsurface horizon to the surface horizon. Predominant vegetation cover on coarse gravel attached to the edges of the polygons. Occurrence of *Usnea auranteacoater*, *Sanionia uncinata*, *Sanionia george-uncinata, Andreae gainni, Deschampsia antarctica, Himenthoria lugubris, Cladonea regalis, Cistocoleo niger, Ocholecria frigida, Psoroma hypnorum, Placopsis contortuplicata, Politrichum alpino, Bractecium austrosalebrosum, Andreae depressinervis, Hypnum Revolution, Cladonia metacolarifera, Psoroma*

				cynamomeum, Stereocalum glabrum, Caloplata atalina and *Rizocarpum geograficum*.
13	'Glacic' Typic Cryopsamments/ Endoreductaquic Endoglacic Cryosol (Pantoorthodystric, Pantoarenic, Orthofluvic, Ochric, Pantonechic, Raptic)	62° 39' 30.7" S 61° 57' 03" W	74	Soil developed on a raised beaches arched, discontinuous, and not reported in previous studies. Soil derived from Holocene marine sediment. Rock fragments arrested and rounded on the surface and rounded on the subsurface, demarcating an area of glacier accumulation. Paraglacial landscape in wavy concave relief. Poorly drained soil with ice below 50 cm deep. No plant cover.

[1/] World Geodetic System (WGS 1984).

Table S2. Morphological properties of soils

Horizon	Depth (cm)	Boundary (distinctness, topography)	Moist color	Structure (grade, size, type)	Consistence (dry, moist, wetter, cementation)	Nodules color	Rock fragments (%, roundness, size)	Temperature (°C)
P1 - "Sulfuric" Typic Haploturbels/ Cambic Turbic Cryosols (Pantoorthodistric, Loamic, Ochric, Pantosulfidic, Epiyermic)								
Ajjj	0-10	C-S	5YR 5/8	1, f, sbk	-, FR, ss, po, NC		30, VA, f	6.7
Bcij	10-43	C-S	10R 3/3	1, f, sbk	-, FR, so, po, NC	10R 3/6	80, VA, m	4.6
Bij	43-80	C-S	7.5YR 5/4	1, f, sbk	-, FR, so, po, NC		10, VA, f	3.0
Ccrjf	80-115+		10R 4/8	0, -, sbk/gr	-, L, so, po, NC	10R 3/6	-, VA, m	0.3
P2 - Aquic Haploturbels/ Cambic Endoreductaquic Turbic Cryosols (Geoabruptic, Pantohypereutric, Clayic, Ochric, Clayinovic, Endorapitic)								
Ajj	0-10	C-S	2.5Y 3/2	2, f, sbk	-, FR, ss, ps, NC		10, VA, f	7.9
Bi_1	10-40	C-S	5Y 3/1	2, f, sbk	-, FR, vs, ps, NC		5, AN, f	4.7
Bi_2	40-60	A-S	5Y 4/2	2, m, sbk	-, FR, s, ps, NC		10, VA, m	3.4
2Crf	60-105+		GLEY1 2.5/N	0, -, m	-, FR, s, po, NC		60, AN, f	0.1
P3 - "Leptic" Skeleptic Typic Haploturbels/ Hyperskeletic Leptic Turbic Cryosols (Hypereutric, Clayic, Ochric)								
Ajj	0-10	C-S	10YR 3/1	1, f, sbk	-, -, so, po, NC		40, VA, f/m	6.7
Crf	10-70	C-S	10YR 3/2	1, f, sbk	-, -, so, po, NC		90, VA, f/m/c	0.3
R	70+							-
P4 - Typic Endoaquents/ Pantohypereutric Reductigleyic Endoreductic Gleysols (Endoclayic, Ochric, Skeletic)								
A	0-20	C-S	5Y 2/1	1, f, sbk	-, -, so, po, NC		60, VA, f/m	5.0

C	20-35	C-S	5Y 3/2	1, f, sbk	-, -, s, ps, NC	35, VA, f	3.3
W	35+						-
P5 –Typic Cryaquents/ Orthodystric EndoReductic Gleysols (Loamic, Ochirc, Skeletic, Turbic)							
Ajj	0-10	C-S	5Y 6/4	2, f, sbk	-, -, ss, po, NC	15, VA, f/m	4.8
C_1	10-30	C-S	5Y 5/3	1, f, sbk	-, -, so, po, NC	40, VA, m	2.7
C_2	30-45+		5Y 4/2	1, f, sbk	-, -, so, po, NC	20, VA, f/m	1.2
P6 - Lythic Cryorthents/ Oligoeutric Cambic Umbric Leptosol (Clayic, Humic, Skeletic, Epiturbic)							
A	0-10	C-S	5Y 2/2	2, f, gr	-, -, ss, ps, NC	30, VA, m	3.6
Bi	10-20	A-W	5Y 3/2	1, f, sbk	-, -, s, p, NC	5, AN, f	4.0
R	20+						-
P7 - Typic Cryaquents/ Pantohyperdystric Fluvic Someriumbric Subaquatic Gleysol (Pantoarenic, Humic, Limnic, Pantonechic)							
A	0-10	-	5Y 2/2	1, f, sbk	-, -, so, po, NC	30, VA, f/m	4.0
W	10+						-
P8 - Typic Cryopsamments/ Pantohyperdystric Protic Akrofluvic Arenosol (Ochric, Pantonechic, Endoraptic)							
A	0-15	A-S	5Y 3/1	0, -, sg	-, -, so, po, NC	5, VA, vf/f	-
C_1	15-20	A-S	5Y 3/1	0, -, sg	-, -, so, po, NC	30, RO, vf/f	-
C_2	20-45	A-S	5Y 4/3	0, -, sg	-, -, so, po, NC	25, RO, vf/f/m	-
C_3	45-65	A-S	5Y 3/2	0, -, sg	-, -, so, po, NC	≤5, RO, vf	-
C_4	65-70	A-S	5Y 4/2	0, -, sg	-, -, so, po, NC	30, RO, vf/f/m	-

C_5	70-90	A-S	5Y 4/2	0, -, sg	-, -, so, po, NC	≤1, RO, vf	-
C_6	90-95	A-S	5Y 4/4	0, -, sg	-, -, so, po, NC	50, RO, vf/f/m	-
C_7	95-115	C-S	5Y 3/2	0, -, sg	-, -, so, po, NC	30, RO, vf/f	-
C_8	115-205	A-S	5Y 3/2	0, -, sg	-, -, so, po, NC	20, RO, vf/f/m	-
R	205+						-
P9 - Typic Cryopsamments/ Pantoorthodystric Protic Akrofluvic Arenosol (Ochric, Pantonechic, Raptic)							
A	0-35	C-S	5Y 2/1	0, -, sg	-, -, so, po, NC	10, VA, vf/f	8.5
$2C_1$	35-50	C-S	5Y 3/1	0, -, sg	-, -, so, po, NC	50, VA, vf/f/m	5.2
$3C_2$	50-80	C-S	5Y 4/4	0, -, sg	-, -, so, po, NC	45, VA, f/m	5.1
$4C_3$	80-115	C-S	5Y 4/1	0, -, sg	-, -, so, po, NC	≤1, VA, vf	4.2
$4C_4$	115-130	A-S	5Y 2/1	0, -, sg	-, -, so, po, NC	20, VA, vf/f	3.9
R	130+						-
P10 - Glacic Haploturbels/ Cambic Epiturbic Amphiglacic Cryosol (Pantohypereutric, Clayic, Humic)							
Ajj	0-30	C-S	5Y 4/4	1, f, sbk	-, -, so, ps, NC	30, VA, f/m	1.6
Cf	30-50	A-S	5Y 2/1	1, f, sbk	-, -, so, ps, NC	5, AN, m	0.6
P11 - Humic Eutrocryepts/ Pantohypereutric Endoleptic Cambisol (Clayic, Humic, Epiturbic)							
Ajj	0-23	C-S	5YR 3/4	2, f, sbk	-, -, so, po, NC	30, VA, m	8.1
Bi	23-60	G-S	7.5YR 4/4	2, f, sbk	-, -, vs, ps, NC	60, VA, co	2.8
C	60-80	C-S	7.5YR 3/2	2, f, sbk	-, -, vs, ps, NC	30, VA, m	1.7

R	80+						-
P12 - Typic Haploturbels/ Pantocambic Endoleptic Turbic Cryosol (Pantohypereutric, Clayic, Humic, Skeletic)							
Ajj	0-35 (25-45)	A-W	7.5YR3/2	2, f, sbk	-, -, so, po, NC	10, VA, f/m	3.7
Cjj	35-50	C-S	10G 7/6	0, -, m	-, -, vs,p, NC	>1, VA, f	2.6
C	50-70	C-S	10G 5/6	0, -, m	-, -, vs, p, NC	0, -, -	1.5
Rf	70+						0.4
P13 - 'Glacic' Typic Cryopsamments/ Endoreductaquic Endoglacic Cryosol (Pantoorthodystric, Pantoarenic, Orthofluvic, Ochric, Pantonechic, Raptic)							
A	0-30	C-S	5Y 2/1	0, -, sg	-, -, so, po, NC	30, RO, f/m	4.8
Cf	30-50	A-S	5Y 3/2	0, -, sg	-, -, so, po, NC	60, RO, f/m/co	0.3

Distinctness: A=abrupt, C=clear. Topography: S=smooth, W=wavy. Structure: Grade: 0=structureless, 1=weak, 2=moderate. Size: f=fine, m=medium. Type: gr=granular, m=massive, sbk= subangular block, sg=single grain. /=principal structure parting to secondary one. Redoximorphic features: Kind: FSN=ironstone. Quantity: f=few, m=many. Size: 2=medium, 3=coarse, 4=very coarse. Contrast: P=prominent. State: D=dry. Hardness: I=indurated. Boundary: S=sharp. Consistence: Dry: EH=extreme hard, EF=extreme firm, HA=hard, L= loose, S=soft, SH=slightly hard. Moist: FR= friable, L=loose. Wetter: so=nonsticky, vs= very sticky, ss= slightly sticky, s=moderately sticky, p=moderately plastic, po=nonplastic, ps= slightly plastic. Cementation: NC= non-cemented. Rock fragments: VA=very angular, AN=angular, RO= rounded. Size: co=coarse, f=fine, very fine= vf, m= medium.

Table S3. Isotopic composition of SOM fractions and C and N levels

Sample	C %	$\delta^{13}C$ (‰)	C (mg g soil^{-1})	N %	$\delta^{15}N$ (‰)	N (mg g soil^{-1})	C/N Ratio	C %	$\delta^{13}C$ (‰)	C (mg g soil^{-1})	N %	$\delta^{15}N$ (‰)	N (mg g soil^{-1})	C/N Ratio	$\delta^{13}C$ (‰)	$\delta^{15}N$ (‰)
	Particulate organic matter (POM)							Mineral-Associated Organic Matter (MAOM)							weighted means	
P1H1	0.17	-26.25	1.33	0.02	18.43	0.12	11.28	0.29	-27.73	0.68	0.04	3.89	0.08	8.05	-26.8	12.4
P1H2	0.17	-26.54	1.05	0.01	8.98	0.09	12.15	0.17	-27.29	0.65	0.02	5.95	0.09	7.52	-26.8	7.5
P1H3	0.09	-26.60	0.52	0.01	6.79	0.08	6.28	0.18	-26.96	0.79	0.02	5.24	0.11	7.39	-26.8	5.9
P1H4	0.12	-26.88	0.99	0.02	7.95	0.13	7.58	0.22	-27.11	0.34	0.03	3.91	0.04	8.14	-26.9	7.0
P2H1	0.48	-26.27	3.18	0.04	3.84	0.27	11.67	0.86	-23.02	2.88	0.08	1.93	0.28	10.12	-24.7	2.9
P2H2	0.59	-26.36	1.76	0.04	5.57	0.12	15.07	0.70	-25.31	4.91	0.04	4.87	0.31	15.64	-25.6	5.1
P2H3	0.45	-26.39	1.91	0.03	4.67	0.14	13.54	0.87	-23.36	4.94	0.07	3.59	0.39	12.60	-24.2	3.9
P2H4	0.58	-27.36	2.16	0.05	4.89	0.18	11.72	0.42	-26.57	2.66	0.03	5.26	0.21	12.80	-26.9	5.1
P3H1	0.15	-25.68	1.32	0.05	17.71	0.43	3.05	2.14	-26.12	2.45	0.30	4.19	0.34	7.15	-26.0	11.7
P3H2	0.50	-24.39	3.40	0.07	6.44	0.45	7.60	2.04	-25.70	6.50	0.23	1.00	0.73	8.94	-25.2	3.1
P4H1	0.78	-27.03	5.76	0.11	4.18	0.80	7.21	1.17	-26.38	3.02	0.18	2.85	0.46	6.57	-26.8	3.7
P4H2	0.91	-27.19	6.62	0.14	3.98	1.01	6.58	1.01	-26.04	2.77	0.15	4.38	0.42	6.55	-26.8	4.1

P5H1	0.04	-25.77	0.19	<DL	0.00	0.00	0.00	0.27	-26.55	1.49	0.02	2.04	0.14	10.74	-26.5	2.0
P5H2	0.04	-25.84	0.23	<DL	0.00	0.00	0.00	0.26	-26.23	1.27	0.02	1.91	0.10	12.25	-26.2	1.9
P5H3	0.05	-25.70	0.21	<DL	0.00	0.00	0.00	0.20	-26.62	1.18	0.02	2.80	0.10	12.19	-26.5	2.8
P6H1	0.45	-21.99	2.58	0.04	-0.23	0.22	11.69	1.63	-22.72	6.99	0.19	-0.08	0.79	8.80	-22.5	-0.1
P6H2	0.25	-23.11	0.81	0.02	0.41	0.05	16.45	1.20	-24.22	8.10	0.12	0.05	0.79	10.22	-24.1	0.1
P7H1	0.13	-21.55	1.17	<DL	0.00	0.00	0.00	1.75	-21.36	1.88	0.19	3.64	0.21	9.15	-21.4	3.6
P8H1	0.04	-24.32	0.41	<DL	0.00	0.00	0.00	0.75	-24.26	0.45	0.11	13.84	0.06	7.08	-24.3	13.8
P8H2	0.04	-24.08	0.37	<DL	0.00	0.00	0.00	0.41	-22.96	0.17	0.05	12.97	0.02	8.83	-23.7	13.0
P8H3	0.05	-24.24	0.51	<DL	0.00	0.00	0.00	0.42	-20.81	0.18	0.04	11.17	0.02	9.53	-23.4	11.2
P8H4	0.04	-24.54	0.39	<DL	0.00	0.00	0.00	0.35	-22.06	0.12	0.03	11.36	0.01	11.11	-23.9	11.4
P8H5	0.05	-24.30	0.43	<DL	0.00	0.00	0.00	0.30	-21.84	0.16	0.03	11.37	0.01	12.06	-23.6	11.4
P8H6	0.05	-24.28	0.45	<DL	0.00	0.00	0.00	0.30	-21.47	0.13	0.03	11.87	0.01	11.62	-23.7	11.9
P8H7	0.05	-24.58	0.49	<DL	0.00	0.00	0.00	0.28	-21.98	0.17	0.02	12.29	0.01	13.37	-23.9	12.3
P8H8	0.04	-24.59	0.38	<DL	0.00	0.00	0.00	0.27	-21.20	0.12	0.02	13.13	0.01	11.50	-23.8	13.1
P8H9	0.07	-23.19	0.66	<DL	0.00	0.00	0.00	0.96	-20.73	0.57	0.12	11.10	0.07	8.34	-22.0	11.1
P9H1	0.04	-25.31	0.41	<DL	0.00	0.00	0.00	1.06	-24.73	0.37	0.17	16.31	0.06	6.25	-25.0	16.3

P9H2	0.04	-27.20	0.42	<DL	0.00	0.00	0.00	0.40	-22.23	0.15	0.04	11.43	0.02	9.21	-25.9	11.4
P9H3	0.03	-24.94	0.31	<DL	0.00	0.00	0.00	0.19	-23.21	0.17	0.01	10.64	0.01	12.77	-24.3	10.6
P9H4	0.04	-24.85	0.34	<DL	0.00	0.00	0.00	0.54	-23.12	0.29	0.05	6.90	0.03	10.17	-24.1	6.9
P9H5	0.05	-24.57	0.46	<DL	0.00	0.00	0.00	0.52	-23.76	0.35	0.05	6.89	0.03	11.04	-24.2	6.9
P10H1	0.26	-23.75	1.53	0.01	1.53	0.08	19.80	1.09	-26.41	4.48	0.10	-0.36	0.41	10.94	-25.7	-0.1
P10H2	0.32	-23.25	2.11	0.02	0.98	0.11	19.42	1.02	-23.98	3.42	0.09	-0.87	0.30	11.38	-23.7	-0.4
P11H1	0.12	-23.12	0.91	<DL	0.00	0.00	0.00	0.83	-22.05	1.82	0.08	0.94	0.18	10.21	-22.4	0.9
P11H2	0.03	-24.81	0.14	<DL	0.00	0.00	0.00	0.03	-23.39	0.19	<DL	0.00	0.00	0.00	-24.0	0.0
P11H3	0.03	-24.66	0.14	<DL	0.00	0.00	0.00	0.03	-23.66	0.17	<DL	0.00	0.00	0.00	-24.1	0.0
P12H1	0.05	-24.44	0.26	<DL	0.00	0.00	0.00	0.49	-23.48	2.12	0.05	3.76	0.23	9.26	-23.6	3.8
P12H2	0.09	-23.95	0.38	<DL	0.00	0.00	0.00	0.28	-23.01	1.59	0.02	4.78	0.14	11.49	-23.2	4.8
P12H3	0.06	-25.32	0.13	<DL	0.00	0.00	0.00	0.06	-23.89	0.48	<DL	0.00	0.00	0.00	-24.2	0.0
P13H1	0.03	-17.44	0.27	<DL	0.00	0.00	0.00	0.17	-19.98	0.28	0.01	5.95	0.02	11.74	-18.8	6.0
P13H2	0.03	-23.62	0.24	<DL	0.00	0.00	0.00	0.18	-20.28	0.16	0.01	4.53	0.01	12.18	-22.3	4.5

* <DL – below detection limit

Table S4. Physical properties of soil profiles sampled on the Byers Peninsula, Livingston Island.

Profile	Depth (cm)	CS[a]	FS[b]	Sand	Silt	Clay	Textural Class	CDW[c]	PD[d]	SD[e]	Gravel
		kg/kg			%			kg/kg	g/cm^3	g/cm^3	%
P1 - "Sulfuric" Typic Haploturbels/ Cambic Turbic Cryosols (Pantoorthodistric, Loamic, Ochric, Pantosulfidic, Epiyermic)											
Ajjj	0-10	0.61	0.091	70.1	17.3	12.5	sandy loam	0.056	2.67	1.62	39.72
Bcij	10-43	0.497	0.052	54.9	16.2	28.9	sandy clay loam	0.003	2.67	1.62	0.40
Bij	43-80	0.742	0.049	79.1	10.7	10.1	sandy loam	0.199	2.63	1.61	16.66
Ccrjf	80-115+	0.626	0.027	65.3	31.1	3.6	sandy loam	0.009	2.7	1.63	4.91
P2 - Aquic Haploturbels/ Cambic Endoreductaquic Turbic Cryosols (Geoabruptic, Pantohypereutric, Clayic, Ochric, Clayinovic, Endorapitic)											
Ajj	0-10	0.138	0.065	20.3	62.4	17.3	silt loam	0.003	2.41	1.76	21.31
Bi_1	10-40	0.165	0.076	24.1	41	34.9	clay loam	0.179	2.5	1.79	44.44
Bi_2	40-60	0.194	0.116	31	41.5	27.5	clay loam	0.111	2.41	1.76	34.08
2Crf	60-105+	0.132	0.061	19.3	48	32.6	silty clay loam	0.134	2.47	1.78	23.25
P3 - "Leptic" Skeleptic Typic Haploturbels/ Hyperskeletic Leptic Turbic Cryosols (Hypereutric, Clayic, Ochric)											
Ajj	0-10	0.727	0.054	78.1	4.5	17.4	sandy loam	0.002	2.78	1.60	1.92
Crf	10-70	0.421	0.199	62	27.5	10.5	sandy loam	0.004	2.63	1.60	59.54
P4 - Typic Endoaquents/ Pantohypereutric Reductigleyic Endoreductic Gleysols (Endoclayic, Ochric)											
A	0-20	0.663	0.07	73.3	16.3	10.3	sandy loam	0.052	2.67	1.32	48.88
C	20-35	0.608	0.07	67.8	16.1	16.1	sandy loam	0.112	2.67	1.32	53.78
P5 –Typic Cryaquents/ Orthodystric EndoReductic Gleysols (Loamic, Ochirc, Turbic)											
Ajj	0-10	0.396	0.131	52.7	43.2	4.1	sandy loam	0.033	2.47	1.48	45.52
C_1	10-30	0.385	0.126	51.1	39.2	9.7	loam	0.044	2.53	1.49	60.18

C_2	30-45+	0.548	0.162	71	13.4	15.6	sandy loam	0.2	2.63	1.51	56.50
P6 - Lythic Cryorthents/ Oligoeutric Cambic Umbric Leptosol (Clayic, Humic, Epiturbic)											
A	0-10	0.332	0.322	65.4	19.4	15.2	sandy loam	0.013	2.56	1.64	25.39
Bi	10-20	0.301	0.074	37.5	50.2	12.3	silt loam	0.054	2.44	1.61	47.14
P7 - Typic Cryaquents/ Pantohyperdystric Fluvic Someriumbric Subaquatic Gleysol (Pantoarenic, Humic, Limnic, Pantonechic)											
A	0-10	0.784	0.078	86.2	7.2	6.6	loamy sand	0.003	2.7	1.81	26.96
P8 - Typic Cryopsamments/ Pantohyperdystric Protic Akrofluvic Arenosol (Ochric, Pantonechic, Endoraptic)											
A	0-15	0.887	0.015	90.2	6.6	3.2	sand	0.018	2.7	1.84	24.58
C_1	15-20	0.961	0.011	97.2	1.7	1.2	sand	0.001	2.78	1.87	0.00
C_2	20-45	0.98	0.008	98.8	0.5	0.7	sand	0.005	2.7	1.84	7.07
C_3	45-65	0.87	0.008	87.8	2.5	9.6	loamy sand	0.01	2.7	1.84	4.69
C_4	65-70	0.82	0.009	82.9	1.5	15.6	sandy loam	0.005	2.7	1.84	7.88
C_5	70-90	0.866	0.025	89.1	10.2	0.8	sand	0.003	2.7	1.84	2.63
C_6	90-95	0.965	0.012	97.7	1.3	1	sand	0.004	2.67	1.83	13.97
C_7	95-115	0.978	0.009	98.7	0.4	0.8	sand	0.007	2.7	1.84	0.31
C_8	115-205	0.9	0.062	96.2	0.5	3.3	sand	0.004	2.6	1.81	26.61
P9 - Typic Cryopsamments/ Pantoorthodystric Protic Akrofluvic Arenosol (Ochric, Pantonechic, Raptic)											
A	0-35	0.967	0.012	97.9	1.3	0.7	sand	0.006	2.74	1.54	17.05
$2C_1$	35-50	0.974	0.013	98.7	0.6	0.6	sand	0.004	2.74	1.54	36.78
$3C_2$	50-80	0.967	0.021	98.8	0.4	0.8	sand	0.003	2.7	1.54	25.13
$4C_3$	80-115	0.961	0.02	98.1	1.4	0.5	sand	0.003	2.74	1.54	2.67
$4C_4$	115-130	0.969	0.019	98.8	0.4	0.7	sand	0.059	2.74	1.54	5.20
P10 - Glacic Haploturbels/ Cambic Epiturbic Amphiglacic Cryosol (Pantohypereutric, Clayic, Humic)											

Ajj	0-30	0.578	0.253	83.1	11.7	5.3	loamy sand	0.032	2.47	1.80	57.84
Cf	30-50	0.638	0.275	91.3	3.9	4.7	sand	0.041	2.63	1.85	46.97
P11 - Humic Eutrocryepts/ Pantohypereutric Endoleptic Cambisol (Clayic, Humic, Epiturbic)											
Ajj	0-23	0.622	0.149	77.1	18.4	4.5	loamy sand	0.037	2.67	1.59	34.54
Bi	23-60	0.302	0.151	45.3	41.2	13.5	loam	0.126	2.53	1.56	45.47
C	60-80	0.275	0.119	39.4	31.6	29	clay loam	0.109	2.63	1.58	46.08
P12 - Typic Haploturbels/ Pantocambic Endoleptic Turbic Cryosol (Pantohypereutric, Clayic, Humic)											
Ajj	0-35	0.494	0.124	61.8	25.1	13.1	sandy loam	0.031	2.67	1.36	36.58
Cjj	35-50	0.246	0.099	34.5	43.8	21.7	loam	0.075	2.35	1.32	44.40
C	50-70	0.209	0.066	27.5	37.5	35	clay loam	0.117	2.44	1.33	56.94
P13 - 'Glacic' Typic Cryopsamments/ Endoreductaquic Endoglacic Cryosol (Pantoorthodystric, Pantoarenic, Orthofluvic, Ochric, Pantonechic, Raptic)											
A	0-30	0.757	0.122	87.9	3.6	8.6	loamy sand	0.004	2.67	2.07	23.39
Cf	30-50	0.766	0.089	85.5	6.1	8.4	loamy sand	0.004	2.67	2.07	50.23

[a]Coarse sand; [b]Fine sand; [c]Clay dispersed in water; [d]Particle density; [e]Soil density

Table S5. Chemical analysis of soil profiles sampled on the Byers Peninsula, Livingston Island.

Profile	Depth	pH	pH	P	K^+	Na^+	Ca^{2+}	Mg^{2+}	Al^{3+}	H+Al	BS	ECEC	CEC	V	m	ISNa	S	P-Rem	Cu	Mn	Fe	Zn
	cm	H_2O	KCl	------- (mg dm^{-3}) -----			---------- (cmolc/dm^3) ----------							------- (%) ----			(mg/dm^3)	mg L^{-1}	-------- (mg/dm^3) -----			
P1 - “Sulfuric” Typic Haploturbels/ Cambic Turbic Cryosols (Pantoorthodistric, Loamic, Ochric, Pantosulfidic, Epiyermic)																						
Ajjj	0-10	5.00	3.67	3.8	62	167.85	7.16	1.85	14.50	18.8	9.90	24.40	28.70	35	59	2	164.4	3.9	0.60	11.5	123.5	0.96
Bcij	10-43	4.14	3.32	0.9	40	157.92	5.20	0.53	14.31	20.6	6.52	20.83	27.12	24	69	2	403.0	3.0	0.81	8.6	213.0	1.44
Bij	43-80	3.92	3.25	3.3	24	136.08	21.29	0.28	10.80	16.5	22.22	33.02	38.72	57	33	2	745.2	11.8	0.51	3.8	178.6	1.62
Ccrjf	80-115+	3.69	3.25	1.5	22	155.93	29.64	0.51	12.55	18.9	30.88	43.43	49.78	62	29	1	761.6	18.3	0.76	7.3	237.4	1.42
P2 - Aquic Haploturbels/ Cambic Endoreductaquic Turbic Cryosols (Geoabruptic, Pantohypereutric, Clayic, Ochric, Clayinovic, Endorapitic)																						
Ajj	0-10	6.90	5.12	55.7	138	177.78	12.76	10.10	<0.1	1.1	23.99	23.99	25.09	96	0	3	7.6	30.2	1.54	53.4	227.6	4.46
Bi_1	10-40	7.34	5.45	144.2	138	175.79	18.93	12.02	<0.1	0.3	32.07	32.07	32.37	99	0	2	2.9	34.6	1.09	66.9	207.8	5.37
Bi_2	40-60	7.72	5.82	94.6	130	169.83	20.26	9.20	<0.1	0.3	30.53	30.53	30.83	99	0	2	0.3	32.4	1.97	59.9	235.9	6.26
2Crf	60-105+	7.59	6.10	953.8	48	140.05	31.95	9.71	<0.1	0.5	42.40	42.40	42.90	99	0	1	0.0	25.2	1.18	152.9	112.9	23.82
P3 - “Leptic” Skeleptic Typic Haploturbels/ Hyperskeletic Leptic Turbic Cryosols (Hypereutric, Clayic, Ochric)																						
Ajj	0-10	6.91	4.91	133.0	94	157.92	5.05	1.44	<0.1	2.1	7.42	7.42	9.52	78	0	7	16.9	28.2	1.91	77.0	212.2	1.49
Crf	10-70	7.26	5.53	109.3	134	200.66	5.70	3.01	<0.1	2.1	9.93	9.93	12.03	83	0	7	0.0	20.0	3.55	40.0	266.2	2.28
P4 - Typic Endoaquents/ Pantohypereutric Reductigleyic Endoreductic Gleysols (Endoclayic, Ochric)																						
A	0-20	7.18	5.69	132.1	82	134.09	11.96	6.79	<0.1	0.5	19.56	19.56	20.06	98	0	3	6.3	37.0	1.75	110.3	363.6	6.34
C	20-35	7.69	5.95	199.7	126	132.10	11.30	5.86	<0.1	0.5	18.06	18.06	18.56	97	0	3	4.1	35.0	1.40	101.9	264.8	7.89
P5 –Typic Cryaquents/ Orthodystric EndoReductic Gleysols (Loamic, Ochirc, Turbic)																						
Ajj	0-10	7.37	5.12	26.4	138	224.49	10.02	10.08	<0.1	0.6	21.43	21.43	22.03	97	0	4	0.0	32.0	1.00	41.2	262.0	5.45
C_1	10-30	7.47	5.19	27.2	110	204.63	8.57	10.13	<0.1	0.5	19.89	19.89	20.39	98	0	4	2.7	36.1	0.92	31.5	247.4	5.10
C_2	30-45+	8.00	5.83	24.8	90	200.66	8.44	8.49	<0.1	0.3	18.03	18.03	18.33	98	0	5	4.1	36.9	1.14	25.9	282.3	4.10
P6 - Oligoeutric Cambic Umbric Leptosol (Clayic, Humic, Epiturbic)/ Lythic Cryorthents																						

A	0-10	7.33	5.20	22.3	219	299.95	5.60	8.33	<0.1	2.1	15.80	15.80	17.90	88	0	7	0.0	23.1	2.65	54.8	270.8	2.60
Bi	10-20	7.74	5.62	29.9	259	315.84	10.10	13.63	<0.1	1.3	25.77	25.77	27.07	95	0	5	0.0	25.6	3.34	20.9	176.9	3.47
P7 - Pantohyperdystric Fluvic Someriumbric Subaquatic Gleysol (Pantoarenic, Humic, Limnic, Pantonechic)/ Typic Cryaquents																					
A	0-10	7.48	5.24	58.0	153	232.43	3.79	4.10	<0.1	1.0	9.29	9.29	10.29	90	0	10	18.5	39.4	1.72	25.8	152.0	1.22
P8 - Pantohyperdystric Protic Akrofluvic Arenosol (Ochric, Pantonechic, Endoraptic)/ Typic Cryopsamments																					
A	0-15	6.85	4.40	51.7	211	181.75	4.03	3.24	0.19	1.4	8.60	8.79	10.00	86	2	8	20.1	41.0	1.02	12.8	154.7	1.43
C_1	15-20	7.14	4.35	54.2	311	204.63	7.20	5.42	0.19	1.0	14.31	14.50	15.31	94	1	6	7.6	45.4	1.66	15.2	171.0	1.30
C_2	20-45	7.26	4.40	62.1	588	216.55	5.39	9.28	<0.1	0.8	17.12	17.12	17.92	6	0	5	7.0	46.1	2.56	18.3	174.3	1.39
C_3	45-65	6.95	4.60	66.0	347	200.66	8.83	5.97	<0.1	0.8	16.56	16.56	17.36	95	0	5	9.4	41.5	2.58	16.9	172.5	1.27
C_4	65-70	7.15	4.62	60.7	327	204.63	9.04	5.79	<0.1	1.0	16.56	16.56	17.56	94	0	5	8.3	42.8	2.57	18.6	174.5	1.34
C_5	70-90	7.24	4.59	72.1	351	204.63	9.83	7.58	<0.1	0.8	19.20	19.20	20.00	96	0	4	5.6	41.4	2.99	25.7	163.5	1.43
C_6	90-95	7.16	4.59	71.2	387	200.66	6.72	7.54	<0.1	0.8	16.12	16.12	16.92	95	0	5	6.3	44.8	3.00	27.1	155.5	1.37
C_7	95-115	7.21	4.62	70.0	508	204.63	5.75	9.52	<0.1	0.6	17.46	17.46	18.06	97	0	4	6.1	44.4	2.86	22.0	155.5	1.27
C_8	115-205	6.66	4.24	38.5	159	189.69	4.18	3.90	0.58	2.2	9.31	9.89	11.51	81	6	7	20.1	35.5	0.81	5.4	103.3	1.06
P9 - Pantoorthodystric Protic Akrofluvic Arenosol (Ochric, Pantonechic, Raptic)/ Typic Cryopsamments																					
A	0-35	6.04	3.73	47.1	307	134.09	2.22	2.92	0.78	1.8	6.51	7.29	8.31	78	11	7	21.8	45.6	1.62	15.2	110.8	1.28
$2C_1$	35-50	6.79	3.97	57.2	307	240.38	1.04	5.41	0.19	1.0	8.28	8.47	9.28	89	2	11	22.0	46.5	2.45	11.4	128.0	1.21
$3C_2$	50-80	7.32	3.99	64.7	371	670.45	1.72	2.92	0.19	0.8	8.51	8.70	9.31	91	2	31	22.0	49.8	2.53	10.4	117.9	1.20
$4C_3$	80-115	7.51	4.25	79.2	379	749.88	1.44	2.62	<0.1	0.8	8.29	8.29	9.09	91	0	36	11.6	48.9	2.47	9.4	125.1	1.45
$4C_4$	115-130	7.71	4.52	88.4	387	799.53	1.28	2.45	<0.1	0.8	8.20	8.20	9.00	91	0	39	13.0	44.0	2.29	13.7	121.2	1.21
P10 - Cambic Epiturbic Amphiglacic Cryosol (Pantohypereutric, Clayic, Humic)/ Glacic Haploturbels																					
Ajj	0-30	7.58	5.39	47.1	84	581.09	9.05	8.61	<0.1	1.0	20.40	20.40	21.40	95	0	12	0.0	30.9	1.89	39.0	251.0	4.77
Cf	30-50	7.91	5.82	47.6	78	591.02	8.80	7.84	<0.1	0.3	19.41	19.41	19.71	99	0	13	2.9	38.2	2.02	50.2	259.4	4.60
P11 - Pantohypereutric Endoleptic Cambisol (Clayic, Humic, Epiturbic)/ Humic Eutrocryepts																					
Ajj	0-23	7.48	5.18	47.9	122	144.02	6.50	7.77	<0.1	1.0	15.21	15.21	16.21	94	0	4	10.1	33.4	3.06	11.4	292.7	1.63

Bi	23-60	7.91	5.35	172.7	32	185.72	13.45	15.92	<0.1	0.2	30.26	30.26	30.46	99	0.	3	3.2	43.3	2.68	19.5	170.2	1.17
C	60-80	8.29	5.84	206.0	46	216.55	13.37	14.16	<0.1	<0.1	28.59	28.59	28.59	100	0	3	2.5	45.7	4.64	31.4	243.0	1.34
P12 - Pantocambic Endoleptic Turbic Cryosol (Pantohypereutric, Clayic, Humic)/ Typic Haploturbels																						
Ajj	0-35	7.56	5.17	30.8	161	295.98	6.46	9.01	<0.1	1.0	17.17	17.17	18.17	95	0	7	7.0	35.6	0.99	15.1	175.2	2.40
Cjj	35-50	7.97	5.55	45.8	157	630.73	14.50	18.44	<0.1	0.3	36.08	36.08	36.38	99	0	8	0.5	39.1	1.18	24.0	168.2	3.03
C	50-70	7.82	5.63	89.5	110	315.84	15.83	21.05	<0.1	<0.1	38.54	38.54	38.54	100	0	4	2.5	46.8	0.35	60.6	130.7	3.22
P13 - Endoreductaquic Endoglacic Cryosol (Pantoorthodystric, Pantoarenic, Orthofluvic, Ochric, Pantonechic, Raptic)/ ‘Glacic’ Typic Cryopsamments																						
A	0-30	7.89	6.37	50.9	82	146.00	3.93	0.95	<0.1	<0.1	5.73	5.73	5.73	100	0	11	22.7	52.2	3.39	43.1	304.4	1.57
Cf	30-50	7.76	6.10	44.4	86	157.92	4.01	1.61	<0.1	<0.1	6.53	6.53	6.53	100	0	11	25.1	51.2	2.79	42.2	292.1	1.53

.

Supplementary Text 1.

The differences between soil groups are noticeable (Figure 4a). The sulfated soil located in the desert pavement (P1) showed an association mainly between the variables associated with potential soil acidity (H + Al and Al^{3+}) and with S and B, with these showing a positive correlation with each other. The soil profiles with pattern showed a broader association of attributes, where the silt and clay fractions were positively correlated, the cation exchange capacity is strongly influenced by the high contents of Ca, resulting in a positive correlation between these, and the P contents in these profiles positively correlated with Ca, Mn and Zn contents. The profiles inserted in the high platforms of Byers Peninsula, together with those associated with fields of soils with patterns in these high environments, showed a mixed association between attributes associated with soils with pattern and variables such as Fe contents, base saturation (V), and at pH in H_2O, these last two attributes being positively correlated and strongly influenced by Mg contents. As for the terraces, the variables associated with this environment were very specific and of great relevance for the characterization of this environment, these being the contents of K, Na, and a high percentage of sand, a striking feature of marine terraces. In addition to these variables, the marine terraces were associated with the contents of Cu and P-rem.

Both total stocks and SOM fractions showed a negative correlation with P-rem. In turn, they showed a positive correlation with Mn, except for N stock MAOM (Supplementary Material Figure S1). Once total stocks of C and N are correlated, as well C and N stocks in the plysical fractions, these nutrients are derived from the same source.

The C stock showed to be positively correlated with Zn, due to the correlation of this element with the C stock in the POM and MAOM fractions. The N stock was positively correlated with Fe due to the positive correlation of this element with the N stock in the POM fraction. In the MAOM fraction, the C and N stocks showed relatively higher values than in the POM fraction, in terms of contribution to the total stocks, thus the stocks in the MAOM fraction showed a high positive correlation with the total stocks of C and N.

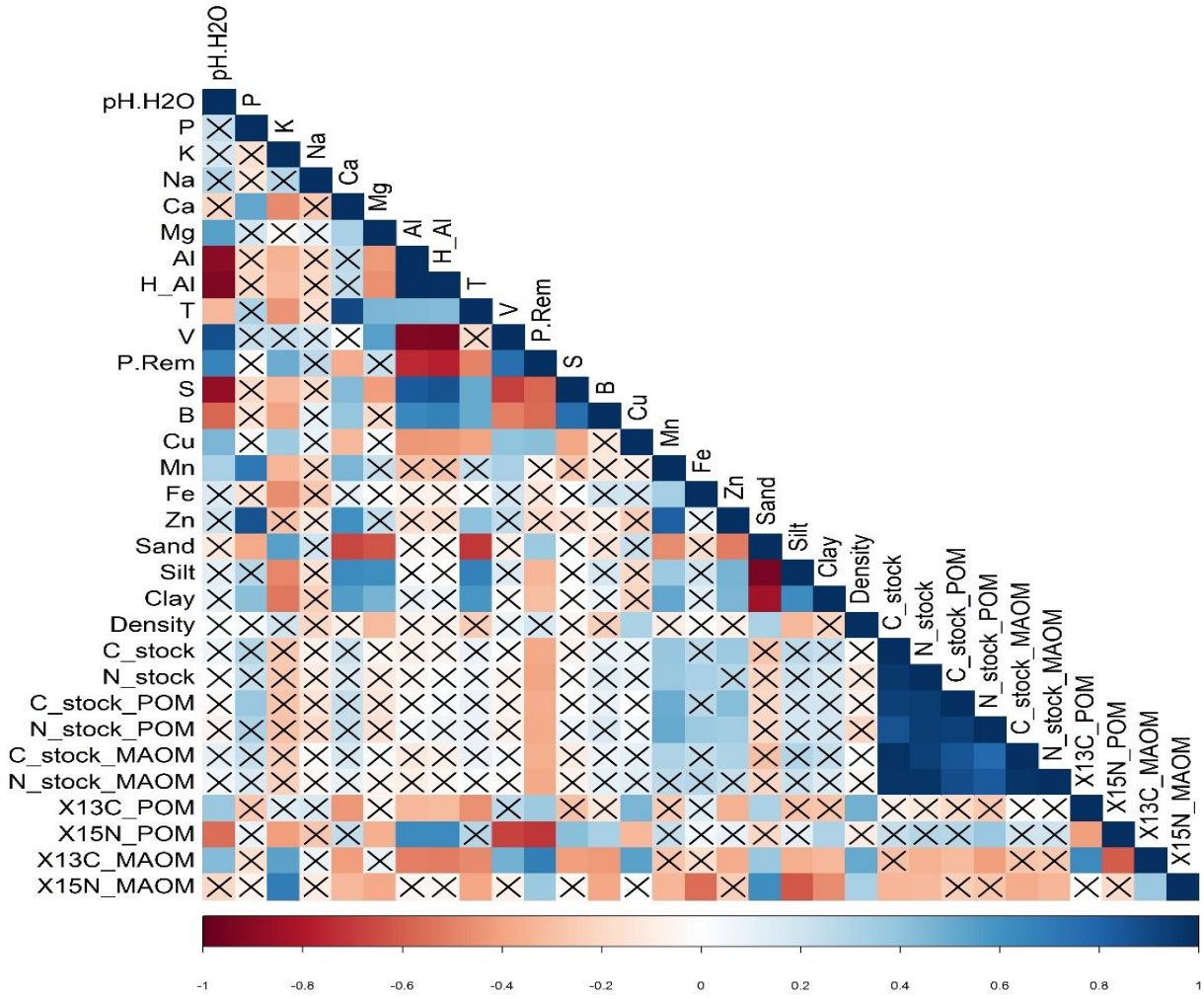

Figure S1. Spearman correlation data. Correlation between chemical, physical soil attributes and SOM. Where, the positive correlation is indicated in blue color and negative correlations in red color. Cells with X, indicate that the correlation was not significant at 5% probability.

Supplementary Text 2.

The total C and N stocks and the stocks in the POM and MAOM fractions showed a high association with the profiles of the high and low platforms, as well as the clay, silt, Mn, Zn, and P contents (Figure S2). The $\delta^{13}C$ and P-rem values showed a high association with one of the raised beaches (P13), because of its high levels of P-rem, and $\delta^{13}C$. The $\delta^{15}N$ of MAOM fraction showed a high association with raised beaches due to the higher values observed in this group of soils, showing high enrichment than in the other areas. The $\delta^{15}N$ in

the POM fraction was more associated with the acid-sulfated soil profile (P1) and the highest platform (P3), where the highest values of $\delta^{15}N$ signature were observed.

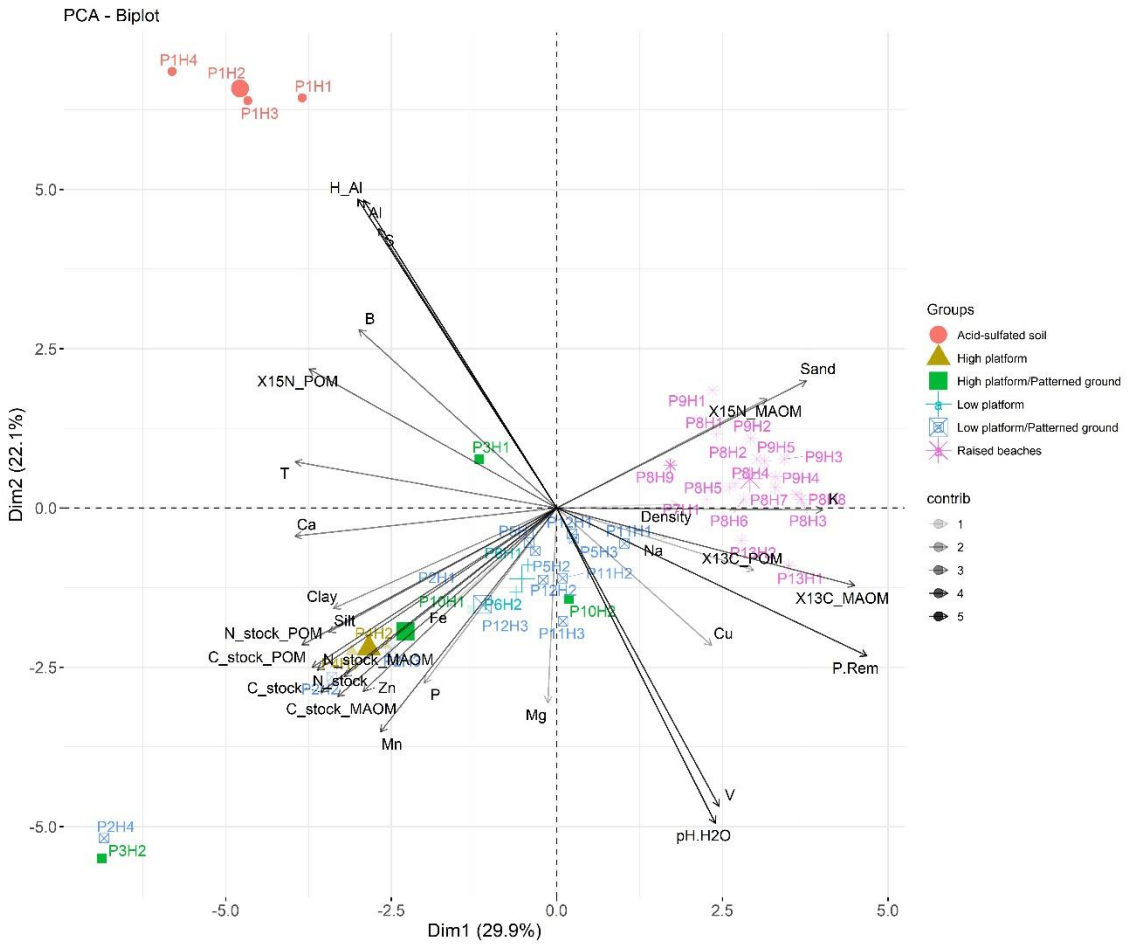

Figure S2. Principal component analysis - PCA indicating the separation of soil groups according to chemical (pH H_2O, P, K, Na^+, Ca^{2+}, Mg^{2+}, Al^{3+}, H + Al, T, V, P-rem, S, B, Cu, Mn, Fe, and Zn) and physical (sand, silt, clay and soil density) attributes of the soil and soil organic matter characteristics (stock total of C and N, stock of C-POM, C-MAOM, N-POM and N-MAOM, $\delta^{13}C$ and $\delta^{15}N$ of POM and MAOM fractions,). Dim1 e Dim2: axis of dimensions.

APPENDIX B. SUPPLEMENTARY DATA (PAPER 2)

Table S1. Overview of sequencing number before and after each step of analyses.

Marker	Sample ID	Zhang-Huang's coverage	Input reads	Filtered reads	Percentage of input that passed in filter	Denoised reads	Merged reads	Percentage of input reads that were merged	Non chimeric	Percentage of input reads that are non chimeric
16S	P10	1	207356	189571	91.4 %2	182725	153943	74.24	127711	61.59
16S	P11	1	219482	200134	91.18	193611	169978	77.45	155002	70.62
16S	P2H1	1	197912	181046	91.48	177275	162696	82.21	149483	75.53
16S	P3H1	1	184968	172343	93.17	167398	147478	79.73	127174	68.75
16S	P3H2	1	195159	176069	90.22	170324	147193	75.42	123801	63.44
16S	P4H1	1	186894	168641	90.23	161315	128680	68.85	107491	57.51
16S	P4H2	1	198430	179438	90.43	174024	156487	78.86	136803	68.94
16S	P5H1	1	200398	183163	91.4	177564	152286	75.99	130543	65.14
16S	P6H1	1	208608	189329	90.76	180989	147062	70.5	121541	58.26
16S	P6H2	1	183759	165250	89.93	159826	136177	74.11	115860	63.05
16S	P7H1	1	202260	184813	91.37	177301	148346	73.34	128722	63.64

16S	P9H1	1	203725	185224	90.92	179863	159947		78.51	135338	66.43
ITS	P10	1	43951	43257	98.42	43069	NA	-		42801	97.38
ITS	P11	1	94392	93063	98.59	92905	NA	-		92559	98.06
ITS	P2H1	1	91781	90711	98.83	90406	NA	-		90290	98.38
ITS	P3H1	1	52896	47491	89.78	47331	NA	-		46702	88.29
ITS	P3H2	1	44915	42702	95.07	42350	NA	-		40754	90.74
ITS	P4H1	1	53058	52398	98.76	51971	NA	-		51032	96.18
ITS	P5H1	1	12931	12744	98.55	12559	NA	-		12491	96.6
ITS	P6H1	1	86034	84671	98.42	84478	NA	-		84173	97.84
ITS	P7H1	1	36533	36041	98.65	35625	NA	-		35114	96.12
ITS	P9H1	1	69987	69156	98.81	68930	NA	-		63477	90.7

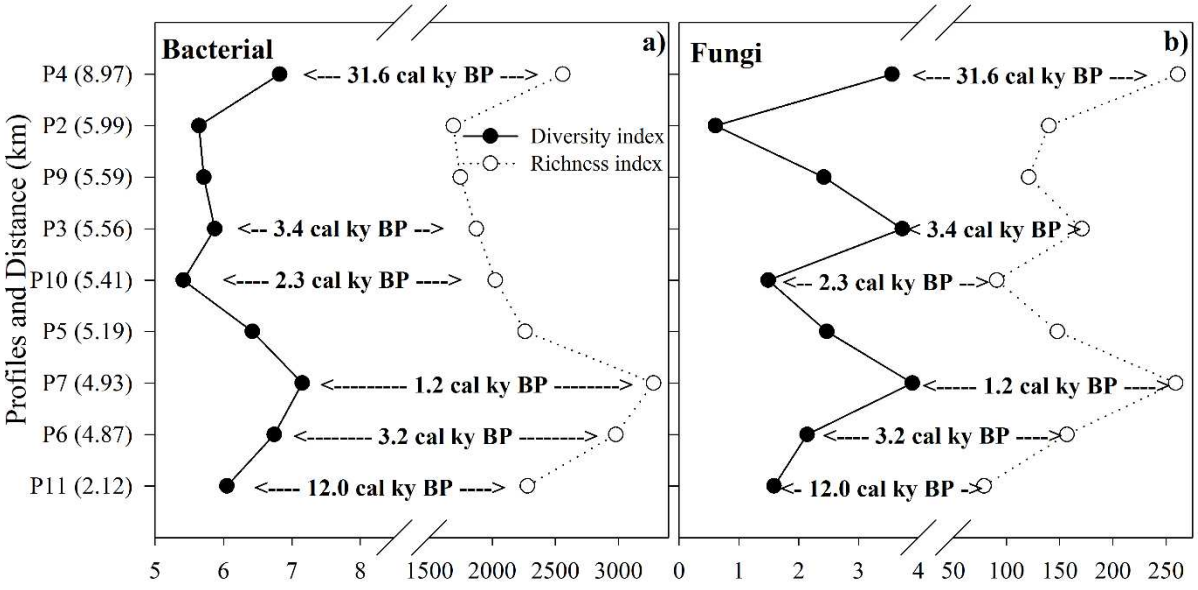

Figure S1. Microbial indices for a) bacteria and b) fungi as a function of linear distance between the profiles and the glacier and ^{14}C dating.

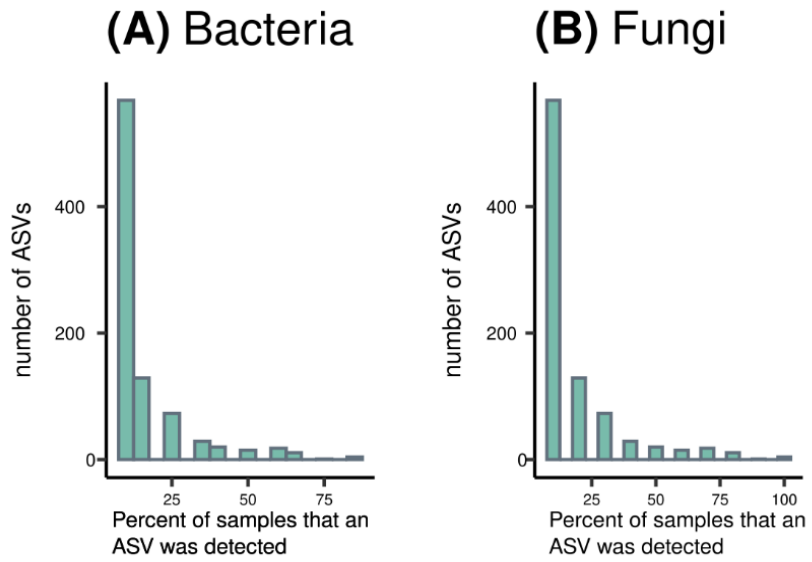

Figure S2. Histogram of frequency detection of ASVs in the samples. Most ASVs were detected in only one or two samples.

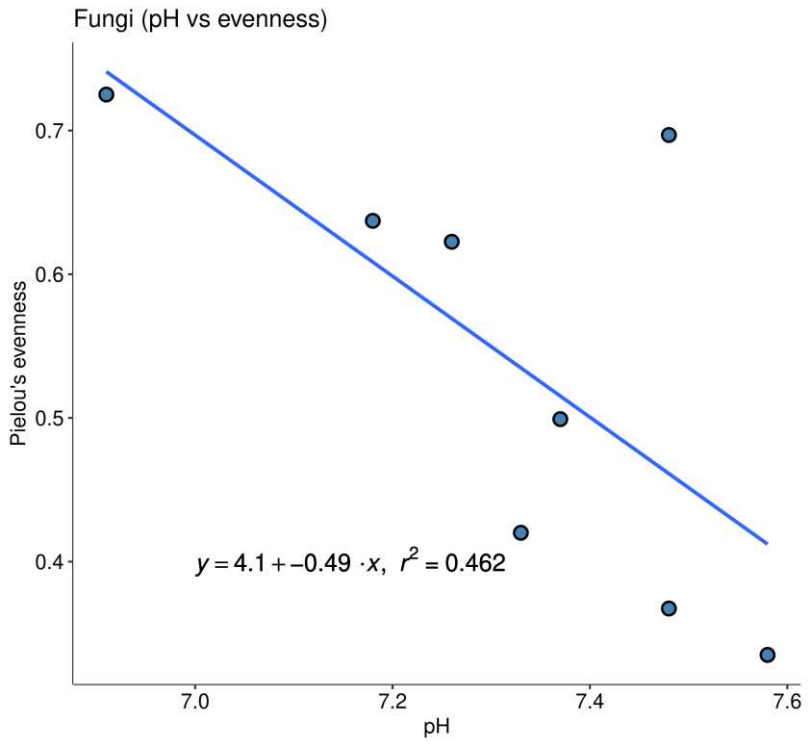

Figure S3. Correlation between pH and fungal evenness

Figure S3. Chemical and organic values of soil traits measured in each sample.

APPENDIX C. SUPPLEMENTARY DATA (PAPER 3)

Table S1. C and N stocks in the SOM fractions, total and percentage representativity of the fractions to the total stocks

	C-POM stock	N- POM stock	C- MAOM stock	N- MAOM stock	Total C stock	Total N stock	% total C stock		% total N stock	
Profiles	----------Mg ha^{-1}----------						POM	MAOM	POM	MAOM
P1	17.32	2.02	12.56	1.66	29.89	3.68	57.96	42.04	54.96	45.04
P2	39.06	3.08	70.15	5.23	109.21	8.31	35.76	64.24	37.04	62.96
P3	34.76	4.99	66.34	7.53	101.10	12.52	34.38	65.62	39.84	60.16
P4	28.36	4.11	13.48	2.06	41.85	6.16	67.78	32.22	66.65	33.35
P5	1.44	0.00	8.66	0.73	10.09	0.73	14.25	85.75	0.00	100.00
P6	5.53	0.44	24.49	2.58	30.02	3.02	18.43	81.57	14.61	85.39
P7	2.11	0.00	3.41	0.37	5.53	0.37	38.27	61.73	0.00	100.00
P8	19.84	0.00	13.15	1.53	32.99	1.53	60.15	39.85	0.00	100.00
P9	7.58	0.00	5.50	0.65	13.08	0.65	57.96	42.04	0.00	100.00
P10	16.11	0.82	36.93	3.33	53.04	4.15	30.38	69.62	19.79	80.21
P11	4.57	0.00	8.33	0.65	12.90	0.65	35.43	64.57	0.00	100.00

P12	2.35	0.00	14.51	1.36	16.86	1.36	13.91	86.09	0.00	100.00
P13	2.65	0.00	2.43	0.21	5.08	0.21	52.12	47.88	0.00	100.00

Table S2. List of organic compounds by the functional group with their respective stoichiometry in the POM and MAOM fraction

Lignin	**Stoichiometry**	**Carbon Chain**	**Present fraction**
2-Propenoic acid, 3-(3,4-dimethoxyphenyl)-, methyl ester	$C_{12}H_{14}O_4$	Aromatic	Vegetable
2-Propenoic acid, 3-(4-methoxyphenyl)-, methyl ester, (E)-	$C_{18}H_{26}O_3$	Aromatic	MAOM/Vegetable
Amino acid			
2,4(1H,3H)-Pyrimidinedione, 1,3,5-trimethyl-	$C_7H_{10}N_2O_2$	Alicyclic	MAOM
2,4(1H,3H)-Pyrimidinedione, 1,3-dimethyl-	$C_6H_8N_2O_2$	Alicyclic	MAOM
2,5-Pyrrolidinedione, 1-methyl-	$C_5H_7NO_2$	Alicyclic	MAOM
2-Pyrrolidone-5-carboxylic acid, N-methyl, methyl ester	$C_7H_{11}NO_3$	Alicyclic	MAOM/Vegetable
Caffeine	$C_8H_{10}N_4O_2$	Aromatic	MAOM
9H-Purin-6-amine, N,N,9-trimethyl-	$C_8H_{11}N_5$	Aromatic	MAOM
DL-Proline, 5-oxo-, methyl ester	$C_6H_9NO_3$	Aliphatic	MAOM
Protein			
1H-Isoindole-1,3(2H)-dione, 2-methyl-	$C_9H_7NO_2$	Aromatic	MAOM
5,10-Diethoxy-2,3,7,8-tetrahydro-1H,6H-dipyrrolo[1,2-a:1',2'-d]pyrazine	$C_{14}H_{22}N_2O_2$	Aromatic	MAOM
N-bearing			
(Dimethylamino)ethyl methacrylate	$C_8H_{15}NO_2$	Aliphatic	MAOM
13-Docosenamide, (Z)-	$C_{22}H_{43}NO$	Aliphatic	MAOM
1-Methyl-2-piperidinemethanol	$C_7H_{15}NO$	Alicyclic	MAOM
2(1H)-Pyridinone, 3,6-dimethyl-	C_7H_9NO	Alicyclic	MAOM
3-Oxo-1,4-diazabicyclo[3.2.2]nonane	$C_7H_{12}N_2O$	Alicyclic	MAOM
Formamide, N,N-dibutyl-	$C_9H_{19}NO$	Aliphatic	MAOM

1-Heptadecanamine, N,N-dimethyl-	$C_{19}H_{41}N$	Aliphatic	Vegetable
1-Nonadecanamine, N,N-dimethyl-	$C_{21}H_{45}N$	Aliphatic	Vegetable
1-Dodecanamine, N,N-dimethyl-	C14H31N	Aliphatic	MAOM
1-Heptadecanamine, N,N-dimethyl-	C19H41N	Aliphatic	MAOM/Vegetable
1-Nonadecanamine, N,N-dimethyl-	C21H45N	Aliphatic	MAOM/POM
1-Methyldodecylamine	C13H29N	Aliphatic	MAOM
1-Pentadecanamine, N,N-dimethyl-	C17H37N	Aliphatic	MAOM
1-Tetradecanamine, N,N-dimethyl-	C16H35N	Aliphatic	MAOM
1-Tridecanamine, N,N-dimethyl-	C15H33N	Aliphatic	MAOM
2(1H)-Pyridinone, 3,6-dimethyl-	C7H9NO	Alicyclic	MAOM
2-Pentanamine, 2,4,4-trimethyl-	C8H19N	Aliphatic	MAOM
Benzedrex	C10H21N	Alicyclic	MAOM
N,1-Dimethylhexylamine	C8H19N	Aliphatic	MAOM
N-Dodecylmethylamine	C13H29N	Aliphatic	MAOM
Carbohydrate			
1,4-Dioxaspiro[2.4]heptan-5-one, 7,7-dimethyl-	$C_7H_{10}O_3$	Alicyclic	MAOM/POM
1-Hexadecanol	$C_{16}H_{34}O$	Alicyclic	MAOM
2,3,4-Trimethyl-d-xylose	$C_8H_{16}O$	Alicyclic	MAOM
2,3,4-Trimethyllevoglucosan	$C_9H_{16}O_5$	Alicyclic	MAOM/POM
.alpha.-D-Glucopyranoside, phenyl 2,3,4,6-tetra-O-methyl-	$C_{16}H_{24}O_6$	Alicyclic	Vegetable
1,2,3,4-Tetramethylmannose	$C_{10}H_{20}O_6$	Aliphatic	Vegetable
1,2,4-Trimethoxybenzene	$C_9H_{12}O_3$	Aromatic	Vegetable

Cutin			
Octadecanoic acid, butyl ester	$C_{22}H_{44}O_2$	Aliphatic	MAOM/Vegetable
Tetracosanoic acid, methyl ester	$C_{25}H_{50}O_2$	Aliphatic	MAOM/Vegetable
Pentacosane	$C_{25}H_{52}$	Aliphatic	POM/Vegetable
8,11-Octadecadienoic acid, methyl ester	$C_{19}H_{34}O_2$	Aliphatic	Vegetable
9-Hexadecenoic acid, methyl ester, (Z)-	$C_{17}H_{32}O_2$	Aliphatic	Vegetable
9-Octadecenoic acid, methyl ester, (E)-	$C_{19}H_{36}O_2$	Aliphatic	Vegetable
Nonanedioic acid, dimethyl ester	$C_{11}H_{20}O_4$	Aliphatic	Vegetable
Octadecanoic acid	$C_{18}H_{36}O_2$	Aliphatic	Vegetable
Octadecanoic acid, butyl ester	$C_{22}H_{44}O_2$	Aliphatic	Vegetable
Suberin			
1-Docosanol, methyl ether	$C_{23}H_{48}O$	Aliphatic	MAOM/POM/Vegetable
Hexacosanoic acid, methyl ester	$C_{27}H_{54}O_2$	Aliphatic	MAOM/Vegetable
MAM			
Hexadecanoic acid, ethyl ester	$C_{18}H_{36}O_2$	Aliphatic	MAOM
Methyl stearate	$C_{19}H_{38}O_2$	Aliphatic	MAOM
n-Hexadecanoic acid	$C_{16}H_{32}O_2$	Aliphatic	MAOM/POM
Octadecanoic acid	$C_{18}H_{36}O_2$	Aliphatic	MAOM/POM
Bioactive			
1,2-Benzenedicarboxylic acid, bis(2-methylpropyl) ester	$C_{16}H_{22}O_4$	Aromatic	MAOM/POM/Vegetable
1-Heptadecene	C17H34	Aliphatic	MAOM
1-Nonadecene	C19H38	Aliphatic	MAOM

2-methylhexacosane	$C_{27}H_{56}$	Aliphatic	MAOM
2-methyloctacosane	$C_{29}H_{60}$	Aliphatic	MAOM
2-Isopropyl-5-methyl-1-heptanol	$C_{11}H_{24}O$	Aliphatic	MAOM/POM
2-Propenoic acid, tridecyl ester	$C_{16}H_{30}O_2$	Aliphatic	MAOM
7,9-Di-tert-butyl-1-oxaspiro(4,5)deca-6,9-diene-2,8-dione	$C_{17}H_{24}O_3$	Alicyclic	MAOM/POM
Benzene, (1,3,3-trimethylnonyl)-	C18H30	Aromatic	MAOM
Benzeneacetic acid, 2-tetradecyl ester	$C_{22}H_{36}O_2$	Aromatic	MAOM
Butane, 1-isothiocyanato-	C5H9NS	Aliphatic	MAOM
Diphenyl sulfone	$C_{12}H_{10}O_2S$	Aromatic	MAOM
E-11,13-Tetradecadien-1-ol	$C_{14}H_{26}O$	Aliphatic	MAOM
Heptafluorobutyric acid, n-octadecyl ester	$C_{22}H_{37}F_7O_2$	Aliphatic	MAOM
Hexadecanoic acid, 2-hydroxy-1-(hydroxymethyl)ethyl ester	$C_{19}H_{38}O_4$	Aliphatic	MAOM/POM
Hexadecanoic acid, butyl ester	$C_{20}H_{40}O_2$	Aliphatic	MAOM/Vegetable
n-Heptadecanol-1	$C_{24}H_{50}O$	Aliphatic	MAOM
Nonahexacontanoic acid	$C_{69}H_{138}O_2$	Aliphatic	MAOM
Nonanal	$C_9H_{18}O$	Aliphatic	MAOM/POM
Nonane, 5-butyl-	C13H28	Aliphatic	MAOM
Tetradecanal	$C_{14}H_{28}O$	Aliphatic	MAOM/POM
Undecanal, 2-methyl-	$C_{12}H_{24}O$	Aliphatic	MAOM
10-Methylnonadecane	$C_{20}H_{42}$	Aliphatic	POM
1-Pentadecene	$C_{15}H_{30}$	Aliphatic	POM
1-Undecene	$C_{11}H_{22}$	Aliphatic	POM

2-methyltetracosane	$C_{25}H_{52}$	Aliphatic	MAOM/POM
3,7,11,15-Tetramethyl-2-hexadecen-1-ol	$C_{20}H_{40}O$	Aliphatic	POM
Decane, 5-ethyl-5-methyl-	$C_{13}H_{28}$	Aliphatic	POM
Decane, 6-ethyl-2-methyl-	$C_{13}H_{28}$	Aliphatic	POM
Dichloroacetic acid, 4-hexadecyl ester	$C_{18}H_{34}Cl_2O_2$	Aliphatic	POM
Dodecane, 2,6,11-trimethyl-	$C_{15}H_{32}$	Aliphatic	POM
Eicosane, 2,4-dimethyl-	$C_{22}H_{46}$	Aliphatic	POM
Eicosane, 10-methyl-	C21H44	Aliphatic	MAOM
Heneicosane	$C_{21}H_{44}$	Aliphatic	POM/Vegetable
Heptadecane	$C_{17}H_{36}$	Aliphatic	POM/Vegetable
Heptadecane, 2,6,10,14-tetramethyl-	$C_{21}H_{44}$	Aliphatic	POM
Heptadecane, 2,6,10,15-tetramethyl-	$C_{21}H_{44}$	Aliphatic	POM
Hexacosane	$C_{26}H_{54}$	Aliphatic	POM
Hexadecane	$C_{16}H_{34}$	Aliphatic	POM
Hexadecane, 2,6,10,14-tetramethyl-	$C_{20}H_{42}$	Aliphatic	POM
Hexadecane, 2,6,11,15-tetramethyl-	$C_{20}H_{42}$	Aliphatic	POM
Nonacosane	$C_{29}H_{60}$	Aliphatic	POM/Vegetable
Nonadecane	$C_{19}H_{40}$	Aliphatic	POM
Octadecane	$C_{18}H_{38}$	Aliphatic	POM
Octadecane, 5-methyl-	$C_{19}H_{40}$	Aliphatic	POM
Oxalic acid, 6-ethyloct-3-yl hexyl ester	$C_{18}H_{34}O_4$	Aliphatic	POM
Oxalic acid, bis(6-ethyloct-3-yl) ester	$C_{22}H_{42}O_4$	Aliphatic	POM

Pentadecane, 8-hexyl-	$C_{21}H_{44}$	Aliphatic	POM
Tetracosane	$C_{24}H_{50}$	Aliphatic	POM/Vegetable
Tetradecane, 2,6,10-trimethyl-	$C_{17}H_{36}$	Aliphatic	POM
Tridecanal	$C_{13}H_{26}O$	Aliphatic	POM
Tridecanol, 2-ethyl-2-methyl-	$C_{16}H_{34}O$	Aliphatic	POM
Tetratriacontane	C34H70	Aliphatic	MAOM
Hexadecanoic acid, methyl ester	$C_{17}H_{34}O_2$	Aliphatic	Vegetable
Other lipids			
1-Decanol, 2-hexyl-	$C_{16}H_{34}O$	Aliphatic	MAOM/POM
1-Dodecanol	$C_{12}H_{26}O$	Aliphatic	MAOM/POM/Vegetable
1-Dodecanol, 2-hexyl-	$C_{18}H_{38}O$	Aliphatic	MAOM
1-Octanol, 2-butyl-	$C_{12}H_{26}O$	Aliphatic	MAOM
1-Tetradecanol	$C_{14}H_{30}O$	Aliphatic	MAOM
2-Propenoic acid, pentadecyl ester	$C_{18}H_{34}O_2$	Aliphatic	MAOM
9-Octadecenoic acid (Z)-, octadecyl ester	$C_{36}H_{70}O_2$	Aliphatic	MAOM
Docosanoic acid, methyl ester	$C_{23}H_{46}O_2$	Aliphatic	MAOM/Vegetable
Dodecanal	$C_{12}H_{24}O$	Aliphatic	MAOM/POM/Vegetable
Heptadecanoic acid, 16-methyl-, methyl ester	$C_{19}H_{38}O_2$	Aliphatic	MAOM
Hexadecanal	$C_{16}H_{32}O$	Aliphatic	MAOM/POM
Methyl 18-methylnonadecanoate	$C_{21}H_{42}O_2$	Aliphatic	MAOM
Octadecanoic acid, 2-hydroxy-1,3-propanediyl ester	$C_{39}H_{76}O_5$	Aliphatic	MAOM
Octadecanoic acid, 2-methylpropyl ester	$C_{22}H_{44}O_2$	Aliphatic	MAOM

Octadecanoic acid, 2-propenyl ester	$C_{21}H_{40}O_2$	Aliphatic	MAOM
Pentadecanal-	$C_{15}H_{30}O$	Aliphatic	MAOM
Pentatriacontane	C35H72	Aliphatic	MAOM
Squalene	C30H50	Aliphatic	MAOM
Z-2-Dodecenol	$C_{12}H_{24}O$	Aliphatic	MAOM
1-Tetradecene	$C_{14}H_{28}$	Aliphatic	POM
2-Nonen-1-ol	$C_9H_{18}O$	Aliphatic	POM
Decane, 3,7-dimethyl-	$C_{12}H_{26}$	Aliphatic	POM
Dodecane	$C_{12}H_{26}$	Aliphatic	POM
Eicosane	$C_{20}H_{42}$	Aliphatic	POM/Vegetable
Octacosane	$C_{28}H_{58}$	Aliphatic	POM
Tetradecane	$C_{14}H_{30}$	Aliphatic	POM
Tetrapentacontane	$C_{54}H_{110}$	Aliphatic	POM
Tridecanoic acid	$C_{13}H_{26}O_2$	Aliphatic	POM
Cyclobutanecarboxylic acid, dodecyl ester	$C_{17}H_{32}O_2$	Alicyclic	Vegetable
Formic acid, decyl ester	$C_{11}H_{22}O_2$	Aliphatic	Vegetable
Others			
1-Hexanol, 5-methyl-2-(1-methylethyl)-	C10H22O	Aliphatic	MAOM
1-Octadecanesulphonyl chloride	C18H37ClO2S	Aliphatic	MAOM
2-Ethyl-1-dodecanol	C14H30O	Aliphatic	MAOM
3-Chloropropionic acid, 4-hexadecyl ester	C19H37ClO2	Aliphatic	MAOM
Benzaldehyde, 2,4-dimethyl-	C9H10O	Aromatic	MAOM/POM

Chloroacetic acid, pentadecyl ester	C17H33ClO2	Aliphatic	MAOM
Decane, 1,1'-oxybis-	C20H42O	Aliphatic	MAOM
Hexadecanal, 2-methyl-	C17H34O	Aliphatic	MAOM
Octadecanal	C18H36O	Aliphatic	MAOM
Phenol, 2,4-bis(1,1-dimethylethyl)-	C14H22O	Aromatic	MAOM/POM/Vegetable
Phenol, 4,6-di(1,1-dimethylethyl)-2-methyl-	C15H24O	Aromatic	MAOM
Propanoic acid, 3,3'-thiobis-, didodecyl ester	C30H58O4S	Aliphatic	MAOM
Sulfurous acid, hexyl octyl ester	C14H30O3S	Aliphatic	MAOM
1,1':3',1"-Terphenyl, 5'-phenyl-	C24H18	Aromatic	POM
1,1'-Biphenyl, 2,2',5,5'-tetramethyl-	C16H18	Aromatic	MAOM
1-Bromoeicosane	C20H41Br	Aliphatic	MAOM
1-Chloroeicosane	C20H41Cl	Aliphatic	POM
1-Chloroundecane	C11H23Cl	Aliphatic	POM
1-Decene	C10H20	Aliphatic	POM
1-Dodecene	C12H24	Aliphatic	POM/Vegetable
1-Tridecene	C13H26	Aliphatic	POM
1-Eicosene	C20H40	Aliphatic	MAOM
1-Hexacosene	C26H52	Aliphatic	MAOM
2-Bromo dodecane	C12H25Br	Aliphatic	POM
2-Bromotetradecane	C14H29Br	Aliphatic	POM
2-Trifluoroacetoxytetradecane	C18H33F3O2	Aliphatic	POM
3-Hexadecene, (Z)-	C16H32	Aliphatic	POM

3-Tetradecene, (E)-	C14H28	Aliphatic	POM
3-Tetradecene, (Z)-	C14H28	Aliphatic	POM/Vegetable
5,5-Diethylheptadecane	C21H44	Aliphatic	POM
5,5-Diethylpentadecane	C19H40	Aliphatic	POM
5-Dodecene, (E)-	C12H24	Aliphatic	MAOM
6,6-Diethylhoctadecane	C22H46	Aliphatic	MAOM
7-Hexadecene, (Z)-	C16H32	Aliphatic	MAOM
6,6-Diethylhexadecane	C20H42	Aliphatic	POM
8-Heptadecene	C17H34	Aliphatic	POM
Behenyl chloride	C22H45Cl	Aliphatic	POM
Benzene, (1-butylheptyl)-	C17H28	Aromatic	POM
Benzene, (1-butyloctyl)-	C18H30	Aromatic	POM
Benzene, (1-ethyldecyl)-	C18H30	Aromatic	POM
Benzene, (1-ethylnonyl)-	C17H28	Aromatic	POM
Benzene, (1-ethyloctyl)-	C16H26	Aromatic	POM
Benzene, (1-methyldecyl)-	C17H28	Aromatic	POM
Benzene, (1-methylnonyl)-	C16H26	Aromatic	POM
Benzene, (1-methylundecyl)-	C18H30	Aromatic	POM
Benzene, (1-pentylheptyl)-	C18H30	Aromatic	POM
Benzene, (1-pentylhexyl)-	C17H28	Aromatic	POM
Benzene, (1-propylheptadecyl)-	C26H46	Aromatic	POM
Benzene, (1-propylnonyl)-	C18H30	Aromatic	POM

Benzene, (1-propyloctyl)-	C17H28	Aromatic	POM
Benzene, 1,3-dichloro-	C6H4Cl2	Aromatic	POM
Cyclopropane, nonyl-	C12H24	Alicyclic	POM
Decane, 1-iodo-	C10H21I	Aliphatic	POM/Vegetable
Decane, 2,3,4-trimethyl-	C13H28	Aliphatic	POM
Decane, 2,3,5,8-tetramethyl-	C14H30	Aliphatic	POM
Decane, 2,3,5-trimethyl-	C13H28	Aliphatic	POM
Dodecane, 1-chloro-	C12H25Cl	Aliphatic	POM
Dodecane, 1-iodo-	C12H25I	Aliphatic	POM
Dodecane, 2-methyl-	C13H28	Aliphatic	POM
Dodecane, 4,6-dimethyl-	C14H30	Aliphatic	POM/Vegetable
Dodecane, 4-methyl-	C13H28	Aliphatic	POM
Dotriacontane	C32H66	Aliphatic	POM
Heptacosane, 1-chloro-	C27H55Cl	Aliphatic	POM
Heptadecane, 8-methyl-	C18H38	Aliphatic	POM
Hexadecanal, 2-methyl-	C17H34O	Aliphatic	MAOM
Hexadecane, 1,16-dichloro-	C16H32Cl2	Aliphatic	MAOM
Hexadecane, 1-chloro-	C16H33Cl	Aliphatic	POM
Hexadecane, 1-iodo-	C16H33I	Aliphatic	POM
Hexatriacontane	C36H74	Aliphatic	MAOM
Hexadecane, 2-methyl-	C17H36	Aliphatic	POM
Nonane, 2-methyl-5-propyl-	C13H28	Aliphatic	POM

Nonane, 3-methyl-5-propyl-	C13H28	Aliphatic	POM
Nonane, 5-(1-methylpropyl)-	C13H28	Aliphatic	POM
Nonane, 5-methyl-5-propyl-	C13H28	Aliphatic	POM
Octadecane, 1-chloro-	C18H37Cl	Aliphatic	POM
Pentadecane	C15H32	Aliphatic	POM
Sulfurous acid, hexyl octyl ester	C14H30O3S	Aliphatic	POM
Tetracontane	C40H82	Aliphatic	POM
Tetradecane, 1-chloro-	C14H29Cl	Aliphatic	POM
Tetradecane, 4-methyl-	C15H32	Aliphatic	POM
Tetradecane, 5-methyl-	C15H32	Aliphatic	POM
Tetrapentacontane, 1,54-dibromo-	C54H108Br2	Aliphatic	POM
Tetratetracontane	C44H90	Aliphatic	POM
Triacontane, 1-bromo-	C30H61Br	Aliphatic	MAOM
Tridecane, 1-iodo-	C14H29I	Aliphatic	MAOM
Tridecane	C13H28	Aliphatic	POM
Tridecane, 4,8-dimethyl-	C15H32	Aliphatic	POM
Undecane, 3,8-dimethyl-	C13H28	Aliphatic	POM
Undecane, 3-ethyl-	C13H28	Aliphatic	POM
Undecane, 3-methyl-	C13H28	Aliphatic	POM
2,4,6-Trimethoxyacetophenone	C11H14O4	Aromatic	Vegetable
3-Octadecene, (E)-	C18H36	Aliphatic	Vegetable
Benzoic acid, 3,5-dimethoxy-, methyl ester	C10H12O4	Aromatic	Vegetable

Tetradecane	C14H30	Aliphatic	Vegetable

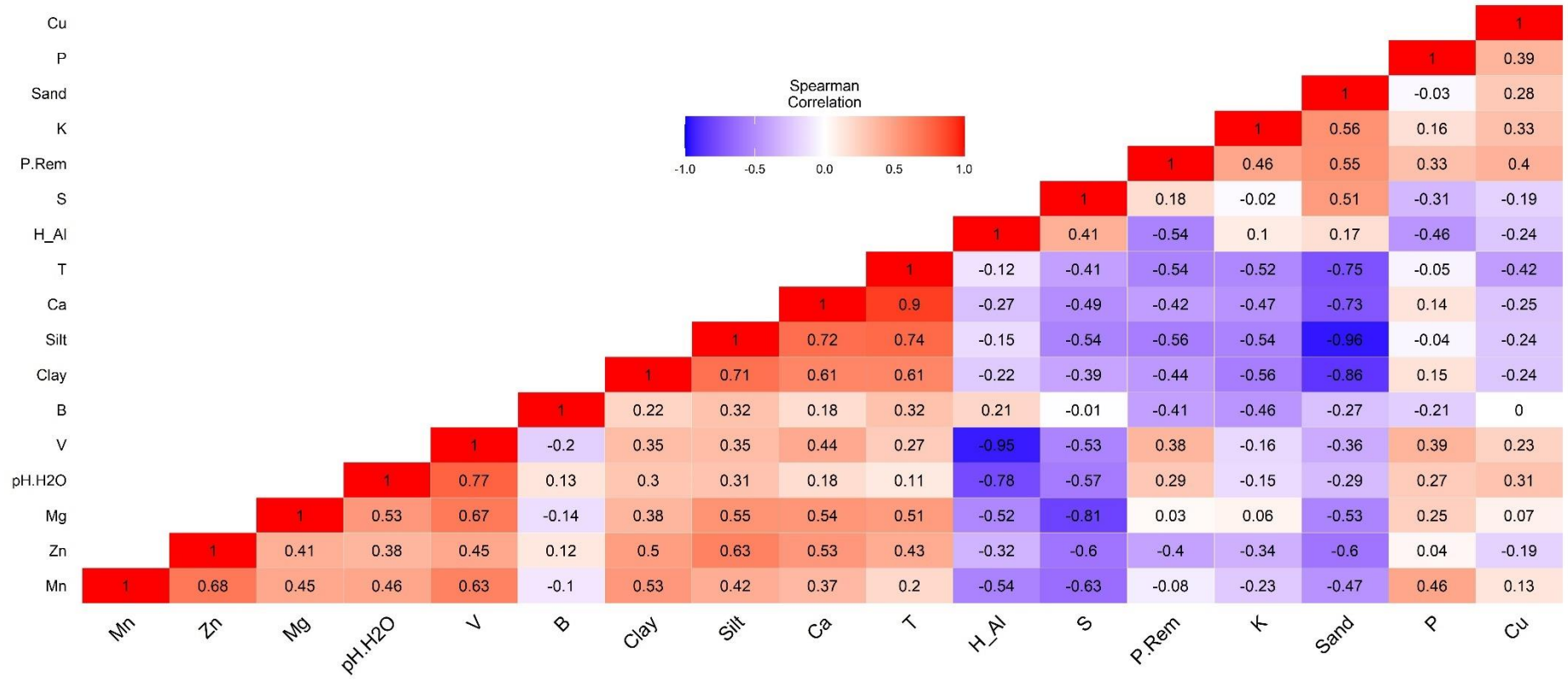

Figure S1. Spearman correlation data between chemical and physical soil attributes. Where, positive correlation is indicated in red color and negative correlations in Blue color. Cells with values above 0.5 or less than -0.5, indicate that the correlation was significant at 5% probability.

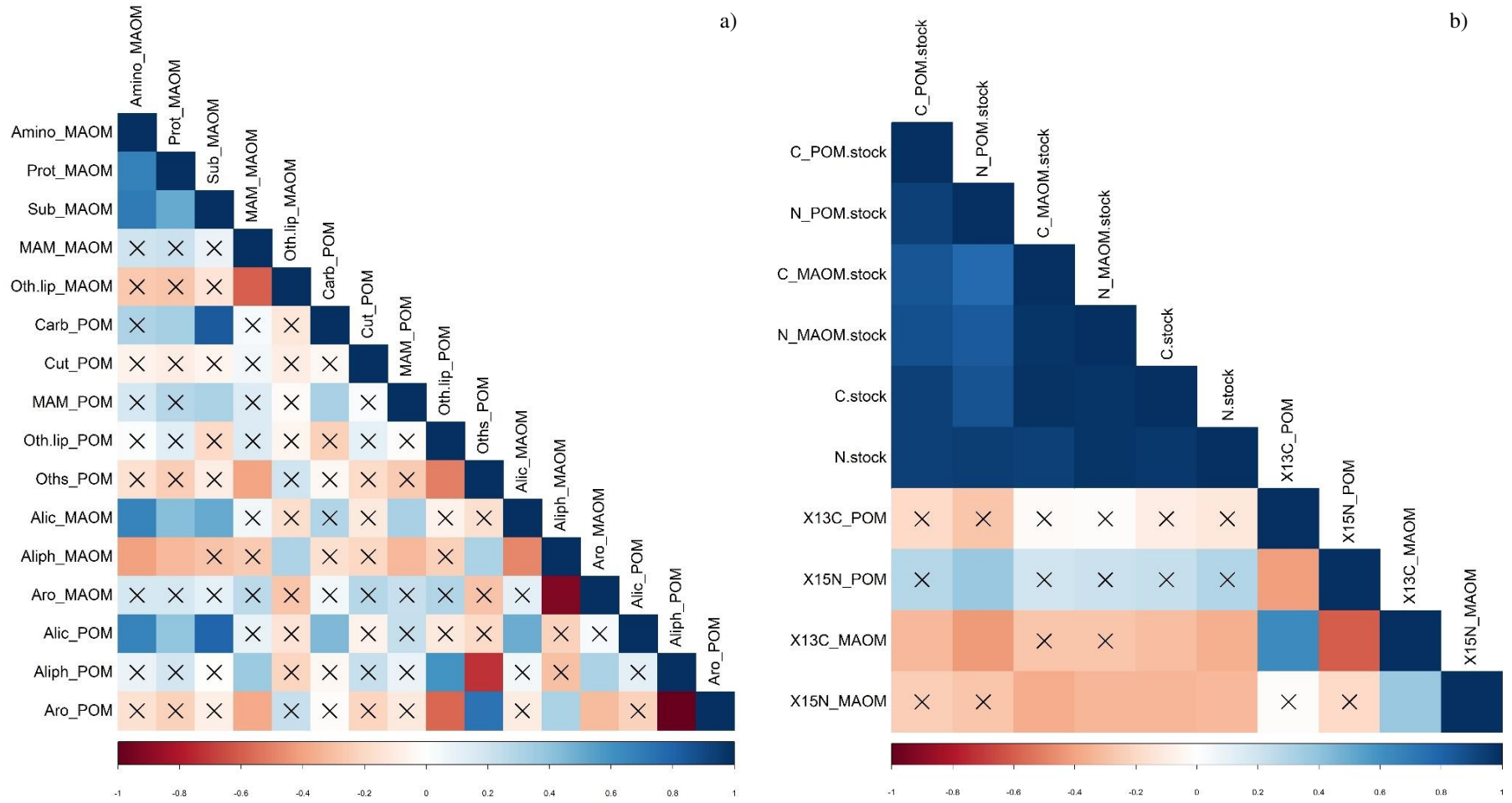

Figure S2. Spearman correlation data. a) Correlation between SOM biochemical composition variables, b) Correlation between C and N stocks and the isotopic signatures of SOM fractions. Where, positive correlation is indicated in blue color and negative correlations in red color. Cells with X, indicate that the correlation was not significant at 5% probability.